Universitat Jaume I
Departament d'Enginyeria de Sistemes Industrials i Disseny

Estimation and fault diagnosis strategies for networked control systems

A dissertation submitted in partial fulfillment of the requirements for the degree of Doctor of Philosophy

AUTHOR
Daniel Dolz Algaba

ADVISORS
Dr. Ignacio Peñarrocha Alós
Dr. Roberto Sanchis Llopis

Castellón de la Plana, November 2014

Universitat Jaume I
Departament d'Enginyeria de Sistemes Industrials i Disseny

Estrategias de estimación y diagnóstico de fallos para sistemas de control en red

Documento remitido en cumplimiento parcial de los requisitos para la obtención del grado de Doctor

AUTOR
Daniel Dolz Algaba

DIRECTORES
Dr. Ignacio Peñarrocha Alós
Dr. Roberto Sanchis Llopis

Castellón de la Plana, Noviembre 2014

To my family.
To Raquel.

Resumen

La utilización de redes de comunicación para entornos industriales ha incrementado la flexibilidad de conexionado de nuevos dispositivos a los sistemas existentes de monitorización, supervisión y control industriales reduciendo además el coste de explotación y mantenimiento. Sin embargo, a diferencia de la comunicación punto a punto donde se tienen mediciones continuas y sin retardos, la transmisión de datos a través de una red de comunicación puede sufrir retardos temporales e incluso pérdidas debido a diversos motivos. Además, la reciente expansión de dispositivos inalámbricos, introduce todavía más flexibilidad en la explotación del sistema en detrimento de una transmisión de datos eficaz desde el punto de vista de la monitorización, supervisión y control de procesos.

Con el auge de la utilización de las redes de comunicación para sistemas industriales también se ha visto incrementada la cantidad de recursos necesarios para garantizar ciertas prestaciones de comunicación. Por ejemplo, en el caso de transmisores inalámbricos, para aumentar la fiabilidad de las transmisiones de datos y así mejorar las prestaciones del sistema, es necesario utilizar una mayor potencia en la transmisión. Sin embargo, estos dispositivos están alimentados por baterías que son caras y difíciles de cambiar, donde además el proceso de transmisión es el más costoso en términos de energía. Esto muestra que, además de afrontar el diseño de sistemas monitorización, supervisión o control de procesos con retardos temporales y pérdidas de datos, también es necesario actuar sobre el funcionamiento de la red para ahorrar recursos, lo que se conoce como problema de codiseño del sistema de procesamiento.

Esta tesis aporta contribuciones novedosas para resolver los problemas de estimación y diagnóstico de fallos para sistemas discretos lineales, donde tanto las acciones de control como las mediciones de los sensores se envían a través de redes de comunicación. Además, también aborda el problema conocido como codiseño donde se realiza el diseño conjunto de estimadores y del funcionamiento de la red.

Más concretamente, la presente tesis tiene los siguientes objetivos generales:

- Modelado de los efectos inducidos por la redes de comunicación industriales en la transmisión de datos como pérdidas, retardos temporales, transmisión sin acuse de recibe, entre otros.
- Diseño de estrategias de estimación de señales y diagnóstico de fallos de bajo coste computacional que adapten su funcionamiento a las características de transmisión de la red de comunicación.
- Análisis del compromiso entre las prestaciones de las estrategias estimación de señales y diagnóstico de fallos frente a la complejidad computacional de las mismas.
- Análisis de estrategias de bajo coste computacional para la implementación de transmisión de datos basada en eventos.
- Diseño de estrategias de estimación de señales para transmisión de datos basada en eventos a través de redes de comunicación.
- Modelado del coste asociado a la transmisión de datos a través de redes de comunicación.

- Diseño conjunto de estimadores y algoritmos para decidir las características de transmisión de tal forma que se minimice la necesidad de utilización de recursos de red a la vez que se asegure ciertas prestaciones de estimación.

La metodología seguida para conseguir estos objetivos se ha basado en cuatro puntos fundamentales: estudio bibliográfico de los antecedentes de los problemas tratados; establecimiento de las hipótesis de trabajo; modelado matemático del problema y verificación de los resultados obtenidos mediante simulaciones.

Los resultados de la investigación llevada a cabo para cumplir con los anteriores objetivos, así como los conceptos y resultados previos necesarios, se han plasmado en el presente documento que contiene cuatro partes diferenciadas por su contenido. En los dos primeros capítulos se describen y se motivan en detalle los problemas de interés. En esta primera parte también se presenta el marco teórico de trabajo, modelando los posibles escenarios de transmisión de datos para diferentes tipos de redes de comunicación así como de políticas de envíos (periódicas o basadas en eventos).

En la segunda parte (Capítulos 3, 4, 5 y 6) se estudia el problema de estimación. Con el propósito de reducir el coste computacional de implementación de estimadores de Luenberger, se propone el uso de observadores con ganancias predefinidas que dependen de las diferentes condiciones de transmisión de la red.

En general, en esta tesis se proponen estimadores con ganancias conmutadas que dependen de los diferentes escenarios de recepción de mediciones ocasionados por la red. Así se define la complejidad del estimador en función del número de ganancias diferentes almacenadas. Bajo probabilidades constantes de éxito en las transmisiones, se diseñan observadores con ganancias conmutadas de forma que se garantiza un compromiso aceptable entre su complejidad y sus prestaciones de estimación. El problema de diseño se expresa mediante un problema de optimización basado en desigualdades lineales matriciales (LMI). Utilizando este tipo de estimadores se muestra que se pueden obtener prestaciones de estimación similares a las ofrecidas por el filtro de Kalman, con un coste computacional muy inferior.

Sin embargo, la probabilidad de llevar a cabo una transmisión con éxito puede variar con el tiempo y además ser desconocida a priori. En este caso, siempre se puede llevar a cabo una estimación de ésta utilizando los instantes de adquisición de nuevos datos. Bajo este supuesto, se propone un estimador con planificación de ganancias a partir de funciones racionales dependientes de la estimación de la tasa de llegada de datos. El problema de diseño se expresa mediante un problema de optimización sobre polinomios que se resuelve numéricamente utilizando técnicas basadas en suma de cuadrados (SOS). Así, a medida que se va aumentando el orden de los polinomios de las funciones racionales, este tipo de estimadores ofrecen prestaciones de estimación similares a las del filtro de Kalman pero con un menor coste computacional de implementación.

En la tercera parte (Capítulos 4 y 6), con el propósito de reducir la necesidad de utilización de recursos de red asegurando ciertas prestaciones de estimación, se estudia el diseño conjunto de las condiciones de transmisión de la red así como del estimador con ganancias conmutadas a utilizar (codiseño). Este paradigma de diseño se aborda considerando redes de comunicación inalámbricas con nodos alimentados por baterías, donde el mecanismo de transmisión es el mayor responsable del consumo de energía. Para reducir el número de transmisiones, y así aumentar la vida útil de los dispositivos

inalámbricos, se analizan dos opciones: transmisiones basadas en eventos y transmisiones de potencia controlada.

Como transmisiones basadas en eventos, se utiliza un protocolo de bajo coste de implementación conocido como Send-on-Delta (SOD). El SOD sólo transmite nuevas mediciones cuando la diferencia entre el valor de la medición actual con respecto a la última enviada sobrepasa cierto umbral. Al aumentar el valor del umbral, se consigue reducir el número de envíos y por lo tanto incrementar la vida útil de los dispositivos inalámbricos. Sin embargo, el problema de esta estrategia de envío es que impide conocer a priori cuál va a ser la probabilidad de envío de nuevos datos ya que ésta depende de la evolución del proceso. Así, bajo el supuesto de una transmisión ideal durante el envío de nuevos datos, se obtienen cotas sobra la probabilidad de nuevas transmisiones. Esto reduce el conservadurismo al efectuar el codiseño y obtener los umbrales de transmisión y las ganancias del estimador. El codiseño se aborda con un algoritmo que resuelve iterativamente problemas de optimización sobre polinomios, los cuales a su vez se resuelven numéricamente utilizando técnicas basadas en SOS.

El control de la potencia de transmisión se analiza para redes inalámbricas multisalto con canales sujetos a desvanecimiento. En este tipo de redes, los datos se transmiten desde el emisor hasta el receptor a través de nodos repetidores aumentando así la fiabilidad de transmisión pero introduciendo un retraso unitario al pasar por cada uno de éstos. Además, debido al efecto de desvanecimiento en los canales de comunicación se producen pérdidas en los envíos que pueden aliviarse incrementando la potencia de transmisión. Sin embargo, cuanta más potencia de transmisión se use, más rápido se consumirán las baterías. En este caso, se consideran funciones de control de potencia paramétricas que pueden depender del estado del canal. Así, el resultado del codiseño estará compuesto por las ganancias del estimador y por los parámetros que definen las funciones de control de potencia. El codiseño se aborda con un algoritmo que resuelve iterativamente problemas de optimización sobre restricciones LMI.

Finalmente, en la cuarta parte (Capítulos 7 y 8), con el propósito de garantizar la seguridad del comportamiento de los procesos controlados a través de redes de comunicación, se estudia el problema del diagnóstico de fallos. Se propone de nuevo el uso de estimadores con ganancia conmutada para estimar los fallos. Con la estimación de los fallos se construye un residuo cuya comparación con un umbral alertará de la presencia de fallos en el sistema. En esta tesis se estudia y se pone en evidencia el compromiso existente entre la detección rápida de un fallo y la capacidad de estimar su evolución con precisión. Las estrategias de diseño de diagnosticadores de fallos desarrolladas permiten elegir al usuario los fallos mínimos detectables, la tasa de falsas alarmas y el tiempo de respuesta frente a fallos deseado. El procedimiento de diseño se expresa mediante un problema de optimización basado en LMIs. Además, imponiendo cierta estructura al residuo se logra caracterizar su distribución de probabilidad obteniendo una cota sobre la tasa de falsas alarmas más precisa que las existentes.

También se analiza el caso en que tanto las acciones de control como las mediciones se envían a través de redes de comunicación sin acuse de recibo. En este caso el diagnosticador de fallos desconoce cuál es el valor exacto de las acciones de control que se están aplicando en el proceso. Entonces, se propone un diagnosticador de fallos basado en un estimador con planificación de ganancias a partir de funciones racionales dependientes de un estadístico finito de la diferencia entre las acciones de control aplicadas en el proceso y las utilizadas en el estimador (error de control). De nuevo, el diseño se expresa mediante

un problema de optimización sobre polinomios que se resuelve numéricamente utilizando técnicas basadas en SOS. Se muestra que la estrategia propuesta mejora las prestaciones del clásico diagnosticador de fallos diseñado para el peor caso cuando el valor del error de control es inferior a su máximo.

Las aportaciones de esta tesis abren camino a numerosas líneas de trabajo futuro (detalladas en la memoria) entre las que se destacan las siguientes:

- Caracterización analítica del compromiso entre complejidad y prestaciones de estimación para estimadores con ganancias conmutadas. Esto podría desarrollarse efectuando un análisis de sensibilidad de la función de optimización correspondiente a través de los multiplicadores de Lagrange. En este caso, los multiplicadores de Lagrange indicarían el coste de introducir una restricción de igualdad en el conjunto de las ganancias del estimador (aliviando así el coste computacional) sobre las prestaciones de estimación.

- Extensión de los resultados obtenidos para sistemas con incertidumbre de modelado.

- Diseño de la topología de la red multisalto. Este problema consistiría en decidir el emplazamiento de los nodos retransmisores para minimizar el consumo de energía mientras se asegura ciertas condiciones de recepción de datos. Se puede ver este problema como una extensión del problema de codiseño aquí presentado, donde además de obtener las ganancias del estimador y las leyes de control de potencia, también se obtendrían las localizaciones de los nodos intermediarios, es decir, se estaría imponiendo ciertas características en los canales sujetos a desvanecimiento.

- Análisis del uso de polinomios homogéneos para reemplazar las condiciones de tipo SOS que aseguran la positividad de polinomios. Las técnicas basadas en polinomios homogéneos permiten derivar condiciones menos conservadores que las derivadas de utilizar SOS para polinomios sin estructura definida.

- Desarrollo de técnicas de diagnóstico de fallos en sistemas de control en red con transmisiones basadas en eventos.

- Diseño de controladores inferenciales que usen los estimadores aquí propuestos para cerrar el lazo de control.

Abstract

Communication networks increase flexibility of industrial monitoring, supervisory and control systems. However, they introduce delays or even dropouts on the transmitted information that affect the performance and robustness on the decision and control mechanisms in the system. This thesis contributes theoretically to the state estimation and fault diagnosis problem over networks.

First, we study the state estimation problem. Motivated by reducing the implementation computational load of Luenberger-type estimators, we focus on predefined gain approaches for different network transmission conditions.

In general, we propose jump estimators whose gains are related to the different network-induced data reception scenarios. We define the estimator complexity in terms of the number of different stored gains. Considering constant successful transmission probabilities, our main contribution here is the design of jump linear estimators to attain favorable trade-offs between estimation performance and estimator complexity. We show that one can reduce the estimator complexity while guaranteeing a similar performance than the optimal Kalman Filter.

When dropouts are governed by a non-stationary stochastic process, the successful transmission probability is time-varying and may be unknown. For this case, we propose an estimator whose gains are scheduled in real-time with rational functions of the estimated packet arrival rate. We turn the design procedure into an optimization problem over polynomials that is numerically solved employing sum-of-squares (SOS) decomposition techniques.

Second, motivated by reducing the network resource consumption without considerably degrading the estimation performance, we study the jointly design of jump linear estimators and predefined network operation conditions (co-design) to guarantee a favorable trade-off. Focusing on wireless networks with self-powered nodes, where transmitting is the most energy consuming task, we analyze two approaches for the network operation: event-based transmissions and power control.

For the event-based approach, we use a Send-on-Delta protocol which reduces the number of transmissions with respect to transmitting at each sampling instant. However, it leads to an unknown successful transmission probability. For this framework, we contribute by characterizing this uncertainty and including it on the stochastic behavior of the estimator by means of a SOS-based design.

Power control strategies are developed over a multi-hop wireless network with fading channels. Instead of reducing the number of transmission, power control acts directly on the transmission power. Higher transmission powers imply higher successful transmission probability values.

Finally, motivated by the need of assuring a reliable operation of the networked system, we study the fault diagnosis problem. We explore and point out the trade-offs between fast fault detection and fault tracking conditions. We design jump estimator-based fault diagnosers in which we can specify the minimum detectable faults, false alarm rate and response time to faults. Another contribution is a tightened version of existing false alarm rate bounds.

Moreover, we also address the case when the control input is transmitted through a network without delivery acknowledgement. In this case, we improve fault diagnosis

accuracy by scheduling in real time the estimator jumping gains with rational functions that depend on a statistic of the control input error (difference between the control command being applied in the process and the one being used in the estimator). Again, we use a SOS-based solution approach to make the design problem tractable.

Acknowledgments

May the reader forgive me the discourtesy of following my wish to write the acknowledgements in my mother tongue.

En primer lugar, me gustaría dar las gracias a mis directores de tesis Roberto Sanchis e Ignacio Peñarrocha por la confianza que depositaron en mi desde el primer momento, por el tiempo que me han dedicado, por los consejos que me han dado (incluso sobre aspectos fuera del ámbito académico) y por compartir sus inquietudes conmigo. Podríamos decir que esta etapa que concluye con la redacción de este documento, empezó con la beca de colaboración en 2011 dirigida por Nacho. Aunque en esa época ya tenía idea de realizar un doctorado, aún no tenía claro dónde hacerlo. Su saber hacer, dedicación y confianza me hizo darme cuenta que el mejor sitio para seguir aprendiendo era aquí. Sin vuestra ayuda esta tesis no hubiera sido posible.

También quisiera acordarme de todos los miembros del ESID y compañeros del TC2124 con los que he podido interactuar durante estos años. Me gustaría agradecer especialmente a Julio Romero y a Néstor Aparicio haber podido colaborar con ellos. Durante este tiempo en el ESID he aprendido una valiosa lección: cualquier fecha límite dentro del mundo académico finaliza a las 6 a.m.. Además, quiero agradecer a la *Universitat Jaume I* por haber financiado durante 36 meses la realización de esta tesis doctoral través del *Pla de promoció de la investigació de la Universitat Jaume I 2011* (código de la ayuda PREDOC/2011/37)

En segundo lugar, estoy especialmente agradecido a Daniel Quevedo por haberme acogido durante 4 meses en la University of Newcastle (Australia). Gracias por tus consejos y dedicación. También quiero agradecer a Alex Leong, Juan Carlos Agüero, Ramón Delgado y Ricardo Aguilera haber podido colaborar con ellos durante mi estancia. Tampoco puedo olvidarme de todos los amigos que hice mientras viví allí, gracias entre otros a Diego, Alejandro, Boris, Michael y Yuzhe por hacer mi estancia más agradable.

En tercer lugar, quiero agradecer a mis amigos su gran apoyo. A Luis por sus increíbles consejos y por ser mi compañero de fatigas. A Marc y Adrián por todos los momentos inolvidables que hemos disfrutado juntos. A Sonia por sus estupendas cenas. A Rubén, Pascual y Carlos por su esfuerzo en adecuar nuestras quedadas a mi ajetreado horario. A mi compi Ester por ayudarme a desconectar en mis momentos de estrés. A mis amigos del INSA de Toulouse, de la UJI y demás.

En cuarto lugar, quiero reconocer la labor de mis padres. Gracias a la educación que me han dado, a los esfuerzos que han hecho por mi, a su apoyo incondicional y a sus consejos, he podido crecer como persona y alcanzar todas las metas que me he propuesto. También quiero agradecer a mi hermano por los buenos ratos que hemos pasado.

Finalmente, quiero dedicar estas últimas líneas a ella. Gracias por entender mis ausencias, gracias por estar siempre a mi lado, gracias por tu apoyo, gracias por alegrarme los días, gracias por hacerme feliz. A ti, Raquel.

Contents

Resumen **i**

Abstract **v**

Acknowledgments **vii**

1 Introduction **1**
1.1 Motivation Example . . . 3
1.2 Challenging Problems . . . 4
1.3 Thesis outline and Contributions . . . 6
1.4 Abbreviations . . . 11
1.5 Notation . . . 12

2 Networked Control Systems **13**
2.1 Process model . . . 13
2.1.1 Faulty process . . . 14
2.2 Sensing link . . . 16
2.2.1 Probabilistic framework . . . 20
2.3 Specific sensing link: wireless multi-hop networks with fading channels . . . 24
2.3.1 Fading channel characterization . . . 26
2.3.2 End-to-end transmission . . . 27
2.4 Control link . . . 30
2.5 Event-based sampling . . . 32
2.6 Estimation over networks . . . 33
2.7 Fault diagnosis over networks . . . 36
2.8 Co-design . . . 38

I Estimation over networks **41**

3 Jump state estimation with multiple sensors with packet dropping and delaying channels **43**
3.1 Problem approach . . . 44
3.2 Observer design . . . 49
3.3 Numerical computation . . . 51
3.4 Complexity reduction . . . 52
3.5 Examples . . . 53
3.5.1 Example 1 . . . 53
3.5.2 Example 2 . . . 56
3.5.3 Example 3 . . . 57
3.6 Conclusions . . . 59

4 Co-design of jump estimators for wireless multi-hop networks with fading channels 61
4.1 Problem description . . . 63
4.2 Multi-hop wireless network . . . 63
4.3 Markovian jump filter . . . 65
4.3.1 Proposed filter . . . 65
4.3.2 Filter design . . . 66
4.3.3 Boundedness of the error covariance . . . 67
4.3.4 Necessary network conditions . . . 67
4.3.5 Numerical computation . . . 68
4.4 Power allocation . . . 69
4.5 Co-design . . . 69
4.5.1 Co-design trade-offs . . . 71
4.6 Example . . . 73
4.7 Conclusions . . . 75

5 Polynomial observers in networked control systems with unknown packet dropout rate. 77
5.1 Problem statement . . . 78
5.1.1 System description . . . 78
5.1.2 Proposed state estimation algorithm . . . 79
5.2 Observer design . . . 80
5.2.1 Proposed optimization procedure . . . 81
5.3 Examples . . . 84
5.4 Conclusions . . . 87

6 Co-design of H-infinity jump observers for event-based measurements over networks 89
6.1 Problem Statement . . . 90
6.2 Observer design . . . 92
6.2.1 Deterministic approach . . . 93
6.2.2 Stochastic approach . . . 93
6.2.3 Optimization design procedure . . . 97
6.3 Observer co-design . . . 98
6.4 Examples . . . 100
6.5 Conclusions . . . 104

II Fault diagnosis over networks 105

7 Performance trade-offs for networked jump observer-based fault diagnosis 107
7.1 Introduction . . . 107
7.2 Problem Formulation . . . 109
7.2.1 Network transmissions characterization . . . 110
7.2.2 Fault diagnosis method . . . 111
7.3 Fault diagnoser design: dropout-free . . . 112
7.4 Application to networked transmission . . . 115
7.5 Fault diagnosis strategies . . . 118

7.6 Example . . . 119
7.7 Conclusion . . . 122

8 Networked gain-scheduled fault diagnosis under control input dropouts without data delivery acknowledgement 125
8.1 Problem setup . . . 126
8.1.1 Sampled measurement reception modeling . . . 128
8.1.2 Control input update modelling . . . 129
8.1.3 Fault diagnosis algorithm . . . 130
8.2 Fault diagnoser design . . . 131
8.2.1 SOS decomposition . . . 133
8.2.2 Fault diagnosis design strategy . . . 135
8.3 Examples . . . 137
8.3.1 Example 1 . . . 137
8.3.2 Example 2 . . . 140
8.4 Conclusion . . . 142

III Conclusions of the thesis 143

9 Conclusions and future work 145
9.1 Contributions . . . 145
9.2 Future work . . . 147

IV Appendixes and Bibliography 149

A Linear matrix inequalities 151
A.1 Convex optimization . . . 151
A.2 Matrix inequalities . . . 151
A.3 Solving nonconvex inequalities . . . 153
A.3.1 Convexifying algorithm . . . 153
A.3.2 Rank-constrained problems . . . 155

B SOS decomposition 157

C Auxiliary results and proofs 159
C.3 Proofs of Chapter 3 . . . 159
C.3.1 Proof of Theorem 3.1 . . . 159
C.3.2 Proof of Theorem 3.4 . . . 160
C.3.3 Proof of Theorem 3.5 . . . 160
C.4 Proofs of Chapter 4 . . . 161
C.4.1 Proof of Theorem 4.1 . . . 161
C.4.2 Proof of Theorem 4.3 . . . 161
C.4.3 Proof of Theorem 4.4 . . . 162
C.5 Proofs of Chapter 5 . . . 163
C.5.1 Proof of Theorem 5.1 . . . 163
C.6 Proofs of Chapter 6 . . . 164
C.6.1 Proof of Theorem 6.1 . . . 164

C.6.2 Probabilities and variances computation 165
C.6.3 Proof of Theorem 6.2 167
C.7 Proofs of Chapter 7 167
C.7.1 Proof of Theorem 7.1 168
C.7.2 Proof of Theorem 7.2 168
C.7.3 Proof of Theorem 7.3 169
C.7.4 Proof of Theorem 7.4 170
C.7.5 Proof of Theorem 7.5 170
C.7.6 Proof of Theorem 7.6 172
C.8 Proofs of Chapter 8 172
C.8.1 Proof of Theorem 8.1 172
C.8.2 Proof of Theorem 8.2 174

Bibliography **175**

Chapter 1

Introduction

Control engineering relies on the possibility to acquire information from a system state for decision-making on control undertakings and to transmit the control decisions to act on the system. Traditional control methods consider an ideal information transmission between sensors, controllers and actuators that can only be obtained in practice with a wired point-to-point connection. However, breaking free of these point-to-point communications by employing a wired or wireless communication network can benefit tremendously the operation and maintenance of modern industries containing many decentralized processes [44, 150]. When the transfer of information is performed through a network, then the control system is defined as a **Networked Control System (NCS)**, see Fig. 1.1.

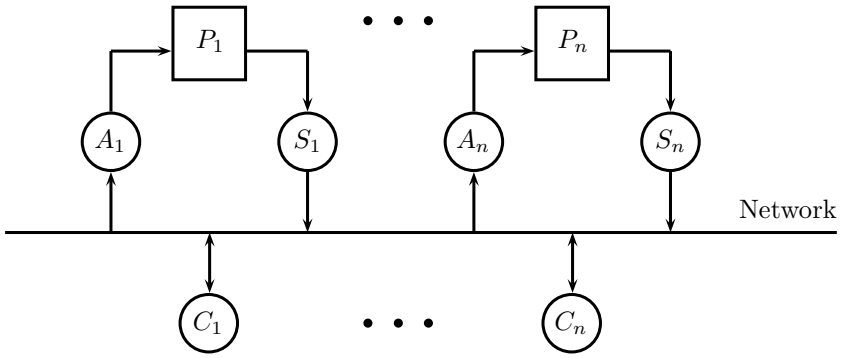

Figure 1.1: Network Control System architecture. A: actuator, P: process, S: sensor, C: controller.

Communicating through networks introduces numerous advantages with respect to point-to-point communication. For instance,

Low cost: Using a shared network decreases the number of wires and connections. Then, both maintenance and operation costs are cut.

Operation: Accessing to the whole system information and performing new acting strategies can be done from a single position without visiting each process.

Maintenance: Reducing the wiring complexity alleviates the maintenance operation on the system.

Flexibility: Including additional elements (sensors, actuators, controllers or processes) in an existing installation takes little effort as neither software, nor hardware significant changes have to be made.

Accessibility: Employing wireless devices allows transferring information from and to unreachable locations where wired connections cannot arrive.

Such advantages have been extensively exploited in many real-life applications through different kinds of networks. Nowadays vehicles use a Controller Area Network (CAN) bus to transmit data between the different modules, e.g., break, engine, transmission, steering and climate control [61]. Other applications can be found in remote surgery [88], water transportation systems [12], industrial automation [94] and wind farms [62].

But, in addition to the aforementioned advantages, the introduction of communication networks bring some network-induced issues [51, 14] such as,

Time delays: Delays appear due to the congestion of the network and may cause the reception of disordered data in time.

Dropouts: Data can be lost after transmission because of collisions or can be corrupted by the communication environment causing a rejection by the reception mechanism.

Accessibility constraints: When multiple devices share a network and try to transmit, a competition between them is performed and some of them may not be able to communicate during their allocated transmission time-slot.

These problems may degrade the system operation performances or even cause its instability. So, how do we design control methods providing some performance guarantees to work under communication networks?

A first approach that may rise in ones mind is to focus on the network itself and improve the communication reliability so traditional control methods can be applied. This is usually known as **control of network**. Contrarily, we can develop new control theories leading to robust designs that overcome the network-induced issues, which is regularly called **control over network**. An intermediate approach between both of them is to design both controllers and networks to operate in harmony, leading to the so-called **co-design**. Therefore, the study of NCS implies dealing with three different research areas: control theory, telecommunications systems and computer science (see Fig. 1.2).

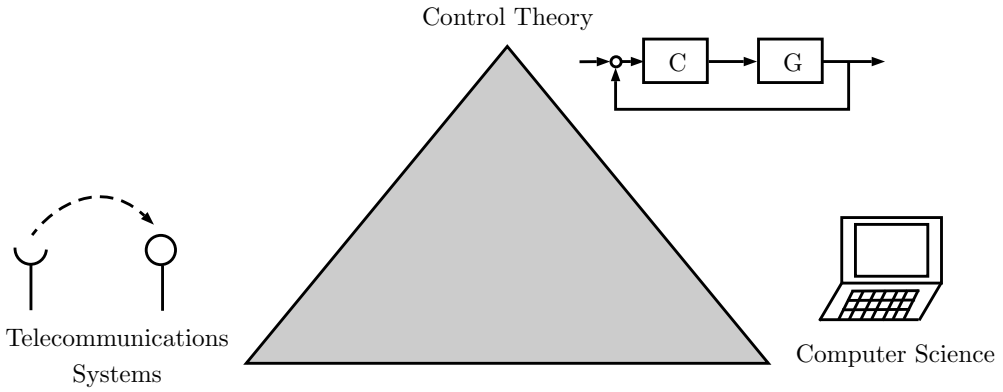

Figure 1.2: NCS as a multidisciplinary research field.

Not only control methods are affected by the use of the networks and need to be adapted. The **state estimation** problem, which is of great importance for control or fault diagnosis purposes, must be also readdressed to deal with the network-induced

issues. Moreover, owing to the need for reliability, safety and efficient operation in control systems, it is required to adapt conventional **fault diagnosis** methods to the networked environment.

This thesis discusses in further details the network-induced problems, proposes some methods to address the problem of estimation and fault diagnosis over networks and gives some approaches to deal with the co-design. In this chapter, we first give a motivation example to show how control performances can be deteriorated when using traditional control methods to control a process over a network. In this example, we also illustrate how estimation helps to overcome the design of new controllers. After that, we present the main challenging problems with which we deal in this thesis. Finally, we conclude the chapter with the thesis outline and contributions, and give a list of notation and abbreviations.

1.1 Motivation Example

The aim of this example is to show that traditional control techniques are not suitable for networked environments. Consider the NCS in Fig. 1.3 where we want to control some process with a discrete-time transfer function given by

$$P(z) = \frac{0.06z^{-1} + 0.05z^{-2}}{1 - 1.61z^{-1} + 0.61z^{-2}}$$

where the sampling time is $T = 65ms$. In this case only measurements are sent through a network that can only assure a 50% of successful transmissions without following any pattern (see Fig. 1.4). Control input transmissions are loss-free.

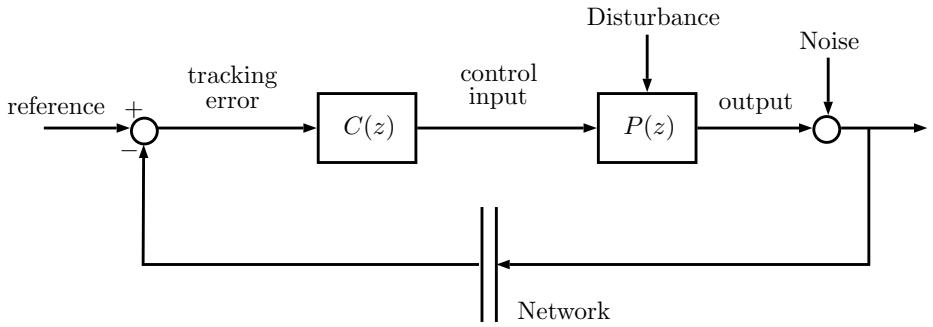

Figure 1.3: A simple networked control system with data losses.

Without any doubt, the most deployed controller in the industry is the PID. One of the most common techniques to tune it is using relay feedback auto-tuning techniques [5]. With that, the discrete-time version of the PID controller has the following transfer function [2]

$$C(z) = \underbrace{K_p}_{Proportional} + \underbrace{\frac{q_i}{1 - z^{-1}}}_{Integral} + \underbrace{\frac{q_d(1 - z^{-1})}{1 + p_d z^{-1}}}_{Derivative}$$

where the parameters for the studied problem are $K_p = 1.06$, $q_i = 0.08$, $q_d = 3.02$, $p_d = 0.11$.

Fig. 1.4 shows the reference tracking performance provided by the PID when the communication is ideal (without losses) and when the network is used to transfer the data. We appreciate that the control performances are deteriorated when using the network leading to a high overshoot of 140%. However if we estimate the system output by means of a Kalman Filter (KF) adapted to the network scenario [129] (which is implemented in the controller) and use this estimation to close the loop, then we obtain a similar behavior than when there was no measurement losses. This shows that traditional control methods can be used under networks scenarios if we are able to estimate properly, for instance, the process outputs., what will require the knowledge of a model of the process.

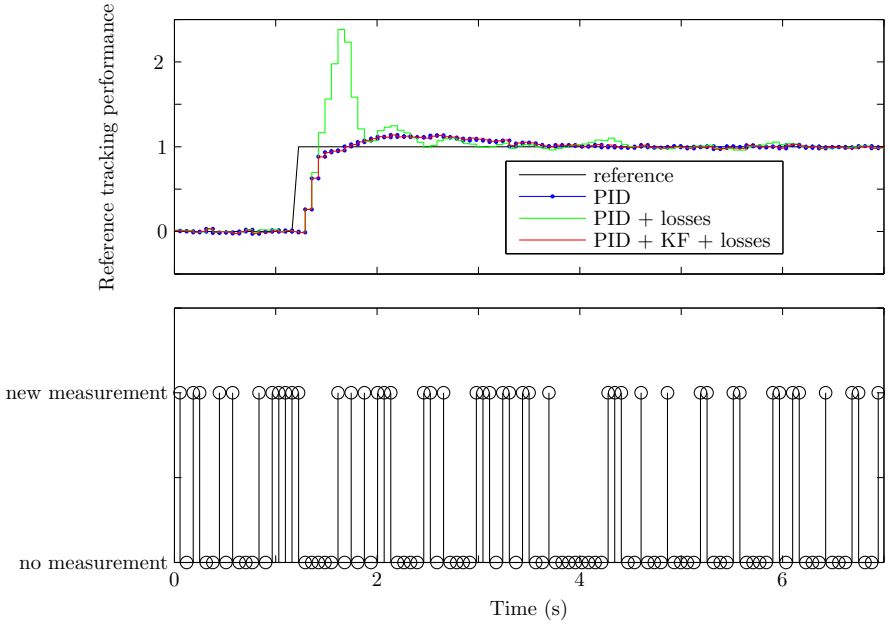

Figure 1.4: Networked effects over reference tracking PID with 50% of measurement losses.

1.2 Challenging Problems

This thesis deals with the problems of state estimation and fault diagnosis of Linear Time-Invariant (LTI) Discrete-Time Systems (DTS) over networks with different characteristics. Moreover, we discuss some techniques to address the co-design problem for the proposed scenarios. In the following we briefly describe the major concerns of the current thesis. For brevity let us just focus on the estimation problem. However, all the next also applies to the fault diagnosis case.

Network-based estimation methods

In the last decades much effort has been put into developing recursive estimation techniques to work under network-based communications [14, 35]. KF solutions have been greatly employed since the seminal works [78, 129] to overcome issues such as

measurement dropouts and delays. However, even if these approaches may give optimal estimation performance, they lead to time-varying filter gains that must be computed in real time even for LTI systems. Seeking to reduce the on-line computational effort, in [130] the authors showed that the gains obtained with a KF depend on the history of combination of measurement availability and proposed a finite history jump linear estimator. Several questions arise from this observation:

Q1 How can we model the effects of network on the data transmission as dropouts, delays and unknown deliverance state?

Q2 How can we design estimation strategies with low implementation cost that adapt their behavior to the network?

Q3 Can we explore the trade-offs between the performance and the complexity of these estimation methods?

Event-based measurement transmissions

With the increasing use of network technologies for process control, researchers have focused recently on the reduction of the network data flow to increase flexibility under the addition of new devices [14, 93]. For instance, sensors can reduce their data transmission employing an event-based sending strategy [85], what furthermore helps to decrease maintenance costs. Then, new promising problems come out:

Q4 Which event-based strategies should be implemented to keep a low sensor computational effort?

Q5 How can we adapt the previous estimation methods to deal with event-based transmissions? How the network-induced problems affect these strategies?

Co-design

In the last two topics we only focused on the design of estimators to work over networks. However network operation efficiency has gained much interest in the last years. As mentioned before, event-based transmissions help to alleviate the data traffic, but as we reduce the available data, we also reduce the estimation performance. In a similar aim, with the growth of wireless networks, a great deal of attention has been focused on reducing the power consumption, where data transmission is the most power expensive task [34]. This shows the existence of a compromise between network resource consumption and estimation performance that make us ask about:

Q6 How can we model the network resource consumption?

Q7 How can we approach both the design of estimation methods and the network use to guarantee a favorable trade-off between estimation performance and network operation efficiency?

1.3 Thesis outline and Contributions

The main goal of this thesis is to develop techniques to design estimators and fault diagnosers to work under diverse network scenarios, as well as to derive methods to design them together with the network use.

The current thesis follows a reasonable base line. First, we model some network scenarios (Chapter 2). Second, we address the estimation problem (Chapter 3, 4, 5 and 6). Third, we deal with the fault diagnosis problem that can be seen as the estimation problem of an unknown input signal (Chapter 7 and 8). Co-design strategies are included in some chapters (Chapter 4 and 6). Finally we draw conclusions and give some directions for future works (Chapter 9). Details on preexisting theory used to develop the results on this thesis is collected in the appendixes.

Note that each chapter is self-consistent and can be mostly read independently of the others. Let us now introduce an extended summary of the thesis with references to the publications related to each chapter.

Chapter 2: Background

This chapter aims to give a common framework for the studied problems. We first give further details on network control systems. We then study different kinds of networks and derive models to describe the effects of the network on the data transmission. More specifically, we analyze a multi-hop network with fading channels. After that, we introduce an event-based sending mechanism and discuss its choice. Finally, we present the estimation and fault diagnosis problems, as well as the co-design, and give some discussion on the main contributions.

Chapter 3: Jump state estimation with multiple sensors with packet dropping and delaying channels

In this chapter we address questions **Q1**-**Q3**. We deal with the estimator design for systems whose outputs are measured through a communication network. The samples from each sensor node are assumed to arrive randomly on time, scarcely and with a time-varying delay. We model the plant and the network sample scenarios such as we cover the cases of multiple sensors, out-of-sequence measurements, buffered measurements on a single packet and multi-rate sensor measurement samples. We derive jump estimators that select a different gain depending on the number of time instants elapsed between successfully received samples and on the available data. A finite set of gains is precalculated off-line with a tractable optimization problem, where the complexity of the estimator implementation is a design parameter. The computational effort of the estimator implementation is much lower than in the KF, whilst the performance is similar. Numerical examples are provided to illustrate the effectiveness of the theory in the chapter.

The results of this chapter were mainly addressed in:

- D. Dolz, I. Peñarrocha, and R. Sanchis. Jump state estimation with multiple sensors with packet dropping and delaying channels. *International Journal of Systems Science*, pages 1–12, 2014

- D. Dolz, I. Peñarrocha, and R. Sanchis. Estrategias de control y estimacion robustas para sistemas de control en red. In *XI Simposio CEA de ingeniería de control*, pages 67–73, 2013

- I. Peñarrocha, D. Dolz, and R. Sanchis. Estimación óptima en redes de sensores con pérdida de datos aleatoria y retardos variantes. In *XXXII Jornadas de Automática*, 2011

Chapter 4: Co-design of jump estimators for wireless multi-hop networks with fading channels

In this chapter we address questions **Q1**-**Q3** and **Q4**-**Q5**. We study transmission power budget minimization of battery-powered nodes in the remote state estimation problem over multi-hop wireless networks. Measurement samples from distributed sensors may hop through several relay nodes until arriving to the estimator node. Passing through a relay introduces an additional unitary delay in the end-to-end transmission. Communication links between nodes are subject to block-fading generating random dropouts. Motivated by offering low computational implementation cost estimators, we propose a jump estimator whose modes depend on the measurement sample transmission outcome over a finite interval. We also give some necessary estimator existence conditions on the network behavior. Transmission power helps to increase the reliability of transmissions at the expense of reducing the lifetime of the node batteries. Motivated by reducing the power budget, we also address the design of power control laws of the form of parametric functions that may depend on the fading channel gain values. We derive an iterative tractable procedure based on semi-definite programming problems to design the precalculated finite set of estimator gains and the power control law parameters to minimize the power budget while guaranteeing a certain estimation performance. This procedure allows us to trade the complexity of the estimator implementation for achieved performance and power budget. Numerical examples are provided to illustrate the effectiveness of the theory in the chapter.

The results of this chapter were mainly addressed in:

- D. Dolz, D. E. Quevedo, I. Peñarrocha, A. S. Leong, and R. Sanchis. Co-design of Markovian jump estimators for wireless multi-hop networks with fading channels. *To be submitted for journal publication*, 2014

- D. Dolz, D. E. Quevedo, I. Peñarrocha, and R. Sanchis. Performance vs complexity trade-offs for markovian networked jump estimators. In *19th World Congress of The International Federation of Automatic Control*, pages 7412–7417, 2014

Chapter 5: Polynomial observers in networked control systems with unknown packet dropout rate.

In this chapter we address questions **Q1**-**Q3**. We study the observer design for systems operating over communication networks with previously unknown packet arrival rate (PAR). We assume that the PAR is time-varying and that can be estimated on-line by means of the acknowledgement on new data arrival. The observer gains depend on the estimated PAR and are designed by minimizing the H_∞ norm from disturbances and measurement noises to estimation error over all the possible PARs. The observer gains

are rational functions of the estimated PAR. Exploiting sum-of-squares decomposition techniques, the design procedure becomes an optimization problem over polynomials. Numerical examples are provided to illustrate the effectiveness of the theory in the chapter.

The results of this chapter were mainly addressed in:

- I. Peñarrocha, D. Dolz, and R. Sanchis. A polynomial approach for observer design in networked control systems with unknown packet dropout rate. In *52nd IEEE Conference on Decision and Control*, pages 5933–5938, 2013

Chapter 6: Co-design of H-infinity jump observers for event-based measurements over networks

In this chapter we address questions **Q4-Q7**. We present a strategy to minimize the network usage and the energy consumption of wireless battery-powered sensors in the observer problem over networks. The sensor nodes implement a periodic Send-on-Delta (SOD) approach, sending a new measurement sample when it deviates considerably from the previous sent one. The estimator node implements a jump observer whose gains are computed off-line and depend on the combination of available new measurement samples, leading to few computational resources in both the estimator and sensor nodes. We bound the estimator performance as a function of the sending policies and then state the design procedure of the observer under fixed sending thresholds as a semi-definite programming problem. We then bound the network usage and obtain an iterative procedure for the design of the policy for message sending, guaranteeing a prescribed estimation performance. Numerical examples are provided to illustrate the effectiveness of the theory in the chapter.

The results of this chapter were mainly addressed in:

- I. Peñarrocha, D. Dolz, J. A. Romero, and R. Sanchis. Co-design of H-infinity jump observers for event-based measurements over networks. *Submitted for journal publication*, may 2014

- I. Peñarrocha, D. Dolz, J. A. Romero, and R. Sanchis. Codesign strategy of inferential controllers for wireless sensor networks. In *4th International Congress on Ultra Modern Telecommunications and Control Systems and Workshops*, pages 28–33, 2012

- I. Peñarrocha, D. Dolz, J. Romero, and R. Sanchis. State estimation and Send on Delta strategy codesign for networked control systems. In *9th International Conference on Informatics in Control, Automation and Robotics*, pages 499–504, 2012

- I. Peñarrocha, D. Dolz, J. A. Romero, and R. Sanchis. Estrategia de codiseño de controladores inferenciales para su implementación mediante sensores inalámbricos. In *XXXIII Jornadas de Automática*, pages 361–367, 2012

Chapter 7: Performance trade-offs for networked jump observer-based fault diagnosis

In this chapter we address questions **Q1-Q3**. We study the fault diagnosis problem for discrete-time multi-sensor networked control systems under dropouts. We use the

measurement sample outcomes to model the sample reception scenarios. Based on this, we propose the use of a jump observer to diagnose multiple faults. We model the faults as slow time-varying signals and introduce this dynamic in the observer to estimate the faults and to generate a residual. The fault detection is assured by comparing the residual signal with a prescribed threshold. We design the jump observer, the residual and the threshold to attain disturbance attenuation, fault tracking and detection conditions and a given false alarm rate. The false alarm rate is upper bounded by means of Markov's inequality. We explore the trade-offs between the minimum detectable faults, the false alarm rate and the dynamic of the fault diagnoser. By imposing the disturbances and measurement noises to be Gaussian, we tighten the false alarm rate bound which improves the time needed to detect a fault. Numerical examples are provided to illustrate the effectiveness of the theory in the chapter.

The results of this chapter were mainly addressed in:

- D. Dolz, I. Peñarrocha, and R. Sanchis. Performance trade-offs for networked jump observer-based fault diagnosis. *Submitted for journal publication*, may and november 2014

- D. Dolz, I. Peñarrocha, and R. Sanchis. Accurate fault diagnosis in sensor networks with markovian transmission dropouts. *Submitted for journal publication*, september 2014

Chapter 8: Networked gain-scheduled fault diagnosis under control input dropouts without data delivery acknowledgement

In this chapter we address questions **Q1**-**Q3**. We investigate the fault diagnosis problem for discrete-time networked control systems under dropouts in both control and sensing channel with no delivery acknowledgment. We propose to use an observer-based fault diagnoser collocated with the controller. The observer estimates the faults and computes a residual signal whose comparison with a threshold alarms the fault appearance. We employ the expected value of the arriving control input for the open loop estimation and the measurement sample reception scenario for the correction with a jump observer. The jumping gains are scheduled in real time with rational functions depending on a statistic of the difference between the control command being applied in the plant and the one being used in the observer. We design the observer, the residual and the threshold to maximize the sensitivity under faults while guaranteeing some minimum detectable faults under a predefined false alarm rate. Exploiting sum-of-squares decomposition techniques, the design procedure becomes an optimization problem over polynomials. Numerical examples are provided to illustrate the effectiveness of the theory in the chapter.

The results of this chapter were mainly addressed in:

- D. Dolz, I. Peñarrocha, and R. Sanchis. Networked gain-scheduled fault diagnosis under control input dropouts without data delivery acknowledgement. *Submitted for journal publication*, july and november 2014

Chapter 9: Conclusions and future work

This last chapter draws conclusions on the current thesis and discusses exciting research problems for further development on a near future.

Contributions by the author

The results presented in this thesis correspond mainly to works developed with the author's supervisors where the author has played a key role. Results in Chapter 4 were also developed in collaboration with D. E. Quevedo and A. S. Leong, while the problematic presented in Chapter 6 was also addressed in collaboration with J. A. Romero.

The author has also collaborated and contributed in other fields of the NCS research area, such as control or estimation of uncertain systems:

- R. P. Aguilera, R. Delgado, D. Dolz, and J. C. Agüero. Quadratic MPC with ℓ_0-input constraint. In *19th World Congress of The International Federation of Automatic Control*, pages 10888–10893, 2014

- I. Peñarrocha, D. Dolz, and R. Sanchis. Inferential networked control with accessibility constraints in both the sensor and actuator channels. *International Journal of Systems Science*, 45(5):1180–1195, 2014

- D. Dolz, D. E. Quevedo, I. Peñarrocha, and R. Sanchis. A jump filter for uncertain dynamic systems with dropouts. In *To appear in 53rd IEEE Conference on Decision and Control*, 2014

These works can be seen as a first approach for future lines of research.

Other contributions of the author during these years on a completely different research area, but that have been helpful to develop new tools adopted in this thesis, are:

- I. Peñarrocha, D. Dolz, N. Aparicio, and R. Sanchis. Synthesis of nonlinear controller for wind turbines stability when providing grid support. *International Journal of Robust Nonlinear Control*, 2013

- D. Dolz, I. Peñarrocha, N. Aparicio, and R. Sanchis. Virtual torque control in wind generation with doubly fed induction generator. In *38th Annual Conference on IEEE Industrial Electronics Society*, pages 2536–2541, 2012

- D. Dolz, I. Peñarrocha, N. Aparicio, and R. Sanchis. Control de aerogeneradores mediante controladores dependientes de la velocidad y turbulencia del viento. In *XXXIII Jornadas de Automática*, pages 443–450, 2012

- I. Peñarrocha, D. Dolz, N. Aparicio, R. Sanchis, R. Vidal, and E. Belenguer. Power analysis in wind generation with doubly fed induction generator with polynomial optimization tools. In *20th Mediterranean Conference on Control & Automation*, pages 1316–1321, 2012

1.4 Abbreviations

A/D	Analog-to-digital converter
CAN	Controller area network
CDF	Cumulative distribution function
D/A	Digital-to-analog converter
DTS	Discrete-time systems
FAR	False alarm rate
FLOP	Floating-point operation
i.i.d.	Independent and identically distributed
KF	Kalman filter
LTI	Linear time-invariant
NCS	Networked control system
PAR	Packet arrival rate
PDF	Probability density function
PDR	Packet dropout rate
PID	Proportional-integral-derivative
SOD	Send-on-Delta
SOS	Sum-of-squares
TCP	Transmission control protocol
TDMA	Time division multiple access
UDP	User datagram protocol
ZOH	Zero order holder

1.5 Notation

$\mathbb{R}$ and $\mathbb{R}_{\geq 0}$	Real and real positive numbers set
$\lvert\mathcal{X}\rvert$	Cardinal of the set $\mathcal{X}$
$x(\tau)$	Continuous-time signal at time τ
$x[t]$, x_t	Discrete-time signal at discrete-time instant t
$x[t_k]$, x_k	Discrete-time signal at sample reception $t = t_k$
$\lVert x\rVert_2$	ℓ_2 norm of x_t over time, $\sqrt{\sum_{t=0}^{\infty} x_t^T x_t}$
$\lVert x_t\rVert_2$	ℓ_2 norm of x_t at instant t, $\sqrt{x_t^T x_t}$
$\lVert x\rVert_{\text{RMS}}$	RMS norm of x_t over time, $\lim_{T\to\infty} \sqrt{\frac{1}{T}\sum_{t=0}^{T-1} x_t^T x_t}$
$\lVert x\rVert_\infty$	ℓ_∞ norm of x_t over time, $\max_t(\max(\lvert x_t\rvert))$
$\lVert x_t\rVert_\infty$	ℓ_∞ norm of x_t at instant t, $\max(\lvert x_t\rvert)$
$\mathbf{E}\{x_t\}$	Expected value of x_t at instant t
$\mathbf{Pr}\{x_t > y\}$	Probability of the event $x_t > y$ at instant t
x^T	Transpose of vector x
$A \bigoplus B$	Block diagonal matrix with A and B on its diagonal
$\text{diag}(A)$	Column vector with the main diagonal of matrix A
$\text{vec}(A)$	Generates a vector by stacking the columns of matrix A.
$\text{vec}^{-1}(x)$	Generates a matrix by reordering the elements of vector x into columns.
$\overline{\lambda}(A)$, $\underline{\lambda}(A)$	Maximum and minimum eigenvalue of A.
$\rho(A)$	Spectral radius of matrix A
$A \prec B$, $A \succ B$	Matrix $A-B$ is negative definite. Matrix $A-B$ is positive definite
$A \preceq B$, $A \succeq B$	Matrix $A-B$ is negative semi-definite. Matrix $A-B$ is positive semi-definite
$\bigvee$	logical "or" operator
$\bigwedge$	logical "and" operator
$\neg$	logical "not" operator
$\lceil\cdot\rceil$	Operator that rounds its argument to the nearest integer towards infinity

Chapter 2

Networked Control Systems

We present a general NCS architecture in Fig. 2.1. Some sensors send some information of a process to a central unit through a network. We call this communication link as the sensing link. This central unit process the acquired information to perform some desired operation (control, estimation, etc.) and send some control inputs, to be applied on the process, to some actuators through a network (which can be different from the one in the sensing link). This communication link is the so-called control link.

In this thesis we consider networks with stochastic events, such as data dropouts and random delays that can be modeled in a probabilistic framework. Such events may happen, for instance, on Ethernet [36, 22] or IEEE 802.15.4 networks (such as Zigbee or WirelessHART) [133, 43] that have been widely used in the industry.

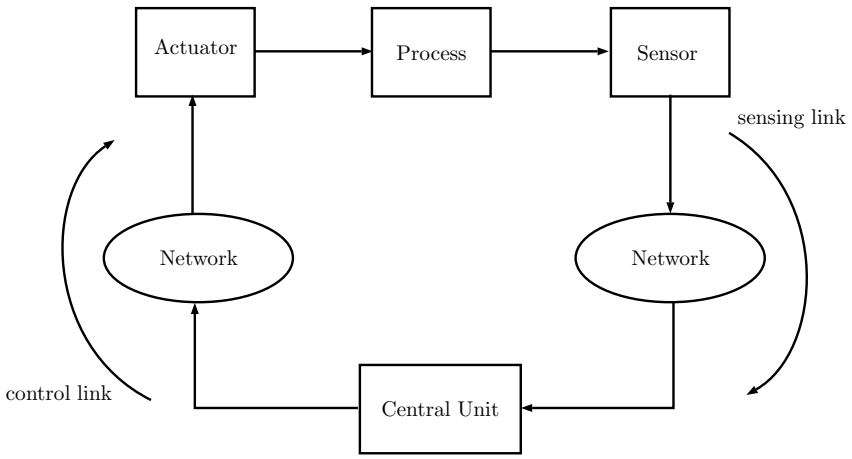

Figure 2.1: Simplified NCS architecture.

This chapter aims to provide a common framework for the problems that will be addressed in the next chapters. First, a full description of the considered types of processes is given. Second, we characterize in general both sensing and control link, and model the influence of possible network-induced problems on the data availability. Moreover, we examine one specific type of network. After that, we present an event-based strategy for sending measurements that allows reducing the network traffic. Finally we discuss the main design problems focused on this thesis and give some hints on the adopted solutions highlighting the differences with related works.

2.1 Process model

Industrial processes can be modeled by continuous-time differential equations that can be linear or nonlinear. In this last case, a linearization around an equilibrium point can be carried out to obtain a linear model. Then, we will consider linear continuous-time processes with several control inputs $u(\tau)$ applied by some actuators and several

controlled outputs $y(\tau)$ that can be measured by some sensors. One way to describe the dynamic of the process is through a state-space representation such as

$$\dot{x}(\tau) = A_c\, x(\tau) + B_c\, u(\tau) + B_{w,c}\, w_c(\tau), \tag{2.1a}$$
$$y(\tau) = C\, x(\tau) \tag{2.1b}$$

where all the signals are continuous-time, being $u(\tau) \in \mathbb{R}^{n_u}$ the input of the process, $y(\tau) \in \mathbb{R}^{n_y}$ the output, $x(\tau) \in \mathbb{R}^n$ the state and $w_c(\tau) \in \mathbb{R}^{n_w}$ the process disturbance. A_c, B_c, $B_{w,c}$ and C are matrices of proper dimensions. Some sensors measure the process outputs and introduce some measurement noise $v(\tau) \in \mathbb{R}^{n_y}$ leading to a continuous-time measurement

$$m(\tau) = C\, x(\tau) + v(\tau). \tag{2.2}$$

Even if the process operates in continuous-time it can only be controlled changing its inputs at discrete intervals. Then, it is convenient to obtain a discretization of the process. If the continuous-time control input signals of the actuators $u(\tau)$ are updated every T seconds through a zero-order holder (ZOH) with the value of each correspondent discrete-time $u[t]$ (see Fig. 2.2) and the sensors measurements $m(\tau)$ are sampled every T seconds (see Fig. 2.3), then, considering that both mechanisms are synchronized, we can obtain an equivalent sampled data model of (2.1) at sampling period T as

$$x[t+1] = A\, x[t] + B\, u[t] + B_w\, w[t], \tag{2.3a}$$
$$m[t] = C\, x[t] + v[t]. \tag{2.3b}$$

where all the signals are discrete-time sampled data signals, being $u[t] = u(tT)$ the control inputs, $m[t] = m(tT)$ the sampled outputs, $x[t] = x(tT)$ the discrete state, $B_w\, w[t] = \int_{tT}^{(t+1)T} e^{A_c(T-\tau)} B_{w,c} w_c(\tau) d\tau$ the equivalent discrete process disturbance and $v[t] = v(tT)$ the sensor measurement noise at time tT. A, B, B_w are matrices of proper dimensions that can be obtained from the matrices of the continuous model by

$$A = e^{A_c T}, \quad B = \int_0^T e^{A_c(T-\tau)} B_c d\tau. \tag{2.4}$$

and $B_w = \int_{tT}^{(t+1)T} e^{A_c(T-\tau)} B_{w,c} d\tau$ if $w_c(\tau)$ is constant. We write each single sample as $m_s[t]$ from sensor $s = 1$ to sensor $s = n_y$ with

$$m_s[t] = c_s\, x[t] + v_s[t] \tag{2.5}$$

where c_s and $v_s[t]$ are the s-th row of C and $v[t]$, respectively. Note that we do not consider quantization errors in the analog-to-digital (A/D) conversion, however we can implicitly include these errors in the measurement noise.

From now on we will only focus on LTI DTS defined by equation (2.3). When possible we will write $x[t]$ as x_t to alleviate notation. Further discussions on process model and discretization can be found in references [42, 2].

2.1.1 Faulty process

Industrial processes are complex systems with many parts that must offer a reliable, safe and efficient operation. However, malfunctions in the process can appear due for

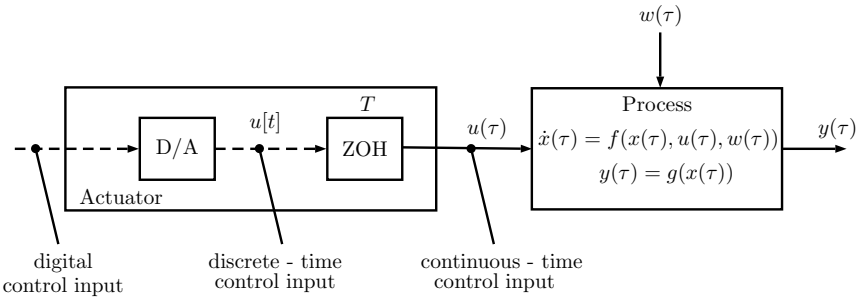

Figure 2.2: Control procedure. Functions $f(\cdot)$ and $g(\cdot)$ refer to the state-space model in (2.1). A solid line denotes continuously transmitted signals while a dashed line denotes a periodically transmitted signal.

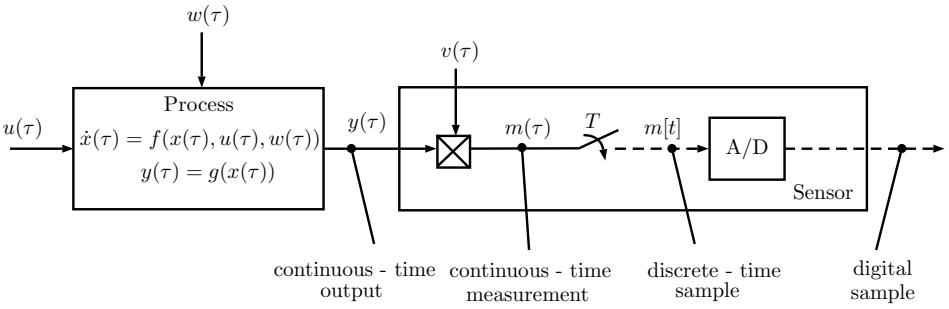

Figure 2.3: Measure procedure. Functions $f(\cdot)$ and $g(\cdot)$ refer to the state-space model in (2.1). A solid line denotes continuously transmitted signals while a dashed line denotes a periodically transmitted signal.

instance to fatigue fracture of some pieces. Moreover, actuators and sensors can also present failures that constraint the process behavior (see Fig. 2.4). One possible way to model a faulty process, is to rewrite the linear discrete-time system (2.3) to include possible faults as additive signals:

$$x[t+1] = A\,x[t] + B\,u[t] + B_w\,w[t] + B_f\,f[t] \tag{2.6a}$$

$$m[t] = C\,x[t] + H\,f[t] + v[t] \tag{2.6b}$$

where $f[t] \in \mathbb{R}^{n_f}$ is the fault vector and B_f and H matrices of appropriate dimensions.

In the current thesis, we model the fault signal as a slow time-varying one (cf. [13, 149]), i.e.,

$$f[t+1] = f[t] + \Delta f[t] \tag{2.7}$$

where $\Delta f[t]$ is the variation of the fault from instant t to $t+1$. Equation (2.7) allows modeling, for instance, step signals ($\Delta f[t]$ only takes a nonzero value at the time the fault appears) or ramp signals ($\Delta f[t]$ takes a constant value), that have been widely used in the literature to analyze the behavior of fault detection algorithms [15, 58].

Remark 2.1. The appearance of faults will be addressed in Chapter 7 and Chapter 8.

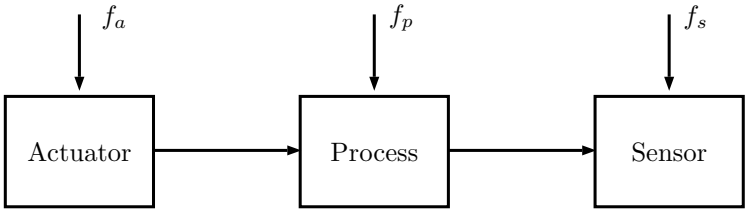

Figure 2.4: Plant model with possible faults on the actuators (f_a), on the process (f_p) and on the sensors (f_s).

2.2 Sensing link

We present a general NCS architecture in Fig. 2.5 that extends the control update and measurement procedure described in Fig. 2.2 and Fig. 2.3. Let us focus on the sensing link in this section.

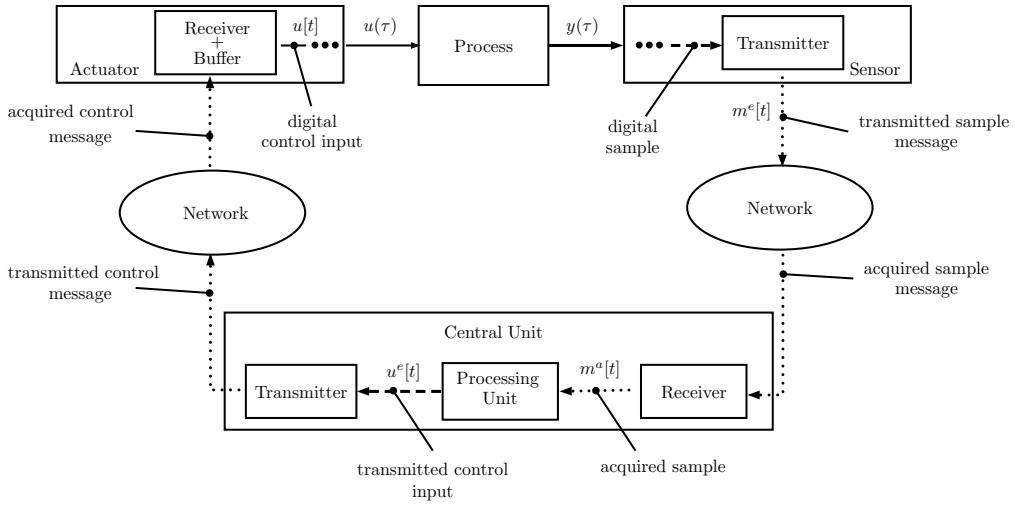

Figure 2.5: NCS detailed architecture. A solid line denotes continuously signals, a dashed line denotes a periodically signals and dotted line denotes sporadic signals.

We assume that all sensors and actuators are synchronized. At each instant of time t, each sensor s encapsulates its measurement sample $m_s[t]$ in a time-tagged packet $m_s^e[t]$ and sends it, independently of the others sensors, to a central unit through an unreliable network that induces time-varying delays and dropouts. We denote by

$$\tau_s[t] \in \mathbb{N} \tag{2.8}$$

the induced delay on the delivery of the t-th sample from sensor s, where $\tau_s[t] = \infty$ represents a sample loss. The induced delay $\tau_s[t]$ is unbounded but we assume that the central unit implements an acceptance protocol. Samples with higher delays than a certain $\bar{d}$ will be discarded. Then, the network induced delay for all sensors can take values in a finite range $\tau[t] \in \{0, 1, \ldots, \bar{d}, \infty\}$.

Remark 2.2. The role of $\bar{d}$ in the estimation problem will be analyzed in depth in Chapter 3. Note that $\bar{d} = 0$ corresponds to the dropout case without delays, i.e., a sample either arrives without delay or is lost (discarded if arrives with some delay).

Current available samples

The available information at instant t at the estimator unit is the pair $(m^a_{s,d}[t], \alpha_{s,d}[t])$ for all $s = 1, \ldots, n_y$ and $d = 0, 1, \ldots, \bar{d}$ being the induced delay, where

$$m^a_{s,d}[t] = \alpha_{s,d}[t]\, m^e_s[t-d], \tag{2.9}$$

and

$$\alpha_{s,d}[t] = \begin{cases} 1 & \text{if } m^e_s[t-d] \text{ is received at instant } t, \\ 0 & \text{otherwise.} \end{cases} \tag{2.10}$$

Note that $\alpha_{s,d}[t] = 1$ represents that the induced delay of the measurement from sensor s sampled at instant $t-d$ is $\tau_s[t-d] = d$. We consider $m^a_{s,d}[t] = 0$ if $m^e_s[t-d]$ does not arrive at instant t.

We model the current available samples, also called as the sampling scenario, at instant t with the reception state of each sample (2.10) by means of the matrix α_t defined as

$$\alpha[t] = \bigoplus_{s=1}^{n_y} \left(\bigoplus_{d=0}^{\bar{d}} \alpha_{s,d}[t] \right), \tag{2.11}$$

where the values of the current acquired samples are in the vector

$$m^a[t] = [m^a_{1,0}[t],\ \ldots,\ m^a_{1,\bar{d}}[t],\ \ldots,\ m^a_{n_y,\bar{d}}[t]]^T. \tag{2.12}$$

The possible values of α_t are within a known finite set

$$\alpha[t] \in \Xi = \{\eta_0, \eta_1, \ldots, \eta_q\}, \tag{2.13}$$

where η_i (for $i = 1, \ldots, q$) denotes each possible available sample combination, being η_0 the scenario without available samples, (i.e., $\eta_0 = 0$). In the general case, any combination of available sensor sample and delay is possible, leading to $q = 2^{\bar{n}_y} - 1$ with $\bar{n}_y = n_y(1+\bar{d})$.

Remark 2.3. This network description will be used in Chapter 3.

Consecutive sample receptions

We call sampling instant, and write it as $t_k = t$, to the instant of some sample reception, i.e., when $\alpha_t \neq 0$. Then, we denote by $N_k = N[t_k]$ the number of instants between two consecutive sample reception, i.e.,

$$N_k = t_k - t_{k-1} \tag{2.14}$$

With that, $N_k - 1$ is the number of consecutive instants without sample reception (consecutive dropouts).

Remark 2.4. This network description will be used in Chapter 3.

Historic available samples

While α_t describes the current sampling scenario (without history), N_k refers to a serie of past events (consecutive losses). Let us now model the sample reception history over a finite interval, which may include the scenarios described by both α_t and N_k.

Let us define vector $\theta_{s,d}[t]$ which represents the transmission outcomes of sample $m_s^e[t-d]$ at instants $\{t-d,\dots,t\}$, i.e.,

$$\theta_{s,d}[t] = \begin{bmatrix}\alpha_{s,0}[t-d] & \alpha_{s,1}[t-d+1] & \cdots & \alpha_{s,d}[t]\end{bmatrix}. \tag{2.15}$$

Considering all the possible sample delays and sensors we can derive vector θ_t, which captures the sample transmission outcomes at times $\{t-\bar{d},\dots,t\}$, as follows:

$$\theta_s[t] = \begin{bmatrix}\theta_{s,0}[t] & \cdots & \theta_{s,\bar{d}}[t]\end{bmatrix}, \tag{2.16a}$$

$$\theta[t] = \begin{bmatrix}\theta_1[t] & \cdots & \theta_{n_y}[t]\end{bmatrix}^T. \tag{2.16b}$$

θ_t is a binary column vector of length $n_\theta = \frac{\bar{n}_y(\bar{d}+2)}{2}$. Note that α_t is the result of applying a surjective function on θ_t that leads to (2.11).

We assume that the central unit will only accept sample $m_s^e[t-d]$ once, i.e., duplicated copies of $m_s^e[t-d]$ with higher delays will be discarded. This implies that $\|\theta_{s,d}[t]\|_1 \leq 1$ with $\|\theta_{s,d}[t]\|_1 = \sum_{\delta=0}^{\bar{d}} \alpha_{s,\delta}[t-d+\delta]$. With that, $\theta[t]$ that can take values in the finite set

$$\theta_t \in \Theta = \{\vartheta_0, \vartheta_1, \dots, \vartheta_r\},\ r = ((\bar{d}+2)!)^{n_y} - 1 \tag{2.17}$$

where ϑ_i (for $i = 0,\dots,r$) denotes each possible combination of the historical measurement transmission outcomes. $\vartheta_0 = 0$ denotes the case where neither of the samples from $t-\bar{d}$ to t is received.

Remark 2.5. Parameter $\bar{d}$ can describe both the presence of induced time-varying delays and the history of sample receptions.

Remark 2.6. The pair (α_k, N_k), at sampling instant $t_k = t$, may represent events that are not included in θ_k. Let us assume some $\bar{d}$ and $N_k = N$. If $\bar{d}+1 < N$ then θ_k do not include the information given by (α_k, N_k). To include it, we can increase $\bar{d}$ at the expense of increasing the elements of the set Θ in (2.17).

Remark 2.7. This network description will be used in Chapter 4.

Packetized samples

What we have presented until now is the case when samples are sent independently from each other. This is sometimes called as the multi-sensor case. Another possibility, which reduces the modeling complexity and the data traffic, is that all the sensors aggregate their samples on a single packet and send it to the central unit. This is known as the packetized case. In this case, considering that the reception state is given by

$$\alpha_d[t] = \begin{cases} 1 & \text{if } m^e[t-] \text{ is received at instant } t, \\ 0 & \text{otherwise.} \end{cases} \tag{2.18}$$

we can easily extend the previous models.

Remark 2.8. This network description will be used in Chapter 5.

Further discussion of these models will be given in later chapters. Let us now present a brief example to illustrate the different defined variables.

Example 2.1

Let us consider a system with one sensor and $\bar{d} = 1$. In this case θ_t and α_t model the reception state of the following samples

$$\theta_t = \begin{bmatrix} m_t \text{ at } t \\ m_{t-1} \text{ at } t-1 \\ m_{[t-1} \text{ at } t \end{bmatrix}, \quad \text{diag}(\alpha_t) = \begin{bmatrix} m_t \text{ at } t \\ m_{t-1} \text{ at } t \end{bmatrix}.$$

Then the sets Θ in (2.17) and Ξ in (2.13) are as follows

$$\Theta = \left\{ \begin{bmatrix}0\\0\\0\end{bmatrix}, \begin{bmatrix}1\\0\\0\end{bmatrix}, \begin{bmatrix}0\\1\\0\end{bmatrix}, \begin{bmatrix}1\\1\\0\end{bmatrix}, \begin{bmatrix}0\\0\\1\end{bmatrix}, \begin{bmatrix}1\\0\\1\end{bmatrix} \right\}$$
$$\Xi = \left\{ \begin{bmatrix}0\\0\end{bmatrix}, \begin{bmatrix}1\\0\end{bmatrix}, \begin{bmatrix}0\\0\end{bmatrix}, \begin{bmatrix}1\\0\end{bmatrix}, \begin{bmatrix}0\\1\end{bmatrix}, \begin{bmatrix}1\\1\end{bmatrix} \right\} = \left\{ \begin{bmatrix}0\\0\end{bmatrix}, \begin{bmatrix}1\\0\end{bmatrix}, \begin{bmatrix}0\\1\end{bmatrix}, \begin{bmatrix}1\\1\end{bmatrix} \right\},$$

where only the diagonal terms of η_i have been represented. Fig. 2.6 illustrates some possible transmission outcomes and the values that θ_t, α_t and N_k would take. For instance, at instant $t+3$ the central unit receive m_{t+1} (with $d = 2$) and m_{t+1} (with $d = 1$), however m_{t+1} is discarded as the maximum allowed delay is $\bar{d} = 1$. In this case, the pair (α_{t+3}, N_{t+3}) describes the fact that central unit receives a sample with a unitary delay after have not being able to acquire any sample in two consecutive time instants. However, with θ_t we can only know that in the last instant nothing was received. To include this case we can increase the maximum considered delay to $\bar{d} = 2$ at the expense of increasing the elements of Θ from 6 to 24. Finally let us remark the differences between t and t_k. As shown in the example, t refers to each instant of time, while t_k is only defined at certain events, when we received some samples.

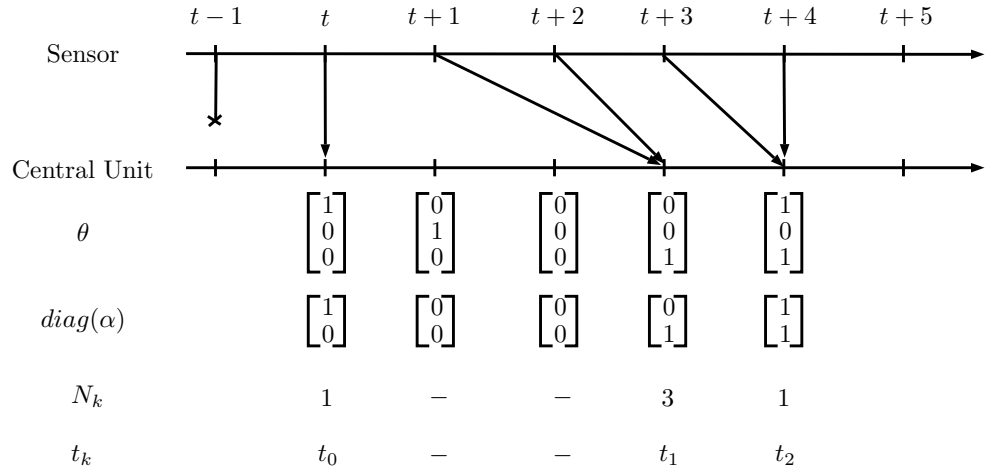

Figure 2.6: Example of received sample scenarios for $n_y = 1$ and $\bar{d} = 1$.

■

2.2.1 Probabilistic framework

There exist different possibilities to characterize the sample transmissions in a probabilistic framework. In the following we present the options used in this thesis.

Node-to-node

Let us first focus on a node-to-node transmission between one sensor and the central unit, which is the most basic communication process. As we remarked in the beginning of the section, we consider networks where dropouts and delays are governed by some stochastic process.

For ease of explanation, let us just consider the dropout case (i.e., when $\bar{d} = 0$). In the vast majority of the networked literature, the probability of receiving a sample is time-invariant, i.e., $\mathbf{Pr}\{\alpha[t] = 1\} = \beta$. From a practical point of view, this probability is computed by implementing an experiment with the common network conditions and then taking the time-average, over a large enough time-window, of the outcomes of $\alpha[t]$, i.e.,

$$\beta = \lim_{T\to\infty} \frac{1}{T} \sum_{t=0}^{T} \alpha[t]. \tag{2.19}$$

This approach meets the probability of receiving a sample at each instant t, i.e. $\mathbf{Pr}\{\alpha[t] = 1\}$, when the dropouts are governed by a stationary stochastic process as the expected value of the reception state variable $\mathbf{E}\{\alpha[t]\} = \beta$ is constant, see Fig. 2.7(a).

This practical approach, which takes the temporal average behavior of the network, is useful to avoid time-varying probabilities that appear when the dropouts are governed by a non-stationary process, i.e. $\mathbf{Pr}\{\alpha[t] = 1\} = \beta[t]$, see Fig. 2.7(b). By the moment, let us study the case of time-invariant probabilities. The time-varying case will be analyzed at the end of this section.

In a network with time-varying delays and dropouts the probability of receiving a given sample with a given delay can be modeled in different ways. We consider the following two alternatives:

- The delays $\tau_s[t]$ are independent and identically distributed (i.i.d.) random variables with

  $$\beta_{s,d} = \mathbf{Pr}\{\tau_s[t] = d\} \tag{2.20}$$

  for $d = 0, \ldots, \bar{d}$ where $\sum_{d=0}^{\bar{d}} \beta_{s,d} \leq 1$. Note that $\mathbf{Pr}\{\alpha_{s,d}[t] = 1\} = \mathbf{Pr}\{\tau_s[t] = d\} = \beta_{s,d}$. Let us denote the tail probabilities by

  $$\bar{\beta}_{s,d} = \mathbf{Pr}\{\tau_s[t] > d\} \tag{2.21}$$

  where $\mathbf{Pr}\{\tau_s[t] > d\} = \mathbf{Pr}\{\|\theta_{s,d}[t]\|_1 = 0\}$.

- The delays $\tau_s[t]$ follow a mutually independent Markovian process with transition probabilities given by

  $$\lambda_{s,i,j} = \mathbf{Pr}\{\tau_s[t+1] = j | \tau_s[t] = i\} \tag{2.22}$$

  for $i, j = 0, \ldots, \bar{d}$.

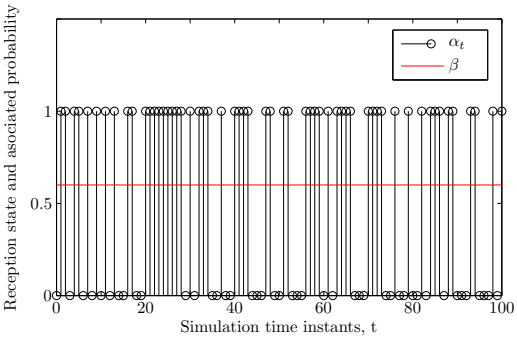

(a) Dropouts governed by a stationary stochastic process with $\mathbf{E}\{\alpha_t\} = \beta = 0.6$.

(b) Dropouts governed by a non-stationary stochastic process with $\mathbf{E}\{\alpha_t\} = \beta_t$ and $\mathbf{E}\{\beta_t\} = \beta$.

Figure 2.7: Node-to-node probability scenarios.

Current available sample and consecutive dropouts, (α_k, N_k)

Let us consider the description on the network given by the pair (α_k, N_k). The probability of having a given sampling scenario at instant t is given by

$$p_i = \mathbf{Pr}\{\alpha_t = \eta_i\}, \tag{2.23}$$

where $\eta_i \in \Xi$ in (2.13). The probability p_0 denotes the probability of having no sample. Once some samples arrive at $t_k = t$ at the central unit, the probability of having $N-1$ consecutive instants without data is given by

$$\mathbf{Pr}\left\{\bigcap_{t=t_k+1}^{t_k+(N-1)} \alpha_t = \eta_0\right\} = p_0^{N-1}. \tag{2.24}$$

For instance, if the arrival of samples from each sensor with a given delay is governed by an i.i.d. process (which implies the independency of each $\alpha_{s,d}[t]$), we compute the probabilities of each sampling scenario as follows. Let us denote by $\vec{\beta} \in \mathbb{R}^{\bar{n}_y}$ the vector containing all the $\beta_{s,d}$ probabilities defined in (2.20) such as

$$\vec{\beta} = \left[\beta_{1,0} \ \ldots \ \beta_{1,\bar{d}} \ \ldots \ \beta_{n_y,0} \ \ldots \ \beta_{n_y,\bar{d}}\right]^T \tag{2.25}$$

where $\vec{\beta}_j$ refers to the j-th row of $\vec{\beta}$. With that, te probability of having no sample available at a given instant is

$$p_0 = \mathbf{Pr}\{\alpha_t = \eta_0\} = \prod_{j=1}^{\bar{n}_y}(1 - \vec{\beta}_j). \tag{2.26}$$

The probability of having some sensors available is $\mathbf{Pr}\{\alpha[t] \in \bar{\Xi}\} = 1 - p_0$, and the probability of having a given combination of available sensors $\eta_i \in \bar{\Xi}$ is

$$p_i = \mathbf{Pr}\{\alpha_t = \eta_i\} = \left(\prod_{\substack{j=1 \\ \forall \eta_{i,j}=0}}^{\bar{n}_m} (1 - \vec{\beta}_j)\right)\left(\prod_{\substack{j=1 \\ \forall \eta_{i,j}=1}}^{\bar{n}_m} \vec{\beta}_j\right), \ i = 1, \ldots, r \tag{2.27}$$

where $\eta_{i,j}$ refers to the j-th diagonal entry of η_i.

Example 2.2

Let us consider a system with one sensor and $\bar{d} = 1$. The probability of having $\alpha_t = \eta_1$ with $\text{diag}(\eta_1) = [1\ \ 0]^T$ can be computed as

$$\mathbf{Pr}\{\alpha_t = \eta_1\} = \mathbf{Pr}\{\alpha_0[t] = 1,\, \alpha_1[t] = 0\} = \beta_0(1 - \beta_1),$$

where we have considered that $\alpha_0[t]$ and $\alpha_1[t]$ are independent. ■

Remark 2.9. This network characterization will be used in Chapter 3.

Historic available samples, θ_t

After describing the probabilistic framework of the pair (α_k, N_k), let us consider now θ_t that, as we mentioned before, may generalize the events described by (α_k, N_k).

The behavior of θ_t can be described by an ergodic[1] Markov chain where the transition probability matrix is $\Lambda = [p_{i,j}]$ with $p_{i,j} = \mathbf{Pr}\{\theta[t+1] = \vartheta_j \big| \theta[t] = \vartheta_i\}$. For instance, if the arrival of samples from each sensor with a given delay is governed by an i.i.d. process, the transition probabilities can be calculated as

$$\mathbf{Pr}\{\theta[t+1] \big| \theta[t]\} = \prod_{s=1}^{n_y} g(t+1, \bar{d}, s)/g(t, \bar{d}-1, s), \tag{2.28}$$

where

$$g(t, \bar{d}, s) = \left(\prod_{\substack{d=0 \\ d:\, \|\theta_{s,d}[t+1]\|_1 = 0}}^{\bar{d}} \bar{\beta}_{s,d} \right) \left(\prod_{\substack{d=0 \\ d:\, \alpha_{s,d}[t+1] = 1}}^{\bar{d}} \beta_{s,d} \right). \tag{2.29}$$

The result from equation (2.28) is only nonzero for feasible transitions. A transition is feasible if $\alpha_{s,d}[t-h]$ have the same value in both $\theta[t]$ and $\theta[t+1]$, for all $s = 1, \ldots, n_y$, $d = 0, \ldots, \bar{d} - 1$ and $h = 0, \ldots, \bar{d} - 1 - d$.

Example 2.3

Let us consider a system with $s = 1$ and $\bar{d} = 1$. The transition probability $\mathbf{Pr}\{\theta[t+1] = \vartheta_1 | \theta[t] = \vartheta_0\}$ of the events illustrated in Fig. 2.8 can be calculated as follows

$$\begin{aligned}
&\mathbf{Pr}\{\tau[t+1] = 0, \tau[t] > 1 | \tau[t] > 0, \tau[t-1] > 1\} = \mathbf{Pr}\{\tau[t+1] = 0, \tau[t] > 1 | \tau[t] > 0\} \\
&\quad = \mathbf{Pr}\{\tau[t+1] = 0\}\, \mathbf{Pr}\{\tau[t] > 1 | \tau[t] > 0\} \\
&\quad = \mathbf{Pr}\{\alpha_0[t+1] = 1\}\, \mathbf{Pr}\Big\{ \|\theta_1[t+1]\|_1 = 0 \Big| \|\theta_0[t]\|_1 = 0 \Big\} \\
&\quad = \mathbf{Pr}\{\alpha_0[t+1] = 1\}\, \mathbf{Pr}\{\|\theta_1[t+1]\|_1 = 0\} / \mathbf{Pr}\{\|\theta_0[t]\|_1 = 0\} = \beta_0 \bar{\beta}_1 / \bar{\beta}_0.
\end{aligned}$$

■

Remark 2.10. This network characterization will be used in Chapter 4.

[1] In an ergordic Markov chain every state can be reached from every state in a finite time.

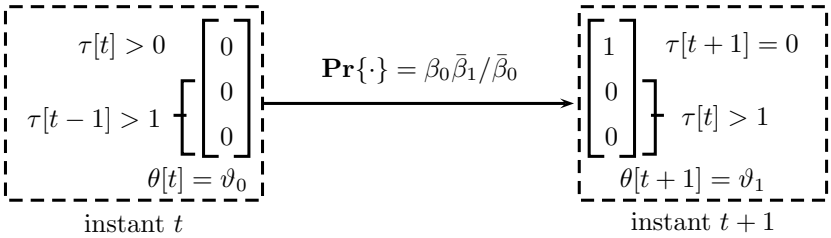

Figure 2.8: Markovian transitions example.

Time-varying probability

In the above descriptions we have considered time-invariant probabilities, either because the stochastic process was stationary or because we have considered the time-average probability (see (2.19)). However, taking into account the possibility of time-varying ones is a novel and challenging problem.

For ease of analysis, let us just focus on the dropout case (with $\bar{d} = 0$) for packetized samples. If the dropouts are governed by a non-stationary stochastic process, then the so called packet arrival rate (PAR) at each instant t is a time dependent probability defined as

$$\beta_t = \mathbf{Pr}\{\alpha_t = 1\}, \tag{2.30}$$

The probability β_t can change on time with a bounded rate of change as

$$\beta_t = \beta_{t-1} + \varepsilon_t, \quad |\varepsilon_t| \leq \bar{\varepsilon}, \tag{2.31}$$

where ε_t is the rate of change and $\bar{\varepsilon}$ its bound.

Moreover, we can go further and consider that the probability is unknown but can be estimated in real time by means of an estimator $\hat{\beta}_t = f_\beta(\hat{\beta}_{t-1}, \alpha_t)$ that makes use of the arrived packets α_t. A simple estimator is the following first order filter

$$\hat{\beta}_t = a\,\hat{\beta}_{t-1} + (1-a)\alpha_t, \tag{2.32}$$

where $0 < a \lesssim 1$ is a tuning parameter that should produce soft variations of $\hat{\beta}_t$, but fast enough to fit the variations of β_t along time. The actual PAR estimation error is defined as

$$\tilde{\beta}_t = \beta_t - \hat{\beta}_t, \tag{2.33}$$

and it is assumed that, as a consequence of the chosen estimator f_β (i.e., the value chosen for a in the case of the first order filter) and of the bound on PAR variations ε_t, the error is bounded by a value $0 < \bar{\mu} < 1$ as

$$|\tilde{\beta}_t| \leq \bar{\mu}. \tag{2.34}$$

Remark 2.11. This kind of network description will be analyzed in Chapter 5.

2.3 Specific sensing link: wireless multi-hop networks with fading channels

In Section 2.2 we have just studied and described the behavior of general networks without entering into details on the network topology. In this section we present a specific wireless network architecture used to transmit measurement samples. More information about wireless networks can be found in [92].

Wireless communication technologies have been considerably upgraded in the last years in terms of reliability and transmission rate [147], which have favored their use for control and estimation purposes [142, 14] instead of wired technologies.

Briefly, transmitter wireless nodes broadcast a signal with some energy trough a wireless digital link. Receiver nodes will acquire the signal if it is strong enough, i.e., if the signal to noise ratio for the digital communication channel is high enough. The strength of the signal can be attenuated due to the phenomenon of fading leading to dropouts. Fading may be due to multi-path propagation or to the presence of obstacles in the path. Using higher transmission power levels alleviates the fading effect leading to lower dropouts. But, transmission is the most power expensive task [34].

Due to the distance between transmitters and receivers or to the presence of obstacles in the path, point-to-point transmissions through wireless fading channels may be highly unlikely or extremely power consuming [92]. In the aim to improve sample delivery and reducing power budget, we will derive a model for multi-hop wireless networks where some nodes (called relays) consciously help to transmit the information from the source to the final destination. These topologies profit from the fact that node data broadcasts are more likely to be acquired from intermediate nodes.

We assume that the multi-hop network topology is given and fixed, i.e. the nodes that comprise the network and the communication links between them are known and fixed. In the interest of simplicity, we assume that nodes work in a half-duplex mode with mutually orthogonal wireless links [92], i.e., simultaneous transmissions on different channels are allowed and there is no interference between nodes. Moreover, we suppose that the nodes access the communication channels with a time division multiple access (TDMA) method using a predefined protocol. Thus, we assume that nodes are time-driven and synchronized.

In this thesis, we consider multi-hop wireless networks that can be described via an acyclic directed graph [7], see Fig. 2.9. This implies the absence of cycles in the network topology. We denote the set of network nodes by $\mathcal{N} = \{N_1, \ldots, N_M, N_{M+1}\}$ being M the number of transmitter nodes, where $\mathcal{S} = \{N_1, \ldots, N_{n_y}\} \subset \mathcal{N}$ corresponds to the sensor nodes set and N_{M+1} to the central unit. The network topology is classified and ordered by node layers depending on the maximum number of hops (longest path) for a sample to arrive to the central unit from each node. We assume that the number of different layers is bounded by $\bar{d}+2$ (which defines the depth of the graph). The set of nodes in the d-layer are denoted by $\mathcal{N}_d \subset \mathcal{N}$ and a node N_a belongs to the d-layer if $N_a \in \mathcal{N}_d$. The 0-layer refers to the central unit, $(\bar{d}+1)$-layer alludes to only sensor nodes and all the other layers may contain relay nodes (intermediate node that helps to retransmits the data) and sensors, see Fig. 2.9. While relay nodes are used to retransmit data, sensors can only send their own samples (this allows keeping sensors simple).

The central unit sends to each node through a reliable channel (without dropouts and delays) their transmission powers when necessary (not necessarily at each instant t). If a node transmission power is not updated the node keeps its previous transmission power.

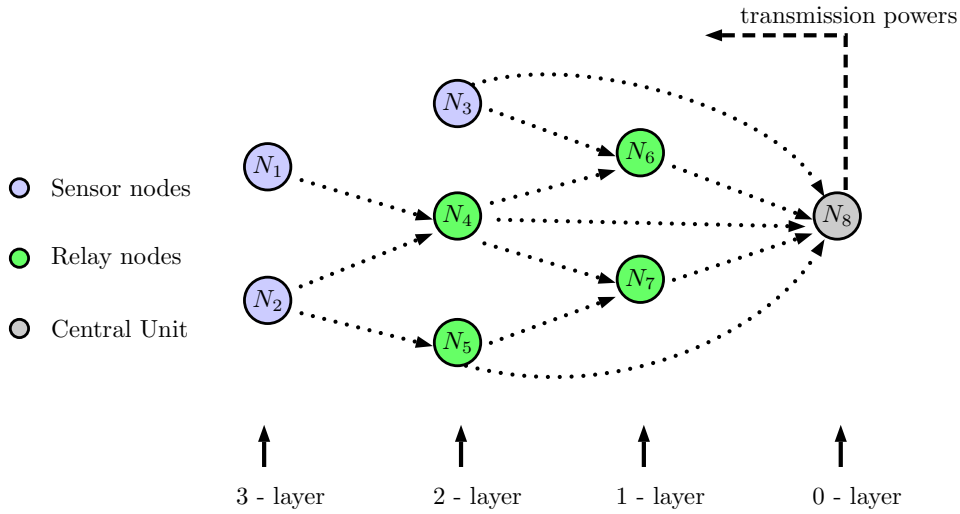

Figure 2.9: Multi-hop wireless network with 8 nodes and 4 layers ($\bar{d} = 2$).

Each node N_a aggregates all its available samples in a single time-stamped packet and broadcasts it with the assigned transmission power, but only some nodes will listen to its transmission. Nodes belonging to the same layer degree or to a higher layer degree than the transmitter node (i.e. between d_1-layer and d_2-layer with $d_2 \geq d_1$) will ignore its transmission. Only nodes with lower layer degree will listen to it (i.e. between nodes in d_1-layer with d_2-layer, with $d_2 < d_1$). With that, a node may receive multiple measurement sample packets from higher layer degree nodes and may forward its information to many lower layer degree nodes. Whenever a relay node has nothing to retransmit it frees its channel. We denote the whole set of wireless links by $\mathcal{I}$.

In the aim of [126, 17], we assume that communicating through each relay introduces an additional unitary delay (equivalent to one sampling period) on the data reception at the next receiver node. Considering this, a sample being transmitted at t by sensor $N_s \in \mathcal{S}$ belonging to the ($\bar{d}$+1)-layer, i.e. $N_s \in \mathcal{N}_{\bar{d}+1}$, may arrive with an end-to-end delay up to $\bar{d}$ depending on the number of intermediate layers it went through.

The central unit will discard measurement samples already received, i.e., only the samples that have hopped with the least number of times will be accepted (smallest delay). Let us denote by $\mathcal{I}_{s,d} = \{\mathcal{I}^1_{s,d}, \ldots, \mathcal{I}^\iota_{s,d}\}$ the ordered set of links for a sample from sensor s to arrive to the central unit with $d + 1$ hops.

Example 2.4

The multi-hop wireless network of Fig. 2.9 has 8 nodes and 3 layers. The depth of the graph is given by $\bar{d} = 2$ and the sensor nodes set is $\mathcal{S} = \{N_1, N_2, N_3\}$. A sample leaving sensor N_2 may hop twice (e.g., through N_5) or three times (e.g., through N_5 and N_7) before arriving to the central unit. The available links for a sample from sensor N_2 to hop twice until reaching the central unit are $\mathcal{I}_{2,1} = \{\{(N_2, N_4), (N_4, N_8)\}, \{(N_2, N_5), (N_5, N_8)\}\}$. If the same sample from sensor N_3 (taken at t) arrives directly to the central unit (at t) and through relay N_6 (at $t + 1$) , this last one will be discarded. ■

2.3.1 Fading channel characterization

In this thesis, we model the fading wireless channels as i.i.d. block fading ones, where the channel gains remain invariant over a block (representing the coherence time of the channel [11]), but may vary i.i.d. from block to block. The channel fading gain can be seen as the attenuation or amplification of the signal transmitted power at the receiver node due to the state of communication link. We denote the channel fading gain associated to the communication link $(N_a, N_l) \in \mathcal{I}$ by $h_{a,l}[t]$. We assume that the value of all the fading channel gains at each instant t are known, which can be attained in practice by means of channel estimation algorithms (see references in [115]), where

$$h_{a,l}[t] \in \Omega_{a,l} \subset \mathbb{R}_{\geq 0}, \quad \Omega_a = \{\Omega_{a,l}, \ldots, \Omega_{a,o}\}, \quad \Omega = \{\Omega_1, \ldots, \Omega_M\} \tag{2.35}$$

with $a, l, o \in \{1, \ldots, M+1\}$ such that $(N_a, N_l) \in \mathcal{I}$ and $(N_a, N_o) \in \mathcal{I}$.

To model the unreliable transmission through the wireless links, we introduce the following binary variable

$$\gamma_{a,l}[t] = \begin{cases} 1 & \text{if node } N_l \text{ receives an error-free packet from node } N_a \text{ at } t, \\ 0 & \text{if packet from node } N_a \text{ received at node } N_l \text{ contains errors at } t. \end{cases} \tag{2.36}$$

Whenever a packet contains errors, it will be rejected. Then, the success probabilities of acquiring a transmitted packet are defined by the state of the communication link $h_{a,l}[t]$ and, with abuse of notation, by the transmission power $u_m[t] \in [0,\, \bar{u}]$ such that

$$\mathbf{Pr}\{\gamma_{a,l}[t] = 1 | h_{a,l}[t] = h,\, u_a[t] = u\} = f_{a,l}(hu) \tag{2.37}$$

where the function $f_{a,l}$ is monotonically increasing and differentiable, and depends on the employed modulation scheme (see [114]).

Remark 2.12. If we consider that the digital communication uses binary phase shift keying (BPSK) transmission [114] with b bits per packet, we have

$$f_{a,l}(hu) = \left(\int_{-\infty}^{\sqrt{hu}} \frac{1}{\sqrt{2\pi}} e^{-k^2/2} \mathrm{d}k \right)^b. \tag{2.38}$$

Note that as the transmission power increases, the successful transmission probability is higher. Moreover, assuming Rayleigh fading, the fading channel gains are exponentially distributed with probability density function (PDF)

$$g_{a,l}(h) = \frac{1}{\bar{h}} e^{-h/\bar{h}},\ h \in \mathbb{R}_{\geq 0}, \tag{2.39}$$

with $\bar{h}$ being its mean.

Let us denote by $H_a[t] \in \Omega_a$ the vector that defines the fading channel gains of the links through which node N_a can transmit at instant t, i.e, $H_a[t] = [h_{a,l}[t] \ \cdots \ h_{a,o}[t]]^T$ with $\{(N_a, N_l), \ldots, (N_a, N_o)\} \subset \mathcal{I}$. Then, the vector containing all the fading gains involved in the communications at instant t is $H[t] = [H_1[t]^T \ \cdots \ H_M[t]^T]^T$ where $H[t] \in \Omega$. We use $\Upsilon_a[t]$ to represent whether node N_a have received any sample at instant t

$$\Upsilon_a[t] = \bigvee_{\forall l\,:\,(N_l, N_a) \in \mathcal{I}} \gamma_{l,a}[t]. \tag{2.40}$$

With that, we denote by $D_a[t]$ the vector containing all the available data characterizing the broadcast of node N_a at instant t, i.e.

$$D_a[t] = [H_a[t]^T \; u_a[t] \; \Upsilon_a[t-1]]^T \tag{2.41}$$

where $D[t] = [D_1[t]^T \; \cdots \; D_M[t]^T]^T$. Taking into account that when node N_a has no available information it does not try to transmit, the probability of acquiring a packet from node N_a at node N_l is

$$\mathbf{Pr}\{\gamma_{a,l}[t] = 1 | D_a[t] = D\} = \begin{cases} f_{a,l}(hu) & \text{if } \Upsilon_a[t-1] = 1, \\ 0 & \text{if } \Upsilon_a[t-1] = 0. \end{cases} \tag{2.42}$$

where Υ_a is always one when the transmitter node is a sensor, i.e., when $N_a \in \mathcal{S}$. When there is nothing to transmit, the transmitted power is considered to be $u_a[t] = 0$. Let us assume that the transmission outcomes from node N_a to node N_l at instant t_1 ($\gamma_{a,l}[t_1]$) and from node N_o to node N_j at instant t_2 ($\gamma_{o,j}[t_2]$) are conditionally independent given $D_a[t_1]$ and $D_o[t_2]$.

Remark 2.13. The sample successful transmission probability depends on the value of fading gain channel when transmitting, which is governed by a stochastic process, see (2.37) and (2.42). Then, this probability may vary over time. However in this thesis, we will adopt the practical point of view and consider that the successful transmission probability between nodes is time-invariant with a value given by its expected value, i.e.,

$$\beta_{a,l} = \int_{\Omega_a} g(H_a) \, \mathbf{Pr}\{\gamma_{a,l}[t] = 1 | h_{a,l}[t], \, u_a[t]\} \mathrm{d}H_a \tag{2.43}$$

where

$$g(H_a) = \prod_{\forall l \, : \, (N_a, N_l) \in \mathcal{I}} g_{a,l}(h_{a,l}). \tag{2.44}$$

is the joint PDF of all the fading channel gains of the communication links available for node N_a.

2.3.2 End-to-end transmission

To conclude this section, let us show how the historic available sample description θ_t, introduced in Section 2.2, can be used in this context.

Considering that the number of layers is bounded by $\bar{d} + 2$ (and so the hops), the maximum possible end-to-end delay is $\bar{d}$, which means that the induced delay is $\tau_s[t] \in \{0, 1, \ldots, \bar{d}, \infty\}$. Then $\tau_s[t] > \bar{d}$ (equivalent to $\tau_s[t] = \infty$) means that the sample sent at t is lost. Let us denote by $\Gamma_s(\tau[t])$ the boolean combinations (logical "and", "or" operations) of variables $\gamma_{a,l}[t + d]$ that define the possible paths a sample from sensor N_s sent at t may take to arrive to the central unit with $\tau[t] \in \{0, 1, \ldots, \bar{d}, \infty\}$ delays. Based on $\Gamma_s(\tau[t])$ the next lemma shows how to compute the transition probabilities of θ_t.

Lemma 2.1. *The transition probabilities* $p_{i,j} = \mathbf{Pr}\{\theta_t = \vartheta_j | \theta_{t-1} = \vartheta_i\}$ *of* θ_t *can be computed as*

$$p_{i,j} = \mathbf{Pr}\left\{\varphi(t, \bar{d}) \middle| \varphi(t-1, \bar{d})\right\} \tag{2.45}$$

with

$$\varphi(t,\bar{d}) = \bigwedge_{s=0}^{n_y} \left(\left(\bigwedge_{\substack{d=0 \\ \{d,\delta\}:\, \alpha_{s,\delta}[t-d+\delta]=1}}^{\bar{d}} \bigwedge_{\delta=0}^{d} \Gamma_s(\tau[t-d]=\delta) \right) \bigwedge \left(\bigwedge_{\substack{d=0 \\ d:\, \|\theta_{s,d}[t]\|_1=0}}^{\bar{d}} \Gamma_s(\tau[t-d]>d) \right) \right). \tag{2.46}$$

Proof. From the definition of the binary variable $\alpha_{s,d}[t-d]$ in (2.10) and of vector $\theta[t]$ (see (2.15)-(2.16b)) we know that $\alpha_{s,\delta}[t-d+\delta]=1$ models that $\tau_s[t-d]=\delta$ and that $\|\theta_{s,d}[t]\|_1=0$ states that $\tau_s[t-d]>d$. Then, exploring the whole vector θ_t and taking into account that $\Gamma_s(\tau[t])$ models the state of the links that characterize the end-to-end transmission outcome, one can obtain (2.46). ■

Example 2.5

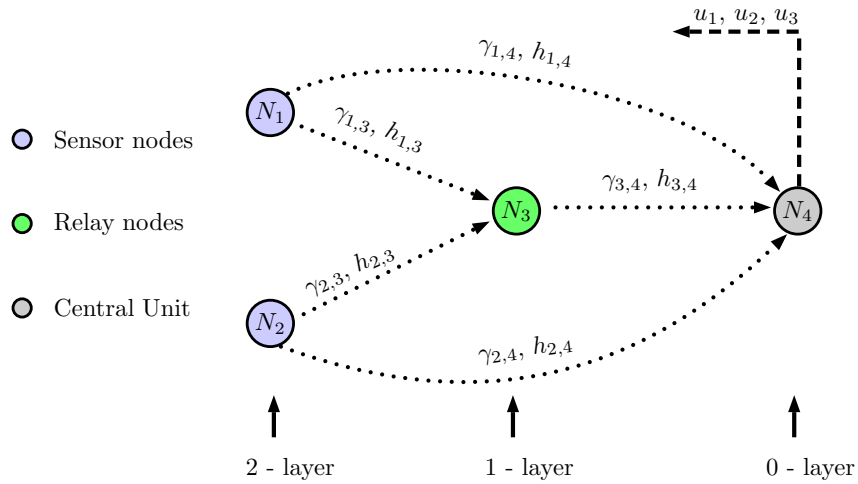

Figure 2.10: Multi-hop wireless network with 4 nodes and 3 layers ($\bar{d}=1$).

Let us consider that the network topology on Fig. 2.10, where $n_y=2$ and $\bar{d}=1$. With that θ_t represents the following reception events:

$$\theta_t = \begin{bmatrix} m_1[t] & \text{at} & t \\ m_1[t-1] & \text{at} & t-1 \\ m_1[t-1] & \text{at} & t \\ m_2[t] & \text{at} & t \\ m_2[t-1] & \text{at} & t-1 \\ m_2[t-1] & \text{at} & t \end{bmatrix},$$

where sample m_1 comes from sensor node N_1 and sample m_2 comes from sensor node N_2. For instance, let us analyze what represents

$$\theta[t-1] = \begin{bmatrix} 1 & 0 & 0 & 0 & 0 & 1 \end{bmatrix}^T$$

in terms of the communication occurrences between the different nodes. In this case, $\theta[t-1]$ models the following:

- $m_1[t-1]$ from sensor node N_1 has been directly acquired by the central unit at $t-1$, which implies $\tau_1[t-1]=0$ and $\gamma_{1,4}[t]=1$.

- $m_1[t-2]$ from sensor node N_1 has not been received neither directly nor through relay node N_3 (sample is lost), which implies $\tau_1[t-2] > 1$. This might have happened because neither N_3 nor N_4 have acquired $m_1[t-2]$ at $t-2$ (which implies $\gamma_{1,4}[t-2]=0$ and $\gamma_{1,3}[t-2]=0$) or because communication through N_3 has failed at instant $t-1$ (which implies $\gamma_{1,4}[t-2]=0$, $\gamma_{1,3}[t-2]=1$ and $\gamma_{3,4}[t-1]=0$).

- $m_2[t-1]$ from sensor node N_2 has not has not been received yet, which implies $\tau_2[t-1]>0$. This means that direct communication has failed, $\gamma_{2,4}[t-1]=0$, and the sample may arrive or not at t.

- $m_2[t-2]$ from sensor node N_2 has only arrived through relay node N_3 at $t-1$ (direct communication with the central unit failed at $t-2$), which implies $\tau_2[t-1]=1$, $\gamma_{2,4}[t-2]=0$, $\gamma_{2,3}[t-2]=1$ and $\gamma_{3,4}[t-1]=1$.

Considering that $\gamma_{a,l}[t]$ denotes $\gamma_{a,l}[t]=1$ while $\neg\gamma_{a,l}[t]=0$, Table 2.1 extends the above comments and shows the different possible node to node transmission scenarios (outcomes of $\gamma_{a,l}$) causing the delayed state of a sample sent from sensor node N_s sent at instant t, $\Gamma_s(\tau[t])$.

To conclude the example let us show how to compute the transition probability between the states

$$\theta[t-1]=\begin{bmatrix}1 & 0 & 0 & 0 & 0 & 1\end{bmatrix}^T, \text{ and } \theta[t]=\begin{bmatrix}0 & 1 & 0 & 1 & 0 & 1\end{bmatrix}^T.$$

In this case $\theta[t]$ models the reception scenario where

$$(\tau_1[t]>0)\wedge(\tau_1[t-1]=0)\wedge(\tau_2[t]=0)\wedge(\tau_2[t-1]=1).$$

Applying the definition of conditional probability, expression (2.45) leads to

$$\mathbf{Pr}\{\theta[t]|\theta[t-1]\}=\frac{\mathbf{Pr}\{\varphi(t,1)\wedge\varphi(t-1,1)\}}{\mathbf{Pr}\{\varphi(t-1,1)\}}$$

where

$$\begin{aligned}\varphi(t,1)\wedge\varphi(t-1,1)=&\neg\gamma_{1,4}[t]\wedge\gamma_{1,4}[t-1]\wedge\gamma_{2,4}[t]\wedge\neg\gamma_{2,4}[t-1]\wedge\gamma_{2,3}[t-1]\wedge\gamma_{3,4}[t]\wedge\\&\neg\gamma_{1,4}[t-2]\wedge\neg\gamma_{1,3}[t-2]\wedge\neg\gamma_{2,4}[t-2]\wedge\gamma_{2,3}[t-2]\wedge\gamma_{3,4}[t-1],\\\varphi(t-1,1)=&\gamma_{1,4}[t-1]\wedge\neg\gamma_{1,4}[t-2]\wedge\neg\gamma_{1,3}[t-2]\wedge\neg\gamma_{2,4}[t-1]\wedge\neg\gamma_{2,4}[t-2]\wedge\\&\gamma_{2,3}[t-2]\wedge\gamma_{3,4}[t-1].\end{aligned}$$

Finally using (2.42) and (2.43), we get

$$\mathbf{Pr}\{\theta[t]|\theta[t-1]\}=(1-\beta_{1,4})\,\beta_{2,4}\,\beta_{2,3}\,\beta_{3,4}.$$

■

Remark 2.14. This kind of network will be employed in Chapter 4.

Table 2.1: End-to-end transmissions for Fig. 2.10

Case	From sensor node N_1	From sensor node N_2
$\Gamma_s(\tau[t]=0)$	$\gamma_{1,4}[t]$	$\gamma_{2,4}[t]$
$\Gamma_s(\tau[t]=1)$	$\neg\gamma_{1,4}[t] \wedge \gamma_{1,3}[t] \wedge \gamma_{3,4}[t+1]$	$\neg\gamma_{2,4}[t] \wedge \gamma_{2,3}[t] \wedge \gamma_{3,4}[t+1]$
$\Gamma_s(\tau[t]>0)$	$\neg\gamma_{1,4}[t]$	$\neg\gamma_{2,4}[t]$
$\Gamma_s(\tau[t]>1)$	$(\neg\gamma_{1,4}[t] \wedge \neg\gamma_{1,3}[t]) \vee (\neg\gamma_{1,4}[t] \wedge \gamma_{1,3}[t] \wedge \neg\gamma_{3,4}[t+1])$	$(\neg\gamma_{2,4}[t] \wedge \neg\gamma_{2,3}[t]) \vee (\neg\gamma_{2,4}[t] \wedge \gamma_{2,3}[t] \wedge \neg\gamma_{3,4}[t+1])$

2.4 Control link

Let us now turn our attention to the control link illustrated in Fig. 2.5. Let us describe the considered control input update. At each instant $t-1$, the controller sends to the actuators (through the network) a single packet with all the control inputs to be used at instant t[2]. We denote with u_t^e the control input transmitted from the controller (at $t-1$) to be applied at instant t. We will only consider the dropout case and then, we model the control input reception at instant $t-1$ with

$$\gamma_{t-1}^u = \begin{cases} 1 & \text{if } u_t^e \text{ is received at instant } t-1, \\ 0 & \text{if } u_t^e \text{ is lost.} \end{cases} \tag{2.47}$$

Each actuator implements a ZOH strategy (see Fig. 2.2) , i.e.,

$$u_t = \begin{cases} u_t^e & \text{if } \gamma_{t-1}^u = 1 \\ u_{t-1} & \text{otherwise.} \end{cases} \tag{2.48}$$

With this control input update procedure, in this thesis we consider two cases depending on whether there exist a control reception acknowledgement.

TCP-like networks

TCP-like networks provide to the central unit a delivery acknowledgment on the control input transmission, and therefore the central unit knows which are the control inputs being applied on the process at each instant of time. This is the most frequently considered case in the works on estimation and fault diagnosis over networks.

UDP-like networks

When the communication network implements an UDP protocol (motivated by reducing the network resource consumption, e.g., power and bandwidth) there is no acknowledgement of successful delivery and we ignore at the central unit the exact value of the control input being applied at each instant. Here, we will assume that the probability of being applying at instant t the control input transmitted at $t-\tau-1$ is known, i.e.

$$\varphi_\tau = \mathbf{Pr}\{u_t = u_{t-\tau}^e\}, \qquad \tau = 0, \ldots, N_u, \qquad \sum_{\tau=0}^{N_u} \varphi_\tau = 1, \tag{2.49}$$

[2]This control strategy is used to overcome delays up to one instant, see [110].

where N_u denotes the maximum integer number of consecutive packet dropouts from the central unit to the actuators.

Remark 2.15. Let us suppose that the dropouts in the controller to actuator link follow a Markovian process with

$$\begin{aligned}\mathbf{Pr}\{\gamma_t^u = 0|\gamma_{t-1}^u = 0\} &= q_u,\\ \mathbf{Pr}\{\gamma_t^u = 1|\gamma_{t-1}^u = 1\} &= p_u.\end{aligned}$$

If the actuators implement a time-triggered protocol that forces the controller to assure the successful control command transmission when the consecutive number of packet dropout is N_u, then the probabilities in (2.49) can be obtained as

$$\begin{aligned}\varphi_0 &= \frac{1}{p_{0,u}}\,\pi_{1,u},\\ \varphi_\tau &= \frac{1}{p_{0,u}}\,q_u^{\tau-1}\,(1-p_u)\,\pi_{1,u}, \quad \forall \tau > 0\end{aligned}$$

where

$$p_{0,u} = \pi_{1,u} + \sum_{\tau=1}^{N_u} q_u^{\tau-1}\,(1-p_u)\,\pi_{1,u}$$

denotes the tail probability originated by the bounded number of consecutive dropouts N_u. $\pi_{1,u}$ is the probability of updating the control inputs (i.e., $\pi_{1,u} = \mathbf{Pr}\{\gamma_t^u = 1\}$) that can be computed as $\pi_u = \pi_u \Lambda_u$, where $\pi_u = [\pi_{0,u}\ \pi_{1,u}]$ and Λ_u is the associated transition probability matrix of γ_t^u (being $\pi_{0,u} = \mathbf{Pr}\{\gamma_t^u = 0\}$).

The value of the real control input being applied to the system is unknown, but the central unit has acces to its expected value $\mathbf{E}\{u_t\}$. Let us denote $\mathbf{E}\{u_t\}$ by u_t^c where

$$u_t^c = \sum_{d=0}^{N_u} \varphi_d\, u_{t-d}^e. \tag{2.50}$$

With that definition, the control error $\tilde{u}_t = u_t - u_t^c$ can be expressed as

$$\tilde{u}_t = u_t - \sum_{d=0}^{N_u} \varphi_d\, u_{t-d}^e. \tag{2.51}$$

The next lemma characterizes some statistics of $\tilde{u}_t$.

Lemma 2.2. *The control error $\tilde{u}_t$ has the following properties:*

$$\mathbf{E}\{\tilde{u}_t\} = 0, \tag{2.52a}$$

$$\mathbf{E}\{\tilde{u}_t^T \tilde{u}_t\} = \sum_{d=0}^{N_u} \varphi_d \left(u_{t-d}^e - \sum_{d=0}^{N_u} \varphi_d\, u_{t-d}^e\right)^T \left(u_{t-d}^e - \sum_{d=0}^{N_u} \varphi_d\, u_{t-d}^e\right). \tag{2.52b}$$

Proof. The expected value of $\tilde{u}_t$ is zero by definition of u_t^c, see (2.50). The expected value of $\tilde{u}_t^T \tilde{u}_t$ can be expressed as

$$\mathbf{E}\{\tilde{u}_t^T \tilde{u}_t\} = \mathbf{E}\left\{ \left(u_t - \sum_{d=0}^{N_u} \varphi_d \, u_{t-d}^e \right)^T \left(u_t - \sum_{d=0}^{N_u} \varphi_d \, u_{t-d}^e \right) \right\}$$
$$= \sum_{d=0}^{N_u} P\{u_t = u_{t-d}^e\} \, \mathbf{E}\left\{ \left(u_t - \sum_{d=0}^{N_u} \varphi_d \, u_{t-d}^e \right)^T \left(u_t - \sum_{d=0}^{N_u} \varphi_d \, u_{t-d}^e \right) \middle| u_t = u_{t-d}^e \right\}$$

where the total probability law has been applied, proving (2.52b). ■

Remark 2.16. UPD-like networks on the control link will be considered in Chapter 8. The rest of the chapters deal with TCP-like networks.

2.5 Event-based sampling

Data traffic is an important issue in NCS due to the increasing number of processes that are branched to the same communication network. Usually, sensors send their sample periodically (at each sampling instant t) in a time-triggered strategy. However some of this information may be redundant, for instance, when the process is stabilized at a certain point and there is no disturbance. In the aim to reduce sensor transmission we can rather use and event-based strategy where an event triggers the transmission. Moreover, this will also help to increase battery lifetime of wireless sensor nodes. In the work [4] a comparison between periodical and event-based sampling is done. In [67, 77] a survey of different event-based strategies are presented.

In this thesis we focus on the periodical Send-on-Delta (SOD) strategy [90] where the sensor node decides to send a new sample if the current one differs more than a given threshold with respect to the last sent one, see Fig. 2.11. The main motivation to use this approach is to keep the sensors as simple as possible. Other strategies, as the one presented in [49], needs sensors with additional computational capabilities to preprocess the samples, which increase the cost of the sensors.

In the following we describe the SOD strategy. Let us assume that the sensor node s has sent a sample to the central unit through the communication network at instant $t = t_{k_s}$ and we call it $m_{s,k_s}^e = m_s^e[t_{k_i}]$ (where k_s enumerates the sent data from sensor s). Then, a new sample will be sent if the following condition holds

$$|m_s[t] - m_{s,k_s}^e| \geq \Delta_s, \quad \Delta_s > 0, \quad t > t_{k_s} \tag{2.53}$$

where Δ_s is the allowed deviation threshold, see Fig. 2.11. In that case, the sensor sends the $(k_s + 1)$-th measurement, and $m_s^a[t]$ becomes m_{s,k_s+1}^e. If there is no dropout neither delays induced by the network, the s-th component of the acquired samples $m^a[t]$ at the central unit remains constant while there is no new sample from sensor s, i.e.,

$$m_s^a[t] = m_{s,k_s}^e, \qquad t_{k_s} \leq t < t_{k_s+1}.$$

With that, we can reuse the sample state reception variable presented in (2.10) to describe when the central unit receives a new sample as follows

$$\alpha_s[t] = \begin{cases} 1 & \text{if there is a new sample received at instant } t, \\ 0 & \text{otherwise.} \end{cases} \tag{2.54}$$

Note that a higher value of Δ_s will reduce the number of transmitted samples from sensor s.

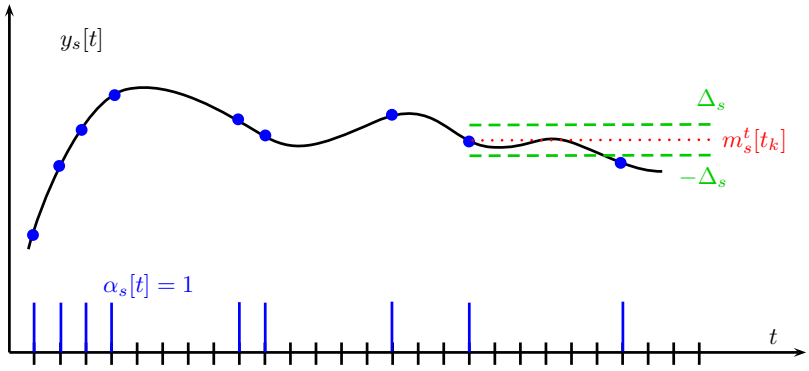

Figure 2.11: Send-on-Delta sampling.

Remark 2.17. SOD sampling will be employed in Chapter 6.

2.6 Estimation over networks

Traditional estimation methods must be adapted to overcome the issues induced by the use of communication networks such as packet dropout, delays or intermittent partial observations when acquiring samples from sensors. For ease of explanation let us focus here on the estimation problem with packetized dropouts. A common Luenberger-type estimation algorithm for this case is given by

$$\hat{x}_{t^-} = A\,\hat{x}_{t-1} + B_u\,u_{t-1}, \tag{2.55a}$$
$$\hat{x}_t = \hat{x}_{t^-} + L_t(m_t^a - \alpha_t\,C\,\hat{x}_{t^-}). \tag{2.55b}$$

At each instant of time t, we run the open loop estimation (2.55a) using the control input being applied at the plant u_{t-1}. When some measurements are available at the central unit $\alpha_t \neq 0$, we update the estimation by means of the updating gain matrix L_t, see (2.55b). Otherwise, we hold the open loop, i.e., $\hat{x}_t = \hat{x}_{t^-}$ (note that m_t^a is zero under dropouts, see (2.9)).

The KF approach is one of the most employed methods to obtain gains L_t [64]. It tackles the state estimation over networks problem updating the estimator gain at each instant of time with the corresponding observation matrix. In [129] the authors provided the following modified optimal KF

$$P_{t^-} = A\,P_t\,A^T + B_w\,W\,B_w^T, \tag{2.56a}$$
$$L_t = P_{t^-}\,C^T\,(C\,P_{t^-}\,C^T + V)^{-1}, \tag{2.56b}$$
$$P_t = (I - \alpha_t\,L_t\,C)\,P_{t^-} \tag{2.56c}$$

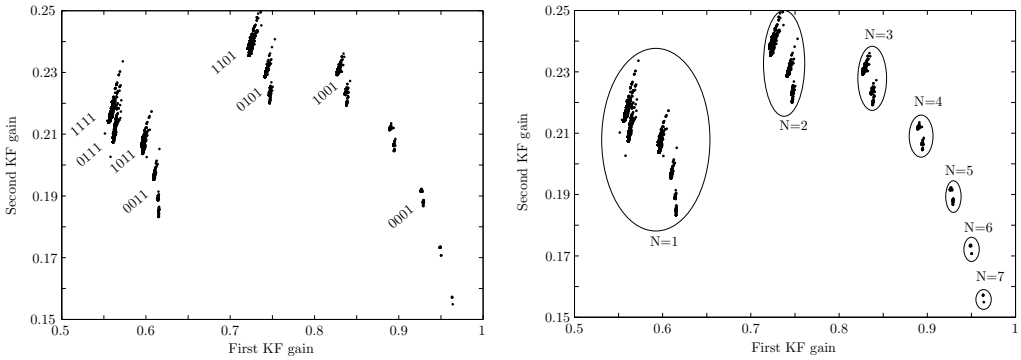

(a) Dependency on the history of transmission outcomes, $[\alpha_{t-3}\ \alpha_{t-2}\ \alpha_{t-1}\ \alpha_t]$.

(b) Dependency on the number of instants between two consecutive sample receptions, N.

Figure 2.12: Components of the updating gains given by the Kalman filter applied to the double integrator system with dropouts presented in [130].

where $W = \mathbf{E}\{w_t w_t^T\}$ and $V = \mathbf{E}\{v_t v_t^T\}$ are the disturbance and measurement noise covariances (or tuning parameters if the covariances are unknown). As we can see, this approach leads to a time varying gain that must be computed on-line even for LTI systems. The on-line computational burden of the KF may be unaffordable for some applications, what motivates the search for computationally low cost alternatives.

Jump estimators

The authors in [130] showed in their motivation example that the gains of the KF depend on the history of combination of samples availability. Based on this observation, they proposed a finite history jump linear estimator with pre-calculated gains that depend on the historical transmission outcomes. The use of pre-calculated gains reduce the on-line computational effort, but increases the estimation error and requires both storage and a mechanism to choose the appropriate gain at each sampling time.

Let us reproduce their motivation example and show the obtained KF gains in Fig. 2.12. As we can see from Fig. 2.12(a), it is obvious that there exists a high correlation between the KF gains and the sample reception history. In this case it extremely depends on the outcomes of the last four reception instants, i.e., on $[\alpha_{t-3}\ \alpha_{t-2}\ \alpha_{t-1}\ \alpha_t]$. Using their approach this would lead to 8 different observer gains. Note that their finite history jump linear estimator is similar to relate the observer gain to our θ_t, defined (2.16b), where in this case $\bar{d}$ defines the considered history.

However, one can observe that there exist other relationships between the KF gains and the sample reception scenario. For instance, as illustrated in Fig. 2.12(b), the gains also depend on the number of instants between two consecutive sample reception N_k (see (2.14)). In this case, relating the observer gains to N_k will lead to 7 different gains (one less than before). It is obvious that as we consider more reception scenarios, and assign a different estimator gain to each of them, we improve the estimation performance. Therefore, is there any set of possible sample reception scenarios that allows reducing the number of stored gains while guaranteeing some estimation performance?

Motivated by reducing the jump linear estimator complexity (in terms of storage

and selection mechanism), in Chapter 3 and Chapter 4 we study the design of a set of estimator gains that gives favorable trade-offs between estimator complexity and estimation performance for different network scenarios with multi-sensor transmission with both time-varying delays and dropouts (in [130] only the packetized case with dropouts were studied). In order to be able to compare the results with the KF we address the estimator design through a covariance-based procedure. Moreover, we also show how the models for the sensing link presented in Section 2.2 can describe other transmission policies used on the networked estimation literature.

Dealing with delayed samples

In the literature there exist mainly two approaches to deal with delayed measurements in the estimation problem with KF methods:

- **Stack solutions:** augment the state and the measurement space with the maximum number of possible delays, e.g. [84, 91], as

$$\bar{x}[t+1] = \bar{A}\,\bar{x}[t] + \bar{B}\,u[t] + \bar{B}_w\,w[t], \tag{2.57a}$$

$$\bar{m}^a[t] = \alpha[t]\left(\bar{C}\,\bar{x}[t] + \bar{v}[t]\right) \tag{2.57b}$$

  where $\bar{x}[t] = \begin{bmatrix} x[t]^T & \cdots & x[t-\bar{d}]^T \end{bmatrix}^T$, $\bar{v}[t] = \begin{bmatrix} \bar{v}_1[t] & \cdots & \bar{v}_{\bar{n}_y}[t] \end{bmatrix}^T$, $\bar{v}_s[t] = \begin{bmatrix} v_s[t] & \cdots & v_s[t-\bar{d}] \end{bmatrix}$ and

$$\bar{A} = \begin{bmatrix} A & 0 & \cdots & 0 \\ I & \cdots & 0 & \vdots \\ \vdots & \ddots & \vdots & \vdots \\ 0 & \cdots & I & 0 \end{bmatrix}, \quad \bar{B} = \begin{bmatrix} B \\ 0 \end{bmatrix}, \quad \bar{B}_w = \begin{bmatrix} B_w \\ 0 \end{bmatrix}, \tag{2.58a}$$

$$\bar{C} = \begin{bmatrix} \bar{c}_1 \\ \vdots \\ \bar{c}_{n_y} \end{bmatrix}, \quad \bar{c}_s = \begin{bmatrix} \bar{c}_{s,0} \\ \vdots \\ \bar{c}_{s,\bar{d}} \end{bmatrix}, \quad \bar{c}_{s,d} = \begin{bmatrix} 0_{1\times n\cdot d} & c_s & 0_{1\times n\cdot(\bar{d}-d)} \end{bmatrix}. \tag{2.58b}$$

  This approach can be seen as incorporating additional fictitious sensors for each actual sensor with a different constant delay and therefore the estimation method (2.56) with the KF in (2.55) can be directly used. However, even if it could be very computationally expensive due to the increased size of the involved matrices, its sparsity can be used to reduce the computational load.

- **Re-compute solutions:** re-compute all the state estimations from the more delayed measurement, e.g. [123, 45]. This approach requieres the inversion of each of the involved KF gains, which could be a very computational consuming task.

Considering the stability of systems with delays, in [52] the authors demonstrateed the equivalence between the Lyapunov-Krasovskii methods and the use of a common Lyapunov function with the stack approach. Motivated by this and in the aim of simplicity, in this thesis, in Chapters 3 and Chapter 4, we adopt the stack solution to design jump estimator over networks with delays.

SOD-based estimators

Following the same research line (relating estimator gains to the sampling scenarios), in Chapter 6 we introduce the SOD mechanism to transmit multi-sensor samples through a network with dropouts and propose a jump linear estimator whose gains are related to the sample reception scenarios. Moreover, we characterize in a probabilistic framework the SOD-based transmission. As we shall see, the probability of having available a new sample turns to be time-varying and a priori unknown, but bounded. Therefore, we design the estimator to guarantee some estimation performances under these circumstances.

Gain-scheduled estimators

In the previous items, sample losses and therefore the different reception scenarios (if samples are transmitted at each instant of time) are due to the unreliability of the communication link where there exists some probability of being able to perform a successful transmission. So, this probability is the fundamental process behind the reception scenarios. In the previous sections, we considered that dropouts were governed by a stationary process that leads to a time-invariant dropout probability. But, what would happen if the PAR, as described in Section 2.2, is time-dependent and we only have access to an estimated value (see (2.32))? Can we relate the estimator gains to the origin of dropouts?

Motivated by adapting the estimator to the changes produced on the network, in Chapter 5 we study the design of estimators where their gains are scheduled in real time with rational functions depending on the estimated PAR.

2.7 Fault diagnosis over networks

Let us first introduce the following definitions borrowed from [15, 58].

- **Fault:** forbidden deviation of at least one characteristic of the system.
- **Fault detection:** to determine the presence of faults with a binary decision and time of detection.
- **Fault isolation:** to determine the kind, location (e.g. sensor or actuator) and time of detection.
- **Fault identification:** to determine the size and time-variant behavior of a fault.
- **Fault diagnosis:** to determine the kind, size, location and time of detection of the fault. Include fault detection, isolation and identification.

The needs for reliability, safety and efficient operation in control systems, make the design of model-based fault diagnosis methods a key issue. In this thesis we focus on observer-based methods. Fault detection when using an observer-based fault detection scheme is addressed by the comparison between a residual signal generated with the estimated system outputs and a threshold. The residual is conceived to balance the robustness against disturbances and the sensitivity to faults. Fault isolation is usually guaranteed by assigning a residual signal to each possible fault that is insensitive to the other faults. Finally, estimating the fault signals leads to fault diagnosis. Further information can be found in [15, 58].

Unlike in the state estimation problem where we know the dynamic of states and have some knowledge about the behavior of the disturbances and measurement noises (e.g., their covariances), in the fault diagnosis problem we aim to estimate a completely unknown input signal. We may want to reliably detect as fast as possible the presence of faults (higher response time to faults) to prevent damages or we may need to estimate accurately the magnitude and time behavior of the fault to decide whether the malfunction is important. Therefore, the performance of a fault diagnosis algorithm can be defined by means of the trade-off between the fault tracking conditions (that includes the minimum detectable fault), the response time to faults and the false alarm rate [57, 55]. Let us define these concepts:

- **Fault tracking conditions:** refers to how accurate the estimated faults follow the real faults.
- **Minimum detectable fault:** refers to the fault that drives the residual to its threshold, provided no other faults, disturbances and measurement noises are present.
- **Response time to faults:** refers to the sensitivity to faults which affects indistinctively the time elapsed between the appearance of a fault and its detection, and the response time of the fault estimation algorithm under faults.
- **False Alarm Rate (FAR):** refers to probability of alarming of the presence of fault when in fact there is no fault.

The ideal fault diagnoser would provide a fast response time to faults (fast detection), a low (or null) FAR and an accurate fault estimation. We can obtain a fast response under faults by increasing the sensitivity of the algorithm. Then, both the residual signal and the estimated fault signal become more aggressive and react faster under faults. However, this reduces the robustness against disturbances leading to an increasing number of false alarms and to more disturbed estimated fault signals (as well as higher minimum detectable faults). Decreasing the sensitivity of the algorithm reduces the false alarm rate and leads to a smooth estimated fault behavior (as well as lower minimum detectable faults). But, this increases the response time to faults.

The use of a network to transmit information enhances the difficulty of meeting the ideal goals and makes more evident the compromise between them. How can we detect faults under measurement sample dropouts? How can we assure a given false alarm rate under the loss? Can we assure the detectability of some desired fault magnitudes? Can we relate explicitly the compromise between these three goals under the network paradigm? How far can we push the fault diagnosis algorithm? These five last questions do not have proper answers on the networked fault diagnosis literature.

In Chapter 7 we show how to adapt the estimator (2.55) to perform fault diagnosis over networks and give an answer to the above questions. Following the research line of the last section, we also relate the estimator gains to the sample reception scenarios.

UDP-like networks

Fault diagnosis is carried out using an extended version of the estimator (2.55) that uses the control input being applied in the process. If the control action is sent through a TCP-like network then the central unit (where the fault diagnosis is performed) knows which are the control inputs being applied to the process. However, if the control link

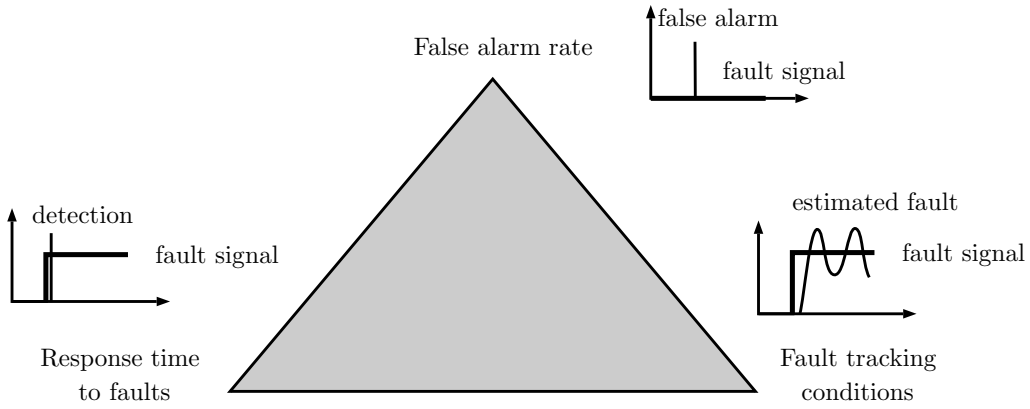

Figure 2.13: Fault diagnosis objectives: response time to faults, false alarm rate and fault tracking conditions.

is given by an UDP-like network, then the central unit ignores the control inputs at the plant and only knows the sent ones, as described in Section 2.4. Then, how this affects the fault diagnosis performance?

In Chapter 8 we extend the results presented in Chapter 7 for the case when the control input is transmitted through an UDP-like network. We use the expected value of the real control input being applied to the system to update the open-loop estimation. In the aim to relate the estimator gains to the network conditions, we propose the use of jumping gains that are scheduled in real time with rational functions depending on a statistic of the difference between the control command being applied in the plant and the one being used in the observer, see (2.52b).

2.8 Co-design

In the last two sections we have presented the estimation and fault diagnosis over networks problem. Let us just focus on the estimation problem. In Section 2.6 the data transmission context was fixed and we gave some hints on the addressed methodologies to overcome the network induced problems. But, what if we can control the data transmission rate?

Saving network resources is a key issue. Reducing the data traffic over a network increases its reliability and favors the inclusion of new devices that share the network. This can be achieved by increasing the threshold Δ_s of the SOD sending mechanism (see Section 2.5) or by assigning lower transmission power levels to the transmitter nodes (see Section 2.3). Moreover, decreasing the number of transmissions helps to increase the battery lifetime of wireless self-powered nodes. However, having less data available at the central unit deteriorates the performance of the estimation methods. These observations arise the following question: would it be possible to design both the transmission mechanisms and the estimators to minimize the network resource consumption while guaranteeing a prescribed estimation performance? This is the so-called co-design problem.

In Chapter 4 we address the co-design problem considering the minimization of the power budget consumed by the wireless nodes, while in Chapter 6 we deal with the

minimization of the sensor transmissions that implements a SOD policy. The approaches presented in these chapters can be adapted to the fault diagnosis problem with not much effort.

Part I

Estimation over networks

Chapter 3

Jump state estimation with multiple sensors with packet dropping and delaying channels

ABSTRACT: *This chapter addresses the estimator design for networked multi-sensor systems. Samples from each sensor node are considered to arrive randomly on time, scarcely and with a time-varying delay. The derived model of the plant and the network sample scenarios covers the cases of: multiple sensors, out-of-sequence measurements, buffered measurements on a single packet and multi-rate sensor measurement samples. We propose jump estimators that select a different gain depending on the number of time instants elapsed between successfully received samples and on the available data. Then, we precalculate a finite set of gains with a tractable optimization problem, where the complexity of the estimator implementation is a design parameter. The computational effort of the estimator implementation is much lower than in the KF, whilst the performance is similar.*

In the last years many processes in industry are controlled or supervised through sensors, actuators and controllers connected to a shared network (wired or wireless), see [44]. The use of a network causes packet dropout, delays or intermittent partial observations when acquiring data from sensors, and the control and estimation through a network must overcome these problems.

The KF tackles the state estimation over networks problem updating the observer gain at each sampling time with the corresponding observation matrix. This approach leads to a time varying gain that must be computed on-line even for linear time invariant systems (e.g. [129, 122, 123]). The computational cost of the on-line implementation is unaffordable for some applications, what motivates the search for computationally low cost alternatives.

The use of precalculated gains reduces the implementation cost in terms of computing capacity, but increases the estimation error and requires both storage and a mechanism to choose the appropriate gain at each sampling time (e.g. [130, 119, 101]). A constant gain approach leads to lower storage requirements but also to lower performance. The jump linear estimator approach [37] improves the estimation with a set of precalculated gains that are used at each sampling time depending on the actual available measurement samples, requiring both storage and the implementation of a selection algorithm. If the set of gains is also a function of the history of sample availabilities (called finite loss history estimator in [130]) a better performance is achieved at the cost of more implementation complexity in the selection of the appropriate gain. An intermediate approach in terms of storage and selector complexity consists of a dependency on the current available samples and on the number of consecutive dropouts since last available sample ([101, 110]).

Computing the gains off-line requires prior knowledge about the network dropout. When the network behaves as a Markov chain, the design uses the transition probabilities ([130]), and when the Markov chain is irreducible and aperiodic (i.e., Bernoulli distribution), the reception probabilities (stationary distribution of the Markov chain) give enough information for design or analysis purposes ([129]). Under unknown statistic information and scarce measurement samples, the maximum possible number of consecutive dropouts, if it is assumed to be bounded, gives useful information for the design ([101]).

In this chapter we propose a jump linear estimator that leads to low cost implementation and acceptable performance for networks with Bernoulli distributions. The gains depend on the combination of actual available measurements and on the number of consecutive time instants without data since the last data arrived. As that number is unbounded for Bernoulli distributions, we propose to use a constant gain when the number of consecutive dropouts exceeds a given threshold, and derive an expression to determine the effect of this threshold on the achievable performance. Furthermore, we propose to reduce the number of stored gains by means of sharing the use of each gain for different combinations of available samples.

The main difference with the work [130] is an important reduction in the number of gains and in the complexity of the gain selection mechanism under scarce measurements, while leading to a similar performance. With respect to work [101], the main differences are that we do not need to assume that the number of consecutive packet dropouts is bounded, and that we do not discard the samples from which the state is not detectable. Other differences with those previous works are the integration of delayed measurements and irregular sampling scenarios as out-of-sequence or buffered measurements, and the proposal of different strategies to reduce the complexity of the observer in order to find a compromise between implementation cost and performance.

The chapter has the following structure: in Section 3.1 we describe the process, present the observer algorithm and derive the estimation error. In Section 3.2 we develop the convex optimization based observer design, and demonstrate the convergence of the estimator. In Section 3.4 we propose some possible grouping scenarios to find a compromise between implementation cost and performance. In Section 3.5 several examples show the validity of the proposal, compared to the KF approach. Finally, the main conclusions are summarized in Section 3.6.

3.1 Problem approach

Let us assume a LTI DTS defined by equations

$$x_{t+1} = A\,x_t + B\,u_t + B_w\,w_t \tag{3.1}$$

where $x \in \mathbb{R}^n$ is the state, $u \in \mathbb{R}^{n_u}$ is the input, and $w \in \mathbb{R}^{n_w}$ is the state disturbance, assumed as a random signals with zero mean and known covariance $\mathbf{E}\{w_t\,w_t^T\} = W$. Throughout this chapter we assume that the control input is causally available at all times (see Fig. 3.1).

Let us assume that samples from several sensors are taken synchronously with the input update but received through a network with packet dropouts and induced time-varying delays. We denote by t_k the instant of sample reception, and define the acquired

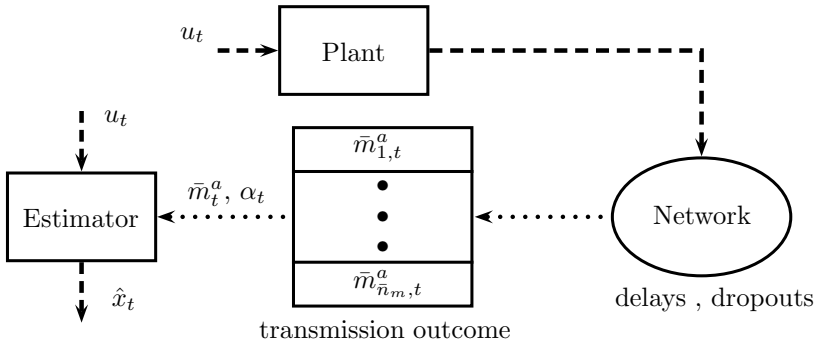

Figure 3.1: Estimation over networks problem.

measurement value by

$$m^a_{s,k} = c_{s,k}[t_k]\, x[t_k - d_{s,k}] + v_{s,k}, \qquad s = 1, \ldots, n_m \tag{3.2}$$

where $m_{s,k}$ represents the k-th measurement sample of sensor s, and $v_{s,k}$ the sensor noise on the k-th sample, assumed an independent random signal with zero mean and known variance $\mathbf{E}\{v^2_{i,k}\} = \sigma^2_i$. We assume synchronization between sensors and the estimator unit and time-tagged message sending, that allows us to know the transmission delay. $d_{s,k} \in \mathbb{N}$ is the network induced delay measured in number of time instants. We introduce an extended order model to avoid running backwards the model when dealing with delayed measurements. We take into account in the model delays up to a value $\bar{d} \in \mathbb{N}$ that must be selected in the estimator design procedure.

Remark 3.1. In the observer to be designed we discard samples with a delay higher than $\bar{d}$. Note that $\bar{d}$ is not a network parameter (the network could have unbounded delays), but an observer design parameter (see Fig.2 in [123]). As $\bar{d}$ may be lower than the bound on the real delays, reducing $\bar{d}$ may decrease the probability of having available samples, but will also reduce the model order and hence, the complexity of the estimator. For a given delay distribution, the selection of $\bar{d}$ is a trade-off between estimator complexity (related to the order) and achievable performance (related to the amount of available data used by the estimator to be designed). Example 3.5.2 illustrates this compromise in the choice of $\bar{d}$.

The model including the delayed states is

$$\bar{x}_{t+1} = \bar{A}\, \bar{x}_t + \bar{B}\, u_t + \bar{B}_w\, w_t, \tag{3.3}$$

where $\bar{x}_{t+1} = \begin{bmatrix} x^T_{t+1} & \cdots & x^T_{t-\bar{d}+1} \end{bmatrix}^T$ and

$$\bar{A} = \begin{bmatrix} A & 0 & \cdots & 0 \\ I & \cdots & 0 & \vdots \\ \vdots & \ddots & \vdots & \vdots \\ 0 & \cdots & I & 0 \end{bmatrix}, \quad \bar{B} = \begin{bmatrix} B \\ 0 \end{bmatrix}, \quad \bar{B}_w = \begin{bmatrix} B_w \\ 0 \end{bmatrix},$$

with the acquired measurement equation

$$m^a_{s,k} = \underbrace{[0_{1\times(n)d_{s,k}}\ c_s\ 0_{1\times(n)(\bar{d}-d_{s,k})}]}_{c_{s,k}}\ \bar{x}_k + v_{s,k}. \tag{3.4}$$

As $c_{s,k}$ can take $\bar{d}+1$ different values (depending on the delay $d_{s,k}$), we enumerate with $j \in [1, n_m(1+\bar{d})]$ each combination of sensor $s = 1, \ldots, n_m$ plus possible delay $d = 0, \ldots, \bar{d}$, and consider each one of those combinations as if they were measurements from different (fictitious) sensors. The enumeration we choose follows the law $j = (s-1)(1+\bar{d}) + (d+1)$, and we express the acquired measurement equations of the fictitious sensors j with a constant output matrix as

$$\bar{m}^a_{j,k} = \bar{c}_j \bar{x}_k + \bar{v}_{j,k}, \quad j = 1, \ldots, \bar{n}_m \tag{3.5}$$

with $\bar{n}_m = n_m(1+\bar{d})$ the number of total (real and fictitious) sensors, and

$$\bar{c}_j = [0_{1\times(n)d}\ c_i\ 0_{1\times(n)(\bar{d}-d)}].$$

This notation allows us to deal with out-of-sequence received measurements, with received packets including measurements from one sensor sampled on different instants (i.e., buffered measurements), and avoids the use of time varying matrices $c_{s,k}$.

We propose the following state estimation algorithm. At each instant t, the model is run in open loop leading to

$$\hat{\bar{x}}^-_t = \bar{A}\,\hat{\bar{x}}_{t-1} + \bar{B}\,u_{t-1}. \tag{3.6}$$

If no measurement sample is received, the best estimation of the system state is the open loop one, i.e., $\hat{\bar{x}}_t = \hat{\bar{x}}^-_t$. If some messages arrive at time $t = t_k$, the state is updated as

$$\hat{\bar{x}}_k = \hat{\bar{x}}^-_k + \sum_{j=1}^{\bar{n}_m} l_{j,k}(\bar{m}^a_{j,k} - c_j \hat{\bar{x}}^-_k), \tag{3.7}$$

where $l_{j,k}$ is the updating gain that applies to the k-th sample of sensor j if available at the estimator node. The design of $l_{j,k}$ is one of the main concerns of this chapter and it will be discussed later in detail.

Let us define the sensor availability factor $\alpha_{j,t}$ of the j-th sensor ($j = 1, \ldots, \bar{n}_m$) for every instant t (similar to (2.10)) as

$$\alpha_{j,t} = \begin{cases} 1 & \text{when } \bar{m}^a_j \text{ is acquired in } t, \\ 0 & \text{otherwise.} \end{cases} \tag{3.8}$$

Let us define the availability matrix (cf. (2.11)) as $\alpha_t = \bigoplus_{j=1}^{\bar{n}_m} \alpha_{j,t}$, that is a binary diagonal matrix with ones only at positions jj such that $\alpha_{j,t} = 1$. Using this matrix, we rewrite the acquired samples at instant t as

$$\bar{m}^a_t = \alpha_t \left(\bar{C}\bar{x}_t + \bar{v}_t\right),$$

with $\bar{m}^a_t = [\bar{m}^a_{1,t}\ \cdots\ \bar{m}^a_{\bar{n}_m,t}]^T$, $\bar{v}_t = [\bar{v}_{1,t}\ \cdots\ \bar{v}_{\bar{n}_m,t}]^T$, where a null value is assumed when a sample is lost, the rows of $\bar{C}$ are $\bar{c}_j$, and where $\bar{v}_t$ is the measurement noise vector with covariance

$$\mathbf{E}\{\bar{v}_t \bar{v}_t^T\} = V = \bigoplus_{i=1}^{n_m} \left(\bigoplus_{j=1}^{1+\bar{d}} \sigma_i^2 \right) \tag{3.9}$$

assuming a non correlated noise. An instant t in which all information from sensors is lost leads to $\alpha_t = 0$. If at a given instant t all the information from each sensor is available, then $\alpha_t = I$ (as we assume delayed sample, this means an arrival of a packet with information of each sensor from $t - \bar{d}$ to t).

With the previous notation, and considering a null value on the unavailable samples, we rewrite the update equation (3.7) as

$$\hat{\bar{x}}_k = \hat{\bar{x}}_{k^-} + L_k \alpha_k (\bar{m}_k - \bar{C} \hat{\bar{x}}_{k^-}), \tag{3.10}$$

where L_k is the updating matrix. Defining the estimation error at the updating instant as $\tilde{x}_k = \bar{x}_k - \hat{\bar{x}}_k$, the estimation error dynamic is

$$\tilde{x}_k = (I - L_k \alpha_k \bar{C}) \left(\bar{A}^{N_k} \tilde{x}_{k-1} + \sum_{i=0}^{N_k - 1} \bar{A}^i \bar{B}_w w[t_{k-1} + i] \right) - L_k \alpha_k \bar{v}_k, \tag{3.11}$$

where N_k denotes the number of consecutive time instants without samples, i.e., $N_k = t_k - t_{k-1}$. To obtain equation (3.11) we firstly run the estimator (3.6) in open loop from t_{k-1} to t_k and apply the update equation (3.10), secondly we run the model (3.3) from t_{k-1} to t_k, and finally we subtract the two results.

Each combination of available samples leads to a different value of matrix $\alpha[t]$ at each instant. These values are within a known set

$$\alpha_t \in \Xi = \{\eta_0, \eta_1, \ldots, \eta_r\}, \tag{3.12}$$

where η_i denotes each possible combination (sampling scenario). In the general case, any combination of available sensor measurements and delays is possible, leading to $r = 2^{\bar{n}_m} - 1$. Matrix η_0 denotes the scenario without available measurements, i.e., $\eta_0 = 0$, and the set of scenarios including some available samples is denoted by $\bar{\Xi} = \Xi \setminus \eta_0 = \{\eta_1, \ldots, \eta_r\}$.

Remark 3.2. In each real application, the set Ξ gathers the possible cases, and becomes a parameter design if the sensors have some processing capabilities. If the sensor nodes collect samples on a buffer of size $\bar{b}$ and transmit the full buffer every instant (as in works [123, 91, 152]), then each η_i will have ones in the positions related to the sensors from which the gathered delayed samples are sent, if they are received for the first time and their associated delay is lower than $\bar{d}$. In the multi-rate approach of [75], each η_i will represent the possible measurement sample combinations in the global time instant.

The probability of each case on Ξ characterizes the network and is the prior knowledge that allows us to make a design with stochastic properties. Let us denote the probability of having a given set of samples at time instant t by

$$p_i = \mathbf{Pr}\{\alpha_t = \eta_i\}, \tag{3.13}$$

where p_0 denotes the probability of having no measurements. Once a packet with data from several sensors arrives at t_k, the probability of having $N - 1$ consecutive instants without data is given by

$$\mathbf{Pr}\left\{ \bigcap_{t=t_k+1}^{t_k+(N-1)} \alpha_t = \eta_0 \right\} = p_0^{N-1}. \tag{3.14}$$

Remark 3.3. If the arrival from each sensor with a given delay is an i.i.d. process (as in [140, 145, 60]), we compute the probabilities of each sampling scenario as follows (see Section 2.2). Let us denote by β_j the probability of a sample from fictitious sensor j being available at a given instant, i.e. $\beta_j = \mathbf{Pr}\{\alpha_{j,t} = 1\}$. The complementary probability of failing on receiving an output sample from sensor j is $\mathbf{Pr}\{\alpha_{j,t} = 0\} = 1 - \beta_j$, and the probability of having no sample available at a given instant is

$$p_0 = \mathbf{Pr}\{\alpha_t = \eta_0\} = \prod_{j=1}^{\bar{n}_m} (1 - \beta_j). \tag{3.15}$$

where we have considered the independency of each $\alpha_{j,t}$. The probability of having some sensors available is $\mathbf{Pr}\{\alpha_t \in \bar{\Xi}\} = 1 - p_0$, and the probability of having a given combination of available sensors $\eta_i \in \bar{\Xi}$ is

$$p_i = \mathbf{Pr}\{\alpha_t = \eta_i\} = \left(\prod_{\substack{j=1 \\ \forall \eta_{i,j}=0}}^{\bar{n}_m} (1 - \beta_j) \right) \left(\prod_{\substack{j=1 \\ \forall \eta_{i,j}=1}}^{\bar{n}_m} \beta_j \right), \; i = 1, \ldots, r \tag{3.16}$$

where $\eta_{i,j}$ refers to the j-th diagonal entry of η_i.

The aim of this chapter is to compute the gain matrices L_k that minimize the state estimation error in the mean square sense requiring low computing and storage capabilities (see Section 3.2). We first differentiate the computational cost of on-line and off-line gains computing, and then differentiate the storage requirements between precomputed gains approaches.

Using a KF [123] leads to a time varying gain L_k whose on-line implementation requires $2\bar{n}^3 + \bar{n}^2 n_w + \bar{n} n_w^2 + 4\bar{n}^2 \bar{n}_m + 2\bar{n}\bar{n}_m^2 + 5\bar{n}_m^3 + 2\bar{n}^2 + \bar{n} n_u + 2\bar{n}\bar{n}_m + \bar{n}_m^2 + 2\bar{n} + \bar{n}_m$ (where $\bar{n} = n(\bar{d}+1)$) floating-point operations (FLOPs) per time instant, leading to high computation requirements and to possible numerical problems due to the inversion of a matrix of at most $\bar{n}_m \times \bar{n}_m$. Using a jump linear estimator with a finite set of stored gains leads to $\bar{n}^2 + \bar{n} n_u + 2\bar{n}\bar{n}_m + 2\bar{n} + \bar{n}_m$ FLOPs per instant, that is much lower than the previous one.

In the motivation example in [130] (which has been further developed in Section 2.6), the authors show that the gains obtained with a KF depend on the history of combination of sensor availability . From this observation they propose a finite history jump linear estimator whose gains depend on $\alpha[t]$, $t = t_k - h, \ldots, t_k$, and chose a history bound h, what requires storing $(2^{\bar{n}_m} - 1)\, 2^{\bar{n}_m (h-1)}$ gains. In that motivation example, the gains depend also strongly on the number of consecutive instants without data between receptions (N_k). From that observation, we propose a jump linear estimation that depends both on N_k and α_k and stores at most $(2^{\bar{n}_m} - 1)\, \bar{N}$ gains, with $\bar{N}$ our history bound that must be chosen as a compromise between observer complexity (number of stored gains) and achievable performance. We define the gains as follow

$$L_k = \begin{cases} L_{N,i} & \text{if } N_k = N < \bar{N} \text{ and } \alpha_k = \eta_i \\ L_{\bar{N},i} & \text{if } N_k \geq \bar{N}, \text{ and } \alpha_k = \eta_i \end{cases} \tag{3.17}$$

for $\alpha_k = \eta_1, \ldots, \eta_r$. The matrices are computed off-line leading to the set of matrices

$$L_k \in \mathcal{L} = \{L_{1,1}, \ldots, L_{1,r}, \ldots, L_{\bar{N},r}\}, \tag{3.18}$$

that will be used to implement the jump linear estimator.

Remark 3.4. In this chapter, N_k is assumed to be unbounded and $\bar{N}$ is a tuning parameter that affects to the number of stored gains, but it is not a parameter that describes the network behaviour. In [120, 101] the nodes are assumed to guarantee somehow that N_k remains below $\bar{N} = \max\{N_k\}$, where $\bar{N}$ defines both the network behavior and the number of stored gains.

3.2 Observer design

In the following theorem we obtain the recursion that defines the evolution of the covariance matrix of the state estimation error. We will use this result later to compute the observer gains.

Theorem 3.1. *Let $P_{k-1} = \mathbf{E}\{\tilde{x}_{k-1}\tilde{x}_{k-1}^T\}$ be the covariance matrix for the state estimation error updated at the sampling instant t_{k-1}. Then, the expected value of the covariance matrix at the measurement instant t_k is given by*

$$\begin{aligned}\mathbf{E}\{P_k\} &= \sum_{N=1}^{\bar{N}-1} p_0^{N-1} \sum_{i=1}^{r} p_i L_{N,i}\,\eta_i V \eta_i^T L_{N,i}^T \\ &+ \frac{p_0^{\bar{N}-1}}{1-p_0} \sum_{i=1}^{r} p_i L_{\bar{N},i}\,\eta_i V \eta_i^T L_{\bar{N},i}^T \\ &+ \sum_{N=1}^{\bar{N}-1} p_0^{N-1} \sum_{i=1}^{r} p_i F_{N,i} \left(\bar{A}^N P_{k-1} (\bar{A}^N)^T + S_{W,N}\right) F_{N,i}^T \\ &+ \sum_{i=1}^{r} p_i F_{\bar{N},i} (p_0^{\bar{N}-1} \bar{A}^{\bar{N}} S_{P,k-1} (\bar{A}^{\bar{N}})^T + \bar{S}_W) F_{\bar{N},i}^T \end{aligned} \tag{3.19}$$

where $S_{P,k-1} = \sum_{i=0}^{\infty} p_0^i \bar{A}^i P_{k-1} (\bar{A}^i)^T$, expressed as

$$S_{P,k-1} = \mathrm{vec}^{-1}\left((I - p_0 \bar{A} \otimes \bar{A})^{-1} \mathrm{vec}(P_{k-1})\right), \tag{3.20}$$

fulfills $S_{P,k-1} - p_0 \bar{A} S_{P,k-1} \bar{A}^T = P_{k-1}$, and

$$F_{N,i} = I - L_{N,i}\,\eta_i \bar{C}, \tag{3.21}$$

$$S_{W,N} = \sum_{j=1}^{N} \bar{A}^{j-1} \bar{B}_w W \bar{B}_w^T (\bar{A}^{j-1})^T, \tag{3.22}$$

$$\bar{S}_W = \frac{p_0^{\bar{N}-1}}{1-p_0} \left(S_{W,\bar{N}} + p_0 \bar{A}^{\bar{N}} S'_{W,\infty} (\bar{A}^{\bar{N}})^T\right), \tag{3.23}$$

$$S'_{W,\infty} = \mathrm{vec}^{-1}\left((I - p_0 \bar{A} \otimes \bar{A})^{-1} \mathrm{vec}(\bar{B}_w W \bar{B}_w^T)\right). \tag{3.24}$$

Proof. See Appendix C.3.1. ■

The previous theorem shows a recursion on the covariance matrix that we write $P_k = \mathfrak{E}\{P_{k-1}\}$, being $\mathfrak{E}\{P_{k-1}\}$ the linear operator that returns the right hand of equation (3.19). In order to compute the observer gains off-line, one must find the stable solution to equation $\mathfrak{E}\{P_{k-1}\} = P_{k-1}$, but the relationship between $S_{P,k-1}$ and P_{k-1}

in (3.20) prevents from using standard Riccati solvers. We compute the set of gains $\mathcal{L}$ solving the optimization problem

$$\begin{aligned} \underset{\mathcal{L},P}{\text{minimize}} \quad & \text{tr}(P) \\ \text{subject to} \quad & \mathfrak{E}\{P\} - P \preceq 0, \end{aligned} \tag{3.25}$$

that allows us to include different constraints on the set of gains to reduce the observer complexity. We present the following numerical solution to this problem based on linear matrix inequalities and bilinear equality constraints that makes it easy to include different constraints over observer gains.

Theorem 3.2. *If there exist matrices P, Q, R and a set of matrices $\mathcal{L} = \{L_{1,1}, L_{1,r}, \ldots, L_{\bar{N},r}\}$ such that*

$$\begin{bmatrix} P & \bar{M}\,\bar{\bar{A}} & \bar{M}\,\bar{W} & \bar{X}\,\bar{V} \\ \bar{\bar{A}}^T\,\bar{M}^T & \bar{Q} & 0 & 0 \\ \bar{W}^T\,\bar{M}^T & 0 & \bar{W} & 0 \\ \bar{V}^T\,\bar{X}^T & 0 & 0 & \bar{V} \end{bmatrix} \succeq 0, \tag{3.26}$$

$$P\,Q = I,\ S_P\,R = I, \tag{3.27}$$

with

$$\begin{aligned} S_P &= \text{vec}^{-1}\left((I - p_0\bar{A}\otimes\bar{A})^{-1}\text{vec}(P)\right), \\ \bar{X} &= [\sqrt{p_1}L_{1,1}\,\eta_1\ \cdots\ \sqrt{p_1}L_{1,r}\,\eta_r\ \cdots\ \sqrt{p_N}L_{\bar{N},r}\,\eta_r], \\ \bar{M} &= [M_1\ \cdots\ M_{\bar{N}}],\ M_N = [\sqrt{p_1}F_{N,1}\ \cdots\ \sqrt{p_r}F_{N,r}], \\ \bar{\bar{A}} &= \bigoplus_{N=1}^{\bar{N}} p_0^{N-1}\left(\bigoplus_{i=1}^{r}\bar{A}^N\right), \\ \bar{W} &= \left(\bigoplus_{N=1}^{\bar{N}-1} p_0^{N-1}\left(\bigoplus_{i=1}^{r} S_{W,N}\right)\right) \oplus \left(\bigoplus_{i=1}^{r}\bar{S}_W\right), \\ \bar{V} &= \left(\bigoplus_{N=1}^{\bar{N}-1} p_o^{N-1}\left(\bigoplus_{i=1}^{r} V\right)\right) \oplus \left(\bigoplus_{i=1}^{r}\frac{p_0^{\bar{N}-1}}{1-p_0}V\right), \\ \bar{Q} &= \left(\bigoplus_{N=1}^{\bar{N}-1} p_o^{N-1}\left(\bigoplus_{i=1}^{r} Q\right)\right) \oplus \left(\bigoplus_{i=1}^{r} p_0^{\bar{N}-1}R\right). \end{aligned}$$

then, recursion $\mathfrak{E}\{\cdot\}$ over P fulfills $\mathfrak{E}\{P\} - P \preceq 0$. Furthermore, the optimization problem

$$\begin{aligned} \underset{\mathcal{L},P}{\textit{minimize}} \quad & \text{tr}(P) \\ \textit{subject to} \quad & (3.26),\ (3.27), \end{aligned} \tag{3.28}$$

is a solution of (3.25).

Proof. Applying extended Schur complements on (3.26) and taking into account (3.27) makes problem (3.25) and (3.28) equivalent.

■

We show next that if we apply the gains $\mathcal{L}$ obtained from problem (3.28), then the sequence $\{P_k\}$ converges to the unique solution P obtained in (3.28).

Theorem 3.3. *Suppose that the set $\mathcal{L}$ in* (3.18) *solves problem* (3.25)*, i.e., exists $\bar{P} \succ 0$ such that $\mathfrak{E}\{\bar{P}\} \preceq \bar{P}$. Then, for any initial condition $P_0 \succeq 0$ the sequence $\{P_k\}$ is bounded, i.e., $\{P_k\} \preceq M_P$.*

Proof. Considering the linear operator on Lemma C.1 (see Appendix C.3), we have $\mathfrak{L}(\bar{P}) \prec \mathfrak{E}\{\bar{P}\} \preceq \bar{P}$. Thus, $\mathfrak{L}$ meets the condition of Lemma C.1. The evolution of P_k is expressed as $P_{k+1} = \mathfrak{E}\{P_k\} = \mathfrak{L}(P_k) + U$. Since U contains the disturbance and noise covariance (both positive definite), then $U \succ 0$, leading that $\{P_k\}$ is bounded.

■

Theorem 3.4. *Suppose that the set $\mathcal{L}$ in* (3.18) *solves problem* (3.25)*. Then, for any initial condition $P_0 \succeq 0$, the iteration $P_{k+1} = \mathfrak{E}\{P_k\}$ converges to the unique positive semi-definite solution $\bar{P}$ obtained in problem* (3.25)*, i.e., $\lim_{k\to\infty} P_k = \lim_{k\to\infty} \mathfrak{E}^k\{P_0\} = \bar{P} \succeq 0$, where $\bar{P} = \mathfrak{E}\{\bar{P}\}$*

Proof. See Appendix C.3.2.

■

Problem (3.25) minimizes the expected value of the state estimation error covariance matrix at the updating instants t_k. However, a more representative measure of the estimation performance is the value of the covariance matrix at each instant t. The following theorem allow us to obtain this value.

Theorem 3.5. *Given $P = \mathbf{E}\{\tilde{x}_k \tilde{x}_k^T\}$, the covariance matrix of the estimation error at each instant t is given by*

$$P_t = \mathbf{E}\{\tilde{x}[t]\tilde{x}[t]^T\} = (1-p_0)P + p_0 \operatorname{vec}^{-1}\left((I - p_0 \bar{A} \otimes \bar{A})^{-1} \operatorname{vec}(S_c)\right) \tag{3.29}$$

where $S_c = \left(\bar{A}\, P\, \bar{A}^T + (1-p_0)^{-1} \bar{B}_w W \bar{B}_w^T\right)$.

Proof. See Appendix C.3.3.

■

Remark 3.5. Matrix $P_t = \mathbf{E}\{\tilde{x}[t]\tilde{x}[t]^T\}$ is a linear combination of $P = \mathbf{E}\{\tilde{x}[t_k]\tilde{x}[t_k]^T\}$. We refer to the right hand of (3.29) as a linear operator $\mathfrak{F}\{\cdot\}$ that applies to P as $P_t = \mathfrak{F}\{P\}$. The set of observer gains $\mathcal{L}$ obtained as the solution of the optimization problem

$$\begin{aligned} \underset{\mathcal{L},P}{\text{minimize}} \quad & \operatorname{tr}(\mathfrak{F}\{P\}) \\ \text{subject to} \quad & (3.26),\ (3.27), \end{aligned} \tag{3.30}$$

minimizes the expected value of the covariance matrix at each instant t (with or without measurement samples).

3.3 Numerical computation

Optimization problem (3.28) is a nonconvex optimization problem because of the terms $Q = P^{-1}$ and $R = S_P^{-1}$. One approach to obtain the solution of this problem is the reformulation as a rank-constrained LMI problem, leading to constraints

$$\operatorname{rank}\left(\begin{bmatrix} S_P - p_0 \bar{A}\, S_P\, \bar{A}^T & I \\ I & Q \end{bmatrix}\right) \leq \bar{n}, \quad \operatorname{rank}\left(\begin{bmatrix} R & I \\ I & S_P \end{bmatrix}\right) \leq \bar{n}.$$

In this chapter, we address the rank-constrained LMI problem (3.28) with a cone complementarity linearization algorithm (CCL) [33], leading to

$$\begin{aligned} &\underset{\mathcal{L},P,Q,S_P,R}{\text{minimize}} \quad \text{tr}(PQ + S_P R) \\ &\text{subject to} \quad (3.26),\ \text{tr}(P) < \gamma,\ \begin{bmatrix} P & I \\ I & Q \end{bmatrix} \succeq 0,\ \begin{bmatrix} S_P & I \\ I & R \end{bmatrix} \succeq 0, \end{aligned} \tag{3.31}$$

where S_P is the matrix defined in (3.20) and γ is a real positive value. Condition $\text{tr}(P) < \gamma$ can be replaced by $\text{tr}(\mathfrak{F}\{P\}) < \gamma$ to minimize the expected value of the covariance matrix at every time instant (see Remark 3.5). We solve the nonlinear minimization problem with a bisection algorithm over the CCL as follows.

Algorithm 3.1. CCL algorithm.

Step 1 Choose a large enough initial γ_u such that there exists a feasible solution to LMI conditions (3.26), (3.31) with $\gamma = \gamma_u$. Set $\gamma_l = 0$, and $\gamma = \frac{1}{2}(\gamma_l + \gamma_u)$.

Step 2 Set $k = 0$ and find a feasible solution set $\left[P^0, Q^0, S_P^0, R^0, \mathcal{L}^0\right]$, satisfying (3.26), (3.31).

Step 3 Solve the following LMI problem for the decision variables P, Q, S_P, R and $\mathcal{L}$:

$$\begin{aligned} &\underset{\mathcal{L},P,Q,S_P,R}{\text{minimize}} \quad \text{tr}(P^k Q + Q^k P + S_P^k R + R^k S_P) \\ &\text{subject to} \quad (3.26),\ (3.31), \\ &\text{set} \qquad\quad k = k+1,\ [P^k, Q^k, S_P^k, R^k] = [P, Q, S_P, R]. \end{aligned}$$

Step 4 If $k < k_{\max}$ for a given prescribed maximum number of iterations $k_{\max}$, and (3.26) is unsatisfied after replacing Q by P^{-1} and R by S_P^{-1}, then return to Step 3. If $k < k_{\max}$ and (3.26) are satisfied, update the upper bound on γ as $\gamma_u = \gamma$, store the actual observer gains $L_{N,i}$, and go to Step 5. If $k = k_{\max}$, update the lower bound on γ as $\gamma_l = \gamma$ and go to Step 5.

Step 5 If $\gamma_u - \gamma_l \geq \delta$, for a given small δ, update γ with $\gamma = \frac{1}{2}(\gamma_l + \gamma_u)$ and go to Step 2. If $\gamma_u - \gamma_l < \delta$ exit with the last stored set of gains $\mathcal{L}$ in Step 4.

■

3.4 Complexity reduction

The solution of the previous section leads to a number of stored matrices equal to $|\mathcal{L}| = \bar{N} \cdot r$, each one used for a different pair (N, η_i). We can reduce the complexity of the observer in terms of storage choosing a small $\bar{N}$ and imposing some equality constraints over the set $\mathcal{L}$ as $L_{N,i} = L_{N,j}$. Problem (3.28) allows to easily include equality constraints over the set $\mathcal{L}$, and the choice of $\bar{N}$ only affects on the construction of the matrices of the LMI problem. Reducing the number of gains also simplifies the numerical burden of (3.28), as the number of decision variables and the size of the matrices are decreased. Sharing gains has also implications on the implementation of the selection mechanism. In the aim of implementing an observer with a simple on-line looking-up-table procedure and low storage, we propose the following preconfigured sets of equalities

over the possible sensor availability combinations. The gain selection mechanism is mainly based on counting the number of available sensors and the number of consecutive instants without data.

- **S1**. The observer gains depend only on the intersample instants, leading to $|\mathcal{L}_{S1}| = \bar{N}$, i.e., $L_{N,i} = L_{N,j}$ for any pair $i \neq j$.
- **S2**. The observer gains depend on the number of real sensors from which samples arrive successfully at an instant, leading to $|\mathcal{L}_{S2}| = n_m \cdot \bar{N}$.
- **S3**. The observer gains depend on the number of real and fictitious sensors from which samples arrive successfully at an instant, leading to $|\mathcal{L}_{S3}| = \bar{n}_m \cdot \bar{N}$.
- **S4**. The observer gains are different depending on the sampling scenario (this is the general case), leading to $|\mathcal{L}_{S4}| = (2^{\bar{n}_m} - 1) \cdot \bar{N}$.

The selection of one of the previous gain grouping alternatives, together with the choice of $\bar{N}$, allows to define a compromise between implementation cost and performance. The lowest cost and worst performance is obtained for S1 and a low value of $\bar{N}$, while the highest cost and best performance corresponds to S4 and a high value of $\bar{N}$. The examples illustrate this idea.

3.5 Examples

3.5.1 Example 1

In this example we analyze the different gain scheduling strategies proposed in Section 3.4, as well as the relationship between number of stored gains and achieved performance. We consider three different state matrices

$$A_1 = \begin{bmatrix} 0.8821 & -0.0351 \\ -0.0351 & 0.7347 \end{bmatrix}, A_2 = \begin{bmatrix} 0.8373 & -0.7207 \\ 0.7207 & 0.8373 \end{bmatrix},$$
$$A_3 = \begin{bmatrix} 1.6684 & 0.3197 \\ -0.1003 & 0.6782 \end{bmatrix},$$

where A_1, A_2, A_3 have real stable, complex conjugate unstable and one unstable eigenvalue, respectively. In the three cases we use

$$B = \begin{bmatrix} -0.3359 \\ 0.3466 \end{bmatrix}, C = \begin{bmatrix} 0.5325 & 0.3987 \\ 0.7258 & 0.3584 \end{bmatrix}$$
$$B_w = \begin{bmatrix} 0.0121 & 0.1347 \\ 0.0112 & 0.0831 \end{bmatrix}.$$

and state disturbance and sensor noises with covariances

$$W = \begin{bmatrix} 0.2632 & -0.0027 \\ -0.0027 & 0.2466 \end{bmatrix}, \begin{bmatrix} \sigma_1^2 \\ \sigma_2^2 \end{bmatrix} = \begin{bmatrix} 0.0086 \\ 0.0079 \end{bmatrix}.$$

The samples are independently acquired through a communication network that induces a delay that varies from 0 to 1 time instans. The amount of fictitious sensors is 4, and the number of possible sampling scenarios is $2^4 = 16$. Table 3.1 details the availability

Table 3.1: Probabilities assignment.

sensor	delay	β_{A_1,A_2}	β_{A_3}
1	0	0.1391	0.3340
1	1	0.1751	0.3064
2	0	0.1397	0.3761
2	1	0.1334	0.3403

probabilities that are assumed for each of the fictitious sensors in each example. They are defined such that the problem (3.30) is feasible.

Let us first analyze the observer performance as a function of the number of stored gain matrices in the set (3.18), according to the scheduling approaches detailed on Section 3.4. Fig. 3.2 shows the dependency of the trace of the expected covariance matrix at time instants t, P_t (3.29), with respect to the number of gain matrices for the four proposed scheduling approaches. We considered different intersample instans $\bar{N} = 1, \ldots, 7$, leading to different number of stored gains (each point in the plot means a given value for $\bar{N}$). For the system with state matrix A_1 (stable with real eigenvalues), increasing the number of observer gains either by increasing $\bar{N}$ or due to the possible scheduling approaches do not improve significantly the performance, because the estimation performance ($\mathrm{tr}(P_t)$) of the constant gain approach (S1) is only a 1.7% worse than the optimal performance (with scheduling S4 and $N \to \infty$, $\mathrm{tr}(P_t^\star)$). In this case, a constant gain approach (S1) would be a good compromise between estimation performance and storage or implementation cost. For the system with state matrix A_2 (unstable with complex eigenvalues), the performance of the estimator can be increased significantly by using $\bar{N} \geq 2$ with respect to $\bar{N} = 1$. The effect of using a more complex approach than S2 (with set S3 or S4) is negligible for the performance, but implies a high number of stored gains. In this case, selecting S2 and $\bar{N} = 2$ (storing only 4 gains) leads to an acceptable compromise solution. For the state matrix A_3 it is better to increase the considered scenarios in the scheduling approach in terms of performance and memory storage, rather than increasing $\bar{N}$. In this case a good compromise could be to select S3 and $\bar{N} = 1$ (storing only 4 gains).

Now, let us compare for the case of state matrix A_3 the results of the implementation of a KF algorithm adapted from [123] and the proposed algorithm (in the cases indicated with a black filled symbol in Fig. 3.2(c)). Table 3.2 shows, for each studied case, the number of needed observer gains, the obtained trace of the covariance matrix for the state estimation error at the time instans t (through simulation) and the computational cost (upper-bound of FLOPs per iteration). The KF gives the best performance but needs almost fifteen times more operations than the proposed algorithm, with a slight improvement in performance. Regarding the proposed approach, it can be noticed that

Table 3.2: Observers comparison for system A_3.

Case	S1	S2	S3	S3	S4	KF
$\lvert\mathcal{L}\rvert$	1	2	4	8	60	-
$\mathrm{tr}(P_t)$	0.1585	0.0781	0.0553	0.0498	0.0451	0.0423
FLOP	64	64	64	64	64	976

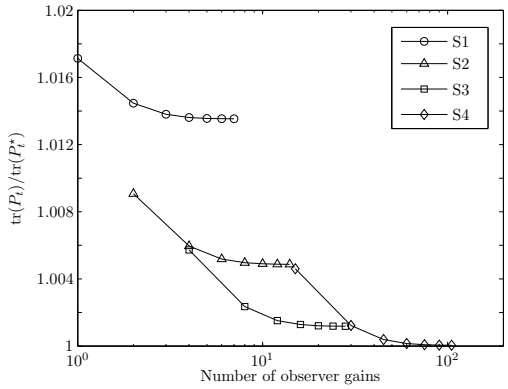

(a) Case of two real stable poles, A_1.

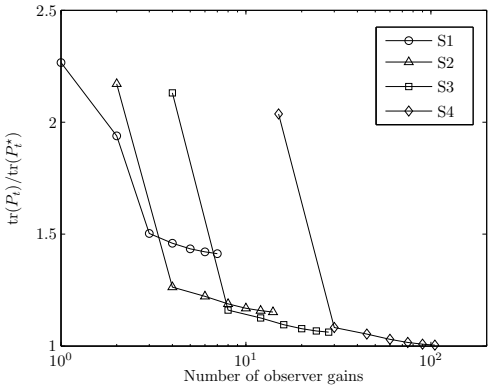

(b) Case of two complex conjugates unstable poles, A_2.

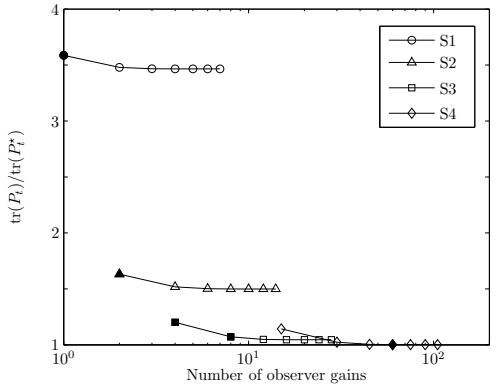

(c) Case of one unstable pole, A_3.

Figure 3.2: Quotient between the trace of the expected value of the estimation error covariance matrix at each time instant $\mathrm{tr}(P_t)$ and the minimum reachable value (with scheduling S4 and $N \to \infty$, $\mathrm{tr}(P_t^\star)$) for different number of observer gains and for different scheduling approaches.

increasing the number of gains improves the performance (getting closer to the Kalman one) but the storage requirement is also increased. Furthermore, the numerical values for $\mathrm{tr}(P_t)$ obtained from simulations (shown in Table 3.2) converge to the optimal values presented graphically in Fig. 3.2(c).

Case S4 with $\bar{N} = 1$ corresponds to the same approach presented in [130] with no history loss. However, adding only one instant of history to improve the estimation performance of [130] implies the use of $15 \cdot 2^{4\cdot(2-1)} = 240$ different gains. Our approach needs to store only 60 gains to achieve a performance, $\mathrm{tr}(P_t)$, just a 6% higher than the one obtained with the KF, and just 8 gains to perform an 18% worse (Table 3.2).

This example shows a compromise between the estimation performance, storage and scheduling complexity. The designer can use this information to decide a maximum

number of observer gains to be stored and then to chose its dependency either on the intersample time instant or on the possible scenarios to minimize the estimation error.

3.5.2 Example 2

This example analyzes the influence of parameter $\bar{d}$ on the estimation performance and on the computational cost. Let us consider the system defined by A_1 and that only samples from the first sensor are available. We assume that the probability of having a sample available from the first sensor with a given delay, i.e $\beta_j = \mathbf{Pr}\{\alpha_j = 1\}, \forall j = 1, \ldots, \infty$, is given by a negative binomial distribution where the probability of success is 0.5 and the number of failures is 3. The assumed probability distribution of the network induced delays is shown in Fig. 3.3. Only the values for $d < 20$ have been plotted as the probability of higher delays is negligible.

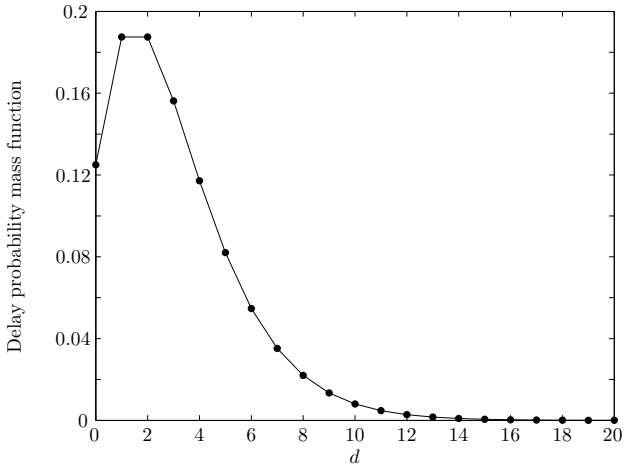

Figure 3.3: Probability distribution of the delays, which follow a negative binomial distribution where the probability of success is 0.5 and the number of failures is 3.

Fig. 3.4 shows the values of $\mathrm{tr}(P_t)$ (defined in (3.29)), the number of FLOPs per time instant (presented in Section 3.1) and the values of the probability of having no sample available p_0 (defined in (3.15)), for different choices of $\bar{d}$ in the set $\{0, 1, \ldots, 6\}$ within case S4. Choosing a higher $\bar{d}$ reduces p_0 and leads to a better performance ($\mathrm{tr}(P_t)$ is lower). However, the order of the observer increases with $\bar{d}$ as well as the computational effort to obtain a solution for problem (3.30) and the number of FLOPs used in the on-line implementation. Moreover, at a given point incrementing the value of $\bar{d}$ does not significantly improve the estimation performance. Therefore, parameter $\bar{d}$ must be chosen as a trade-off between estimation performance and observer complexity (number of FLOPs) plus computational effort to solve the optimization problem.

For the examined example, the case $\bar{d} = 4$ could be a good choice if there is enough on-line computational capability available because the obtained estimation performance is only 7% worst than the optimal (with $\bar{d} \to \infty$). If the number of FLOPs is an important constraint, the cases with $\bar{d} = 3$ and $\bar{d} = 2$ reduce the number of FLOPS in a 29% and

53% respectively at the expense of increasing the estimation error to a 20% and 51% above the optimum.

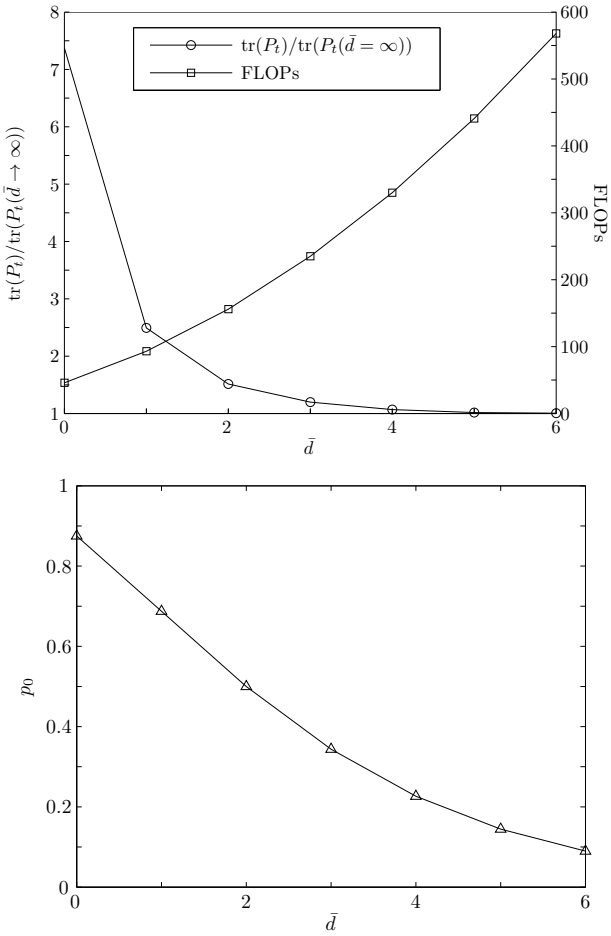

Figure 3.4: Normalized trace of the expected value of the estimation error covariance matrix at each instant $\mathrm{tr}(P_t)$, number of FLOPs, and probability of having no sample available p_0 for different maximum considered delay $\bar{d}$.

3.5.3 Example 3

In this example, we design the observer assuming the application of the buffer approach presented in [123] and explained in Remark 3.2. Let us consider the detectable and unstable system defined by A_3 in the first example. Let us assume that each sensor has a probability of sending a buffered packet (with the actual and the last $\bar{b}$ samples) of $\beta_1 = 0.66$ and $\beta_2 = 0.11$, respectively, but when the packet is received, the delay is 0. A parameter $\bar{d} = \bar{b}$ is selected in this case, to take into account all the measurement samples

present in the received packets. The value of $\mathrm{tr}(P_t)$ decreases when the buffer is enlarged (with scheduling approach S4), and therefore the estimation is improved (Fig. 3.5).

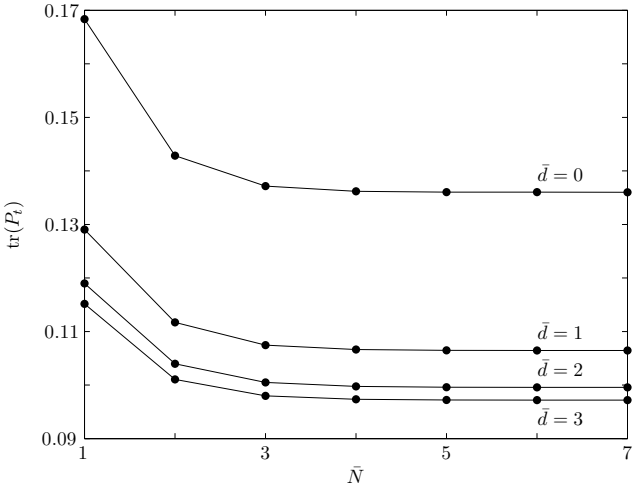

Figure 3.5: Trace of the expected value of the estimation error covariance matrix at each instant $\mathrm{tr}(P_t)$ as a function of the maximum intersample instant $\bar{N}$ (with S4) for different buffer lengths $\bar{b}$.

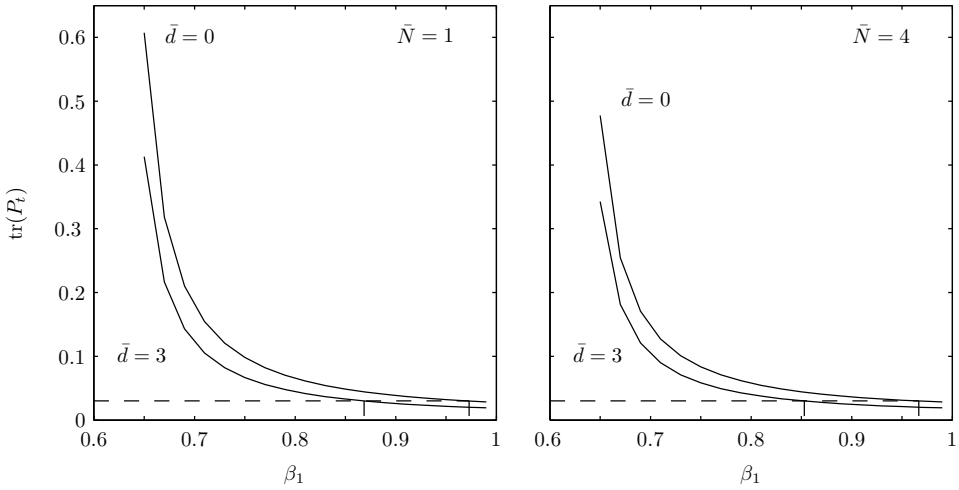

Figure 3.6: Trace of the expected value of the estimation error covariance matrix at each instant $\mathrm{tr}(P_t)$ (with S4) as a function of the probability of having available the measurement sample for different buffer lengths ($\bar{d} = 0$ and $\bar{d} = 3$) and different intersample instants ($\bar{N} = 1$ and $\bar{N} = 4$).

The buffer approach allows to reduce the use of the network. To illustrate this phenomena, let us consider that only the first sensor of the considered systems is available and that we want a performance $\mathrm{tr}(P_t) \leq 0.03$, with the lowest network resources (measured as the probability of available measurement samples). We search for the minimum probability (network usage) with different buffer lengths $\bar{b}$ and different intersampling instants $\bar{N}$. The achievable performance varies with each strategy and with the value of probability β_1 (see Fig. 3.6, with approach S4). Thus, for $\mathrm{tr}(P_t) = 0.03$, the probability of having available samples from the sensor can be decreased in a 12% from the worst case ($\bar{N} = 1$, $\bar{b} = 0$, $\beta_1 = 0.9730$) to the best one ($\bar{N} = 4$, $\bar{b} = 3$, $\beta_1 = 0.8530$).

3.6 Conclusions

In this chapter we designed a jump state estimator for networked control systems where the complexity in terms of storage requirements and selection mechanism is a design parameter, and we quantified the degradation that comes with the reduction of the observer complexity. The proposed approach allows to find a compromise between on-line computational implementation cost and performance. The result is a finite set of gains that are applied depending on the number of consecutive time instants without samples and on the available samples. We modeled the sampling scenario due to the network through the probabilities associated to the successful reception of each sample. As a consequence, the number of instants between consecutive samples, N_k, is unbounded, and the associated delays are time-varying. We used a model that accepts out-of-sequence measurements, buffered measurements on a single packet or multi-rate sensor measurements. The computational cost of the on-line implementation is lower than KF approaches with extended model, while the achieved performance is close to that one. The performance is better than the constant gain approaches at the cost of more storage requirements, and is similar to the one obtained with finite history loss jump estimators, while requiring less storage. Next chapter extends these results to become applicable under Markov chain models of the missing data.

Chapter 4

Co-design of jump estimators for wireless multi-hop networks with fading channels

ABSTRACT: *This chapter studies the transmission power budget minimization of battery-powered nodes in the remote state estimation problem over multi-hop wireless networks. Transmitting measurement samples through an intermediate node (relay) introduces an additional unitary delay in the end-to-end transmission. Communication links between nodes are subject to block-fading generating random dropouts. We propose a jump estimator whose modes depend on the measurement sample transmission outcome over a finite interval. Higher transmission powers increase the reliability of the transmissions at the expense of reducing the lifetime of the node batteries. Motivated by reducing the power budget, we derive an iterative tractable procedure to design the precalculated finite set of estimator gains and the power control laws to minimize the power budget while guaranteeing a predefined estimation error. This procedure allows us to trade the complexity of the estimator implementation for achieved performance and power budget.*

Wireless networks offer several advantages in contrast with wired ones, such as ease of manoeuvre, low cost and self-power. However, they are subject to channel fading that may lead to time-varying delays and packet dropouts [51]. These network-induced issues must be overcome when designing networked control system.

Considering remote estimation over networks, KF approaches may yield to optimal performance at the cost of notable implementation computational complexity, because the time-varying filter gain is computed at each instant in real time (e.g. [129, 123]). Motivated by offering low cost alternatives, we explore in this chapter the use of precalculated gains that alleviates the implementation computing requirements, but needs both selection mechanism and storage to choose the suitable gain [130, 119, 101, 45, 26]. The authors in [130] proposed a Markovian jump linear estimator approach whose gains depend on the history of measurement sample transmission outcomes due to packetized dropouts. Estimation performance improvement is achieved at the expense of enlarging the estimator complexity (storage demands and gain selection mechanism). Intermediate complexity approaches were presented in [45, 26]. In [45] the authors employed a gain dependency on the possible arrivals instants and delay for packetized samples in a finite set, while in [26] (see Chapter 3) we considered the multi-sensor case where the estimator gains jumped with the measurement sample availability and the number of consecutive instants without acquiring any sample.

Recently, a great deal of attention has been focused on designing both the estimator and the network conditions that exploit the relationship between transmission power and dropouts. This problem is sometimes called the co-design problem. Higher transmission

power leads to lower dropouts, which improves estimation performance. But, battery lifetime is of great importance as battery replacement can be difficult and expensive, and transmission is the most power consuming task [34]. Power control helps to save transmission power [116, 115, 68, 127, 73]. Briefly, in these works the authors presented methodologies to minimize the estimation error using a KF while guaranteeing a certain power budget. These works considered point-to-point communication, i.e., only two nodes (sensor and estimator) are concerned in data communication. However, due, e.g., to the distance between transmitters and receivers or to the presence of obstacles in the path, the point-to-point transmission through wireless fading channels may be highly unlikely or extremely power consuming [92].

In the aim to improve measurement sample delivery and reducing power budget, we focus on multi-hop wireless networks, see Section 2.3. In the works [117, 69] the authors studied the estimation (with KF) and power control problem through multi-hop fading networks. However, they neglected any transmission delay when hopping. This is not the case when estimating the states of a fast dynamic system (for instance communicating between nodes through IEEE 802.15.4 networks take typically 10 ms [38, 100]). Motivated by this fact and in the aim of [126, 17], we consider that hopping through a relay introduces a unitary additional delay on the data. While in [126] the authors presented a two-hop network with two power levels (direct transmission or transmission through relay), we analyze more general network structures where multiple relays nodes are present leading to multiple communications paths between sensors and the estimator node (see Section 2.3).

In this chapter we study the transmission power budget minimization of wireless self-powered nodes in the remote state estimation problem for multi-sensor systems over multi-hop networks. The wireless communication links are block-fading and produce random dropouts, while hopping through intermediate nodes introduce an additional unitary delay in the end-to-end transmission. We obtain a finite measurement sample transmission outcome parameter representing the network effects that follows a finite Markov chain. Based on the network average behavior, we propose a Markovian jump linear filter (which extends the one studied in Chapter 3) that provides propitious trade-offs between filter complexity (implementation computational burden) and estimation performance. We also present some necessary conditions related to the network average conditions for the existence of such a filter. We propose the use of power control laws of the form of parametric functions that may depend on the real time channel fading gain values to decide the power transmission of all the nodes (sensors and relays). We study the co-design problem of minimizing the power budget while guaranteeing some estimation performance. As this optimization is nonlinear, we derive a greedy algorithm that solves iteratively semi-definite programming problems to obtain a solution. Furthermore, we analyze the effects of decreasing the number of stored gains (i.e., complexity) and of using diverse power control policies (power budget) on the estimation performances. We show that as the filter complexity is increased (higher number of different gains) we can obtain similar estimation performance as the KF and the power budget can be reduced for a prescribed state estimation error.

Compared with the studied literature, the main contributions on this chapter can be summarized as follows.

1. Differently from [130] and [45] we consider the multi-sensor case with multiple time-varying delays and we present a flexible way to deal with different gain dependency strategies to get a compromise between estimation performance and implementation

cost. Moreover, we consider that the measurement sample transmission outcomes follow a Markov chain, while in [32] they were considered to be independent.

2. To the best of the author's knowledge, the preexisting power control works dealing with state estimation are addressed through KF while here, motivated by reducing the real time computation burden, we employ predefined filter gains and derive a greedy algorithm to solve the co-design problem.

This chapter extends the last one by considering a Markovian model of the network, introducing the estimator necessary existence conditions and dealing with power control issues.

The remainder of this chapter has the following structure. Section 4.1 introduces the problem in hands. In Section 4.2 we remind about the multi-hop network and its operation seen in Section 2.3. The jump filter design and its stability conditions are addressed in Section 4.3. Section 4.4 defines the power control policies considered while in Section 4.5 we present how to deal with the co-design problem. Numerical studies are included in Section 4.6 and Section 4.7 draws conclusions.

4.1 Problem description

We consider LTI DTS defined by

$$x[t+1] = A\,x[t] + B_w\,w[t], \tag{4.1a}$$

$$m_s[t] = c_s\,x[t] + v_s[t] \tag{4.1b}$$

where $x \in \mathbb{R}^n$ is the state, $m_s \in \mathbb{R}$ is the s-th measured output ($s = 1, \dots, n_y$) with $m[t] = [m_1[t] \cdots m_{n_y}[t]]^T$, $w \in \mathbb{R}^{n_w}$ is the state disturbance assumed to be a random signal of zero mean and known covariance $\mathbf{E}\{w[t]\,w[t]^T\} = W$, and $v_s \in \mathbb{R}$ is the s-th sensor noise considered as an independent zero mean random signal with known variance $\mathbf{E}\{v_s[t]^2\} = \sigma_s^2$. Note that in this chapter we do not consider the control input on (4.1). This is motivated by alleviating notation when dealing with the power control problem.

In this chapter, we study the remotely estimation of the system states (4.1) where the received samples at the estimator node (central unit) arrive through an unreliable multi-hop wireless network with fading channels, see Fig. 4.1. We assume that diverse sensors samples the system outputs synchronously with the input update and sent the samples independently through the network to the estimator (which is in the central unit). We aim to explore the trade-offs between power control, estimation performance and estimator complexity.

4.2 Multi-hop wireless network

Let us consider that the samples from different sensors are transmitted (i.e., $m_s^e[t] = m_s[t]$) through the multi-hop network with fading channels described in Section 2.3. In this section we just give a brief reminder on how we can describe the available samples at the estimator node.

The available information at instant t at the estimator node is the pair $(m_{s,d}^a[t], \alpha_{s,d}[t])$ for all $s = 1, \dots, n_y$ and $d = 0, 1, \dots, \bar{d}$, where

$$m_{s,d}^a[t] = \alpha_{s,d}[t]\,m_s^e[t-d], \tag{4.2}$$

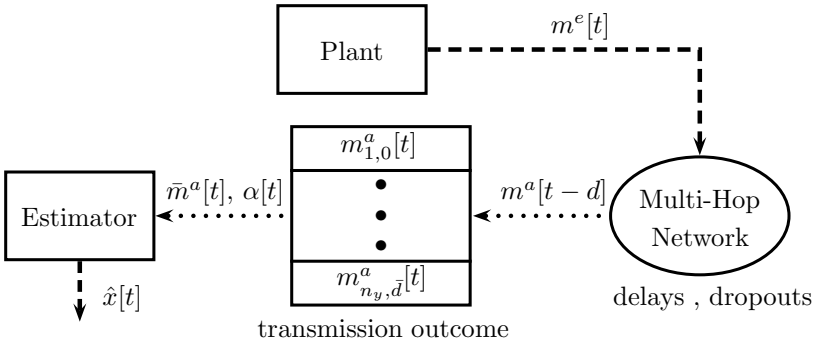

Figure 4.1: Estimation over networks problem.

and $\alpha_{s,d}[t]$ is a binary variable such as

$$\alpha_{s,d}[t] = \begin{cases} 1 & \text{if } m^e_s[t-d] \text{ is received and accepted at instant } t \\ 0 & \text{otherwise} \end{cases} \tag{4.3}$$

When $\alpha_{s,d}[t] = 1$ the sample sent at $t-d$ from sensor node N_s has an induced delay of $\tau_s[t-d] = d$. If $m^e_s[t-d]$ has not arrived yet at instant t, then $m^a_{s,d}[t] = 0$. We can describe the sample transmission outcomes from $t-\bar{d}$ to t with vector $\theta[t]$ such as

$$\theta[t] = \begin{bmatrix} \theta_1[t] & \cdots & \theta_{n_y}[t] \end{bmatrix}^T, \tag{4.4}$$

with $\theta[t]$ a binary column vector of length $n_\theta = \frac{(\bar{d}+1)(\bar{d}+2)}{2} n_y$ and where $\theta_s[t]$ captures the sample reception and acceptance at times $\{t-\bar{d}, \ldots, t\}$ from sensor N_s

$$\theta_s[t] = \begin{bmatrix} \theta_{s,0}[t] & \cdots & \theta_{s,\bar{d}}[t] \end{bmatrix}, \tag{4.5}$$

$$\theta_{s,d}[t] = \begin{bmatrix} \alpha_{s,0}[t-d] & \alpha_{s,1}[t-d+1] & \cdots & \alpha_{s,d}[t] \end{bmatrix}. \tag{4.6}$$

$\theta_{s,d}[t]$ stands for the transmission outcome of sample $m^e_s[t-d]$ at times $\{t-d, \ldots, t\}$. Remember that measurement samples delayed copies will be discarded. This implies that $\|\theta_{s,d}[t]\|_1 \leq 1$, where

$$\|\theta_{s,d}[t]\|_1 = \sum_{\delta=0}^{\bar{d}} \alpha_{s,\delta}[t-d+\delta] \tag{4.7}$$

The outcomes of $\theta[t]$ are governed by an ergodic Markov process and can take values in the finite set

$$\theta[t] \in \Theta = \{\vartheta_0, \vartheta_1, \ldots, \vartheta_r\},\ r = ((\bar{d}+2)!)^{n_y} - 1, \tag{4.8}$$

where ϑ_i (for $i = 0, \ldots, r$) is one of the possible combinations of the historical sample transmission outcomes. We write $\vartheta_0 = 0$ for case where none of the samples from $t-\bar{d}$ to t is received.

As explained in Section 2.3, we just consider the average behavior of the network which leads to time-invariant probabilities (instead of time-varying ones). The probability matrix $\Lambda = [p_{i,j}]$ with $p_{i,j} = \mathbf{Pr}\{\theta[t+1] = \vartheta_j | \theta[t] = \vartheta_i\}$ can be calculated as shown in Lemma 2.1. With that, the total probabilities of being at a given state $\pi_i = \mathbf{Pr}\{\theta[t] = \vartheta_i\}$ can be calculated solving $\pi = \pi\Lambda$ with $\sum_{i=0}^{r} \pi_i = 1$ and $\pi = [\pi_0 \ \cdots \ \pi_r]$.

Finally, let us define the sample availability matrix at instant t as

$$\alpha[t] = \psi(\theta[t]) = \bigoplus_{s=1}^{n_y} \left(\bigoplus_{d=0}^{\bar{d}} \alpha_{s,d}[t] \right). \tag{4.9}$$

The possible values of $\alpha[t]$ belong also to a known set

$$\alpha[t] \in \Xi = \{\eta_0, \eta_1, \ldots, \eta_q\}, \quad q = 2^{\bar{n}_y} - 1 \tag{4.10}$$

where η_i (for $i = 1, \ldots, q$) denotes each possible combination, being η_0 the scenario without available samples, (i.e., $\eta_0 = 0$). α_t is the result of applying a surjective function $\psi : \Theta \to \Xi$ on θ_t.

4.3 Markovian jump filter

To take into account the reception of delayed samples, we propose employing an aggregated model such as

$$\bar{x}[t+1] = \bar{A}\bar{x}[t] + \bar{B}_w w[t], \tag{4.11}$$

where $\bar{x}[t] = \begin{bmatrix} x[t]^T & \cdots & x[t-\bar{d}]^T \end{bmatrix}^T$ and

$$\bar{A} = \begin{bmatrix} A & 0 & \cdots & 0 \\ I & \cdots & 0 & \vdots \\ \vdots & \ddots & \vdots & \vdots \\ 0 & \cdots & I & 0 \end{bmatrix}, \quad \bar{B}_w = \begin{bmatrix} B_w \\ 0 \end{bmatrix}.$$

We express with vector $\bar{m}_s^a[t]$ the availability of the sample at instant t from sensor s sent from $t - \bar{d}$ to t as

$$\bar{m}_s^a[t] = [m_{s,0}^a[t] \cdots m_{s,\bar{d}}^a[t]]^T, \tag{4.12}$$

where $m_{s,d}[t]$ is as defined in (4.2). With that, $\bar{m}^a[t] = [\bar{m}_1^a[t]^T \cdots \bar{m}_{n_y}^a[t]^T]^T$ has a length of $\bar{n}_y = n_y(1+\bar{d})$. Using α_t, we rewrite the received sample information at instant t as

$$\bar{m}^a[t] = \alpha[t] \left(\bar{C}\bar{x}[t] + \bar{v}[t] \right) \tag{4.13}$$

where $\bar{v}[t] = [\bar{v}_1[t] \cdots \bar{v}_{\bar{n}_y}[t]]^T$ and $\bar{v}_s[t] = [v_s[t] \cdots v_s[t-\bar{d}]]$. $\bar{c}_s = [\bar{c}_{s,0} \cdots \bar{c}_{s,\bar{d}}]^T$ with $\bar{c}_{s,d} = [0_{1\times n\cdot d}\ c_s\ 0_{1\times n\cdot(\bar{d}-d)}]^T$ are the rows of matrix $\bar{C}$. In (4.13), $\bar{v}[t]$ is the measurement noise vector with covariance $\mathbf{E}\{\bar{v}[t]\bar{v}[t]^T\} = V = \bigoplus_{s=1}^{n_y} \left(\bigoplus_{d=0}^{\bar{d}} \sigma_s^2 \right)$.

4.3.1 Proposed filter

We propose the next state estimation algorithm

$$\hat{\bar{x}}_t = \bar{A}\,\hat{\bar{x}}_{t-1} + L_t(\bar{m}_t^a - \alpha_t \bar{C}\bar{A}\,\hat{\bar{x}}_{t-1}). \tag{4.14}$$

When no sample is available, the estimator is run in open loop. Otherwise, the state estimation is updated with the updating gain matrix L_t.

Considering (4.11) and (4.13)-(4.14), the dynamic of the estimation error, defined as $\tilde{x}_t = \bar{x}_t - \hat{\bar{x}}_t$, is

$$\tilde{x}_t = (I - L_t\alpha_t\bar{C})\left(\bar{A}\tilde{x}_{t-1} + \bar{B}_w w_{t-1}\right) - L_t\alpha_t\bar{v}_t. \tag{4.15}$$

One of the aims of this chapter is to compute matrices L_t to obtain acceptable estimation performances while requiring low computing and storage capabilities. Using predefined gain filters [130, 32] instead of KFs [123] helps to alleviate the on-line computation burden. The authors in [130] illustrated that the KF gains depend on the history of combination of sensor availability. In the current chapter we extend their result to include multi-sensor transmission and delayed measurement samples. Thus, we propose relating the gains with θ_t as $L_t = L(\theta_t)$. We define the filter gains as

$$L(\theta_t) = \begin{cases} 0 \text{ if } \psi(\theta_t) = 0, \text{(no measurement sample received)} \\ L_i \text{ if } \theta_t = \vartheta_i,\ \psi(\vartheta_i) \neq 0 \end{cases} \tag{4.16}$$

We compute the gain matrices off-line leading to the finite set

$$L(\theta_t) \in \mathcal{L} = \{L_0, \ldots, L_r\}. \tag{4.17}$$

4.3.2 Filter design

The next theorem states the evolution of the state estimation error covariance matrix.

Theorem 4.1. *Let $P_{t,j} = \mathbf{E}\{\tilde{x}_t\tilde{x}_t^T|\theta[t] = \vartheta_i\}$ (with $j = 1, \ldots, r$) be the state estimation error covariance matrix updated at instant t with information $\theta[t] = \vartheta_j$ that can be recursively obtained as*

$$P_{t,j} = \sum_{i=0}^{r} p_{i,j}\frac{\pi_i}{\pi_j}\left(F_j(\bar{A}P_{t-1,i}\bar{A}^T + \bar{B}_w W \bar{B}_w^T)F_j^T + X_j V X_j^T\right), \tag{4.18}$$

with

$$F_j = I - L_j\,\psi(\vartheta_j)\bar{C}, \quad X_j = L_j\psi(\vartheta_j). \tag{4.19}$$

Then, the total expected value of state estimation error covariance matrix at instants t, $\mathbf{E}\{\tilde{x}_t\tilde{x}_t^T\}$, is given by

$$\sum_{j=0}^{r}\mathbf{E}\{\tilde{x}_t\tilde{x}_t^T|\theta[t] = \vartheta_j\}\,\mathbf{Pr}\{\theta[t] = \vartheta_j\} = \sum_{j=0}^{r} P_{t,j}\pi_j. \tag{4.20}$$

Proof. See Appendix C.4.1. ■

The above theorem defines a recursion on the covariance matrix that we write as $\mathcal{P}_t = \mathfrak{E}\{\mathcal{P}_{t-1}\}$, where $\mathcal{P}_t \triangleq (P_{t,0}, \ldots, P_{t,r})$, $\mathfrak{E}\{\cdot\} \triangleq (\mathfrak{E}_0\{\cdot\}, \ldots, \mathfrak{E}_r\{\cdot\})$, being $\mathfrak{E}_i\{\cdot\}$ the linear operator that gives (4.18). To compute a steady state off-line solution, one must address the problem of finding a set of filter gains that satisfies the Riccati equation $\mathfrak{E}\{\mathcal{P}_t\} = \mathcal{P}_t$. When the filter gains jump with all the states of the Markov chain, [130] and [45] show how to get their explicit value. Their methods are not valid if the filter shares the same gain for different modes of the Markov chain, and therefore do not allow

to explore the trade-offs between storage complexity and estimation performance. To address this issue, we adopt the following alternative optimization problem

$$\begin{aligned} \underset{\mathcal{L},\mathcal{P}}{\text{minimize}} \quad & \operatorname{tr}\left(\sum_{j=0}^{r} P_j \pi_j\right) \\ \text{subject to} \quad & \mathfrak{E}\{\mathcal{P}\} - \mathcal{P} \preceq 0, \end{aligned} \tag{4.21}$$

with $\mathcal{P} \triangleq (P_0, \ldots, P_r)$.

We shall prove next that the constraint

$$\mathfrak{E}\{\mathcal{P}\} - \mathcal{P} \preceq 0 \tag{4.22}$$

is a key for guaranteeing the boundedness of $\mathbf{E}\{\tilde{x}_t \tilde{x}_t^T\}$, and therefore the mean square stability of the filter. The next results are independent on the constraints over $\mathcal{L}$.

4.3.3 Boundedness of the error covariance

In the following we present the theorems that demonstrate that applying the gains $\mathcal{L}$ obtained from problem (4.21), the sequence $\{\mathcal{P}_t\}$ (and thus $\{\mathbf{E}\{x_t x_t^T\}\}$) converges to the unique solution $\bar{\mathcal{P}} \triangleq (\bar{P}_1, \ldots, \bar{P}_r)$ obtained in (4.21). Let us write $\bar{\mathcal{P}} \succ 0$ to denote $\bar{P}_i \succ 0$, $\forall i = 1 \ldots, r$ and $\mathfrak{E}^t\{\cdot\}$ to define the recursion of $\mathfrak{E}\{\cdot\}$.

Theorem 4.2. *Let $\mathcal{L}$ in* (4.17) *be a set that fulfills* (4.22)*, i.e., there exists $\bar{\mathcal{P}} \succ 0$ such that $\mathfrak{E}\{\bar{\mathcal{P}}\} \preceq \bar{\mathcal{P}}$. Then, for any initial condition $\mathcal{P}_0 \succeq 0$ the sequence $\{\mathcal{P}_t\}$ is bounded, i.e., $\{\mathcal{P}_t\} \preceq M_{\mathcal{P}}$, with $M_{\mathcal{P}} \triangleq (M_{P_0}, \ldots, M_{P_r})$.*

Proof. Taking into account the linear operator in Lemma C.2 (see Appendix C.4), Theorem 4.1 and constraint (4.22), we have $\mathcal{T}(\bar{\mathcal{P}}) \prec \mathfrak{E}\{\bar{\mathcal{P}}\} \preceq \bar{\mathcal{P}}$. Therefore, $\mathcal{T}(\cdot)$ meets the condition of Lemma C.2. $\mathcal{P}_t$ evolves as $\mathcal{P}_{t+1} = \mathfrak{E}\{\mathcal{P}_t\} = \mathcal{T}(\mathcal{P}_t) + U$. Because U contains the disturbance and noise covariance (both positive definite and bounded), thus, $U \succ 0$ that assures that $\{\mathcal{P}_t\}$ is bounded.

■

Considering the above theorem, the next result states that $\{\mathcal{P}_t\}$ converges to the solution of problem (4.21).

Theorem 4.3. *Let $\mathcal{L}$ in* (4.17) *be a set that solves problem* (4.21)*. Then, for any initial condition $\mathcal{P}_0 \succeq 0$, the iteration $\mathcal{P}_{t+1} = \mathfrak{E}\{\mathcal{P}_t\}$ converges to the unique positive semi-definite solution $\bar{\mathcal{P}}$ obtained in problem* (4.21)*, i.e., $\lim_{t\to\infty} \mathcal{P}_t = \lim_{t\to\infty} \mathfrak{E}^t\{\mathcal{P}_0\} = \bar{\mathcal{P}} \succeq 0$, where $\bar{\mathcal{P}} = \mathfrak{E}\{\bar{\mathcal{P}}\}$.*

Proof. See Appendix C.4.2

■

4.3.4 Necessary network conditions

Theorem 4.2 and Theorem 4.3 show that the feasibility of problem (4.21) is a sufficient condition to guarantee the boundedness of $\mathbf{E}\{\tilde{x}_t \tilde{x}_t^T\}$. Now, we give some necessary conditions (affecting the power transmissions) to assure some network reliability performances that may allow solving (4.21). If these conditions are not fulfilled, problem (4.21) is infeasible.

Theorem 4.4. *A necessary condition to find a solution for problem* (4.21) *is that the transition probabilities of* θ_t *fulfill the following constraints*

$$p_{jj} \cdot \rho(\bar{A})^2 - 1 \leq 0, \quad \forall j : \psi(\vartheta_j) = 0, \tag{4.23a}$$

$$p_{jj} \cdot \rho(\bar{A}_l)^2 - 1 < 0, \quad \forall j : \psi(\vartheta_j) = \eta_l,\ l \in ND, \tag{4.23b}$$

being p_{ij} *the probabilities defined in* (2.45), $\rho(\bar{A})$ *the spectral radius of matrix* $\bar{A}$, *ND the set of reception scenarios* η_l *from which the system is not detectable and* $\rho(\bar{A}_l)$ *the spectral radius of the unobservable subspace of matrix* $\bar{A}$ *from reception scenario* η_l[1].

Proof. See Appendix C.4.3. ■

Remark 4.1. If the system is unstable, and non detectable from the reception scenario η_l the transition probabilities must hold (4.23a) and (4.23b). If the system is unstable, but it is detectable from each possible reception scenario η_l , the transition probabilities must fulfill (4.23a). However, if the system is stable, then it is always possible to find a solution for problem (4.21).

4.3.5 Numerical computation

Problem (4.21) can be solved using the following linear matrix inequalities and bilinear equality constraints,

$$\begin{aligned}
&\underset{\mathcal{L},\mathcal{P},\mathcal{R}}{\text{minimize}} \quad \operatorname{tr}\left(\sum_{j=0}^{r} P_j \pi_j\right) \\
&\text{subject to} \quad \begin{bmatrix} P_j & \bar{\bar{M}}_j \bar{\bar{A}} & \bar{\bar{M}}_j \bar{\bar{W}} & \bar{\bar{X}}_j \bar{\bar{V}} \\ \bar{\bar{A}}^T \bar{\bar{M}}_j^T & \bar{\bar{R}} & 0 & 0 \\ \bar{\bar{W}}^T \bar{\bar{M}}_j^T & 0 & \bar{\bar{W}} & 0 \\ \bar{\bar{V}}^T \bar{\bar{X}}_j^T & 0 & 0 & \bar{\bar{V}} \end{bmatrix} \succeq 0, \quad \forall j = 0, \ldots, r, \\
&\quad \bar{\bar{P}}\,\bar{\bar{R}} = I.
\end{aligned} \tag{4.24}$$

with

$$\bar{\bar{X}}_j = \left[\sqrt{p_{0,j}\pi_0/\pi_j} L_j \psi(\vartheta_j) \ \cdots \ \sqrt{p_{r,j}\pi_r/\pi_j} L_j \psi(\vartheta_j)\right],$$

$$\bar{\bar{M}}_j = \left[\sqrt{p_{0,j}\pi_0/\pi_j} F_j \ \cdots \ \sqrt{p_{r,j}\pi_r/\pi_j} F_j\right], \ \bar{\bar{A}} = \bigoplus_{i=0}^{r} \bar{A},$$

$$\bar{\bar{W}} = \bigoplus_{j=0}^{r} \bar{B}_w W \bar{B}_w^T, \ \bar{\bar{V}} = \bigoplus_{j=0}^{r} V, \ \bar{\bar{R}} = \bigoplus_{j=0}^{r} R_j, \ \bar{\bar{P}} = \bigoplus_{j=0}^{r} P_j,$$

$\mathcal{R} \triangleq (R_1, \ldots, R_r)$ and F_j as defined in (4.19). Applying extended Schur complements on the matrix inequality constraint makes problem (4.21) and (4.24) equivalent.

[1] $\bar{A}_l = \mathcal{O}^T \bar{A} \mathcal{O}$ where $\mathcal{O} = \ker\left(\left[(\eta_l \bar{C})^T \quad (\eta_l \bar{C}\bar{A})^T \quad \cdots \quad (\eta_l \bar{C}\bar{A}^{n-1})^T\right]^T\right)$ is the unobservable subspace.

The optimization problem (4.24) is a nonconvex optimization problem because of the terms $R_j = P_j^{-1}$ involved in the equality constraint. We address this problem with the cone complementarity linearization algorithm [33] over a bisection algorithm. The algorithm is omitted for brevity; an example can be found in Chapter 3.

4.4 Power allocation

One of the goals of the current chapter is to explore the benefits of power control in the estimation problem over multi-hop networks. Note that, from (2.37) (see Section 2.4), the power transmission level alleviates the occurrence of errors and improves the link reliability. However, transmitter nodes are usually self-powered and power control plays a trade-off role between power budget and transmission reliability (that affects the estimation performances). The power level of each transmitter node is calculated at the central unit (estimator node), and sent back to them before the measurement sample transmission procedure. We consider power control laws that may use the channel fading gains to decide in real time the power transmission level as

$$u_a[t] = \kappa_a(H_a[t]), \tag{4.25}$$

with $u_a[t] \in [0,\, \bar{u}]$ and $\kappa_a : \Omega_a \to [0,\, \bar{u}]$ is an integrable function over the domain Ω_a where $H_a[t] \in \Omega_a$. We denote by U_t the vector of power levels, i.e., $U_t = [u_1[t] \;\; \cdots \;\; u_M[t]]^T$. We write as $\mathcal{U}_a$ the set that contains the parameters of function $\kappa_a(\cdot)$ where $\mathcal{U} = \{\mathcal{U}_1, \ldots, \mathcal{U}_M\}$. Using the PDF of the fading channel gains $g(\cdot)$ (2.44), we can compute the expected value of transmission power (i.e. when $\Upsilon_a = 1$) from each node N_a as

$$\mathbf{E}\{u_a | \Upsilon_a = 1\} = \int_{\Omega_a} g(H_a)\kappa_a(H_a)\mathrm{d}H_a. \tag{4.26}$$

For ease of notation let us denote $\mathbf{E}\{u_a|\Upsilon_a = 1\}$ by $\mathbf{E}\{u_a\}$.

Remark 4.2. The proposed control power laws include the case when instead of a continuous range of power levels only some finite number of predefined discrete power levels are available (as proposed in [127]). For instance, one can discretize the fading gain value set of the most favorable communication link and schedule the power levels with the discretized resulting sets. In this case, the parameters of power control functions would be the fading gain value ranges of each discretized set.

4.5 Co-design

Battery life is an important setback for the widespread adoption of wireless based control systems in industry. Batteries need replacement, so reducing power consumption of wireless devices is a key issue. Motivated by this, we aim to compute off-line the parameters that define the power control functions to minimize the network power budget (when transmitting) and the set of filter gains that guarantees a certain estimation performance. Let us characterize the power budget by a function of the expected value of the transmission power of each node as

$$J(U) = \sum_{a=1}^{M} \mu_a \mathbf{E}\{u_a\} \tag{4.27}$$

where $\mu_a \in \mathbb{R}$ are some real constants. Then, the problem in hands can be formulated (when taking into account the average behavior of the network) as

$$\begin{aligned} \underset{\mathcal{L},\mathcal{P},\mathcal{U}}{\text{minimize}} \quad & J(U) \\ \text{subject to} \quad & \operatorname{tr}\left(\sum_{j=0}^{r} P_j \pi_j\right) \leq \gamma_P, \\ & \mathfrak{E}\{\mathcal{P}\} - \mathcal{P} \preceq 0, \\ & u_a[t] \in [0,\, \bar{u}], \quad \forall a = 1, \ldots, M, \end{aligned} \tag{4.28}$$

where γ_P is a prescribed estimation performance to be assured.

This is a nonlinear optimization problem as the transitions probabilities of between the modes of θ_t are also a decision variable (that depends on the power control strategy). This kind of problem can be solved, for instance, by brute force using a gridding approach, by means of heuristic optimization with genetic algorithms, or by implementing a greedy algorithm. To give a fast way to obtain a solution, in this chapter, we propose the use of a greedy algorithm. A greedy algorithm is a tree search where at each step only the branch that locally optimize the problem fulfilling some heuristics is explored, in the hope that this choice will lead to a globally optimal solution. So, this kind of algorithm never comes back to previous solutions to change the search path. Therefore global solutions are not guaranteed. The proposed greedy algorithm is as follows

Algorithm 4.1. Greedy algorithm.

Step 1 For a given $\bar{u}$, choose each set of power control parameters $\mathcal{U}_a^0$ to maximize the power transmission of each node N_a (i.e., the one the leads to the maximum $\mathbf{E}^0\{u_a\}$). For some given constants μ_a, define index J^0 as

$$J^0 = \sum_{a=1}^{M} \mu_a \mathbf{E}^0\{u_a\}.$$

Choose a small positive parameter value $\xi \gtrsim 0$.

Step 2 Set $k = k+1$ and $J^k = J^{k-1} - \xi$. For $a = 1$ to M repeat step 3, then go to step 4.

Step 3 Set $\mathcal{U}_i^k = \mathcal{U}_i^{k-1}$ for all $i \neq a$ with $i = 1, \ldots, M$. Obtain $\mathcal{U}_a^k$ as a power control parameter set resulting from the optimization problem

$$\begin{aligned} \underset{\mathcal{U}_a}{\text{maximize}} \quad & \prod_{\forall l\,:\,(N_a,N_l)\in\mathcal{I}} \int_{\Omega} g(H)\, \beta_{a,l} \mathrm{d}H \\ \text{subject to} \quad & J^k - \sum_{\substack{i=1 \\ i\neq a}}^{M} \mu_i \mathbf{E}\{u_i^k\} - \mu_a \mathbf{E}\{u_a^k\} = 0, \\ & u_a[t] \in [0,\ \bar{u}], \quad \forall a = 1, \ldots, M. \end{aligned}$$

where $\mathbf{E}^k\{u_i\}$ is the obtained power transmission with (4.26) for the set $\mathcal{U}_i^k$. If this problem has no solution set the auxiliary variable γ_a to $\gamma_a = \infty$. Otherwise,

compute the transition probabilities given in (2.45) and check conditions (4.23). If they are not fulfilled, set $\gamma_a = \infty$. Otherwise solve optimization problem (4.21),

$$\begin{aligned} \underset{\mathcal{L}_a, \mathcal{P}_a}{\text{minimize}} \quad & \text{tr}\left(\sum_{j=0}^{r} P_{a,j}\pi_j\right) \\ \text{subject to} \quad & \mathfrak{E}\{\mathcal{P}_a\} - \mathcal{P}_a \preceq 0, \end{aligned}$$

If the problem is infeasible set $\gamma_a = \infty$. Otherwise, store $\mathcal{P}_a$, $\mathcal{L}_a$ and

$$\gamma_a = \text{tr}\left(\sum_{j=0}^{r} P_j \pi_j\right).$$

Step 4 Set $a = \arg\min_a \gamma_a$.

If $\gamma_a \leq \gamma_P$, then
set $\mathcal{U}_i^k = \mathcal{U}_i^{k-1}$ for all $i \neq a$, store $\mathcal{U}^k = \{\mathcal{U}_1^k, \ldots, \mathcal{U}_M^k\}$, $\mathcal{P}^k = \mathcal{P}_a^k$ and $\mathcal{L}^k = \mathcal{L}_a^k$; and go to step 2.
Else, exit, best solution found in iteration $k-1$.

■

As it can be appreciated, the algorithm starts by considering the most favorable power control deliverance where the probabilities of receiving packets are higher (higher transmission power). Then, the power budget $J = \sum_{a=1}^{M} \mu_a \mathbf{E}\{u_a\}$ is minimized while possible. Each time it can be decreased, M sets containing the power control parameters that would lead to the obtained cost are calculated in such a way that each of them maximizes the expected value of probability of successful transmissions through all its communication channels. Then, the proposed heuristic to choose the path selects the solution with the lowest γ_a, i.e., the solution that allows a larger future search before the algorithm ends.

Remark 4.3. We can use the MATLAB function `fmincon` to solve the optimization problem presented in the third step of the greedy algorithm (that may be nonlinear) to obtain each of the power control parameter sets that allows to reduce the network consumption to the given extent. Note that the obtained solution may not be unique.

Remark 4.4. The presented method is not restricted to power budgets in the form of linear functions, more complicated functions can be also explored. The proposed approach also allows including further constraints related to the chosen power control laws. Moreover, one can easily rewrite the algorithm to solve the problem of minimizing the estimation error for a constrained power budget (as proposed in [68, 73, 118]).

4.5.1 Co-design trade-offs

In this chapter, we explore the trade-offs between estimation performance, estimator complexity and power budget.

Let us first analyze the estimator complexity. Because the filter gains jump with the outcomes of θ_t, the solution of the problem (4.21) leads to a number of nonzero different

gains of $|\mathfrak{L}| = (\bar{d}+1)!^{n_y}((\bar{d}+2)^{n_y}-1)$, where $\mathcal{L} = \mathfrak{L}\bigcup\{0\}$ (see (4.17)). We can reduce the filter complexity by imposing some equality constraints over some gain matrices of the set $\mathcal{L}$ as $L_i = L_j$ in problem (4.24). Decreasing the number of gains alleviate the numerical burden of (4.24). To implement a jump filter with a simple gain selection procedure and low storage requirements, we suggest the following predefined sets of equalities over the possible historical measurement sample transmission outcomes:

- **S1**. The filter gain is independent of the sampling scenario, $|\mathfrak{L}_{S1}| = 1$.
- **S2**. The filter gains depend on the number of sensors from which samples arrive successfully at each instant, $|\mathfrak{L}_{S2}| = n_y$.
- **S3**. The filter gains depend on the sampling scenario at a given instant α_t, $|\mathfrak{L}_{S3}| = 2^{\bar{n}_y} - 1$.
- **S4**. The filter gains are related to the historical sample transmission outcomes θ_t, $|\mathfrak{L}_{S4}| = (\bar{d}+1)!^{n_y}((\bar{d}+2)^{n_y}-1)$.

Let us now examine some power allocation strategies. In this chapter, we will study two specific ones:

- **Constant power (P1)**. Each of the transmitter nodes deploy a time-invariant strategy defined as
$$u_a[t] = \bar{u} \tag{4.29}$$
if some samples are available to transmit, otherwise $u_a[t] = 0$. Then, the set of power control parameter for each node is $\mathcal{U}_a = \{\bar{u}\}$. This strategy can be implemented directly in the nodes, helping to not overload the traffic in the network.
- **Saturated inverted channel gain (P2)**. The power control law for each transmitter node is given by
$$u_a[t] = \begin{cases} \dfrac{\delta_a}{h_{a,l}[t]} & \text{if } h_{a,l}[t] \geq h^{\star}_{a,l}, \\ \dfrac{\delta_a}{h^{\star}_{a,l}} & \text{otherwise,} \end{cases} \tag{4.30}$$
if some samples are available to transmit, otherwise $u_a[t] = 0$. We consider that channel gain $h_{a,l}$ refers to the link $(N_a, N_l) \in \mathcal{I}$ that has the best communication conditions, i.e, the lowest $\mathbf{E}\{h_{a,l}\} = \int_{\Omega_{h,l}} g(h_{a,l})h_{a,l}\mathrm{d}h_{a,l}$. Then, the set of power control parameters for each node is $\mathcal{U}_a = \{\delta_a, h^{\star}_{a,l}\}$.

The example section explores these ideas.

4.6 Example

We consider the following system (randomly chosen)

$$A = \begin{bmatrix} 1.05 & -0.1 \\ 0.74 & 1.05 \end{bmatrix}, \quad B_w = \begin{bmatrix} 0.01 & 0.13 \\ 0.01 & 0.08 \end{bmatrix}, \quad C = \begin{bmatrix} 0.53 & 0.39 \\ 0.72 & 0.35 \end{bmatrix},$$

with $B_u = \begin{bmatrix} -0.33 & 0.34 \end{bmatrix}^T$. The state disturbance and sensor noises covariances are

$$W = \begin{bmatrix} 0.26 & -0.003 \\ -0.003 & 0.25 \end{bmatrix}, \begin{bmatrix} \sigma_1^2 \\ \sigma_2^2 \end{bmatrix} = \begin{bmatrix} 0.0086 \\ 0.0079 \end{bmatrix}.$$

Samples are acquired through the multi-hop network in Fig. 4.2 that may induce up to one unit delay in the end-to-end transmission. Thus, the number of different outcomes of θ_t is $|\Theta| = (1+2)!^2 = 36$ (see (4.8)). Nodes transmit using a BPSK modulation with $b = 4$ bits and a transmission power bounded by $\bar{u} = 10$ through Rayleigh fading channels (see Remark 2.12) with

$$\bar{h}_{14} = 0.01,\ \bar{h}_{13} = 1,\ \bar{h}_{24} = 0.1,\ \bar{h}_{23} = 0.3,\ \bar{h}_{34} = 0.5.$$

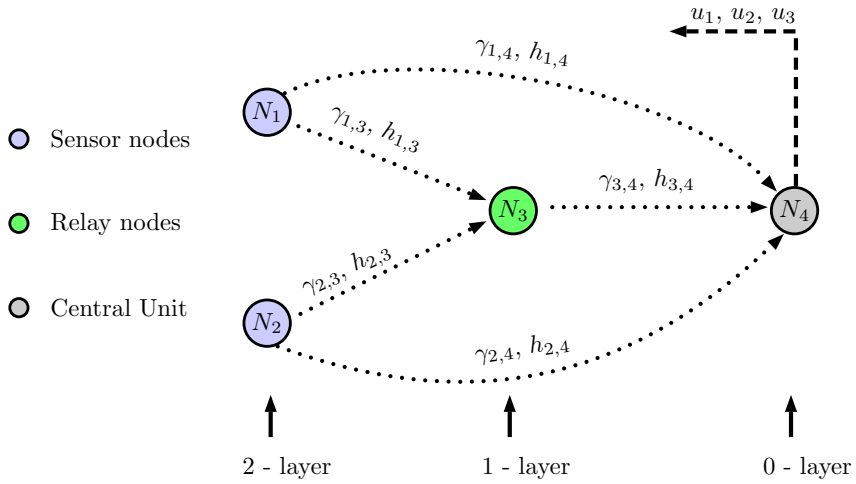

Figure 4.2: Multi-hop wireless network with 4 nodes and 3 layers.

Let us first analyze the effect of having a relay node helping to retransmit the samples. Let us denote the estimation performance index $\mathrm{tr}\left(\sum_{i=0}^{35} C_x P_i C_x^T \pi_i\right)$ as γ where $C_x = [I_n \, 0_{n\times(n\cdot\bar{d})}]$ selects the covariance corresponding to $x[t] - \hat{x}[t|t]$. When the nodes deploy a constant power control strategy equal to its maximum available power (i.e. $u_a[t] = \bar{u}$ for all t and $a \in 1, 2, 3$), we obtain $\gamma = 0.023$, which is the best estimation performance index that can be achieved with the proposed methods. If the relay node is not available, then we obtain $\gamma = 0.075$. This means that the relay node allows improving the estimation performance by a factor of 3 with respect to the case when no relay is available.

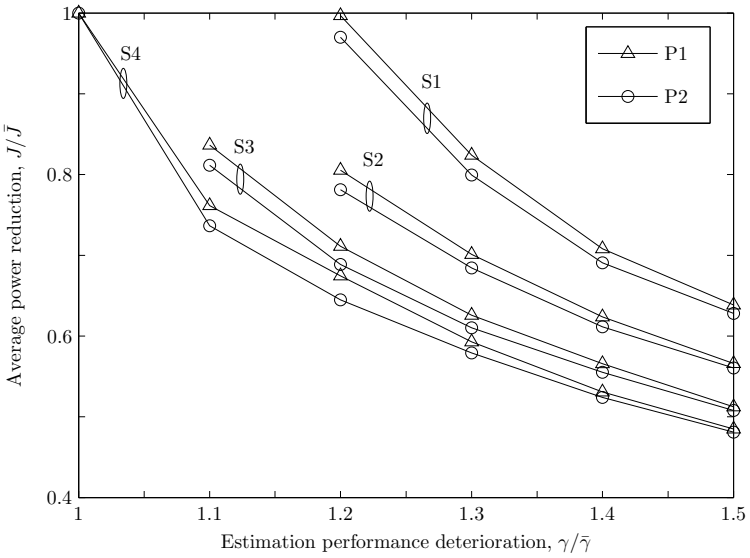

Figure 4.3: Co-design trade-offs between power budget, estimation performances and filter complexity for different power control strategies.

We now explore the co-design trade-offs between power budget, estimation performances and filter complexity for different power control strategies presented in Section 4.5 that can be obtained using the greedy algorithm developed in Section 4.4. Let us define the power budget J as $J = \sum_{a=1}^{3} \mathbf{E}\{u_a\}$ (average power) where the best estimation performance index $\bar{\gamma} = 0.023$ is achieved when $\bar{J} = 30$. Fig. 4.3 shows the compromises between transmitted power, estimation performance and power budget for all the the described cases in Section 4.5. We appreciate that at the expense of only a 10% deterioration from the best estimation performance, we can reduce the power budget by 25% when deploying approach S4, which will increase the node battery lives. Note that for the given example the saturated inverted channel gain power control law (P2) is only able to decrease up to a 5% the power budget with respect to a constant power level (P1). In this case, it is more interesting to deploy strategy P1 to reduce the network traffic. The main obtained differences lie in the estimator complexity. To obtain the same power consumption reduction as case S4, cases S2 and S1 need to deteriorate 10% and 20% more the best estimation performance than case S4. However case S4 uses 32 different gains which increases the estimator complexity (storage requirements). A reasonable trade-off could be to choose case S3 because it reduces the number of stored gains in by 50% and increases the power budget only up to 10% with respect to S4.

Finally, let the transmission powers be $u_1[t] = 4.84$, $u_2[t] = 10$ and $u_3[t] = 8$ for all t (which correspond to the solution of the co-design problem for case S4 with $\gamma/\bar{\gamma} = 1.1$). Fig. 4.4 compares the results of implementing in simulation the KF algorithm adapted from [123] and the proposed jump filters. The estimation performance index obtained with the KF is $\gamma_{\text{Kal}} = 0.0242$ (where $\gamma_K = \text{tr}(C_x \mathbf{E}\{\tilde{x}_t \tilde{x}_t^T\} C_x^T)$. We can appreciate that as the number of stored gains becomes higher, the jump filter performs nearly as well the KF. However, the KF needs to execute at most 976 floating-point operations per

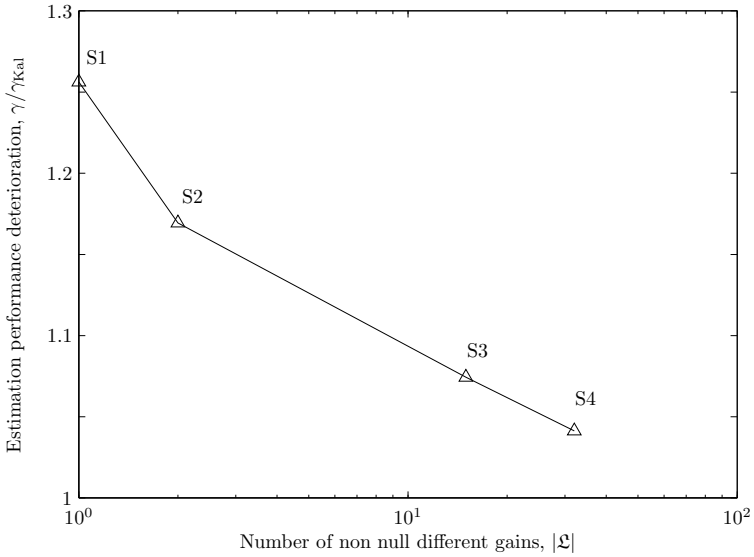

Figure 4.4: Deterioration of the estimation performance w.r.t. the Kalman filter for transmission powers $u_1[t] = 4.84$, $u_2[t] = 10$ and $u_3[t] = 8$ (for all t).

instant, while the off-line methods only need 64 (see Chapter 3 for further information about FLOPs).

4.7 Conclusions

In this chapter we used the model for multi-hop networked estimation with fading channels developed in Section 2.3. Random dropouts are generated due to the fading links while delays are introduced while hopping through relay nodes. We introduced a vector that captures the network behavior by keeping the measurement sample transmission outcomes on an interval, which is governed by Markovian finite process. With the average network behavior, we conceived a jump filter where its complexity can be selected as a trade-off between storage requirements and estimation performance. Moreover, we gave necessary filter existence conditions based on the network conditions. To keep the network operation power-efficient we studied the use of power control laws of the forms of parametric functions. We designed the power policies and the finite set of filter gains to minimize the power budget while guaranteeing a certain level of state estimation error. The design is carried out with an iterative procedure based on semi-definite programming problems. We explored the trade-offs between estimation performance, estimator complexity (by reducing the number of different filter gains) and power budget. Numerical results showed that: 1) intermediates relays helps to reduce the power budget for prescribed estimation performance, 2) increasing estimator complexity allows saving power for prescribed estimation performance, and 3) for the same network conditions the on-line computational burden of the jump filter can be much lower than Kalman filter approaches, while achieving similar estimation performances.

In Chapters 4 and 3 we considered the stationary behavior of the network by assuming constant successful transmission probabilities. In the next chapter we develop a result for the case when the successful transmission probabilities are time-varying.

Chapter 5

Polynomial observers in networked control systems with unknown packet dropout rate.

ABSTRACT: *This chapter studies the estimator design problem for networked systems with previously unknown successful transmission probability. We consider a time-varying PAR that can be estimated in real time by means of the acknowledgement on new data arrival. The estimator gains are rational functions of the estimated PAR and are designed by minimizing the H_∞ norm from disturbances and measurement noises to estimation error over all the possible PARs. The design procedure is an optimization problem over polynomials that is numerically solved using SOS decomposition techniques.*

In the last years many processes in industry are controlled or supervised through sensors, actuators and controllers connected to a shared network (wired or wireless). One of the interesting control problems that arise in those scenarios is the state estimation from measurement samples that are acquired through a network. The main difficulties are the problems of packet dropout, network induced delays, or intermittent partial observations. Most of the proposals in the literature can be classified in two generic groups: KF based algorithms (e.g. [129, 122, 123]), in which the estimator implements a modified KF to compute on line the gains of an estimator, and off-line computed gains strategies (e.g. [119, 132, 76]) in which the estimator gains are previously computed and stored.

The use of a KF with irregular observations that follow a Bernoulli distribution was firstly studied in depth in [129], where the conditions for the existence of an estable estimator were addressed, demonstrating the existence of a critical value for the measurement samples arrival probability to get a bounded filter when dealing with transmission of a packet containing samples from several sensors. The main drawback is that the on-line computation of the gains requires a high computer power, and, furthermore, the algorithm does not give as a result a value of the bound of the estimation error.

On the other hand, the off-line computed gains approaches lead to a low computer cost algorithm and allow to obtain in advance a bound of the estimation error. Previous works (as [119, 132, 76, 86, 53]) propose a constant gain, or a set of constant gains, that are not a function of the packet dropout rate or the successful transmission probability. When these are not known in advance, or are time varying, the resulting observer is very conservative.

In this chapter, we address the design of a rational gain-scheduled observer for networks with packet dropout whose successful transmission ratio is unknown in advance and time-varying. The implemented observer gain at each instant is a function of an estimation of the packet arrival rate on the observer node, as a difference with

previous chapters. This leads to a better estimator performance with a slight increase in the computational cost. We perform the design assuring stochastic stability and H_∞ performance over the disturbance, noises and time-varying and uncertain packet dropout rate. Then, an LMI optimization problem is derived from an optimization over polynomial constraints that tries to minimize the state estimation error covariance for the overall packet successful transmission rate. The degree of the polynomials of the proposed Lyapunov function and the observer gains is a tuning parameter that can be selected as a compromise between the computational complexity of the optimization problem to be solved, and the achievable performance.

In order to overcome the optimization over polynomials, we use the sum-of-squares (SOS) approach (see [16, 113, 59, 99] and [80] or [113] for a tool that allows to implement these methods). The conceptual novelty introduced with respect to previous works with SOS methods is to use them to schedule the observer with the estimation of PAR that depends on the behavior of the network, which is known in real time, and as we shall see, enters on the Lyapunov function.

The chapter has the following structure: in Section 5.1 the system is defined including the characteristics of the network and the proposed state estimation algorithm. In Section 5.2 the proposed solution for the polynomial observer design is presented, including the necessary existing results about SOS decomposition. Finally, in Section 5.3 some examples show the validity of the approach.

5.1 Problem statement

5.1.1 System description

Let us assume a linear time invariant discrete time system defined by equations

$$x_{t+1} = Ax_t + Bu_t + B_w w_t, \tag{5.1a}$$

$$m_t = Cx_t + v_t, \tag{5.1b}$$

where $x \in R^n$ is the state, $u \in \mathbb{R}^{n_u}$ is the input, $w \in \mathbb{R}^{n_w}$ is the state disturbance, $m \in \mathbb{R}^{n_y}$ are the sampled measured outputs and $v \in \mathbb{R}^{n_y}$ the measurement noise. Throughout this chapter we assume that the control input is causally available at all times, Let us assume that the samples m_ta re encapsulated on a single packet m_t^e and transmitted through a network with packet dropout, and let us define the binary variable called availability factor of new data as

$$\alpha_t = \begin{cases} 0, & \text{if } m_t^e \text{ is not received,} \\ 1, & \text{if } m_t^e \text{ is received.} \end{cases} \tag{5.2}$$

Let us define the packet arrival rate (PAR) as the probability of having available new data at a given sampling time as

$$\beta = \mathbf{Pr}\{\alpha_t = 1\}, \quad \forall t \geq 0, \tag{5.3}$$

and the packet dropout rate (PDR) (its complementary) as the probability of having no new data at a given sampling time $P\{\alpha_t = 0\} = 1 - \mathbf{Pr}\{\alpha_t = 1\} = 1 - \beta$. Differently from the last chapters, in thi chapter the PAR is assumed to be non-stationary and, at each sampling time a time dependent probability β_t is defined as

$$\beta_t = \mathbf{Pr}\{\alpha_t = 1\}, \tag{5.4}$$

We assume that probability β_t can change slowly on time with a bounded rate of change as

$$\beta_t = \beta_{t-1} + \delta_t, \quad |\delta_t| \leq \bar{\delta}, \tag{5.5}$$

where δ_t is the change of rate and $\bar{\delta}$ its bound (assumed to be known). We also assume that a PDF $g(\beta_t)$ is previously known for the possible values of the probability β_t along time. The global packet availability rate will be given by

$$\beta = \mathbf{Pr}\{\alpha_t = 1, \forall t\} = \int_0^1 \beta_t g(\beta_t) \mathrm{d}\beta_t.$$

If this PDF is not available, the proposed method can be applied assuming a uniform function.

5.1.2 Proposed state estimation algorithm

The aim of this chapter is to define an state estimator that depends on the previous state estimation, on the availability of new data and on an estimation of the actual PAR as

$$\hat{x}_t = f_x(\hat{x}_{t-1}, u_{t-1}, \alpha_t, \hat{\beta}_t). \tag{5.6}$$

The binary variable α_t is available at each sampling period (simply checking that there are new measurements on the central), and we use it to estimate the actual PAR with a given estimator $\hat{\beta}_t = f_\beta(\hat{\beta}_t, \alpha_t)$. A simple estimator is the following first order filter

$$\hat{\beta}_t = a\,\hat{\beta}_{t-1} + (1-a)\alpha_t, \tag{5.7}$$

where $0 < a \lesssim 1$ is a tuning parameter that should produce soft variations of $\hat{\beta}_t$, but fast enough to fit the variations of β_t along time. The actual PAR estimation error is defined as

$$\tilde{\beta}_t = \beta_t - \hat{\beta}_t, \tag{5.8}$$

and we assume that, as a consequence of the chosen estimator f_β (i.e., the value chosen for a in the case of the first order filter) and of the bound on PAR variations δ_t, it is bounded by a known value $0 < \bar{\mu} < 1$ as

$$|\tilde{\beta}_t| \leq \bar{\mu}. \tag{5.9}$$

The estate estimation algorithm is computed as follows. Initially, the state is estimated in open loop

$$\hat{x}_t^- = A\hat{x}_{t-1} + Bu_{t-1}. \tag{5.10}$$

If the sample m_t^e is not available, the state estimation is the open loop one (i.e. $\hat{x}_t = \hat{x}_t^-$), but, if new data is available, $m_t^a = m_t^e$ when $\alpha_t = 1$, the state is updated by

$$\hat{x}_t = \hat{x}_t^- + L_t(m_t^a - C\hat{x}_t^-), \tag{5.11}$$

where L_t is the updating gain. As shown in previous chapters, we can relate L_t to the sampling scenario α_t to improve estimation performances. In this chapter, we relate L_t to the fundamental process behind the dropouts, i.e., to the PAR. As the real value of the PAR is not available, we relate L_t to its estimation, i.e., $L_t = L(\hat{\beta}_t)$.

This estimation algorithm can be rewritten including the availability factor α_t as

$$\hat{x}_t = A\hat{x}_{t-1} + Bu_{t-1} + \alpha_t\, L(\hat{\beta}_t)(m_t^e - C(A\hat{x}_{t-1} + Bu_{t-1})). \tag{5.12}$$

The state estimation error $\tilde{x}_t = x_t - \hat{x}_t$ can be easily derived, leading to

$$\tilde{x}_t = (I - \alpha_t L(\hat{\beta}_t)C)(A\tilde{x}_{t-1} + B_w w_{t-1}) - \alpha_t L(\hat{\beta}_t)v_t. \tag{5.13}$$

The aim of this chapter is to define a law for the state observer gain $L(\hat{\beta}_t)$ such that stability and performance in the presence of state disturbance and noise measurement is robustly achieved taking into account the possible PAR variations and the error on its estimation, i.e., for any β_t, $\hat{\beta}_t$ and δ_t fulfilling $\{\beta_t, \delta_t, \hat{\beta}_t\} \in S_1 \times S_2 \times S_3 \times S_4$ with

$$S_1 = \{\beta_t : 0 \leq \beta_t \leq 1\}, \tag{5.14a}$$
$$S_2 = \{\delta_t : |\delta_t| < \bar{\delta}\}, \tag{5.14b}$$
$$S_3 = \{\beta_t, \delta_t : 0 \leq \beta_t - \delta_t \leq 1\}, \tag{5.14c}$$
$$S_4 = \{\hat{\beta}_t : 0 \leq \hat{\beta}_t \leq 1\}, \tag{5.14d}$$
$$S_5 = \{\beta_t, \hat{\beta}_t : |\beta_t - \hat{\beta}_t| \leq \bar{\mu}\}\}. \tag{5.14e}$$

Membership to sets S_1, S_3 and S_4 are always fulfilled as the variables are probabilities (in the case of β_t and $\beta_{t-1} = \beta_t - \delta_t$) or the filtered value of a binary variable (in the case of $\hat{\beta}_t$).

5.2 Observer design

In this section we address the design procedure that allows to obtain the law $L(\hat{\beta}_t)$. First, we state a sufficient condition for the observer existence in terms of parameter-dependent matrix inequalities. Then we show that if we choose a Lyapunov function dependent polynomially on the PAR, and a rational gain function $L(\hat{\beta}_t)$, the problem can be solved with numerically efficient algorithms using the SOS approach. The degree of the polynomials is a design parameter to be chosen as a trade-off between achievable performance and complexity of the observer to be implemented.

The next theorem presents the observer design based on parameter-dependent matrix inequalities.

Theorem 5.1. *Let us assume that there exists a positive definite matrix depending on the PAR $P(\beta_t)$, two matrices depending on the estimated PAR $G(\hat{\beta}_t)$ and $X(\hat{\beta}_t)$ and two positive scalar functions depending on the PAR $\gamma_w(\beta_t)$ and $\gamma_v(\beta_t)$ such that the following matrix inequalities hold for any $\{\beta_t, \delta_t, \hat{\beta}_t\} \in S_1 \times S_2 \times S_3 \times S_4$*

$$P(\beta_t) \succ 0, \tag{5.15}$$

$$M(\beta_t, \hat{\beta}_t, \delta_t) = \begin{bmatrix} M_{11} & M_{12} & M_{13} & M_{14} \\ \star & M_{22} & M_{23} & 0 \\ \star & \star & M_{33} & 0 \\ \star & \star & \star & M_{44} \end{bmatrix} \succ 0, \tag{5.16}$$

with entries

$$
\begin{aligned}
M_{11} &= \beta_t \left(G(\hat{\beta}_t)^T + G(\hat{\beta}_t) - P(\beta_t) \right), \\
M_{12} &= \beta_t \left(G(\hat{\beta}_t) - X(\hat{\beta}_t) C \right) A, \\
M_{13} &= \beta_t \left(G(\hat{\beta}_t) - X(\hat{\beta}_t) C \right) B_w, \\
M_{14} &= \beta_t \, X(\hat{\beta}_t), \\
M_{22} &= P(\beta_t - \delta_t) - I - (1 - \beta_t) \, A^T P(\beta_t) A, \\
M_{23} &= -(1 - \beta_t) \, A^T P(\beta_t) B, \\
M_{33} &= \gamma_w(\beta_t) I - (1 - \beta_t) \, B^T P(\beta_t) B_w, \\
M_{44} &= \gamma_v(\beta_t).
\end{aligned}
$$

Then, if the observer gain is defined as $L(\hat{\beta}_t) = G(\hat{\beta}_t)^{-1} X(\hat{\beta}_t)$*, the following conditions are fulfilled: (i) under null disturbances, the system is asymptotically mean square stable; (ii) under null initial conditions, the state estimation error is bounded by*

$$
\mathbf{E}\{\|\tilde{x}\|^2_{\mathrm{RMS}}\} < \bar{\gamma}_w \|w\|^2_{\mathrm{RMS}} + \bar{\gamma}_v \|v\|^2_{\mathrm{RMS}}, \tag{5.17}
$$

with

$$
\bar{\gamma}_i = \int_0^1 g(\beta_t) \gamma_i(\beta_t) \mathrm{d}\beta_t, \qquad i = \{w, v\}. \tag{5.18}
$$

Proof. See Appendix C.5.1. ■

Remark 5.1. The previous theorem also states that, for a constant β_t, the bound achieved for the estimation error will be the one expressed by

$$
\|\tilde{x}\|^2_{\mathrm{RMS}} < \gamma(\beta_t) = \gamma_w(\beta_t) \|w\|^2_{\mathrm{RMS}} + \gamma_v(\beta_t) \|v\|^2_{\mathrm{RMS}}. \tag{5.19}
$$

The solvability of the previous condition (5.16) is infinite-dimensional, as it is the solution space, and the major difficulty is how to verify that condition over the entire parameter space. To approximate the infinite-dimensional functional space, we restrict matrices and functions to be polynomial functions of β_t, $\hat{\beta}_t$ and δ_t of a fixed order. Then, the computationally tractability of the SOS decomposition can be used to derive a numerical solution for the proposed PAR dependent gain.

5.2.1 Proposed optimization procedure

With the basis of the presented SOS decomposition in Appendix B, the following theorem presents a sufficient condition that allows to find numerically the parametric functions and matrices that assure the properties established in Theorem 5.1. We will use β to denote independent SOS variables representing de possible values of β_t.

Theorem 5.2. *Let us assume that there exist polynomial matrices*

$$
P(\beta) = \sum_{i=0}^{d_P} P_i \beta^i, \quad G(\hat{\beta}) = \sum_{i=0}^{d_G} G_i \hat{\beta}^i, \quad X(\hat{\beta}) = \sum_{i=0}^{d_X} X_i \hat{\beta}^i, \tag{5.20}
$$

polynomial functions

$$\gamma_w(\beta) = \sum_{i=0}^{d_w} \gamma_{w,i}\beta^i, \quad \gamma_v(\beta) = \sum_{i=0}^{d_v} \gamma_{v,i}\beta^i, \tag{5.21}$$

where d_i, $i = \{P, G, X, w, v\}$ denotes the order of the polynomial function, and that there also exist eight SOS polynomials s, and some vectors ζ, ν such that the following conditions hold[1]

$$\zeta^T P(\beta)\zeta - s_P(\beta,\zeta)\, h_1(\beta) \in \Sigma(\beta,\zeta), \tag{5.22a}$$

$$\nu^T M(\beta,\hat{\beta},\delta)\nu - s_{M1}(\beta,\hat{\beta},\delta,\nu)\, h_1(\beta) - s_{M2}(\beta,\hat{\beta},\delta,\nu)\, h_2(\delta) - s_{M3}(\beta,\hat{\beta},\delta,\nu)\, h_3(\beta,\delta),$$
$$- s_{M4}(\beta,\hat{\beta},\delta,\nu)\, h_4(\hat{\beta}) - s_{M5}(\beta,\hat{\beta},\delta,\nu)\, h_5(\beta,\hat{\beta}) \in \Sigma(\beta,\hat{\beta},\delta,\nu), \tag{5.22b}$$

$$\gamma_w(\beta) - s_w(\beta)\, h_1(\beta) \in \Sigma(\beta), \tag{5.22c}$$

$$\gamma_v(\beta) - s_v(\beta)\, h_1(\beta) \in \Sigma(\beta), \tag{5.22d}$$

$$s_P \in \Sigma(\beta,\zeta),\ , s_{M1,\ldots,M5}(\beta,\hat{\beta},\delta,\nu) \in \Sigma(\beta,\hat{\beta},\delta,\nu), \tag{5.22e}$$

$$s_w(\beta), s_v(\beta) \in \Sigma(\beta), \tag{5.22f}$$

being $M(\beta,\hat{\beta},\delta)$ the matrix defined in (5.16)*, and where polynomials $h_i(\beta,\hat{\beta},\delta)$ ($i = 1,\ldots,5$) are*

$$h_1(\beta) = \beta(1-\beta), \tag{5.23}$$

$$h_2(\delta) = \bar{\delta}^2 - \delta^2, \tag{5.24}$$

$$h_3(\beta,\delta) = (\beta-\delta)(1-\beta+\delta), \tag{5.25}$$

$$h_4(\hat{\beta}) = \hat{\beta}(1-\hat{\beta}), \tag{5.26}$$

$$h_5(\beta,\hat{\beta}) = \mu^2 - (\beta-\hat{\beta})^2. \tag{5.27}$$

Then, conditions of Theorem 5.1 are fulfilled.

(5.15)-(5.16) are fulfilled for any $\{\beta_t, \delta_t, \hat{\beta}_t\} \in S_1 \times S_2 \times S_3 \times S_4$, and, therefore, the stability condi

Proof. First note that each of the sets S_i ($i = 1,\ldots,5$) can be rewritten with its corresponding polynomial h_i as $S_i = \{\beta,\hat{\beta},\delta : h_i(\beta,\hat{\beta},\delta) \geq 0\}$. Then applying Lemma B.3 and Lemma B.4 it follows that the conditions on Theorem 5.1 are fulfilled for any $\beta = \beta_t$, $\hat{\beta} = \hat{\beta}_t$ and $\delta = \delta_t$.

■

In the above feasibility SOS problem ζ and ν are scalarization vectors used to transform polynomial matrices in polynomials (see Lemma B.4). The decision variables are matrices H_i, G_i, X_i and coefficients $\gamma_{w,i}$ and $\gamma_{v,i}$ plus the coefficients of the SOS polynomials $s\_$ whose degree has not been specified in the previous result. In order to state a feasible SOS problem, the degrees of these polynomials must be first defined. The simplest choice is to select degree zero, i.e., transforming polynomials $s\_$ on positive constants. In order to maximize the degrees of freedom of the previous problem, we choose

[1] The set of SOS polynomials in ζ is denoted by $\Sigma(\zeta)$.

the following degrees on the polynomials $s_{\_}$:

$$\deg\ s_P(\beta,\zeta) = \deg\left\{\beta^{\max\{d_P-2,0\}},\ \zeta^2\right\}, \tag{5.28a}$$

$$\deg\ s_{M1}(\beta,\hat{\beta},\delta,\nu) = \deg\left\{\beta^{\max\{d_\beta-2,0\}},\hat{\beta}^{d_{\hat{\beta}}},\delta^{d_P},\nu^2\right\}, \tag{5.28b}$$

$$\deg\ s_{M2}(\beta,\hat{\beta},\delta,\nu) = \deg\left\{\beta^{d_\beta},\hat{\beta}^{d_{\hat{\beta}}},\delta^{\max\{d_P-2,0\}},\nu^2\right\}, \tag{5.28c}$$

$$\deg\ s_{M3}(\beta,\hat{\beta},\delta,\nu) = \deg\left\{\beta^{\max\{d_\beta-2,0\}},\hat{\beta}^{d_{\hat{\beta}}},\delta^{\max\{d_P-2,0\}},\nu^2\right\}, \tag{5.28d}$$

$$\deg\ s_{M4}(\beta,\hat{\beta},\delta,\nu) = \deg\left\{\beta^{d_\beta},\hat{\beta}^{\max\{d_{\hat{\beta}}-2,0\}},\delta^{d_P},\nu^2\right\}, \tag{5.28e}$$

$$\deg\ s_{M5}(\beta,\hat{\beta},\delta,\nu) = \deg\left\{\beta^{\max\{d_\beta-2,0\}},\hat{\beta}^{\max\{d_{\hat{\beta}}-2,0\}},\delta^{d_P},\nu^2\right\}, \tag{5.28f}$$

$$\deg\ s_w(\beta) = \deg\ \beta^{\max\{d_w-2,0\}}, \tag{5.28g}$$

$$\deg\ s_v(\beta) = \deg\ \beta^{\max\{d_v-2,0\}}, \tag{5.28h}$$

where deg returns the maximum degree for each variable in the involved polynomial and

$$d_\beta = \max\{1+d_P, d_w, d_v\}, \quad d_{\hat{\beta}} = \max\{d_G, d_X\}. \tag{5.29}$$

The values of d_β and $d_{\hat{\beta}}$ refer to the degree of β and $\hat{\beta}$, respectively, in matrix $M(\beta,\hat{\beta},\delta)$. The degree of δ in $M(\beta,\hat{\beta},\delta)$ is always d_P. The idea is to assure that all the addends in problem (5.22) have the same degree on all the variables. Note that the problem stated in Theorem 5.2 does not involve products or inversions of decision variables and, therefore, it can be transformed into a tractable LMI problem.

Remark 5.2. If the RMS values of the disturbance and noises are assumed to be known, then the minimization of the sum

$$J = \int_0^1 g(\beta)(\gamma_w(\beta)\|w\|^2_{\mathrm{RMS}} + \gamma_v(\beta)\|v\|^2_{\mathrm{RMS}})d\beta$$

over constraints (5.22) leads to the gain-scheduled observer that minimizes the RMS value of the state estimation error that can be achieved with the polynomial approach. If the RMS values of the disturbances and noises are not available, then, they can be used as tuning parameters to achieve a given desired behavior. If the PFM $g(\beta)$ is not known, we can assume a uniform distribution.

Remark 5.3. The previous theorems assume that β can take values from 0 to 1. If the probability is known to belong to a range $\beta_{\min} < \beta < \beta_{\max}$ then the optimization can be changed straightforwardly to give less conservative results. This applies for example when the system is unstable but the pair (A, C) is detectable. In those cases, previous results, as [129], show that a necessary condition for the existence of a solution for the previous observer design procedure with a constant β_t is that $\beta_t \geq 1 - \frac{1}{\rho(A)^2}$ being $\rho(A) = \max_i(|\lambda_i(A)|)$ and $\lambda_i(A)$ the eigenvalues of matrix A. Therefore, when the system is unstable, it must be assumed that the network fulfills this bound.

5.3 Examples

Let us consider a stable LTI DTS defined by (5.1) with

$$A = \begin{bmatrix} 0.3147 & 0.4134 & -0.2215 \\ 0.4058 & 0.1324 & 0.0469 \\ -0.3730 & -0.4025 & 0.4575 \end{bmatrix}, \; B = B_w = \begin{bmatrix} 0.9649 \\ 0.1576 \\ 0.9706 \end{bmatrix},$$
$$C = \begin{bmatrix} 0.9572 & 0.4854 & 0.8003 \end{bmatrix},$$

with a sampling period of $T_s = 10ms$ and where $\|w\|^2_{\text{RMS}} = 0.25$ and $\|v\|^2_{\text{RMS}} = 0.04$ with zero mean.

Let us assume that the samples are acquired through a network where the PAR may vary in the range $0.1 \leq \beta_t \leq 0.9$, with a uniform distribution. We also assume that the maximum variation in one time instant is bounded by $\bar{\delta} = 10^{-6}$ (defined in (5.5)). In order to show the effectiveness of the proposed approach, a three hour simulation is carried out where the PAR decreases its value from 0.5 to 0.3 with the prescribed maximum rate. The tuning parameter of (5.7) has been heuristically fixed to $a = 0.9999$ and the maximum computed PAR estimation error is 0.0157 for the previous simulation. The bound $\bar{\mu} = 0.02$ (defined in (5.9)) is assumed for the observer design.

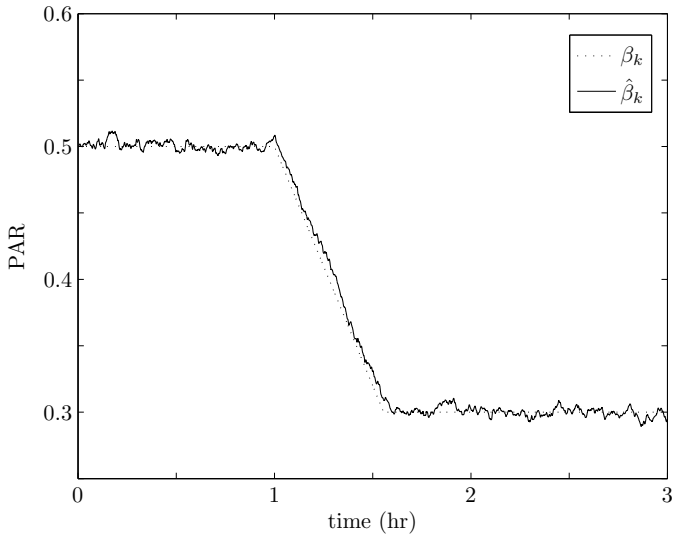

Figure 5.1: Evolution of the real PAR (β_t) and its estimation $\hat{\beta}_t$. Maximum estimation error obtained of 0.0157.

To evaluate the benefits of using a polynomial dependency on the PAR, four cases are considered depending on which variables $(P, G, X, \gamma_w, \gamma_v)$ depend polynomially on the PAR or not. Table 5.1 summarizes the cases, where the numbers represent the degree of the polynomial. Note that $L = G^{-1}X$, and hence, in case C1 the observer gain L is a rational function of the PAR, in C2 it is a polynomial one and in C3 it is simply a constant value. Finally C4 is used to analyze the convenience of using a dependency on the PAR in variables γ_w and γ_v. In this example, the degree of the polynomial has been

chosen to be 4, but in general, it can be selected as a compromise between performance and computation efforts (i.e., high degrees lead to better performances but imply a higher computational cost).

Table 5.1: Considered cases (polynomial degrees)

Case	d_P	d_G	d_X	d_w	d_v	J
C1	4	4	4	4	4	0.4619
C2	4	0	4	4	4	0.4672
C3	4	0	0	4	4	0.5907
C4	4	4	4	0	0	1.0614

Fig. 5.2 and Fig. 5.3 show the results of applying Remark 5.2 to the cases presented in Table 5.1. Case C2 is not included because it is almost coincident with case C1. This is an interesting issue, because the on-line computational cost of case C2 is lower than case C1, while leads to a similar performance. It can be appreciated from these figures that the use of an observer gain depending on the PAR improves the obtained performance with respect the constant gain case. However, the most significant improvement results from considering the variables γ_w and γ_v as polynomial functions of the PAR, instead of constant values.

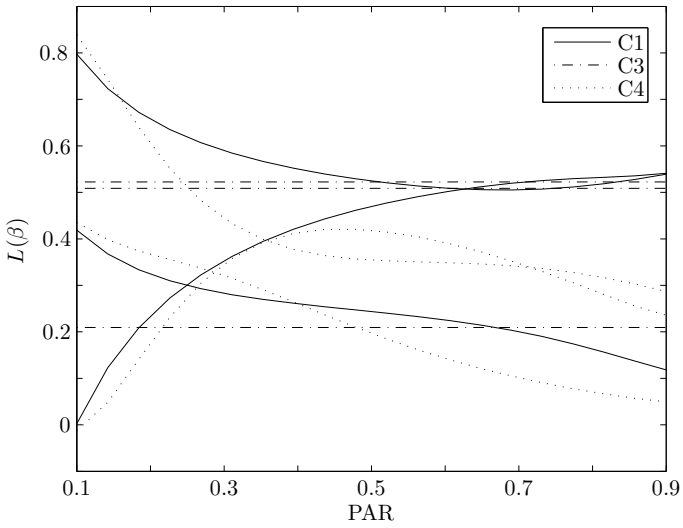

Figure 5.2: Design results. Elements of observer gain $L(\beta)$ as a function of β for the different cases.

Table 5.2 shows the value of $\|\tilde{x}\|^2_{\text{RMS}}$ during the proposed simulation, indicating the RMS during the instants of time in which β_t is constant, as well as the total RMS for the whole simulation. As it can be observed, when $\beta_t = 0.5$ the case C4 results in the worst performance because in its design γ_w and γ_v are constants and therefore the synthesis is not optimal for the whole range of the PAR. However, for $\beta_t = 0.3$ the worst performance is given by C3 due to the non dependency on the PAR in the observer

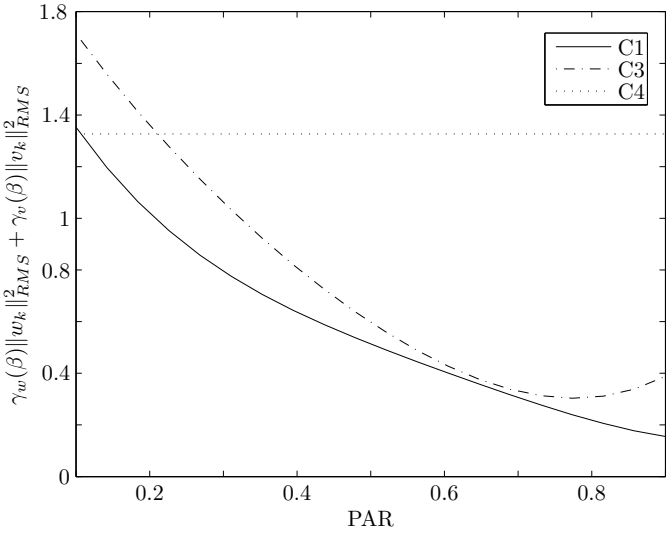

Figure 5.3: Design results. Obtained bound on $\|\tilde{x}\|^2_{\text{RMS}}$ as a function of β for the different cases.

gain. No significant difference appears between cases C1 (rational observer gain) and C2 (polynomial observer gain) leading always to the best performances. Table 5.2 also includes the achieved performances using the KF presented in [129], which improves the performance only in a 7% but with a higher on-line computational effort.

Table 5.2: Simulation Results

Case	$\|\tilde{x}\|^2_{\text{RMS}}$		
	$\beta_t = 0.5$	$\beta_t = 0.3$	all
C1	0.3751	0.5039	0.4371
C2	0.3798	0.5084	0.4395
C3	0.3910	0.6013	0.4901
C4	0.4616	0.5219	0.4854
[129]	0.3587	0.4734	0.4141

Comparing the results from Fig. 5.3 and Table 5.2, we appreciate that the bounds on $\|\tilde{x}\|^2_{\text{RMS}}$ obtained during the observer design for constant β_t are less conservative for the cases C1, C2 and C3, while the ones obtained for C4 are very conservative. This fact justifies the benefits of including a polynomial dependency on $\gamma_w(\beta_t)$ and $\gamma_v(\beta_t)$ in the observer design.

Finally Table 5.3 shows the trade-off between performance (J, see Remark 5.2) and the degree of the polynomials when the gain L is a rational function of the PAR (case C1).

Table 5.3: Polynomial degrees versus performances (case C1)

d	0	1	2	3	4
J	1.4029	0.6085	0.5251	0.4892	0.4619

5.4 Conclusions

In this chapter, we designed a rational gain-scheduled observer for systems whose samples are acquired through a network with packet dropout phenomena. We assumed that the probability of successful packet arrival is time-varying and unknown during the design procedure. We proposed an estimator for the PAR, and a state estimator with a rational gain that depends on the PAR. Sufficient conditions for the existence of that observer have been established leading to an optimization with SOS constraints that are traduced into a tractable LMI problem. The validity of the proposal has been demonstrated through an example, where we illustrated the trade-offs between achievable performance and the complexity of the rational observer.

This chapter and previous ones consider periodical measurement sample transmissions at each sampling instant t. The irregular data availability is due to dropouts and delays caused by transmitting through a network. In the next chapter we extend the obtained results to the case when measurement samples are transmitted sporadically, in order to reduce the network usage.

Chapter 6

Co-design of H-infinity jump observers for event-based measurements over networks

ABSTRACT: *This chapter presents a strategy to minimize the network usage and the energy consumption of wireless battery-powered sensors in the estimation problem over networks. The sensor nodes transmit with a periodic Send-on-Delta (SOD) approach, sending a new measurement sample when it deviates considerably from the previous sent one. We derive a jump observer whose gains are computed off-line and depend on the combination of available new measurement samples. We bound the observer performance as a function of the sending policies and then state the design procedure of the observer under fixed sending thresholds. We then bound the network usage and obtain an iterative tractable procedure for the design of the sending policy, guaranteeing a prescribed estimation performance.*

Previous chapters considered a periodic sensor sample transmission at each instant of time. However, sensor nodes can reduce their data transmissions with an event-based sending strategy (see [85]), what alleviates the the network data flow and increase the flexibility to include new devices over NCS (see [14, 93]).

State estimation plays a key role in NCS as the state of the plant is rarely directly measured for control purposes and because the sampled output measurements are irregularly available due to communication constraints or packet dropouts (see [14]). The approaches found in the literature to address the state estimation problem with event-based sampling can be classified depending on the sending policy, and on the communication or computational resources required on the sensor nodes. The authors in [95, 134] use a Send-on-Delta (SOD) strategy where the sensor node decides whether to send a new sample if the current acquired one differs more than a given threshold with respect to the last sent one. With those samples, the estimator node implements a modified KF that uses the last acquired data and modifies the update equation to account the lack of data by means of including a virtual noise. In the work [96] each node uses the integral of the difference between the last acquired sample and the last sent one to decide whether sending a new sample (Send-on-Area), while the authors in [128] combine SOD and time-triggered strategies in the sensor nodes. In other works like [6, 89] the authors include an state estimator in each sensor node to decide the sending of new data (output or state estimation), while in [144] the authors impose the sensor node to receive and process several information to decide whether it should send the sample.

Under the motivation of reducing the computational effort of the estimator and the sensor nodes, we use a jump linear estimator that at each instant uses a precomputed gain that depends on the availability of new samples, and the nodes implement a SOD strategy with fixed thresholds. With the aim of extending the approaches found in the literature

to a wider class of disturbances, we obtain the gains that guarantee an H_∞ attenuation level based on a LMI problem. With the aim of having less conservative results, we also obtain the range of probabilities of having new samples with the SOD mechanism. In this case we bound the H_∞ attenuation level for all the possible probabilities in the range with SOS techniques [16].

Some works have shown that there is a trade-off between communication rate and estimation quality [144]. The authors in [136, 19, 40, 56] named the problem of optimizing the network usage while assuring an estimation performance as the co-design problem. The works [128, 97] addressed this problem with the time-triggering condition, and [134] addressed it deciding the threshold levels of sensors implementing a SOD strategy. In the last work the authors modeled the network usage with a Gaussian probability distribution of the system outputs.

Motivated by extending the applicability of the co-design procedure to more general cases, we use the bounds on the probability of having new transmissions to measure the network usage, and to guarantee tight bounds of the achievable performance of the estimator.

This chapter is organized as follows. We define the problem in Section 6.1, and present the jump linear estimator design in 6.2. In Section 6.3, we present the co-design iterative procedure. Section 6.4 explores some examples that shows the main differences between the approaches and, finally, in Section 6.5 we summarize the main conclusions.

6.1 Problem Statement

Consider a NCS that updates the control action synchronously with the output measurement and the process model

$$x[t+1] = A\,x[t] + B\,u[t] + B_w\,w[t], \tag{6.1a}$$

$$m[t] = C\,x[t] + v[t], \tag{6.1b}$$

where $x \in \mathbb{R}^n$ is the state, $u \in \mathbb{R}^{n_u}$ is the known input vector, $w \in \mathbb{R}^{n_w}$ is the unmeasurable state disturbance vector, $m \in \mathbb{R}^{n_y}$ is the sampled measured output, and $v \in \mathbb{R}^{n_y}$ the measurement noise. Throughout this chapter we assume that the control input is causally available at all times, see Fig. 6.1.

Let us remember the SOD mechanism presented in Section 2.5. Let us assume that the sensor node s has sent a sample to the central unit through the communication network at time instant $t = t_{k_s}$ and we call it $m^e_{s,k_s} = m^e_s[t_{k_i}]$ (where k_s enumerates the sent data from sensor s). Then, a new sample will be sent if the following condition holds

$$|m_s[t] - m^e_{s,k_s}| \geq \Delta_s, \;\; \Delta_s > 0, \;\; t > t_{k_s} \tag{6.2}$$

where Δ_s is the allowed deviation threshold. In that case, the sensor sends the (k_s+1)-th measurement, and $m^a_s[t]$ becomes m^e_{s,k_s+1}.

The central unit implements a state estimator that estimates the system state using the acquired samples and the equations

$$\hat{x}[t^-] = A\,\hat{x}[t-1] + B\,u[t-1], \tag{6.3a}$$

$$\hat{x}[t] = \hat{x}[t^-] + L[t](m^a[t] - C\,\hat{x}[t^-]), \tag{6.3b}$$

where $L[t]$ is the observer gain. $m^a[t]$ includes both the information of the received samples (m^e_{s,k_s}) and the information of the measurement uncertainty. The s-th component of the acquired samples $m^a[t]$ at the central unit remains constant while there is no new samples from sensor s, i.e.,

$$m^a_s[t] = m^e_{s,k_s}, \qquad t_{k_s} \leq t < t_{k_s+1}$$

and we model its relation with the actual state as

$$m^a_s[t] = \begin{cases} C_s\, x[t] + v_s[t], & t = t_{k_s}, \\ C_s\, x[t] + v_s[t] + \delta_s[t], & t_{k_s} < t < t_{k_s+1}, \end{cases} \tag{6.4}$$

being C_s the s-th row of matrix C, and where $\delta_s[t]$ is a virtual noise fulfilling $\|\delta_s\|_\infty < \Delta_s$, as we have $|m_s[t] - m^e_{s,k_s}| < \Delta_i$ for $t_{k_s} < t < t_{k_s+1}$.

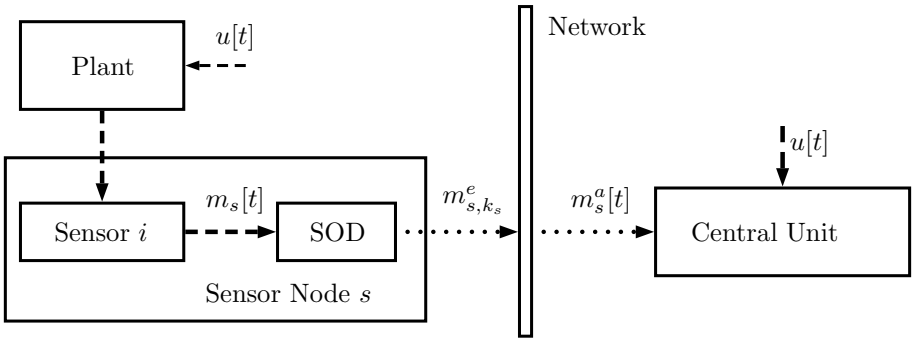

Figure 6.1: Send-On-Delta based networked state estimator.

Let us define $\alpha_s[t]$ as the availability factor for each sensor s, that is a binary variable that takes a value of 1 if there is a new sample received from the sensor node s and 0 otherwise. The availability matrix is the matrix including in its diagonal the availability factor of each sensor, i.e.,

$$\alpha[t] = \text{diag}\{\alpha_1[t], \ldots, \alpha_{n_y}[t]\}.$$

We then model the available samples as

$$m^a[t] = C\, x[t] + v[t] + (I - \alpha[t])\, \delta[t], \tag{6.5}$$

with $\delta[t] = [\delta_1[t] \ \cdots \ \delta_{n_y}[t]]^T$, $\delta_s[t] \in (-\Delta_s, \Delta_s)$.

Matrix $\alpha[t]$ can take different values depending on the sample successful transmission possibilities and they belong to a known set

$$\alpha[t] \in \Xi = \{\eta_0, \eta_1, \ldots, \eta_q\}, \tag{6.6}$$

where η_i denotes a possible combination of available samples at each instant t. We recall those combinations as sampling scenarios. Matrix η_0 denotes the scenario with unavailable samples and q the number of different scenarios with available samples. In the general case, any combination of available sensor samples is possible, leading to $q = 2^{n_y} - 1$.

The first of our goals is to define an observer that uses the scarcely received distributed data and the uncertainty knowledge. We propose the observer equation (6.3) and define

the gain observer law $L[t]$ as

$$L[t] = L(\alpha[t]), \tag{6.7a}$$
$$L(\alpha[t]) = L_j, \quad \text{if } \alpha[t] = \eta_j, \tag{6.7b}$$

what leads to a jump observer. The gains take, in general, $q+1$ different values within a predefined set, i.e.,

$$L(\alpha[t]) \in \mathcal{L} = \{L_0, \ldots, L_q\}. \tag{6.8}$$

The gains are computed off-line once, and the observer chooses the applicable gain depending on the availability of new samples (see [130, 26] for other jump observers applicable on NCS).

With the estimator defined by (6.3) and (6.7), we obtain the state estimation error dynamics given by

$$\tilde{x}[t] = \mathcal{A}(\alpha[t])\tilde{x}[t-1] + \mathcal{B}(\alpha[t])\xi[t], \tag{6.9}$$
$$\xi[t] = \begin{bmatrix} w[t-1]^T & v[t]^T & \delta[t]^T \end{bmatrix}^T,$$

with $\tilde{x}[t] = x[t] - \hat{x}[t]$, and

$$\mathcal{A}(\alpha[t]) = (I - L(\alpha[t])C)A,$$
$$\mathcal{B}(\alpha[t]) = \begin{bmatrix} (I - L(\alpha[t])C)B_w & -L(\alpha[t]) & -L(\alpha[t])(I - \alpha[t]) \end{bmatrix}.$$

As we restrict $L(\alpha[t])$ to take $q+1$ different values depending on the value of matrix $\alpha[t]$, we get a jump linear system with discrete state $\alpha[t]$ and with a finite number of modes.

The second of our goals is to design the observer gains and the thresholds Δ_s that minimize the network usage while guaranteeing a predefined estimation performance. The network usage is proportional to the rate in which (6.2) occurs, so we achieve this goal by minimizing a cost function related to the sending thresholds Δ_s. In this chapter, we present alternatives to bound the estimator performance and the network usage depending on Δ_s. For each of them we calculate the minimum probability of receiving a sample and the maximum variance of the resulting virtual noise $\delta[t]$.

We reformulate the main objective of this chapter as the simultaneous design of the $q+1$ gains L_i and thresholds Δ_s that minimize the network usage, at the same time that guarantee a given bound on the estimation error.

6.2 Observer design

We present two jump observer design approaches for SOD policy with fixed Δ_s that assure stability and H_∞ attenuation level. We propose first a deterministic strategy that does not require any assumption on the output statistics. Then, we propose different assumptions about the statistical information of the output, and then develop a stochastic strategy that allows us to relax the bound on the achievable performance.

6.2.1 Deterministic approach

Theorem 6.1. *Let us consider that observer* (6.3) *with gain* (6.7) *estimates the state of system* (6.1) *that sends its sampled outputs with the SOD policy. If there exist matrices* P_j, Q_j, X_j $(j = 0, 1, \ldots, q)$, *and positive values* γ_w, γ_{v_s} *and* γ_{δ_s} $(s = 1, \ldots, n_y)$ *such that* $P_j = P_j^T \succ 0$, *and for all* $i, j \in \{0, \ldots, q\} \times \{0, \ldots, q\}$[1]

$$\Phi_{j,i} = \begin{bmatrix} Q_j + Q_j^T - P_j & \star & \star & \star & \star \\ ((Q_j - X_j C)A)^T & P_i - I & \star & \star & \star \\ ((Q_j - X_j C)B_w)^T & 0 & \gamma_w I & \star & \star \\ -X_j^T & 0 & 0 & \Gamma_v & \star \\ -(I - \eta_j)X_j^T & 0 & 0 & 0 & \Gamma_\delta \end{bmatrix} \succ 0, \tag{6.10}$$

being $\Gamma_v = \mathrm{diag}\{\gamma_{v_1}, \ldots, \gamma_{v_{n_y}}\}$, $\Gamma_\delta = \mathrm{diag}\{\gamma_{\delta_1}, \ldots, \gamma_{\delta_{n_y}}\}$, *then, defining the observer gains as* $L_j = Q_j^{-1} X_j$ $(j = 0, \ldots, q)$, *the following conditions are fulfilled: under null disturbances, the system is asymptotically stable, and, under null initial conditions, the state estimation error is bounded by*

$$\|\tilde{x}\|_{RMS}^2 < \gamma_w \|w\|_{RMS}^2 + \sum_{s=1}^{n_y} \gamma_{v_s} \|v_s\|_{RMS}^2 + \sum_{s=1}^{n_y} \gamma_{\delta_s} \|\delta_s\|_{RMS}^2. \tag{6.11}$$

Proof. See Appendix C.6.1. ■

6.2.2 Stochastic approach

The previous theorem leads to conservative results due to the consideration of all the possible sequences of new data reception with the same probability. For instance, it can respond satisfactorily to the situation of acquiring just a first samples at the start-up of the observer and then working indefinitely with that unique measurement. If the disturbances and noises are not negligible, we can assume that there is a small probability of acquiring new data, and that is the key in the stochastic approach to reduce the conservativeness. The probability of having available new data at a given sampling instant is

$$\beta_s = \mathbf{Pr}\{\alpha[t] = 1\} = \mathbf{Pr}\{m_s[t] - m_{s,k_s}^e| \geq \Delta_s\}, \quad t > t_{k_s}.$$

The difference $m_s[t] - m_{s,k_s}^e$ depends on the achieved state $x[t_{k_s}]$ during the last sent measurement, the inputs, disturbances and number of elapsed time instants from t_{k_s}, let us call it N, as

$$m_s[t] - m_{s,k_s}^e = m_s[t_{k_s} + N] - m_{s,k_s}^e =$$
$$C_s \left(A^N x[t_{k_s}] + \sum_{j=0}^{N-1} A^{N-1-j} (B\, u[t_{k_s} + j - 1] + B_w w[t_{k_s} + j]) \right) + v[t_{k_s} + N] - v[t_{k_s}].$$

The dependency of that difference on the inputs leads us to a non-stationary probability that can change at every sampling instant, i.e.,

$$\beta_s[t] = \mathbf{Pr}\{|m_s[t] - m_{s,k_s}^e| \geq \Delta_s\}, \quad t > t_{k_s}.$$

[1] the symbol $\star$ refers to the required element to make the matrix symmetric.

As the difference include the stochastic values $w[t]$ and $v[t]$, we assume that the probability belongs to the set

$$\beta_s[t] \in \mathcal{S}_s = \{\beta_s[t] : \beta'_s \leq \beta_s[t] \leq 1\}.$$

$\beta_s[t] = 1$ applies when the control action or the state evolution are sufficiently high to assure a new samples transmission. $\beta_s[t] = \beta'_s$ applies during the less excited time instants (with $x[t_{k_s}] = 0$ and $u[t] = 0$ for $t \geq t_{k_s}$) that leads to the less favorable scenario to acquire new data, when only the disturbance and noise excite the SOD mechanism. If we choose $\beta'_i = 0$ we face again the deterministic approach, but choosing $\beta'_s > 0$ implies assuming that there is at least a small probability of acquiring new data, thus reducing conservatism.

In this chapter, we choose the lower bound β'_s as an explicit function of Δ_s. We first note that during the less excited time instants we have the difference

$$m_s[t] - m^e_{s,k_s} = C_s \sum_{j=0}^{N-1} A^{N-1-j} B_w w[t_{k_s} + j] + v[t_{k_s} + N] - v[t_{k_s}].$$

The lowest probability of having a new sample is in the first new instant, i.e., when $N = 1$. Therefore, we characterize now the lower bound of the probability of having a new sample with the difference

$$m_s[t] - m^e_{s,k_s} = C_s B_w w[t_{k_s}] + v[t_{k_s} + 1] - v[t_{k_s}],$$

and then compute the probability of having new samples from that sensor at instant $t = t_{k_s} + 1$ with law (6.2). This probability is tedious to obtain as it requires to obtain the density function of the sum of several signals with different distribution laws. For this reason, we present a simplification of the computation of the lower bound β'_s that allows us to relate it with Δ_s with tractable expressions. We compute an approximation of β'_s with two different assumptions on the outputs (proofs are given in the Appendix C.6):

- If we assume symmetrically bounded disturbances and noises, we can bound the difference $m_s[t] - m^e_{s,k_s}$ (in the less excited scenario) within $[-r_s, r_s]$ with

$$r_s = \|C_s B_w w\|_\infty + 2\|v\|_\infty. \tag{6.12}$$

  Expression $\|C_s B w\|_\infty$ $(s = 1, \ldots, n_y)$ can be computed as

$$\|C_s B_w w\|_\infty = \sum_{j=1}^{n_w} \left(\sum_{i=1}^{n} |C_{s,k} B_{w_{i,j}}| \right) ||w_j||_\infty.$$

  with w_j the j-th element of vector w, and $\|w_j\|_\infty$ and $\|v\|_\infty$ are assumed to be known. If the outputs are uniformly distributed and fulfill $m_s[t] - m^e_{s,k_s} \in [-r_s, r_s]$ the probability of having a new measurement is bounded by

$$\beta_s[t] = \mathbf{Pr}\{|m_s[t] - m^e_{s,k_s}| \geq \Delta_s\} > \beta'_s = \frac{1}{r_s^2}(r_s - \Delta_s)^2. \tag{6.13}$$

- If the disturbances and noises are distributed with covariances W and V_s and they have zero mean, in the less excited scenario we have that the difference $m_s[t] - m^e_{s,k_s}$ is distributed with variance

$$\sigma_s^2 = C_s B_w W B_w^T C_s^T + 2V_s. \tag{6.14}$$

If our knowledge is the RMS norm of vector w and noises v_s, we can bound σ_s^2 as

$$\sigma_s^2 \leq \mathrm{tr}(B_w^T C_s^T C_s B_w)\|w\|_{\mathrm{RMS}}^2 + 2\|v_s\|_{\mathrm{RMS}}^2. \tag{6.15}$$

If we assume that the difference between two consecutive samples follow a normal distribution with zero mean and variance σ_s^2, the probability of having a new measurement is bounded by

$$\beta_s[t] = \mathbf{Pr}\{|m_s[t] - m_{s,k_s}^e| \geq \Delta_s\} > \beta_s' = 1 - \mathrm{erf}\left(\frac{\Delta_s}{\sqrt{2}\sigma_s}\right), \tag{6.16}$$

being $\mathrm{erf}(x) = \frac{2}{\sqrt{\pi}}\int_0^x e^{-t^2}\mathrm{d}t$ the error function.

The probability of obtaining a sampling scenario η_j $(j = 1, \ldots, q)$ is also non-stationary and is given by

$$p_j[t] = \mathbf{Pr}\{\alpha[t] = \eta_j\} = \prod_{\substack{s=1 \\ \forall \eta_{j,s}=0}}^{n_y} (1 - \beta_s[t]) \prod_{\substack{s=1 \\ \forall \eta_{j,s}=1}}^{n_y} \beta_s[t], \tag{6.17}$$

where $\eta_{j,s}$ refers to the s-th diagonal entry of η_j. The probability of having no measurement available at t is given by

$$p_0[t] = \mathbf{Pr}\{\alpha[t] = \eta_0\} = \prod_{s=1}^{n_y}(1 - \beta_s[t]), \tag{6.18}$$

and the probability of sending some samples is $1 - p_0[t]$.

With the probabilities of the sampling scenarios we can obtain the set of gains that assure an attenuation level for any probability within the set.

Theorem 6.2. *Let us consider that observer* (6.7) *estimates the state of system* (6.1) *that sends its sampled outputs with the SOD policy. Consider that there exist matrices* $P = P^T \succ 0$, Q_j, X_j $(j = 0, \ldots, q)$, *and positive values* γ_w, γ_{v_s} *and* γ_{δ_s} $(s = 1, \ldots, n_y)$ *such that for any* $\{\beta_1, \ldots, \beta_{n_y}\} \in \mathcal{S}_1 \times \mathcal{S}_2 \cdots \times \mathcal{S}_{n_y}$

$$\Psi(\beta) = \begin{bmatrix} M_1 & \star & \star & \star & \star \\ M_2 & P - I & \star & \star & \star \\ M_3 & 0 & \gamma_w I & \star & \star \\ M_4 & 0 & 0 & \Gamma_v & \star \\ M_5 & 0 & 0 & 0 & \Gamma_\delta \end{bmatrix} \succ 0, \tag{6.19}$$

where

$$\begin{aligned}
&M_1 = \mathrm{diag}\{p_0(Q_0 + Q_0^T - P), \ldots, p_q(Q_q + Q_q^T - P)\},\\
&M_2 = [p_0\bar{\mathcal{A}}_0^T \ \cdots \ p_q\bar{\mathcal{A}}_q^T], \quad M_3 = [p_0\bar{\mathcal{B}}_0^T \ \cdots \ p_q\bar{\mathcal{B}}_q^T],\\
&M_4 = [-p_0X_0^T \ \cdots \ -p_qX_q^T],\\
&M_5 = [-p_0(I - \eta_0)X_0^T \ \cdots \ -p_q(I - \eta_q)X_q^T],\\
&\bar{\mathcal{A}}_j = (Q_j - X_jC)A, \quad \bar{\mathcal{B}}_j = (Q_j - X_jC)B_w, \ j = 0, \ldots, q,\\
&\Gamma_v = \mathrm{diag}\{\gamma_{v_1}, \ldots, \gamma_{v_{n_y}}\}, \quad \Gamma_\delta = \mathrm{diag}\{\gamma_{\delta_1}, \ldots, \gamma_{\delta_{n_y}}\},
\end{aligned}$$

and

$$p_j = \prod_{\substack{s=1 \\ \forall \eta_{j,s}=0}}^{n_y} (1-\beta_s) \prod_{\substack{s=1 \\ \forall \eta_{j,s}=1}}^{n_y} \beta_s. \tag{6.20}$$

Then, if the observer gains are defined as $L_j = Q_j^{-1} X_j$ $(j = 0, \ldots, q)$*, the system is asymptotically mean square stable and, under null initial conditions, the state estimation error is bounded by*

$$\|\tilde{x}\|_{RMS}^2 < \gamma_w \|w\|_{RMS}^2 + \sum_{s=1}^{n_y} \gamma_{v_s} \|v_s\|_{RMS}^2 + \sum_{s=1}^{n_y} \gamma_{\delta_s} \|\delta_s\|_{RMS}^2 \tag{6.21}$$

Proof. See Appendix C.6.3.

■

In order to solve numerically the previous problem we use the sum of squares (SOS) decomposition ([16, 109]) to define sufficient conditions to accomplish with the previous guaranteed performance (see Appendix B). We will use β_s and $\beta = [\beta_1 \ \cdots \ \beta_{n_y}]$, to denote independent SOS variables representing de possible values of $\beta_s[t]$ and $\beta[t] = [\beta_1[t] \ \cdots \ \beta_{n_y}[t]]$ for all t.

Theorem 6.3. *Let us assume that there exist matrices* $P = P^T \succ 0$*,* Q_j*,* X_j $(j = 0, \ldots, q)$*, positive values* γ_w*,* γ_{v_s} *and* γ_{δ_s} $(s = 1, \ldots, n_y)$ *and SOS polynomials* $s_s(\beta, z)$ *of fixed degree (with* z *a vector of proper dimensions) such that*[2]

$$\nu^T \Psi(\beta) \nu - \sum_{s=1}^{n_y} s_s(\beta, \nu) h(\beta_s) \in \Sigma(\beta, \nu), \tag{6.22}$$

with

$$h(\beta_s) = (\beta_s - \beta_s')(1 - \beta_s) \tag{6.23}$$

and $\beta = [\beta_1 \ \cdots \ \beta_{n_y}]$*. Then, conditions of Theorem 6.2 are fulfilled.*

Proof. First note that each of the sets $\mathcal{S}_s$ $(i = 1, \ldots, n_y)$ can be rewritten with its corresponding polynomial h_s as $\mathcal{S}_s = \{\beta_s : h(\beta_s) \geq 0\}$. Then, applying Lemmas B.3 and B.4 in Appendix B, it follows that the conditions on Theorem 6.2 are fulfilled for any $\beta_s = \beta_s[t]$.

■

In the above feasibility SOS problem ν is scalarization vectors used to transform the polynomial matrix in polynomial (see Lemma B.4). The decision variables are matrices P, Q_j, X_j and scalars γ_w, γ_{v_s} and γ_{δ_s} plus the coefficients of the SOS polynomials s_s. In order to maximize the degrees of freedom of the previous problem, we choose the following degrees on the polynomials s_s:

$$\deg \ s_s(\beta, \nu) = \deg \left\{ \beta_s^{\max\{n_y-3,0\}}, \beta_{i \neq s}^{\max\{n_y-1,0\}}, \nu^2 \right\}. \tag{6.24}$$

The idea is to assure that all the addends in problem (6.22) have the same degree on all the variables.

[2]The set of SOS polynomials in x is denoted by $\Sigma(x)$.

6.2.3 Optimization design procedure

If we know the values of $\|\delta_s\|_{\text{RMS}}$, $\|v_s\|_{\text{RMS}}$ and $\|w\|_{\text{RMS}}$, the optimization problem

$$\begin{aligned} \text{minimize} \quad & \gamma_w \|w\|_{RMS}^2 + \sum_{s=1}^{n_y} \gamma_{v_s} \|v_s\|_{RMS}^2 + \sum_{s=1}^{n_y} \gamma_{\delta_s} \|\delta_s\|_{RMS}^2 \\ \text{subject to} \quad & \Theta \succ 0, \end{aligned} \tag{6.25}$$

leads to the jump observer that minimizes the RMS value of the state estimation error for that assumption, where $\Theta = \Phi_{j,i}$ (6.10) for the deterministic approach and $\Theta = \Psi(\beta)$ (6.19) for all $\beta_s \in \mathcal{S}_s$ for the stochastic one. If the RMS values of the disturbances are unavailable, they can be used as tuning parameters to achieve a desired behavior.

The previous optimization procedure also applies when we can only bound the disturbances and sensor noises by the norms $\|w\|_\infty$ of $\|v_s\|_\infty$, as the RMS norm is bounded by the ℓ_∞ norm: $\|w\|_{\text{RMS}} < \|w\|_\infty$ and $\|v_s\|_{\text{RMS}} < \|v_s\|_\infty$. In this case, we substitute the RMS norm of the previous optimization procedure by its corresponding ℓ_∞ norm.

In the deterministic approach, we have the bound $\|\delta_s\|_{\text{RMS}} < \|\delta_s\|_\infty < \Delta_s$ from the definition of the virtual noise signal. Under the assumption of uniform distribution of $\delta_s[t]$, using the bound $\|\delta_s\|_{\text{RMS}} < \Delta_s/\sqrt{3}$ relaxes the optimization problem. This distribution assumption is not hard as we assume it over the virtual noise, as generally found in the literature [134].

In the stochastic approach, we compute a bound on $\|\delta_s\|_{\text{RMS}}^2$ under the argument of the less excited instant and the same assumptions as in the probabilities computation (the proofs are in Appendix C.6):

- If we assume that the outputs are uniformly distributed and fulfill $m_s[t] - m_{s,k_s}^e \in [-r_s, r_s]$, we bound the RMS norm with

$$\|\delta_s\|_{\text{RMS}}^2 < \sigma_{\delta_s}^2 = \frac{2\Delta_s^3}{r_s^2}\left(\frac{r_s}{3} - \frac{\Delta_s}{4}\right). \tag{6.26}$$

- If we assume that the difference $m_s[t] - m_{s,k_s}^e$ is normally distributed with zero mean and variance σ_s^2 we bound the RMS norm with

$$\|\delta_s\|_{\text{RMS}}^2 < \sigma_{\delta_s}^2 = \sigma_s^2 \text{erf}\left(\frac{\Delta_s}{\sqrt{2}\sigma_s}\right) - \frac{\sqrt{2}\Delta_s\sigma_s}{\sqrt{\pi}} e^{\frac{-\Delta_s^2}{2\sigma_s^2}}. \tag{6.27}$$

If the system outputs do not follow the previous distributions, we use the values r_s and σ_s as tuning parameters. In that case, we must choose sufficiently small values r_s and σ_s to assure that the computed probability of having new measurements is below the RMS norm of the real virtual noise, and such that the computed variance for the virtual noise is higher than the real one. With that choice, we can at least compute a tightener upper bound of the state estimation error than the one obtained with the deterministic approach.

In any of the previous design approaches we can reduce the computational cost of the observer implementation by means of imposing some restrictions on the gain matrices. We achieve the lower computational cost when the matrices are forced to be equal, thus $L_s = L_j$ for all $i, j = 1, \ldots, q$. This can be achieved imposing equality constraints over matrices Q_j and matrices X_j in problems (6.10) and (6.19).

6.3 Observer co-design

Once we have developed the design procedure to minimize the estimation error for a given SOD policy, we now address the minimization of the network usage guaranteeing a desired estimation error. We first propose the cost indexes to measure the network usage.

For the deterministic approach, without statistical information of the outputs, we propose the index

$$J(\Delta_{1:n_y}) = \sum_{s=1}^{n_y} \frac{g_s}{\Delta_s} \tag{6.28}$$

where g_s are some free weighting factors, that can be used to account for the different range of variation of the different sensors, and $\Delta_{1:n_y} = [\Delta_1 \ \cdots \ \Delta_{n_y}]$.

For the stochastic approach, we propose to use as the cost index, the probability of network usage in the lowest excitation case, that is:

$$J(\Delta_{1:n_y}) = 1 - p_0 = 1 - \prod_{s=1}^{n_y} (1 - \beta'_s(\Delta_s)) \tag{6.29}$$

where $\beta'_s(\Delta_s)$ $(i = 1, \ldots, n_y)$ depends on Δ_s by means of (6.13) or (6.16).

The actual probability of network usage will be close to this cost index only in the case of the lowest excitation (when the change of the output is minumim). When the output change is larger (for example when the input u changes), the probability of network usage will be higher. However, this network usage will be proportional to the cost index, and hence, minimizing the cost index results in minimizing the network usage for the desired estimation error in any case.

We then obtain the observer that assures a prescribed performance and minimizes the network usage $J(\Delta_{1:n_y})$ by solving the following optimization problem:

$$\begin{aligned} &\text{minimize} && J(\Delta_{1:n_y}) \\ &\text{subject to} && \Theta(\Delta_{1:n_y}) \succ 0, \\ & && \gamma_w \left\|w\right\|^2_{\text{RMS}} + \sum_{s=1}^{n_y} \left(\gamma_{v_s} \left\|v_s\right\|^2_{\text{RMS}} + \gamma_{\delta_s} \sigma^2_{\delta_s}(\Delta_{1:n_y})\right) \leq \left\|\tilde{x}\right\|^2_{\text{RMS,max}}. \end{aligned} \tag{6.30}$$

The new decision variable Δ_s appears both on the cost index and in the definition of $\sigma^2_{\delta_s}$ used to bound $\|\delta_s\|^2_{\text{RMS}}$. In the deterministic approach, we express $J(\Delta_{1:n_y})$ as (6.28), $\Theta(\Delta_{1:n_y}) = \Phi_{j,i}$ as in (6.10), and we use the bound $\sigma^2_{\delta_s}(\Delta_{1:n_y}) = \Delta^2_s$. Under the assumption of uniform distribution of $\delta_s[t]$, we can relax the problem using the bound $\sigma^2_{\delta_s}(\Delta_{1:n_y}) = \Delta^2_s/3$.

In the stochastic approach, we express $J(\Delta_{1:n_y})$ as (6.29), $\Theta(\Delta_{1:n_y}) = \Psi(\Delta_{1:n_y})$ as (6.19), and we express $\sigma^2_{\delta_s}(\Delta_{1:n_y})$ as (6.26) or (6.27), depending on the output assumption. In this case Δ_s appears in the bound of the probabilities β_s for which $\Psi(\beta)$ in (6.19) must be positive definite.

The optimization problem (6.30) is nonlinear in the variables Δ_s, but reduces to a LMI problem if we fix the values of Δ_s. Some of the approaches to solve this nonlinear optimization are brute force with a griding approach over Δ_s, heuristic optimization with genetic algorithms, and greedy algorithms. If we use a genetic algorithm and the

stochastic approach, the optimization problem can be written as

$$\begin{aligned}
&\text{minimize} \quad J(\Delta_{1:n_y}) \\
&\text{subject to} \quad x^\star(\Delta_{1:n_y}) - \|\tilde{x}\|^2_{RMS,\max} \leq 0, \\
&\qquad x^\star(\Delta_{1:n_y}) = \left\{ \begin{array}{l} \text{minimize } \gamma_w \|w\|^2_{\text{RMS}} + \sum_{s=1}^{n_y} (\gamma_{v_s} \|v_s\|^2_{\text{RMS}} + \gamma_{\delta_s} \sigma^2_{\delta_s}(\Delta_s)) \\ \text{subject to } \ \Theta(\Delta_{1:n_y}) \succ 0 \end{array} \right.
\end{aligned} \tag{6.31}$$

In this chapter, we propose a greedy algorithm (similar to the one proposed in Section 4.5) as an alternative to the previous optimization problem. The greedy algorithm is as follows.

Algorithm 6.1. Greedy algorithm.

Step 1 Take a small $\epsilon > 0$. Take an initial small $\Delta^0_s \gtrsim 0$ $(s = 1, \ldots, n_y)$ such that $\|\tilde{x}\|_{\text{RMS}} < \|\tilde{x}\|_{RMS,\max}$ is achievable. Set $k = 0$ and $\Delta^k_i = \Delta^0_i$ and $J^0 = J(\Delta^0_{1:n_y})$.

Step 2 Set $k = k + 1$ and $J^k = J^{k-1} - \epsilon$.

Step 3 For $s = 1$ to n_y repeat:
Set $\Delta_j = \Delta^{k-1}_j$, $j \neq s$.
Set $\Delta_s = \Delta^k_s = \arg\{J^k = J(\Delta_{1:n_y})\}$
Compute $\sigma^2_{\delta_j} = \sigma^2_{\delta_j}(\Delta_j)$, $j = 1, \ldots, n_y$.
Compute[3] $\beta'_j = \beta'_j(\Delta_j)$, $j = 1, \ldots, n_y$, and p_l, $l = 0, \ldots, q$.
Solve optimization problem (6.25).
Store $x^\star_s = \gamma_w \|w\|^2_{\text{RMS}} + \sum_{j=1}^{n_y} (\gamma_{v_j} \|v_j\|^2_{\text{RMS}} + \gamma_{\delta_j} \sigma^2_{\delta_j}(\Delta_j))$.

Step 4 Set $s = \arg\min_s \ x^\star_s$.

If $x^\star_s < \|\tilde{x}\|^2_{RMS,\max}$, then
set $\Delta^k_s = \arg\{J^k = J(\Delta_{1:n_y}), \Delta_j = \Delta^{k-1}_j, j \neq s\}$,
$\Delta^k_j = \Delta^{k-1}_j$, $j = 1, \ldots, n_y$, $j \neq s$,
and go to step 2.
Else, exit.

■

The algorithm starts considering small values of Δ_s and $\beta'_s \lesssim 1$, what leads to the standard periodic sampling case. Then it reduces iteratively the communication cost index while possible. At each step, it calculates the n_y new sets $\Delta_{1:n_y}$ that lead to the new cost, changing one of the Δ_s in each set. Then, it selects the set that led to the lowest $x^\star_s$, i.e., the solution allowing a larger future search before the algorithm ends. It changes only one value Δ_s at each step.

[3] Only in the stochastic approach.

6.4 Examples

In the following example we aim to show the performance of the proposed approaches. For brevity, we will only explore the deterministic approach and the uniform output distribution assumption one.

We consider the following discrete-time process (randomly chosen)

$$A = \begin{bmatrix} 1.005 & 0.221 & 0.171 \\ -0.031 & 1.008 & 0.136 \\ 0.049 & 0.038 & 1.028 \end{bmatrix}, B_w = \begin{bmatrix} -0.229 & 0.023 \\ 0.231 & 0.211 \\ -0.186 & 0.245 \end{bmatrix},$$
$$B = \begin{bmatrix} 0.658 & 0.919 \\ 0.342 & 0.584 \\ 0.481 & 0.845 \end{bmatrix}, C = \begin{bmatrix} 0.519 & -0.233 & 0.095 \\ 0.569 & 0 & 0 \end{bmatrix}.$$

The measurement noises are assumed Gaussian signals with zero mean and $\|v_s\|_{\text{RMS}} = 0.032$ (for $s = 1, 2$) while the disturbances are the combination of a Gaussian noise plus a sinusoidal such that $\|w\|_{\text{RMS}} = 0.447$. The Matlab code used for generate the disturbance is

$$w[t] = \begin{bmatrix} 0.010 & 0.004 \\ 0.004 & 0.003 \end{bmatrix} \text{randn}(2, 1) + 0.43 \begin{bmatrix} 1 \\ 1 \end{bmatrix} \sin(5 \cdot 10^{-4} \pi\, t),$$

while the control input is generated by

$$u[t] = -8 \cdot (y[t-1] > 8) + 8 \cdot (y[t-1] < -8),$$

which is a relay-based control with dead zone.

The aim of this example is to show the performance of the co-design approach from Section 6.3, i.e., minimize the network usage while guaranteeing that the estimation error is lower than a prescribed one. For this purpose, the following four approaches are analyzed:

C1 Deterministic approach with jump observer (see Section 6.2.1).

C2 Deterministic approach with constant gain.

C3 Stochastic approach based on uniform distribution assumption for a jump observer (see Section 6.2.2).

C4 Stochastic approach based on uniform distribution assumption for constant gain.

We choose the parameters r_s that define the uniform distribution assumption for each output using expression (6.12). The maximum value of the disturbances and noises are $\|w_t\|_\infty = [0.8\ 0.7]$ and $\|v_t\|_\infty = [0.15\ 0.15]$. Then we obtain $r = [0.9\ 0.75]$.

We quantify the network usage with the two cost functions presented in Section 6.3. For the deterministic cases C1 and C2 we use $J = \frac{r_1}{\Delta_1} + \frac{r_2}{\Delta_2}$ (see (6.28)). However, when we characterize the measurement transmission by its probability (cases C3 and C4), we use $J = 1 - p_0$ that is the probability of having any successful data transmission in the lowest excitation case (see (6.29)).

We denote by $\tilde{x}^\star$ the error $\|\tilde{x}\|^2_{\text{RMS}}$ resulting from the standard measurement transmission (i.e. $\Delta = 0$). In this example we analyze the results of the co-design

procedures when fixing different values of $\|\tilde{x}\|^2_{RMS,\max}$ in (6.31). We denote by μ the ratio between the desired performance and $\tilde{x}^\star$, i.e., $\mu = \frac{\|\tilde{x}\|^2_{RMS,\max}}{\tilde{x}^\star}$.

Fig. 6.2 compares the thresholds Δ_s resulting from conducting the co-design procedure (see Section 6.3), by imposing a ratio in the range $1 \leq \mu \leq 3$. The deterministic approaches C1 and C2 are both conservative and lead to the lowest thresholds, while the stochastic approaches C3 and C4 lead to the highest thresholds, and therefore, to the lowest network usage. The thresholds in C1 and C2 remain equal, what implies that using a jump observer in the deterministic approach does not improves the co-design with a constant gain. However, when we have some knowledge about the probability of the different sampling scenarios (stochastic approach), the use of a jump observer (case C3) enlarges Δ_s at the expense of a higher computational complexity with respect to C4.

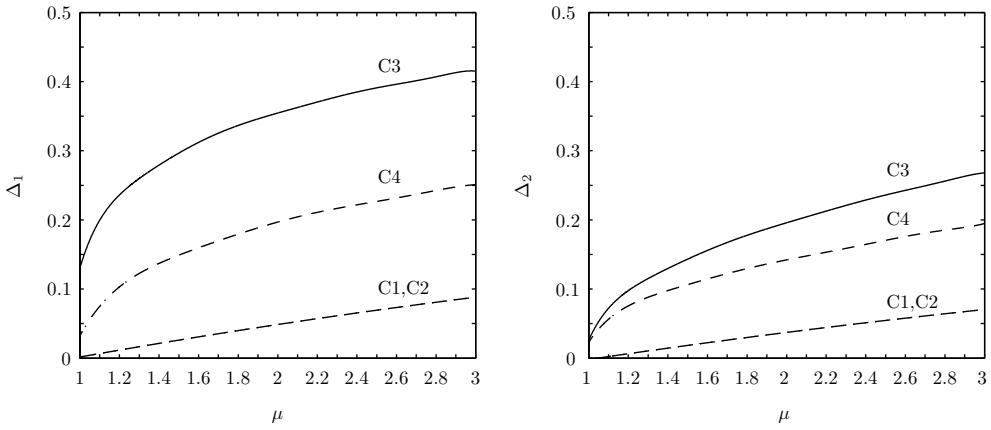

Figure 6.2: Thresholds Δ_s obtained for the co-design approach as a function of the ratio μ.

Fig. 6.3 shows the time-average probability of having a new measurement from a given sensor β_s and its virtual noise RMS norm $\sigma^2_{\delta_s}$ as a function of the Δ_s presented in Fig. 6.2 resulting from a Monte Carlo simulation. It also displays the obtained results of assuming uniform distributed outputs (see (6.13) and (6.26)) and the use of the criterion in [134] ($\sigma^2_{\delta_s} = \Delta^2_s/3$). The choice of $r = [0.9\ 0.75]$ results in lower probabilities and higher variances than in simulation. Therefore the stochastic design will be conservative, but will guarantee the prescribed bound on the estimation error (see Section 6.2.2). The result proposed in [134] for bounding the virtual noise RMS norm assuming it as a uniform variable (i.e. where $\|\delta_s\|^2_{\text{RMS}} < \Delta^2_s/3$) is more conservative than the one resulting from the difference of uniform output signals assumption that we propose in this chapter.

Simulating the estimation algorithm with the SOD procedure for the thresholds in Fig. 6.2 we obtain the number of sent samples indicated in Fig. 6.4 and the performances indicated in Fig. 6.5.

Fig. 6.4 reasserts the conclusions extracted from Fig. 6.2. The case C3 leads to the lowest network consumption, while case C4 improves the network usage of the deterministic approaches requiring less computational requirements than case C3.

Fig. 6.5 shows whether the imposed bound on the estimation error in the co-design procedure is fulfilled in simulation. The deterministic approaches C1 and C2 are far below

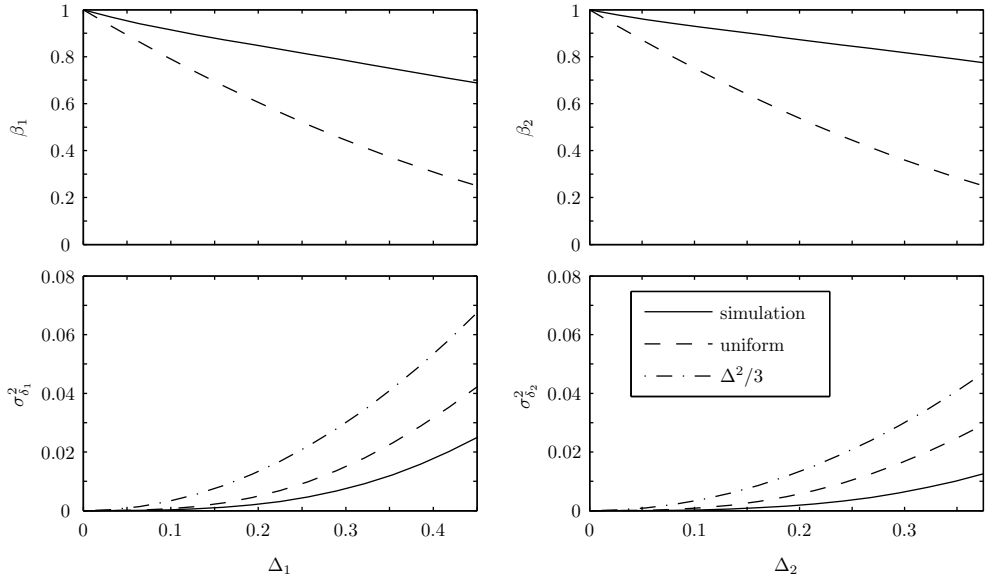

Figure 6.3: Probability of having a new measurements β and variance (RMS norm) of the virtual noise σ^2_δ as a function of Δ. 'simulation': time-average probability and virtual noise RMS norm obtained from simulation, 'uniform': probability and virtual noise variance bounds from the uniform output distribution assumption, '$\Delta^2/3$': bound of the virtual noise RMS norm proposed in [134].

the maximum allowed estimation error. This is due to the conservativeness introduced by the virtual noise variance estimation proposed by [134]. The stochastic approaches C3 and C4 are also below the maximum allowed estimation error, but closer to it. The conservativeness in the stochastic design is introduced by the choice of the parameter r (see Fig. 6.3). Note that the use of a jump observer (C1 and C3) leads to less conservative results (estimation errors closer to the allowed one) than the use of a constant gain observer (C2 and C4). This rapprochement to the allowed error is what allows the jump observer to reach higher thresholds and to reduce the network usage.

In conclusion, this example shows that if no information about the output is known, the deterministic approach is the only option. However, making some assumptions on the output distribution, we can use a stochastic approach during the co-design procedure, that reduces the resulting network usage. We have shown that if we use a jump observer the measurement transmissions can be reduced at the expense of more computational complexity, with respect the use of a constant gain.

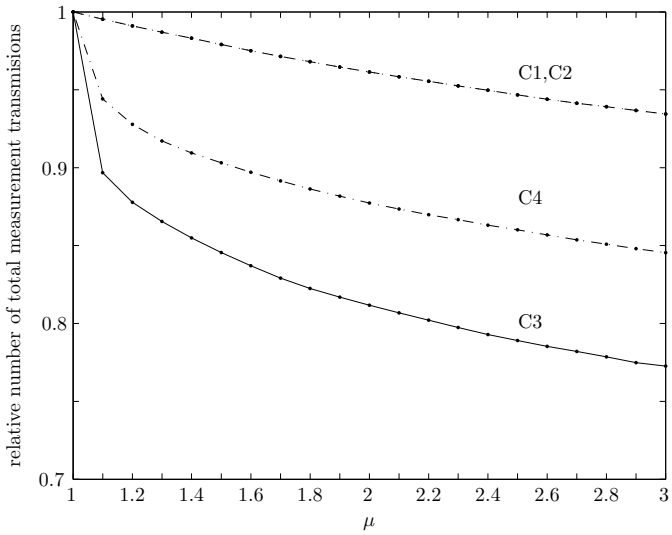

Figure 6.4: Number of total measurement transmission divided by the number of simulation time instants as a function of the ratio μ.

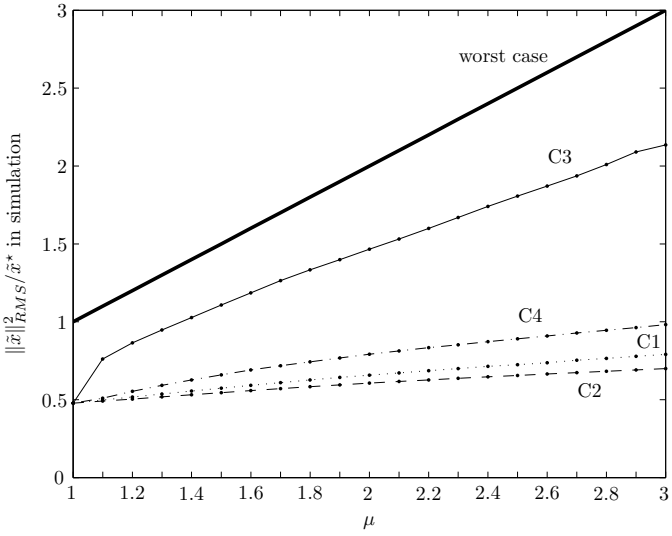

Figure 6.5: Ratio from the $\|\tilde{x}\|^2_{\mathrm{RMS}}$ obtained in simulation to the the standard H_∞ observer performance bound as a function of the ratio μ.

6.5 Conclusions

In this chapter, we addressed an observer co-design procedure for state estimation over networks when using event-based measurements. We used a low computational cost estimation strategy that consists on using a simple Send-on-Delta strategy on the sensor nodes, and a $\mathcal{H}_\infty$ jump linear estimator that uses a gain within a predefined set depending on the combination of available samples at each instant. We included a virtual noise to update the state estimation when new samples are not available. We developed a strategy based on linear matrix inequalities to obtain the observer gains when the thresholds of the sensor nodes are fixed. To reduce conservativeness, we derived a lower bound on the probability of receiving a measurement and an upper bound on the RMS norm of the resulting virtual noise. In this case, we addressed the design of the jump observer by using optimization over polynomial techniques to include the uncertainty on the measurement receiving probability. We then defined two characterizations of the network usage and used them to derive the co-design problem, consisting on finding the thresholds of the sensor nodes and the corresponding observer gains that led to the lowest network usage allowing to reach a prescribed performance on the state estimation error.

Part II

Fault diagnosis over networks

Chapter 7

Performance trade-offs for networked jump observer-based fault diagnosis

ABSTRACT: *This chapter addresses the fault diagnosis problem for multi-sensor NCS under dropouts. We propose the use of a jump observer, whose gains depend on the transmission measurement sample outcome, to diagnose multiple faults. We model the faults as slow time-varying signals and introduce this dynamic in the observer to estimate the faults and to generate a residual. We design the jump observer, the residual and the threshold to attain disturbance attenuation, fault tracking and detection conditions and a given FAR. The FAR is upper bounded by means of Markov's inequality. We explore the trade-offs between the minimum detectable faults, the FAR and the response time to faults. By imposing the disturbances and measurement noises to be Gaussian, we tighten the FAR bound which improves the time needed to detect a fault.*

7.1 Introduction

NCS have been extended to many industrial applications due to the diverse offered advantages, as the reduction on the installation cost or the increase on the flexibility, provided by the communication network [44]. In these kinds of systems, the controller unit, the sensors and the actuator are not collocated and the exchange of information is done through a shared network, leading to some network-induced issues as time delays and dropouts [51, 141]. Owing to the need for reliability, safety and efficient operation in control systems, model-based fault diagnosis methods [15] have been recently introduced in NCS [35, 121].

Fault detection over networks when using an observer-based fault detection scheme is addressed by the comparison between a residual signal generated with the estimated system outputs and a threshold. The residual is conceived to balance the robustness against network effects and disturbances, and the fault sensitivity [87, 139, 72, 137, 82].

Assuring a predefined false alarm rate (FAR) is a key problem. In the majority of the fault detection proposals for NCS the threshold is choosen to reduce the FAR to the minimum [112, 135], but without quantifying it. Some works as [139, 71, 72] characterize the mean and variance of the residual and use Markov's inequality to impose a desired FAR bound. However, Markov's inequality is known to be conservative [98]. The main problem to get a proper FAR bound is to obtain the probability distribution of the residual signal. In [18] the residual was computed as a quadratic form of the outputs estimation error by means of the inverse of the outputs estimation error matrix covariance

given by a Kalman filter. With that, their residual signal follows a chi-squared distribution and an exact FAR can be fixed. But, to the best of the author' knowledge, the extension to observers with predefined gains (which have less implementation cost, see Chapter 3) for NCS with dropouts has not been addressed.

Regarding the fault estimation problem, the most common approach is to make the residual track the fault or a weighted fault signal by guaranteeing some performances of the fault estimation error under disturbances and the network issues [54, 70, 146, 148, 125]. Recently, to improve the fault estimation performances, the authors in [149] introduced a dynamic of the fault signal on the fault estimator. Fault detection and estimation can be combined to attain fault diagnosis.

According to [55], the performance of a fault detection algorithm is defined by means of the trade-offs between the time to detect a fault and the FAR. This definition can be extended to the fault diagnosis case by considering also the convergence speed of a norm of the fault estimation error. The authors in [151] show that there exists a trade-off between the fault detection rate and the FAR. More recently, the existence of a compromise between the time to detect a fault and the fault sensitivity has been demonstrated in [138]. Nevertheless, none of them explores the compromises between the minimum detectable faults, the FAR and the fault diagnosis (detection and estimation) speed.

The dropouts in the fault diagnosis problem have been mainly studied in the packetized case [139, 54, 72]. The multi-sensor case was studied in [47] with an invariant observer gain approach, however the use of jump observers that adapt their gains to the network scenario has been proved to enhance the estimation performances [130] (see Chapter 3). Networked jump observer-based fault estimators have recently started to receive attention [87, 72], but have not been extensively employed.

Motivated by the previous analysis, in this chapter we face the fault diagnosis problem for multi-sensor systems with dropouts through the combination of fault detection and fault estimation. The faults are characterized as slow-time varying signals and the network dropouts are modeled with the combination of available samples at the fault diagnoser. We introduce a jump observer to estimate the faults and define the residual signal as a quadratic form of the estimated fault vector. The design of the jump observer and residual is addressed through an iterative LMI procedure that allows obtaining the predefined set of observer gains and the fault detector parameters. The design is carried out to achieve disturbance and measurement noise attenuation, and fault diagnosis performances under a prescribed FAR. We propose two design strategies: the first one consists of fixing the response speed to faults and minimizing the minimum detectable fault, and the second one consists of fixing the minimum detectable fault and minimizing the response time. The trade-offs between the minimum detectable faults, the FAR and the delay between fault occurrence and detection (response time of the fault estimator) are highlighted. Furthermore, we derive two ways of bounding the FAR depending on whether the residual signal probability distribution is unknown (Markov's inequality approach) or known as a result of assuming Gaussian disturbances and measurement noises (chi-squared approach).

This chapter is organized as follows. We define the problem in Section 7.2, and present the observer-based fault diagnoser design in Sections 7.3 and 7.4. The fault diagnosis strategies are addressed in Section 7.5. Section 7.6 explores some examples and, finally, in Section 7.7 we summarize the main conclusions.

7.2 Problem Formulation

Let us consider linear time invariant discrete-time systems defined by equations

$$x[t+1] = A\,x[t] + B_u\,u[t] + B_w\,w[t] + B_f\,f[t], \tag{7.1}$$

where $x \in \mathbb{R}^n$ is the state, $u \in \mathbb{R}^{n_u}$ is the vector of known inputs, $w \in \mathbb{R}^{n_w}$ is the state disturbance assumed as a random signal, uncorrelated in time, with zero mean and known covariance matrix $\mathbf{E}\{w[t]^T w[t]\} = W$ for all t, and $f \in \mathbb{R}^{n_f}$ is the fault vector. Throughout this chapter we assume that the known input u is causally available at all times, see Fig. 7.1. This general model includes as a particular case a system without known inputs, by simply taking $B_u = 0$.

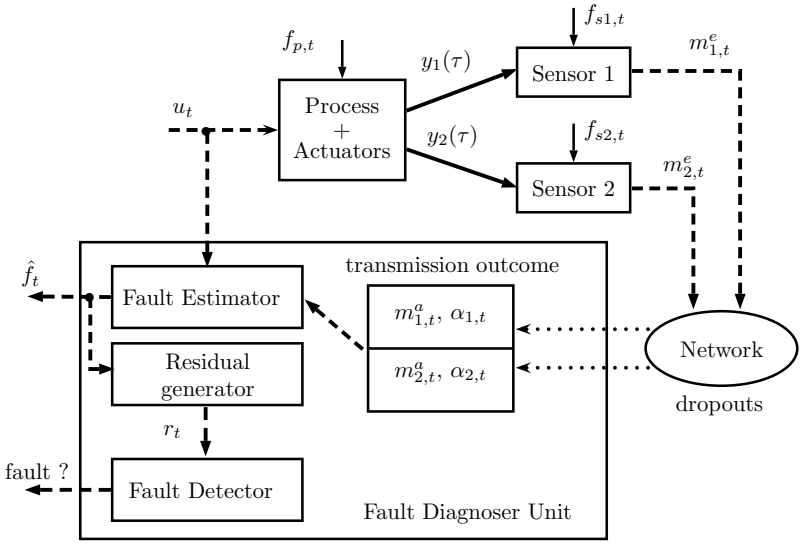

Figure 7.1: Networked fault diagnosis problem for two sensors with possible faults in the plant (f_p for actuators and other faulty components) and in the sensors (f_{s1}, f_{s2}).

The system has n_m measurable outputs. Different sensors with different characteristics on sampling rate or noise, that may have faults, can be connected to one single measurable output, but at least each measurable output is measured by one sensor, having $n_m \geq n_y$ sensors. We define the transmitted sampled measurement as

$$m_s[t] = c_s\,x[t] + h_s\,f[t] + v_s[t], \quad s = 1, \ldots, n_m \tag{7.2}$$

where $m_s[t] \in \mathbb{R}$ represents the t-th measurement of the s-th sensor and $v_s[t] \in \mathbb{R}$ the s-th sensor noise assumed as a zero mean random signal with known variance $\mathbf{E}\{v_s[t]^2\} = \sigma_j^2$ for all t, that is uncorrelated with respect to the time index t. We also consider that v_i is mutually uncorrelated with $v_{s\neq i}$. c_s denotes one row of matrix C (several c_s could be equal and correspond to the same row of C) and h_s denotes each one of the rows of matrix H.

In the current chapter, we model the fault signal as a slow time-varying one (cf. [13, 149]), i.e.,

$$f[t+1] = f[t] + \Delta f[t] \tag{7.3}$$

where $\Delta f[t]$ is the variation of the fault from instant t to $t+1$. Equation (7.3) allows modeling, for instance, step signals ($\Delta f[t]$ only takes a nonzero value at the time the fault appears) or ramp signals ($\Delta f[t]$ takes a constant value), that have been widely used in the literature to analyze the behavior of fault detection algorithms [15]. Along this chapter, we consider that $w[t]$, $v_j[t]$ for all $j = 1, \ldots, n_m$ and $\Delta f[t]$ are mutually uncorrelated for all t.

We introduce an extended order model to include the fault dynamic as

$$z[t+1] = \bar{A}z[t] + \bar{B}_u u[t] + \bar{B}_w w[t] + \bar{B}_f \Delta f[t] \tag{7.4}$$

with $z[t] = \left[x[t]^T \; f[t]^T\right]^T$ and

$$\bar{A} = \begin{bmatrix} A & B_f \\ 0 & I \end{bmatrix}, \; \bar{B}_u = \begin{bmatrix} B_u \\ 0 \end{bmatrix}, \; \bar{B}_w = \begin{bmatrix} B_w \\ 0 \end{bmatrix}, \; \bar{B}_f = \begin{bmatrix} 0 \\ I \end{bmatrix}$$

where $z \in \mathbb{R}^{\bar{n}}$ with $\bar{n} = n + n_f$.

In this chapter we intend to detect and estimate (diagnose) the possible system faults (represented by vector $f[t]$) when the measurement samples are transmitted through a communication network that may induce dropouts. In this case, the system output measurements are not available at every discrete time instant. When the dropout rate is high, the fault estimation problem becomes more difficult and the importance of a fast response to faults and a low FAR becomes more evident.

The transmitted sampled measurements from sensor s at instant t is

$$m_s^e[t] = \bar{c}_s z[t] + v_s[t], \tag{7.5}$$

with $\bar{c}_s = [c_s \; h_s]$ and $s = 1, \ldots, n_m$. We assume that the pair $(\bar{A}, \bar{C})$ is detectable (being $\bar{C}$ the matrix whose rows are $\bar{c}_s$).

Remark 7.1. If the pair $(\bar{A}, \bar{C})$ is not detectable (i.e., $n_f > n_m$), only a combination of the faults can be detected. Then, a previous transformation of the system, as proposed in [74], must be done (leading to new $\bar{n}_f$ faults such that $\bar{n}_f \leq n_m$) before the proposed technique becomes applicable.

7.2.1 Network transmissions characterization

Each sensor samples its output synchronously with the known input update and sends independently a time-tagged packet with the measurement sample $m_s^e[t]$ to the fault diagnoser station, through an unreliable communication network with packet dropouts.

We define the binary variable $\alpha_s[t]$ that indicates the availability of the s-th sensor measurement sample ($s = 1, \ldots, n_m$) at each instant t, as.

$$\alpha_s[t] = \begin{cases} 0 & \text{if } m_s^e[t] \text{ is not received at } t, \\ 1 & \text{if } m_s^e[t] \text{ is received at } t. \end{cases} \tag{7.6}$$

Then, the availability matrix $\alpha[t] = \bigoplus_{s=1}^{n_m} \alpha_s[t]$ is a binary diagonal matrix that can only have ones in its diagonal. Thus, using $\alpha[t]$ we can redefine the available samples at instant t as

$$m^a[t] = \alpha[t] \left(\bar{C}z[t] + v[t]\right). \tag{7.7}$$

Note that a component of vector $m^a[t]$ is null when the corresponding sample is not available. $v[t] = [v_1[t] \cdots v_{n_m}[t]]^T$ is the measurement noise vector with covariance $\mathbf{E}\{v[t]v[t]^T\} = V = \bigoplus_{s=1}^{n_m} \sigma_s^2$ (for all t).

The possible values of $\alpha[t]$ at each instant t belong to a known finite set

$$\alpha[t] \in \Xi = \{\eta_0, \eta_1, \ldots, \eta_q\}, \quad q = 2^{n_m} - 1, \tag{7.8}$$

where η_i denotes each possible combination of the available samples at the fault diagnoser station (sampled measurement reception scenario). Matrix η_0 denotes the scenario in which there is no measurement sample available, i.e., $\eta_0 = 0$. We characterize the network behavior using the total probability of each scenario in Ξ. We denote by $p_i = \mathbf{Pr}\{\alpha[t] = \eta_i\}$ the probability of having the sample reception scenario η_i at instant t. p_0 denotes the probability of having no samples.

In the current chapter, we assume that the arrival probability from each sensor is governed by an independent and identically distributed process [140]. We denote by β_s the probability of having available the measurement samples from sensor s at instant t, i.e., $\beta_s = \mathbf{Pr}\{\alpha_s[t] = 1\}$. Then, the probability of having a given combination of available samples $\eta_i \in \Xi$ is

$$p_i = \mathbf{Pr}\{\alpha[t] = \eta_i\} = \prod_{s \in \mathcal{I}(\eta_i)} (1 - \beta_s) \prod_{s \notin \mathcal{I}(\eta_i)} \beta_s \tag{7.9}$$

for all $i = 0, \ldots, q$ where $\mathcal{I}(\eta_i) \triangleq \{s | \eta_i(s, s) = 0\}$.

7.2.2 Fault diagnosis method

We propose the following fault estimation algorithm for system (7.4)-(7.5). At each instant t, the model is run in open loop leading to

$$\hat{z}[t^-] = \bar{A}\, \hat{z}[t-1] + \bar{B}_u u[t-1]. \tag{7.10}$$

If no measurement sample is received, we keep the open loop estimation, i.e., $\hat{z}[t] = \hat{z}[t^-]$. If a measurement sample arrives at instant $t = t_k$, the state is updated as

$$\hat{z}[t_k] = \hat{z}[t_k^-] + L[t_k]\,(m^a[t_k] - \alpha[t_k]\,\bar{C}\,\hat{z}[t_k^-]), \tag{7.11}$$

where $L[t_k]$ is the updating gain matrix and $m^a[t_k]$ is defined in (7.7).

Remark 7.2. While $t \in \mathbb{N}$ refers to each time instant, t_k (with $k \in \mathbb{N}$) enumerates only the instants where some samples are received. For instance, if we receive some samples only at instants $t_k = 8$ and $t_{k+1} = 10$, but not at $t = 9$, then instant $t_k + 1 = 9$ (or $t_{k+1} - 1 = 9$) refers to instant 9, when no measurement samples is received.

Let us denote $z[t_k]$ by z_k. Defining the extended state estimation error at updating instants as $\tilde{z}_k = z_k - \hat{z}_k$, the estimation error dynamics is given by

$$\begin{aligned} \tilde{z}_k =& (I - L_k \alpha_k \bar{C}) \bar{A}^{N_k} \tilde{z}_{k-1} - L_k \alpha_k v_k \\ &+ \sum_{l=1}^{N_k} (I - L_k \alpha_k \bar{C}) \bar{A}^{l-1} B_{\mathbb{W}} \mathbb{W}[t_{k-1} + l - 1] \end{aligned} \tag{7.12}$$

being $B_{\mathbb{W}} = [\bar{B}_w \;\; \bar{B}_f]$ and $\mathbb{W}[t_{k-1}+l-1] = [w[t_{k-1}+l-1]^T \;\; \Delta f[t_{k-1}+l-1]^T]^T$. N_k denotes the number of consecutive instants without samples (which is unbounded), i.e., $N_k = t_k - t_{k-1}$.

The fault detection algorithm uses the estimated faults to compute a residual signal at instants $t = t_k$ as

$$r_k = \hat{f}_k^T F^{-1} \hat{f}_k, \tag{7.13}$$

where the common fault detection decision is given by

$$\begin{cases} \text{if } r_k \leq r^{\text{th}} & \text{No fault} \\ \text{if } r_k > r^{\text{th}} & \text{Fault} \end{cases}$$

being $r^{\text{th}} > 0$ a threshold to be defined. Then, fault isolation is achieved by means of the combination of fault detection and fault estimation, allowing us to identify which is the origin of the fault.

Remark 7.3. According to [15], the minimum detectable fault is a fault that drives the residual to its threshold, provided no other faults, disturbances and measurement noises are present. Then, assuming a zero fault estimation error (i.e. $\hat{f} = f$), each diagonal element of F in (7.13) multiplied by r^{th} defines the minimum detectable fault as $f_{\min,l} = r^{\text{th}} F(l,l)$ for the corresponding channel ($l = 1, \ldots, n_f$).

Considering the fault detection logic, the FAR is defined as the average probability of rising false alarms over an infinite-time window, i.e.

$$\Psi = \lim_{K \to \infty} \sum_{k=0}^{K-1} \mathbf{Pr}\{r_k > r^{\text{th}} \mid f_k = 0\}. \tag{7.14}$$

The aim of this chapter is to compute the gain matrices L_k, the matrix F, and the threshold r^{th} such that the fault diagnoser attains disturbance and measurement noise attenuation, and fault diagnosis performances for a given FAR. These objectives can be reached with an invariant observer gain (as in the majority of reviewed works), or with a jump one (e.g. [87, 72]). In this chapter, we relate the gain L_k to the sampling scenario α_k, as $L_k = L(\alpha_k)$, with the law $L_k = L_i$ when $\alpha_k = \eta_i$ for $\alpha_k = \eta_1, \ldots, \eta_q$. Then, the matrices are computed off-line leading to the finite set

$$L_k \in \mathcal{L} = \{L_1, \ldots, L_q\}. \tag{7.15}$$

7.3 Fault diagnoser design: dropout-free

Let us first consider the case without measurement dropouts, i.e., $\beta_j = 1$ for all $j = 1, \ldots, n_m$. In this case, $\alpha[t]$ is always the identity, which implies that each instant t is a measurement instant ($t_k = t$) leading to $L_k = L$ and $N_k = 1$, for all k. The following theorem presents how to design the observer gain L and the matrix F that defines the residual (7.13) based on the H_2 norm of system (7.12).

Theorem 7.1. *Consider the estimation algorithm* (7.10)-(7.11) *applied to system* (7.1)-(7.3) *with standard sampling. If there exist symmetric matrices* P, F, Γ_w, Γ_v, Γ_f, *and full matrices* X *fulfilling*

$$\begin{bmatrix} P & \bar{\mathcal{A}} & 0 \\ \bar{\mathcal{A}}^T & P & \bar{B}_f \\ 0 & \bar{B}_f^T & F \end{bmatrix} \succeq 0, \tag{7.16a}$$

$$\begin{bmatrix} P & \bar{\mathcal{B}}_\mu \\ \bar{\mathcal{B}}_\mu^T & \Gamma_\mu \end{bmatrix} \succeq 0, \ \mu = \{w, v, f\} \tag{7.16b}$$

with

$$\bar{\mathcal{A}} = (P - X\bar{C})\bar{A}, \quad \bar{\mathcal{B}}_w = (P - X\bar{C})\bar{B}_w, \quad \bar{\mathcal{B}}_v = -X, \quad \bar{\mathcal{B}}_f = (P - X\bar{C})\bar{B}_f$$

then, defining the observer gain matrices as $L = P^{-1}X$, *the following statements hold:*

i) In the absence of disturbances, faults, and measurement noises the extended state estimation error (7.12) *converges to zero.*

ii) Under null initial conditions, the fault estimation error is bounded by

$$\mathbf{E}\{\|\tilde{f}\|^2_{\mathrm{RMS}}\} \leq \overline{\lambda}(F)\left(\mathrm{tr}(\bar{\Gamma}) + n_f \overline{\lambda}(\Gamma_f)\Delta f^2_{\max}\right), \tag{7.17}$$

where $\bar{\Gamma} = \Gamma_w W + \Gamma_v V$ *and* $\|\Delta f\|_\infty \leq \Delta f_{\max}$.

Proof. See Appendix C.7.1. ■

The above theorem states that F is related to the expected value of the squared RMS norm of the fault estimation error. We can extract from (7.17) that the fault estimation (and therefore the residual signal) is more sensitive to disturbances and measurement noises when the maximum of the minimum detectable faults (by means of $\overline{\lambda}(F)$) is higher. Furthermore, the lower the value $\overline{\lambda}(\Gamma_f)$, the lower the effect of the faults on the estimation error. The next theorem extends the results of the previous one to bound the FAR.

Theorem 7.2. *For a given threshold* $r^{\mathrm{th}} > 0$ *and* $0 \leq \phi \leq 1$, *and under the premisses of Theorem 7.1, if*

$$\mathrm{tr}(\Gamma_w W) + \mathrm{tr}(\Gamma_v V) = \phi\, r^{\mathrm{th}}, \tag{7.18}$$

and constraints (7.16) *are fulfilled, then, the following additional statement holds:*

iii) In the absence of faults and under null initial conditions, the fault detection algorithm assures a FAR (7.14) *bounded by* ϕ.

Proof. See Appendix C.7.2. ■

The next theorem extends the previous one showing how the fault estimation error decays at each measurement instant.

Theorem 7.3. *For a given threshold* $r^{\mathrm{th}} > 0$ *and* $0 \leq \phi \leq 1$, *and under the premisses of Theorem 7.2, if*

$$\Gamma_f - \bar{B}_f^T P \bar{B}_f \succeq 0, \tag{7.19}$$

and constraints (7.16), (7.18) *are fulfilled, then, the following additional statement holds:*

iv) The fault estimation error given by $\mathbf{E}\{\|\tilde{f}_k\|_2^2\}$ *decays with*

$$\rho = 1 - \frac{1}{\overline{\lambda}(\Gamma_f F)}. \tag{7.20}$$

Proof. See Appendix C.7.3. ■

The above theorem shows that $\mathbf{E}\{\|\tilde{f}_k\|_2^2\}$ decays with ρ, from the initial conditions to the steady state region (see (C.25)). ρ depends on the maximum eigenvalue of the product $\Gamma_f F$. If F is fixed to assure the detection of some given minimum faults, Γ_f determines the response time of the fault estimator (by means of ρ) and therefore the time to detect a fault (as the residual is defined with the estimated faults).

Remark 7.4. Under a step-like fault, the number of instants with measurement reception, denoted by $\mathcal{K}$, until the initial value of the fault estimation error is decreased below a 2%, characterizes the settling time of the fault estimation vector (time to achieve the 98% of the final value). $\mathcal{K}$ can be obtained approximately by solving equation $\rho^{k+1} = 0.02$, (see (C.25)) leading to

$$\mathcal{K} = \left\lceil \frac{\log(0.02)}{\log(\rho)} - 1 \right\rceil \tag{7.21}$$

where $\lceil \cdot \rceil$ is the operator that rounds its argument to the nearest integer towards infinity.

Remark 7.5. For a fixed value of F, increasing the FAR by means of ϕ leads to an increase in the values of Γ_w and Γ_v, see (7.18). Higher values on these variables alleviate the constraints over P in (7.16b), increasing the solution space in the search for a feasible matrix P. This would allow, for instance, structure constraints over matrix P. Matrix Γ_f in (7.19) constrains the last diagonal block on P. Then, increasing ϕ can enlarge the solution space to find lower values on Γ_f, i.e., to lead to lower values of ρ (faster fault diagnosers). These ideas are analyzed on the examples section.

We used Markov's inequality in Theorem 7.2 to bound the FAR. However, it is well known that the bound yielded by Markov's inequality may be very conservative (see [98]) because it does not consider the probability distribution of the residual r_k. This may result in a real FAR that is some orders of magnitude lower than the desired one, which, as shown in the examples, may lead to a very slow response of the fault diagnoser (characterized by ρ in Theorem 7.3). Most of the works in the literature share this important drawback. In order to overcome this, a more accurate bound on the FAR must be attained. Assuming that the disturbances w_k and the measurement noises v_k are Gaussian, we show in the next theorem how to impose an appropriate value to matrix F to force the residual r_k follow a chi-squared distribution, which allows us to tighten the FAR bound.

Theorem 7.4. *For the fixed threshold* $r^{\text{th}} = n_f$ *and for a given* $0 \leq \phi \leq 1$*, under the premisses of Theorem 7.3, if*

$$F = \phi^{-1}\Sigma_f \tag{7.22}$$

and constraints (7.16)*,* (7.18)*,* (7.19) *are fulfilled, with*

$$\begin{aligned} \text{vec}(\Sigma_f) &= \left(I - G\bar{A} \otimes G\bar{A}\right)^{-1} \text{vec}\left(Y_1\right), \\ Y_1 &= G\bar{B}_w W \bar{B}_w^T G^T + P^{-1}X\, V\, (P^{-1}X)^T, \\ G &= (I - P^{-1}X\bar{C}), \end{aligned} \tag{7.23}$$

then, in the absence of faults, under null initial conditions and Gaussian disturbances and measurement noises, if the fault diagnoser gain is defined as $L = P^{-1}X$*, then the FAR is given by*

$$\Psi = 1 - \mathrm{CDF}_{\mathcal{X}^2_{n_f}}\left(\frac{r^{\mathrm{th}}}{\phi}\right) \tag{7.24}$$

where $\mathrm{CDF}_{\mathcal{X}^2_{n_f}}(\frac{r^{\mathrm{th}}}{\phi}) = \mathbf{Pr}\{\frac{r_k}{\phi} \leq \frac{r^{\mathrm{th}}}{\phi}\}$ *denotes the cumulative distribution function (CDF) of a chi-squared random variable with* n_f *degrees of freedom,* $\mathcal{X}^2_{n_f}$*.*

Proof. See Appendix C.7.4. ■

Remark 7.6. Following the definition of the CDF of a chi-squared random variable, the value of ϕ needed to obtain a desired FAR ψ with the chi-squared approach is always higher (for any value of n_f) that the one required with the Markov's inequality approach. For instance, if $n_f = 2$ and $\psi = 10^{-3}$ using Theorem 7.2 requires $\phi = 10^{-3}$ while Theorem 7.4 requires $\phi = 0.145$. Following Remark 7.5, this implies that using the chi-squared approach could lead to fault diagnosers with a faster response to faults than employing the result on Theorem 7.2. However, unconstraining F and using Markov's inequality is a more general approach, in the sense that it is valid when disturbances and noises are not Gaussian.

Theorem 7.4 has shown how to reduce the conservatism of the approach when assuming Gaussian disturbances, but at the cost of including new nonlinear equality constraints that are hard to handle. We will show in the design strategies section how to overcome this issue.

7.4 Application to networked transmission

In the previous section we presented how to design the fault diagnoser and to characterize the obtained FAR and response time to faults for sampled measurement transmission without dropouts. In this section we extend the previous results to a more interesting case where measurement information is not always available due to network dropouts. This will stress the need of fast fault detection with a low FAR. The following theorem extends Theorem 7.3 and shows how to find the set of observer gain matrices (7.15) and the matrix that defines the residual (7.13).

Theorem 7.5. *For a given threshold $r^{\text{th}} > 0$ and $0 \leq \phi \leq 1$, consider the estimation algorithm (7.10)-(7.11) applied to system (7.1)-(7.3), and assume that there can be q different measurement reception scenarios η_i $(i = 1, \ldots, q)$ with a probability p_i, being p_0 the probability of failing on the reception of data in a given instant. If there exist symmetric matrices P, Q, F, Γ_v, Γ_w, Γ_f,, and full matrices X_i fulfilling*

$$\begin{bmatrix} P - M_1 & \bar{B}_f \\ \bar{B}_f^T & F \end{bmatrix} \succeq 0, \tag{7.25a}$$

$$\Gamma_w - \bar{B}_w^T M_2 \bar{B}_w \succeq 0, \tag{7.25b}$$

$$\begin{bmatrix} \bigoplus_{l=1}^{q} P & M_3 \\ M_3^T & \Gamma_v \end{bmatrix} \succeq 0, \tag{7.25c}$$

$$\Gamma_f - \bar{B}_f^T (M_5 + M_6) \bar{B}_f \succeq 0, \tag{7.25d}$$

$$\begin{bmatrix} \bigoplus_{l=1}^{q} P & M_4 \\ M_4^T & Q \end{bmatrix} \succeq 0, \tag{7.25e}$$

$$\text{tr}(\Gamma_w W) + \text{tr}(\Gamma_v V) = \phi\, r^{\text{th}}, \tag{7.25f}$$

$$\Gamma_f - \bar{B}_f^T P \bar{B}_f \succeq 0, \tag{7.25g}$$

with

$$\text{vec}(M_1) = \varphi(\bar{A})^{-1} \text{vec}(\bar{A}^T Q \bar{A}),$$

$$M_2 = (1 - p_0) M_5 + \frac{p_0}{1 - p_0} M_1, \quad M_5 = \frac{1}{(1 - p_0)^2} Q,$$

$$M_3 = \begin{bmatrix} \sqrt{\frac{1}{1-p_0} p_1}\, X_1 \eta_1 \\ \vdots \\ \sqrt{\frac{1}{1-p_0} p_q}\, X_q \eta_q \end{bmatrix}, \quad M_4 = \begin{bmatrix} \sqrt{p_1}(P - X_1 \eta_1 \bar{C}) \\ \vdots \\ \sqrt{p_q}(P - X_q \eta_q \bar{C}) \end{bmatrix},$$

$$\text{vec}(M_6) = \varphi(\bar{A})^{-1} \left(\text{vec}(\bar{A}^T M_5 \bar{A}) + \frac{p_0}{1 - p_0} \text{vec}(M_1) \right),$$

and $\varphi(\bar{A}) = I - p_0 \bar{A}^T \otimes \bar{A}^T$, then, defining the observer gain matrices as $L_i = P^{-1} X_i$, the following statements hold:

i) In the absence of disturbances, faults and measurement noises, (7.12) converges to zero in average.

ii) Under null initial conditions, the fault estimation error is bounded by

$$\mathbf{E}\{\|\tilde{f}\|_{\text{RMS}}^2\} \leq \overline{\lambda}(F) \cdot \left(\phi\, r^{\text{th}} + n_f \overline{\lambda}(\Gamma_f) \overline{\Delta f}_{\max}^2 \right), \tag{7.26}$$

where $\overline{\Delta f}_{\max}$ is a constant that depends on the fault magnitude that bounds vector $\overline{\Delta f}_k \in \mathbb{R}^{n_f}$ as $\|\overline{\Delta f}\|_\infty \leq \overline{\Delta f}_{\max}$, being $\overline{\Delta f}_k$ a vector that fulfills for all k that

$$\sum_{N=1}^{\infty} N p_0^{N-1} \sum_{l=0}^{N-1} (\star)^T Q \underbrace{\left(\bar{A}^l \bar{B}_f \Delta f[t_k + l] \right)}_{\star}$$

$$= \overline{\Delta f}_k^{\,T} \left(\sum_{N=1}^{\infty} N p_0^{N-1} \sum_{l=0}^{N-1} \bar{B}_f^T (\bar{A}^l)^T Q \bar{A}^l \bar{B}_f \right) \overline{\Delta f}_k. \tag{7.27}$$

iii) Under null initial conditions and in the absence of faults, the residual evaluation assures a FAR (7.14) *bounded by* ϕ.

iv) The fault estimation error given by $\mathbf{E}\{\|\tilde{f}_k\|_2^2\}$ *decays with*

$$\rho = 1 - \frac{1}{\overline{\lambda}(\Gamma_f F)}. \tag{7.28}$$

Proof. See Appendix C.7.5. ■

Remark 7.7. The existence of vector $\overline{\Delta f}_k$ defined in (7.27) is assured because it represents an equality constrained problem with one equation and n_f degrees of freedom. For instance, under ramp-like faults ($\Delta f[t_k + l]$ is constant), $\Delta f[t_k + l] = \overline{\Delta f}_k$ (for all $l = 0, 1, \ldots$) and $\overline{\Delta f}_{\max} = \|\Delta f\|_\infty$. Furthermore, the exact value of $\overline{\Delta f}_{\max}$ is not relevant for the analysis.

In the aim of reducing the conservativeness introduced by Markov's inequality to bound the FAR, the next theorem extends Theorem 7.4 by forcing r_k to follow a chi-squared distribution when measurement samples are subject to dropouts.

Theorem 7.6. *If the threshold is set as* $r^{\text{th}} = n_f$ *and for a given* $0 \leq \phi \leq 1$, *under the premisses of Theorem 7.5, if*

$$F = \phi^{-1}\Sigma_f \tag{7.29}$$

and constraints (7.25) *are fulfilled for* $i = 1, \ldots, q$, *with*

$$\begin{aligned}
&\Sigma_f = \bar{B}_f^T(R - p_0\bar{A}R\bar{A}^T)\bar{B}_f, \quad \text{vec}(R) = Y_1^{-1}\text{vec}(Y_2),\\
&Y_1 = \varphi(\bar{A}) - (\sum_{i=1}^{q} p_i(G_i\bar{A}) \otimes (G_i\bar{A})),\\
&\varphi(\bar{A}) = I - p_0\bar{A}^T \otimes \bar{A}^T,\\
&Y_2 = \frac{1}{1-p_0}\sum_{i=1}^{q} p_i L_i\,\eta_i V \eta_i^T L_i^T + \sum_{i=1}^{q} p_i G_i(S_W)G_i^T,\\
&S_W = \frac{1}{1-p_0}\left(\bar{B}_w W \bar{B}_w^T + p_0\bar{A}S_{W,\infty}\bar{A}^T\right),\\
&\text{vec}(S_{W,\infty}) = \varphi(\bar{A})^{-1}\text{vec}(\bar{B}_w W \bar{B}_w^T),\\
&L_i = P^{-1}X_i, \;\; G_i = I - L_i\eta_i\bar{C}
\end{aligned}$$

then, in the absence of faults, under null initial conditions and Gaussian disturbances and measurement noises, the FAR is given by (7.24).

Proof. See Appendix C.7.6. ■

7.5 Fault diagnosis strategies

Based on the derived results on Theorem 7.5, we propose the following two strategies to address the design of a fault diagnoser depending on the needs of the application.

First, let us consider that we desire to detect faults over a certain value, i.e to fix the minimum detectable fault on each channel $f_{\min,l}$ (for $l = 1, \ldots, n_f$), with a guaranteed FAR, and to detect as fast as possible the appearance of faults (i.e., with the lowest ρ). The next optimization problem deals with this design problem.

Strategy 7.1. For a given threshold $r^{\text{th}} > 0$, let ψ be the desired FAR, fix ϕ to be $\phi = \psi$, and let $\mathcal{F}$ be a diagonal matrix such that $\mathcal{F} = \bigoplus_{l=1}^{n_f} f_{\min,l}^2 / r^{\text{th}}$. Then, the minimization problem

$$\begin{array}{ll} \text{minimize} & \gamma \\ \text{subject to} & \mathcal{X}_1 = \{(7.25),\ F \preceq \mathcal{F},\ \Gamma_f \mathcal{F} \preceq \gamma I\} \end{array} \tag{7.30}$$

along variables γ, P, Q, F, Γ_v, Γ_w, Γ_f, and X_i (with $i = 1, \ldots, q$), leads to the fault diagnoser with the fastest response under faults, able to detect faults over $f_{\min,l}$ (with $l = 1, \ldots, n_f$) with a FAR below ψ.

Second, let us assume that we desire to impose the response speed under the appearance of faults (by means of ρ) with a guaranteed FAR. Then, the minimum detectable faults can be minimized through the next optimization problem.

Strategy 7.2. For a given threshold $r^{\text{th}} > 0$, let ψ be the desired FAR, fix ϕ to be $\phi = \psi$, and let $\bar{\rho}$ be the given upper bound on how the fault estimation error decays, i.e., $\rho \leq \bar{\rho}$. Then, the minimization problem

$$\begin{array}{ll} \text{minimize} & \gamma \\ \text{subject to} & \mathcal{X}_2 = \left\{ \begin{array}{l} (7.25),\ \text{tr}(F) \leq \gamma, \\ \Gamma_f F \leq (1-\bar{\rho})^{-1} I \end{array} \right\} \end{array} \tag{7.31}$$

along variables γ, P, Q, F, Γ_v, Γ_w, Γ_f and X_i (with $i = 1, \ldots, q$), leads to the fault diagnoser with the minimum value of the sum of the squared minimum detectable faults (defined by matrix F) with $\rho \leq \bar{\rho}$ and a FAR below ψ.

Remark 7.8. Optimization problem (7.31) is nonlinear because of the bilinear matrix inequality (BMI) that affects the product $\Gamma_f F$. This can be solved with the following rank constrained problem

$$\begin{bmatrix} (1-\bar{\rho})^{-1} F & F \\ F & \Lambda \end{bmatrix} \succeq 0, \quad Y = \begin{bmatrix} \Gamma_f & I \\ I & \Lambda \end{bmatrix} \succeq 0, \quad \text{rank}(Y) \leq n_f$$

where a new symmetric decision matrix Λ has been added. This problem can be iteratively handled with the well known cone complementarity linearization algorithm (see Appendix A.3.1).

Both design strategies are still valid when including nonlinear equality constraints (7.29) but need more computational effort. The next strategy extends the previous ones to consider the chi-squared approach presented in Theorem 7.6.

Strategy 7.3. The minimization problem

$$\begin{aligned} &\text{minimize} && \gamma \\ &\text{subject to} && \mathcal{X}_j,\ (7.29), \\ & && \psi = 1 - \text{CDF}_{\mathcal{X}^2_{n_f}}\left(\frac{r^{\text{th}}}{\phi}\right) \end{aligned} \tag{7.32}$$

along variables γ, P, Q, F, Γ_v, Γ_w, Γ_f, and X_i (with $i = 1, \ldots, q$) with $r^{\text{th}} = n_f$, extends the design made in Strategy 7.1, if $j = 1$, or in Strategy 7.2, if $j = 2$, to tighten the FAR bound with the chi-squared approach.

Remark 7.9. Optimization problem (7.32) is nonlinear due to constraint (7.29). This optimization problem can be solved iteratively with LMI constraints by forcing matrix F at each step k to be as $F \preceq \phi^{-1}\Sigma_f(\mathcal{L}^{k-1})$, until $\Sigma_f(\mathcal{L}^{k-1})$ converges to a constant value, where $\Sigma_f(\mathcal{L}^{k-1})$ is the covariance matrix in (7.29) evaluated with the observer gains at step $k-1$.

Remark 7.10. Strategy 7.3 will lead, in general, to minimum detectable faults under $f_{\min,l}$ (for $l = 1, \ldots, n_f$). If we do not intend to detect faults under $f_{\min,l}$, we can first solve the optimization problem involved in Strategy 7.3 and then use $r_k = \hat{f}_k^T \mathcal{F}^{-1} \hat{f}_k$ in the real-time implementation (where $\mathcal{F}$ includes the original prescribed minimum detectable faults, $f_{\min,l}$). In this case, as we impose in the design that $\phi^{-1}\Sigma_f \preceq \mathcal{F}$, the obtained FAR will be upper-bounded by (7.24).

7.6 Example

Let us consider an industrial continuous-stirred tank reactor process (borrowed from [41]) where the discretized state-space model is

$$A = \begin{bmatrix} 0.972 & -0.001 \\ -0.034 & 0.863 \end{bmatrix},\ B_u = \begin{bmatrix} -0.084 & 0.023 \\ 0.076 & 0.414 \end{bmatrix},$$
$$B_w = B_u,\ C = \begin{bmatrix} 1 & 0 \\ 0 & 1 \end{bmatrix}.$$

We desire to detect faults from the second actuator and the first sensor, i.e.

$$B_f = \begin{bmatrix} 0.023 & 0 \\ 0.414 & 0 \end{bmatrix},\ H = \begin{bmatrix} 0 & 1 \\ 0 & 0 \end{bmatrix}.$$

The state disturbances and measurement noises are Gaussian with covariance matrices

$$W = \begin{bmatrix} 0.11 & 0.03 \\ 0.03 & 0.13 \end{bmatrix},\ V = \begin{bmatrix} 0.01 & 0 \\ 0 & 0.01 \end{bmatrix}.$$

We consider that the sampled measurements are independently acquired through a communication network where the probabilities of having available the measurements from each sensor are $\beta = [0.58\ 0.46]$.

For ease of analysis, in this example we will only explore the case when we impose that the minimum detectable faults are below some given values and we try to obtain the fastest response to faults of the fault diagnoser, i.e. we will only analyze Strategies 7.1

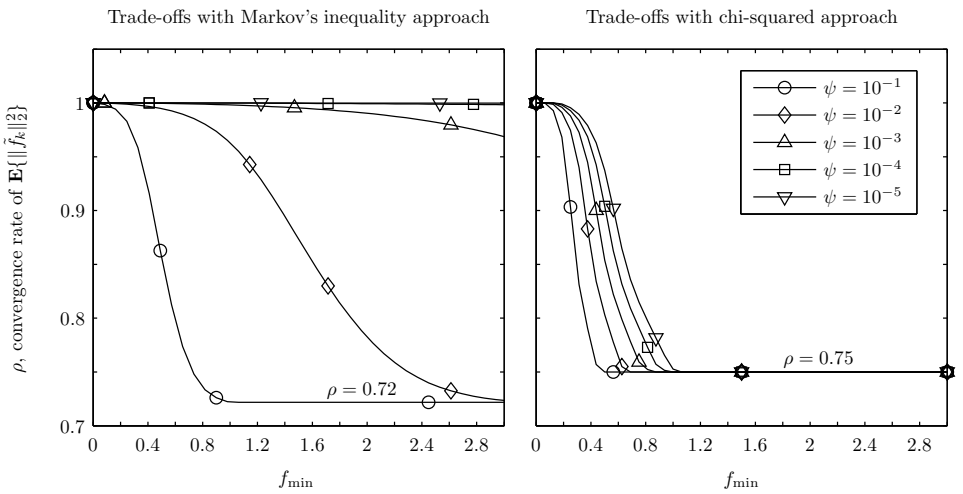

Figure 7.2: Trade-offs on the observer-based fault diagnoser design.

and 7.3. For ease of notation, let us assume that the requirement over the minimum detectable faults is such that $F \preceq f_{\min} I$. In the next, we impose the threshold to be $r^{\text{th}} = n_f$.

First, let us study the compromises between the minimum detectable faults f_{min}, the desired FAR ψ and the speed of the fault diagnoser by means of ρ in the design procedure. Fig. 7.2 illustrates these trade-offs for five different desired FARs with $\psi = [10^{-1}\ 10^{-2}\ 10^{-3}\ 10^{-4}\ 10^{-5}]$ and for the two presented approaches to assure them: through Markov's inequality (left hand side figure, Strategy 7.1) and through characterizing the probability distribution of the residual signal (right hand side figure, Strategy 7.3). We perceive that imposing smaller minimum detectable faults or lower FARs results in a slower response time to faults (ρ higher). We also appreciate that forcing F to be as defined in (7.29) (chi-squared approach) results in a faster response under faults (ρ smaller) for the same minimum detectable faults than using Markov's inequality approach. Furthermore, Fig. 7.2 shows an asymptotic behavior of ρ with respect to $f_{\min}$, leading to a minimum achievable value.

Second, let us study the behaviour of some fault diagnosers in simulation, where $u[t] = 0$ for all t. Table 7.1 compares the fault diagnosis performances for the case when F is unconstrained, case C1 (where Markov's inequality approach is used, Strategy 1) and when F is constrained to be as in (7.29), case C2 (where the chi-squared approach is used, Strategy 3). For both cases we impose $\psi = 10^{-3}$ and $f_{\min} = 0.6$. We also include in Table 7.1 a case C3 where we reduced the $f_{\min}$ from case C2 to the half. The matrices F obtained for the three cases are:

$$F_{\text{C1}} = \begin{bmatrix} 0.18 & 0 \\ 0 & 0.18 \end{bmatrix}, \quad F_{\text{C2}} = \begin{bmatrix} 0.161 & -0.025 \\ -0.025 & 0.107 \end{bmatrix},$$
$$F_{\text{C3}} = \begin{bmatrix} 0.022 & -0.008 \\ -0.008 & 0.041 \end{bmatrix}.$$

As illustrated in Table 7.1, for case C3, we can detect smaller faults than in case C2 at the expense of being slower than in case C2. However, we still are much faster than

in case C1 where the guaranteed detectable faults were higher. Moreover, as stated in Remark 7.10 cases C2 and C3 can detect faults below the imposed $f_{\min}$ ($f_{\min,1}$ for the actuator fault and $f_{\min,2}$ for the sensor fault).

After a simulation of 10^6 instants with no faults, we verify that the FAR obtained in simulation (by dividing the number of risen alarms by the total number of simulation time instants) for case C2 and case C3 is the same as forecasted in the design, but for case C1 is much lower (several orders of magnitude) than the imposed bound. This conservativeness of the Markov's approach results in an extremely slow residual dynamics (as seen in Fig. 7.3), and a huge time to detect the fault (characterized by 6101 measurement instants, see (7.21)), that is useless in practice. To alleviate this conservativeness, we add to the analysis a fourth case C4 (with $F_{C4} = F_{C1}$) where, as a difference from case C1, we impose $\phi = 0.1$ ($\psi \leq 0.1$). Then, we obtain a fault diagnoser similar to C2 with a FAR in simulation of 10^{-4} (see Table 7.1), which is under the desired one of 10^{-3}. This shows that we can compensate the conservativeness of the Markov's approach by increasing the value of ϕ and then verifying in simulation if the prescribed bound is fulfilled, but we cannot guarantee a priori a given tight false alarm rate or minimum detectable faults.

Table 7.1: Fault diagnosers comparison.

Case	Design							Simulation
	$f_{\min}$	$f_{\min,1}$	$f_{\min,2}$	ϕ	ψ	ρ	$\mathcal{K}$	FAR
C1	0.6	0.6	0.6	10^{-3}	10^{-3}	0.999	6101	0
C2	0.56	0.46	0.52	0.145	10^{-3}	0.808	18	10^{-3}
C3	0.21	0.29	0.29	0.145	10^{-3}	0.977	167	10^{-3}
C4	0.6	0.6	0.6	0.1	0.1	0.798	17	10^{-4}

Fig. 7.3 and Fig. 7.4 show the fault estimation and fault detection performances resulting from simulating the fault diagnosers from Table 7.1 under the appearance of two step faults, one for each channel, of an amplitude of 0.7 at time $t = 100$ (disappearing at $t = 400$) for f_1, and at $t = 200$ (disappearing at $t = 500$) for f_2.

The fault diagnosers for case C2 and C4 are the fastest ones to detect the faults and their estimation of the faults have the lowest settling time. However they are the most sensitive under state disturbances and measurement noises (as they have the highest $\phi\overline{\lambda}(F)$ product, see (7.26)). For case C1, the fault detector cannot detect the faults on time because it has a too slow dynamic due to the conservativeness introduced by the Markov's inequality. Case C3, is an intermediate case between C1 and C2. Even if for case C3 the estimated faults converge slower to the faults than for cases C2 and C4, the detection mechanism only takes 6 more instants to detect the fault. This is due to the fact that C3 can detect lower faults than C2 and C4 (note that the diagonal of F_{C3}^{-1} are higher than the ones of F_{C2}^{-1} and F_{C4}^{-1}). Finally, note that the settling time at the 98% for the fault estimation, measured in terms of the number of measurement instants, is in the order of $\mathcal{K}$ (defined in (7.21)). For example, for case C3, the settling time is of 60 measurement instants for $\hat{f}_1$ and of 130 for $\hat{f}_2$, while it was characterized by $\mathcal{K} = 167$ from (7.21).

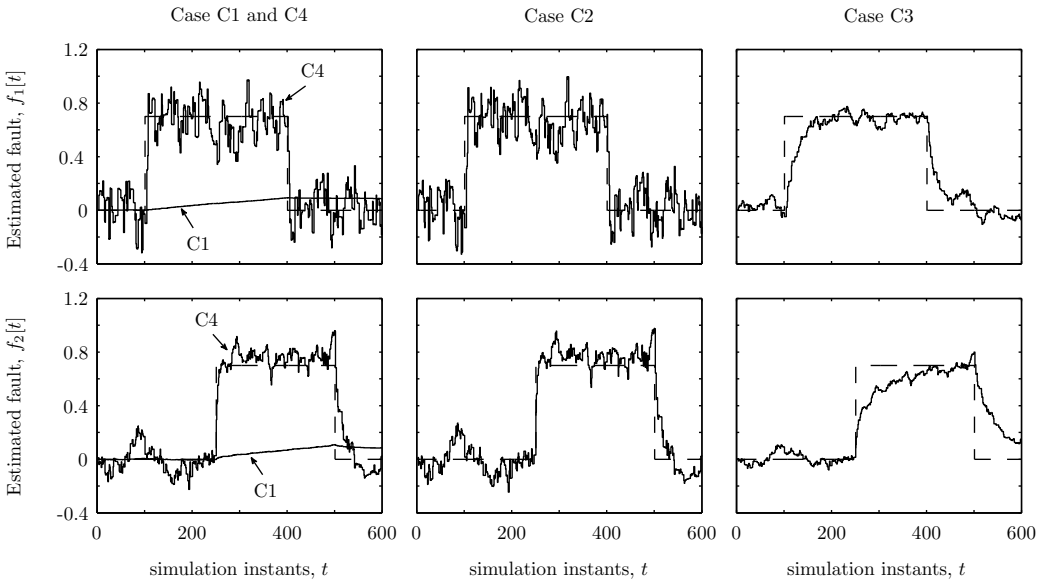

Figure 7.3: Fault estimation performances for the analyzed cases on Table 7.1.

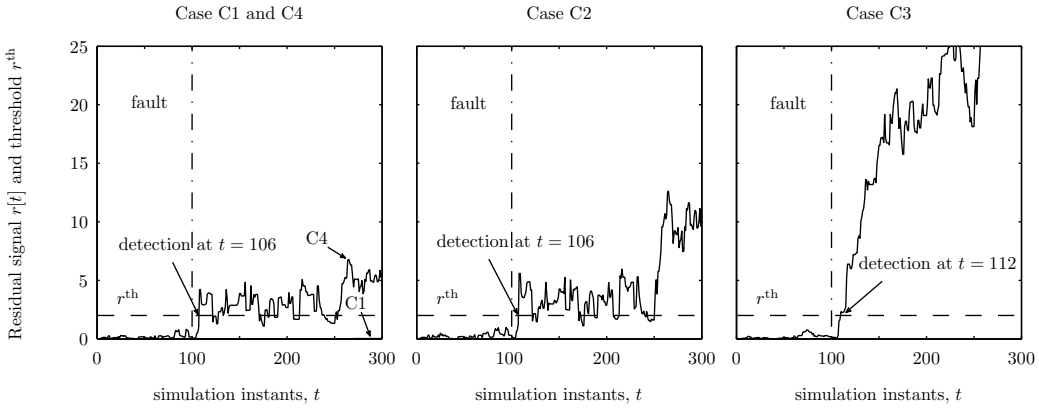

Figure 7.4: Fault detection performances for the analyzed cases on Table 7.1.

7.7 Conclusion

In the current chapter, we designed a jump observer-based fault diagnoser to detect and estimate faults under sampled measurement dropouts. We constructed the residual signal using a quadratic form of the estimated faults. A finite set of observer gains is used to estimate the faults and each gain is applied depending on the sampling scenario. We employed the sample successful reception probabilities from each sensor to describe the possible sampling scenarios.

The proposed design method allows finding a trade-off between the achievable minimum detectable faults and the response time to faults, while guaranteeing a prescribed false alarm rate. Two design strategies can be used: fixing the minimum detectable faults and then minimizing the response time, or fixing the response time and then minimizing the minimum detectable faults.

We developed two ways of imposing a desired false alarm rate depending on the assumed knowledge about the probability distribution of the residual signal. If no information is assumed to be known, the Markov's inequality leads to a very conservative bound on the false alarm rate. If the disturbances and noise are assumed to be Gaussian, a certain condition imposed on matrix F leads to a chi-squared residual distribution. In this case a very precise bound on the false alarm rate is attained, improving the fault diagnosis performance.

In this chapter, we considered that the control input was causally available at the central unit. Next chapter addresses the case when the control input being applied at the process is unknown at the central unit, due to possible dropouts in the transmissions between central unit and actuators trough a network without delivery acknowledgement.

Chapter 8

Networked gain-scheduled fault diagnosis under control input dropouts without data delivery acknowledgement

ABSTRACT: *This chapter investigates the fault diagnosis problem for NCS under dropouts in both control and sensing channel with no delivery acknowledgment. The observer-based fault diagnoser and the controller are collocated. The observer estimates the faults and computes a residual signal whose comparison with a threshold alarms the fault appearance. We use the expected value of the arriving control input for the open loop estimation and the measurement sample reception scenario for the correction with a jump observer. The jumping gains are scheduled in real time with rational functions depending on a statistic of the difference between the control command being applied in the plant and the one being used in the observer. We design the observer, the residual and the threshold to maximize the sensitivity under faults while guaranteeing some minimum detectable faults under a predefined FAR. We use a SOS-based solution approach to make the design problem tractable.*

Control systems in industry are becoming more complex and communication networks enhance flexibility and ease of manoeuvre [44]. However, in NCS, where the elements of the control architecture are not collocated, these benefits are achieved at the expense of introducing some new issues as time delays and dropouts in the information transmission [51, 14]. With the appearance of these network-induced problems, guaranteeing a reliable, safe and efficient operation of NCS has become a challenging concern in the last years, and researches have being adapting and improving traditional model-based fault diagnosis methods [15] to operate in networked environments [35, 121].

Generally, when dealing with dropouts, the existing observer-based fault detection and estimation algorithms only consider sampled measurement losses either by focusing on filter design or by assuming that the control input being applied at the plant is known when updating the observer [87, 48, 72, 146, 83, 81] (see Chapter 7). Concerning samples dropouts, the use of jump observers whose modes are related to the sampled measurement transmission outcome improves estimation performances (with respect to gain invariant approaches, see Chapter 3) and have been employed to fault detection in [87, 72]. But, when the controller and fault diagnoser are collocated, and the controller to actuator link is offered by a network without successful delivery acknowledgement (differently from Chapter 7), the above mentioned methods are not applicable and lead to poor performances.

Some works as [135] and [139] have addressed the problem of dealing with the control error induced by dropouts in the control channel, i.e., with the difference between the applied control input in the process and the one used in the observer. The authors of [135] used the expected value of the control command at the process to update the state estimation and designed the residual signal to guarantee some performances under faults and disturbances. After describing the involved residual signal in terms of the control error, [139] went one step beyond by generating a time-varying threshold adapted in real time to some control error statistics, allowing them to assure a predefined false alarm rate (FAR). However, in both works [135, 139] an observer-based residual generation schema with invariant gains was employed. Owing to guarantee robustness against all possible control errors, those approaches lead to conservative fault detection performance for control errors smaller than foreseen.

In the current chapter, we employ the expected value of the control input being applied at the process to run the open loop fault estimation. We then derive a control error statistic available in real time that can be modelled by a bounded time-varying parameter. Based on [111, 55], the performance of a fault diagnosis algorithm can be defined by means of the trade-offs between the sensitivity to faults and the FAR. Seeking to improve fault diagnosis performances (e.g., time to detect faults), we introduce a gain-scheduled jump observer to estimate the faults. The observer gain jumps with the sampling scenario, modeled as a Markov chain, and follows a function of the aforementioned control error statistic. We define the residual signal as a quadratic form of the estimated fault vector whose comparison with a threshold guarantees fault detection. The major novelty of this chapter lies in scheduling in real time the observer gains with the control error statistic.

We design the gain-scheduled jump observer, the residual and the threshold in order to minimize the response time to faults, by minimizing the H_∞ norm from fault to fault estimation error subject to attain disturbance and measurement noise attenuation and to guarantee fault detection over some minimum detectable faults with a prescribed FAR for all the possible control error occurrences. To handle this optimization procedure we fix the gain-scheduling function to be polynomial and then, we exploit sum-of-squares (SOS) decomposition techniques (see [50, 16]). Some previous works have applied SOS methods to nonlinear polynomial systems [102], to linear parametric varying (LPV) systems [143] or to quasi-LPV systems [3]. The conceptual novelty introduced with respect to those works is the employment of SOS methods (in the aim of Chapter 5) to schedule the observer-based fault diagnoser with a time-varying control error statistic that depends on the behavior of the network and is known in real time.

This chapter is organized as follows. We define the problem in Section 8.1, and present the observer-based fault diagnoser design in 8.2. Section 8.3 explores some examples and, finally, in Section 8.4 we summarize the main conclusions.

8.1 Problem setup

We consider LTI DTS of the form

$$x_{t+1} = A\,x_t + B\,u_t + B_w\,w_t + B_f\,f_t, \tag{8.1}$$

where $x \in \mathbb{R}^n$ is the state, $u \in \mathbb{R}^{n_u}$ is the control input, $w \in \mathbb{R}^{n_w}$ is the state disturbance, and $f \in \mathbb{R}^{n_f}$ is the fault vector. The system has n_m measurable outputs. Each measurable output can be measured by at least one sensor (that may introduce faults), having

$n_y \geq n_m$ sensors. We write the measured and transmitted value as

$$m^e_{s,t} = c_s\, x_t + h_s\, f_t + v_{s,t}, \quad s = 1, \ldots, n_y \tag{8.2}$$

where $m^e_{s,t} \in \mathbb{R}$ is the t-th sampled measurement of the s-th sensor and $v_{s,t} \in \mathbb{R}$ is the s-th sensor noise. c_s denotes a row of matrix $C = [c_1^T \ \cdots \ c_{n_m}^T\ ]^T$ (different c_s can refer to the same row of C) and h_s each of the rows of matrix H. Both the state disturbance input and the measurement noise are assumed to be wide-sense stationary stochastic processes[1] with bounded variances where their RMS norms are bounded by $\|w\|_{\text{RMS}} \leq \bar{w}_{\text{rms}}$ and $\|v\|_{\text{RMS}} \leq \bar{v}_{\text{rms}}$ (with $v_t = [v_{1,t} \ \cdots \ v_{n_y,t}]^T$).

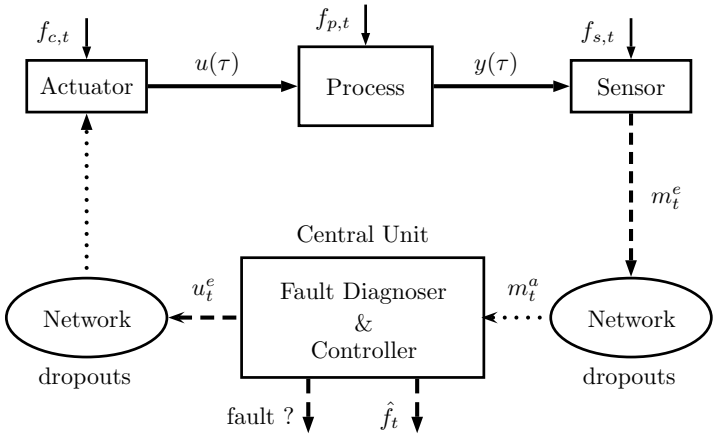

Figure 8.1: Networked fault diagnosis problem under dropouts with possible faults in the actuator (f_c), faulty components in the plant (f_p) and faulty sensor (f_s).

In the current chapter, we model the fault as a slow time-varying signal (cf. [13, 149]), i.e.,

$$f_{t+1} = f_t + \Delta f_t, \ \|\Delta f\|_\infty \leq \overline{\Delta f} \tag{8.3}$$

where Δf_t is the bounded fluctuation of the fault from instant t to $t+1$. This allows us to model, for instance, step signals (Δf_t would only be different from zero when the fault appears) or ramp signals (Δf_t has a constant value) that have been widely used to test fault detection algorithms [15, 58].

We aggregate the evolution of the system state (8.1) and the fault (8.3) leading to an extended order model defined by

$$z_{t+1} = \bar{A}\, z_t + \bar{B}\, u_t + \bar{B}_w\, w_t + \bar{B}_f\, \Delta f_t \tag{8.4}$$

with $z_t = \begin{bmatrix} x_t^T & f_t^T \end{bmatrix}^T$ and

$$\bar{A} = \begin{bmatrix} A & B_f \\ 0 & I \end{bmatrix},\ \bar{B} = \begin{bmatrix} B \\ 0 \end{bmatrix},\ \bar{B}_w = \begin{bmatrix} B_w \\ 0 \end{bmatrix},\ \bar{B}_f = \begin{bmatrix} 0 \\ I \end{bmatrix}$$

[1] If x_t is wide sense stationary its RMS norm becomes $\|x\|_{\text{RMS}} = \sqrt{\mathbf{E}\{x_t^T x_t\}}$, which is a constant value.

where $z \in \mathbb{R}^{\bar{n}}$ with $\bar{n} = n + n_f$. Then, the sampled measurements are

$$m^e_{s,t} = \bar{c}_s z_t + v_{s,t}, \quad s = 1, \ldots, n_y \tag{8.5}$$

with $\bar{c}_s = [c_s \; h_s]$. We consider that the pair $(\bar{A}, \bar{C})$ is detectable (being $\bar{C}$ the matrix whose rows are $\bar{c}_s$), otherwise (i.e., $n_f > n_y$), only a combination of the faults can be detected.

Remark 8.1. A transformation of the system when the pair $(\bar{A}, \bar{C})$ is undetectable must be carried out (leading to new $\bar{n}_f$ faults, a combination of the original faults, with $\bar{n}_f \leq n_y$) before the methods on this chapter become valid, as proposed in [74].

In the current chapter, we consider that the fault diagnoser and the controller are collocated in a central unit. We assume that sensors, central unit and actuators communicate through a network without successful delivery acknowledgement of sent packets (e.g. UDP-like networks) where dropouts are likely to occur (see Fig. 8.1). The control input sent to the actuators is assumed to be known.

8.1.1 Sampled measurement reception modeling

Each sensor measures its output synchronously with the control input update and transmits, independently from each other, a time-tagged packet with the sample $m^e_{s,t}$ to the central unit through the network (see Fig. 8.1). We model the reception state of each sample from sensor $s = 1$ to n_y at instant t with

$$\alpha_{s,t} = \begin{cases} 1 & \text{if } m^e_{s,t} \text{ is acquired at instant } t, \\ 0 & \text{if } m^e_{s,t} \text{ is lost.} \end{cases} \tag{8.6}$$

Then, the available information at instant t at the central unit is the pair $(m^a_{s,t}, \alpha_{s,t})$ for all $s = 1, \ldots, n_y$, where $m^a_{s,t} = \alpha_{s,t}\, m^e_{s,t}$. We use process α_t to model the sampled measurement reception scenario at instant t, where $\alpha_t = \bigoplus_{s=1}^{n_y} \alpha_{s,t}$ is a diagonal matrix with binary variables in its diagonal elements. Thus, we can redefine the acquired samples at instant t as

$$m^a_t = \alpha_t \left(\bar{C}\, z_t + v_t \right), \tag{8.7}$$

where $v_t = [v_{1,t} \cdots v_{n_y,t}]^T$ is the measurement noise vector.

We assume that the outcomes of α_t are governed by a finite ergodic[2] Markov chain [9] whose modes are in the set

$$\alpha_t \in \Xi = \{\eta_0, \eta_1, \ldots, \eta_q\}, \; q = 2^{n_y} - 1, \tag{8.8}$$

where η_i (for $i = 0, \ldots, q$) represents each possible measurement reception scenario. η_0 denotes the case when $\alpha_t = 0$. The transition probability matrix $\Lambda = [p_{i,j}]$ with

$$p_{i,j} = \mathbf{Pr}\{\alpha_{t+1} = \eta_j \big| \alpha_t = \eta_i\}$$

is assumed to be known.

[2] In an ergodic Markov chain every state can be reached from every state in a finite time.

Remark 8.2. Assuming mutually independent Markovian processes for the packet dropouts, i.e.,

$$\begin{aligned}
&\mathbf{Pr}\{\alpha_{s,t}=0|\alpha_{s,t-1}=0\}=q_s,\\
&\mathbf{Pr}\{\alpha_{s,t}=1|\alpha_{s,t-1}=0\}=1-q_s,\\
&\mathbf{Pr}\{\alpha_{s,t}=1|\alpha_{s,t-1}=1\}=p_s,\\
&\mathbf{Pr}\{\alpha_{s,t}=0|\alpha_{s,t-1}=1\}=1-p_s,
\end{aligned}$$

for all $s=1,\ldots,n_y$, each probability of matrix $\Lambda=[p_{i,j}]$ (for $i,j=0,\ldots,q$) is computed as

$$p_{i,j}=\prod_{s=1}^{n_y}\mathbf{Pr}\{\alpha_{s,t}=\eta_{s,j}|\alpha_{s,t-1}=\eta_{s,i}\}$$

where $\eta_{s,i}$ is the s-th diagonal element of η_i.

8.1.2 Control input update modelling

Let us remember here how to model the transmission of control inputs through an UDP-like network (see Section 2.4). At each instant $t-1$, the controller sends to the actuators (through the network) a single packet with all the control inputs to be used at instant t[3]. We denote by u_t^e the control input transmitted from the controller (at $t-1$) to be applied at instant t. We model the control input reception at instant $t-1$ with

$$\gamma_{t-1}^u=\begin{cases}1 & \text{if } u_t^e \text{ is received at instant } t-1,\\ 0 & \text{if } u_t^e \text{ is lost.}\end{cases} \tag{8.9}$$

Each actuator implements a zero order hold strategy, i.e.,

$$u_t=\begin{cases}u_t^e & \text{if } \gamma_{t-1}^u=1\\ u_{t-1} & \text{otherwise.}\end{cases} \tag{8.10}$$

As the network involved in the communication has no acknowledgement of successful delivery, we ignore at the central unit the exact value of the control input being applied at each instant. We assume that the probability of being applying at instant t the control input transmitted at $t-\tau-1$ is known, i.e.

$$\varphi_\tau=\mathbf{Pr}\{u_t=u_{t-\tau}^e\},\qquad \tau=0,\ldots,N_u,\qquad \sum_{\tau=0}^{N_u}\varphi_\tau=1, \tag{8.11}$$

where N_u denotes the maximum integer number of consecutive packet dropouts from the central unit to the actuators. In Remark 2.15 (in Section 2.4) we showed how to obtain each φ_τ.

As the value of the real control input being applied to the process is unknown, we propose the use of its expected value $\mathbf{E}\{u_t\}$ to update the open loop observer estimation. Let us denote $\mathbf{E}\{u_t\}$ by u_t^c where

$$u_t^c=\sum_{d=0}^{N_u}\varphi_d\,u_{t-d}^e. \tag{8.12}$$

[3]This control strategy is used to overcome delays up to one instant, see [110].

With that definition, the control error $\tilde{u}_t = u_t - u_t^c$ (the difference between the control input being applied in the process and the one being used in the observer) can be expressed as

$$\tilde{u}_t = u_t - \sum_{d=0}^{N_u} \varphi_d \, u_{t-d}^e. \tag{8.13}$$

Lemma 2.2 (in Section 2.4) stated that

$$\mathbf{E}\{\tilde{u}_t\} = 0, \tag{8.14}$$

$$\mathbf{E}\{\tilde{u}_t^T \tilde{u}_t\} = \sum_{d=0}^{N_u} \varphi_d \left(u_{t-d}^e - \sum_{d=0}^{N_u} \varphi_d \, u_{t-d}^e \right)^T \left(u_{t-d}^e - \sum_{d=0}^{N_u} \varphi_d \, u_{t-d}^e \right). \tag{8.15}$$

Let us use δ_t to denote $\mathbf{E}\{\tilde{u}_t^T \tilde{u}_t\}$. Note that the value of δ_t is known and can be calculated in real time with (8.15) since the transmitted control input u_t^e is available at the central unit. In the present chapter, we assume that δ_t is a bounded time-varying signal fulfilling $\delta_t \in \mathcal{S}$ with

$$\mathcal{S} = \{\delta_t \, : \, 0 \leq \delta_t \leq \bar{\delta}, \; \forall k\}. \tag{8.16}$$

Remark 8.3. The upper bound $\bar{\delta}$ can be calculated analyzing the system and controller dynamic that may include magnitude saturation and rate limitation. However, the accurate calculation of this bound is not really necessary, since $\bar{\delta}$ only defines the search space of the optimization problem (that will be described later), and hence $\bar{\delta}$ may simply be selected to be a high enough value.

8.1.3 Fault diagnosis algorithm

Taking into account the previous analysis, the proposed fault estimation algorithm is as follows:

$$\hat{z}_t^- = \bar{A} \, \hat{z}_{t-1} + \bar{B} \, u_{t-1}^c, \tag{8.17}$$

$$\hat{z}_t = \hat{z}_t^- + L_t \, (m_t^a - \alpha_t \, \bar{C} \, \hat{z}_t^-). \tag{8.18}$$

At each instant t, we run the model in open loop using the expected value of the control input being applied at the process u_{t-1}^c. When some samples are available at the central unit, we update the estimation by means of the updating gain matrix L_t. Otherwise, we hold the open loop, i.e., $\hat{z}_t = \hat{z}_t^-$ (note that m_t^a is zero under dropouts). Defining the extended state estimation error as $\tilde{z}_t = z_t - \hat{z}_t$, its dynamic is given by

$$\tilde{z}_t = \left(I - L_t \, \alpha_t \, \bar{C}\right) \left(\bar{A} \, \tilde{z}_{t-1} + B_{\mathcal{W}} \, \mathcal{W}_{t-1}\right) - L_t \, \alpha_t \, v_t \tag{8.19}$$

where $B_{\mathcal{W}} = [\bar{B}_w \;\; \bar{B}_f \;\; \bar{B}]$ and $\mathcal{W}_{t-1} = [w_{t-1}^T \;\; \Delta f_{t-1}^T \;\; \tilde{u}_{t-1}^T]^T$.

Using the estimated faults from (8.18), as $\hat{f}_t = [0 \; I] \, \hat{z}_t$, we define the residual signal of the fault detection algorithm as

$$r_t = \hat{f}_t^T \, F^{-1} \, \hat{f}_t, \tag{8.20}$$

where F is some matrix to be defined. Then, the fault detection law is

$$\begin{cases} \text{if } r_t \leq r^{\text{th}} & \text{no fault,} \\ \text{if } r_t > r^{\text{th}} & \text{fault,} \end{cases} \tag{8.21}$$

being r^{th} a constant threshold to be defined. Then, fault isolation is attained by combining fault estimation and fault detection, allowing us to identify the source of the faults.

Remark 8.4. Extending the definition of a minimum detectable fault given in [15], we define a minimum detectable fault as a fault that makes the residual cross a unitary threshold (i.e., $r^{\text{th}} = 1$), provided no other faults, disturbances, measurement noises and control errors are present. Then, under zero fault estimation error (i.e. $\hat{f} = f$), each diagonal element of F in (7.13) multiplied by r^{th} defines the minimum detectable fault as $f_{\min,l} = r^{\text{th}} F(l,l)$ for the corresponding channel ($l = 1, \ldots, n_f$).

Considering the fault detection decision, a false alarm is produced if $r_t > r^{\text{th}}$ when $f_t = 0$ and the FAR is defined as the average probability of rising false alarms over an infinite-time window, i.e.

$$\Psi = \lim_{T\to\infty} \frac{1}{T} \sum_{t=0}^{T-1} \Pr\left\{ r_t > r^{\text{th}} \,\middle|\, f_t = 0 \right\}. \tag{8.22}$$

The aim of this work is to compute gain matrices L_t, matrix F, and threshold r^{th} such that the fault diagnoser attains disturbance and measurement noise attenuation, reaches some fault diagnosis performances, assures a given FAR and overcomes the uncertainty introduced by the control input dropouts for any $\delta_t \in \mathcal{S}$.

Using jump linear estimators that relate their jumps to the measurement reception improves the estimation performance with respect to employing invariant gain estimators [130] and have been recently adapted to fault detection algorithms [87, 72]. When dealing with the uncertainty of the control input update, the authors of [139] propose to adapt the threshold to the mean and variance of the control error in order to improve the performance of their fault detector. However, they used an invariant gain observer approach that leads to conservative fault diagnosis performances for control errors smaller than anticipated. In the current work, in order to improve the fault diagnosis performance, we propose a Markovian jump estimator with a gain-scheduled approach depending on the real time values of δ_t, i.e.

$$L_t = L(\alpha_t, \Delta_{t-1}) = \begin{cases} L_i(\Delta_{t-1}) & \text{if } \alpha_t = \eta_i \text{ for } i = 1, \ldots, q, \\ 0 & \text{if } \alpha_t = \eta_0. \end{cases} \tag{8.23}$$

where

$$\Delta_{t-1} = \begin{bmatrix} \delta_{t-1} & \delta_{t-2} \end{bmatrix}^T. \tag{8.24}$$

We schedule the updating gain L_t with both the current control error statistic δ_{t-1} (at instant k) and the past one δ_{t-2} (at instant $k-1$) to consider the present control uncertainty δ_{t-1} as well as the variation it has suffered from δ_{t-2} to δ_{t-1}. Note that, as the updating gain $L(\alpha_t, \Delta_{t-1})$ is scheduled with α_t and Δ_{t-1}, the residual signal r_t is also related to these parameters.

8.2 Fault diagnoser design

In this section we address the design of the gain-scheduled Markovian jump observer with law $L(\alpha_t, \Delta_{t-1})$ as well as the residual r_t and its threshold r^{th} with an H_∞-based procedure. We first present a sufficient condition for the existence of such a fault diagnoser

based on matrix inequalities that depend on the control error statistic Δ_t. This condition allows bounding the RMS norm of the fault estimation error vector. Second, we derive how to bound the FAR given by the fault diagnoser. Finally, we show that by restricting the dependences to be polynomial, we can solve the design problem in polynomial time through SOS methods.

The next theorem presents the H_∞ observer design based on a parameter-dependent matrix inequality.

Theorem 8.1. *Consider the fault estimation algorithm* (8.17)-(8.18) *applied to system* (8.1)-(8.3). *If there exist positive definite symmetric matrices $P_j(\Delta_t)$ and F, full matrices $G_j(\Delta_t)$ and $X_j(\Delta_t)$, and positive scalar functions $\gamma_w(\Delta_t)$, $\gamma_v(\Delta_t)$, $\gamma_u(\Delta_t)$ and $\gamma_f(\Delta_t)$ for all $i,j=0,\dots,q$ and $\delta_t \in \mathcal{S}$ fulfilling*

$$\Upsilon_i(\Delta_t,\Delta_{t-1}) = \begin{bmatrix} \Omega(\Delta_t) & \bar{M}_{A,i}(\Delta_t) & \bar{M}_{B,i}(\Delta_t) & 0 \\ \bar{M}_{A,i}(\Delta_t)^T & P_i(\Delta_{t-1}) & 0 & \bar{B}_f \\ \bar{M}_{B,i}(\Delta_t)^T & 0 & \Gamma(\Delta_t) & 0 \\ 0 & 0 & \bar{B}_f^T & F \end{bmatrix} \succ 0, \tag{8.25}$$

being Δ_t as in (8.24), *with*

$$\begin{aligned}
\Omega(\Delta_t) &= \bigoplus_{j=0}^{q} G_j(\Delta_t) + G_j(\Delta_t)^T - P_j(\Delta_t), \\
\bar{M}_{A,i}(\Delta_t) &= \left[\sqrt{p_{i,0}} M_{A,0}(\Delta_t)^T \quad \cdots \quad \sqrt{p_{i,q}} M_{A,q}(\Delta_t)^T\right]^T, \\
M_{A,j}(\Delta_t) &= \left(G_j(\Delta_t) - X_j(\Delta_t)\,\eta_j\,\bar{C}\right)\bar{A}, \\
\bar{M}_{B,i}(\Delta_t) &= \left[\sqrt{p_{i,0}} M_{B,0}(\Delta_t)^T \quad \cdots \quad \sqrt{p_{i,q}} M_{B,q}(\Delta_t)^T\right]^T, \\
M_{B,j}(\Delta_t) &= \left[\left(G_j(\Delta_t) - X_j(\Delta_t)\,\eta_j\,\bar{C}\right)\left[\bar{B}_w \quad \bar{B}_u \quad \bar{B}_f\right] \quad -X_j(\Delta_t)\eta_j\right], \\
\Gamma(\Delta_t) &= \gamma_w(\Delta_t)\, I_{n_w} \oplus \gamma_u(\Delta_t)\, I_{n_u} \oplus \gamma_f(\Delta_t)\, I_{n_f} \oplus \gamma_v(\Delta_t)\, I_{n_m},
\end{aligned}$$

then, defining the observer gain matrices as $L_i(\Delta_t) = G_i(\Delta_t)^{-1} X_i(\Delta_t)$, the following statements are fulfilled for all $\alpha_t \in \Xi$, $\delta_t \in \mathcal{S}$, $\|w\|_{\mathrm{RMS}} \le \bar{w}_{\mathrm{rms}}$, $\|v\|_{\mathrm{RMS}} \le \bar{v}_{\mathrm{rms}}$ and $\|\Delta f\|_\infty \le \overline{\Delta f}$:

i) In the absence of disturbances, faults, control errors and measurement noises, the extended state estimation error (8.19) *converges asymptotically to zero in average.*

ii) Under null initial conditions, the expected value of the squared RMS norm of the fault estimation error is bounded by

$$\mathbf{E}\{\|\tilde{f}\|_{\mathrm{RMS}}^2\} < \overline{\lambda}(F)\left(\bar{\gamma}_w \bar{w}_{\mathrm{rms}}^2 + \bar{\gamma}_v \bar{v}_{\mathrm{rms}}^2 + \bar{\gamma}_u + \bar{\gamma}_f\, n_f\, \overline{\Delta f}^2\right), \tag{8.26}$$

where

$$\bar{\gamma}_u = \lim_{K\to\infty} \frac{1}{K} \sum_{k=0}^{K-1} \gamma_u(\Delta_t)\,\delta_t, \quad \bar{\gamma}_\chi = \lim_{K\to\infty} \frac{1}{K} \sum_{k=0}^{K-1} \gamma_\chi(\Delta_t), \quad \chi = \{w,v,f\}. \tag{8.27}$$

Proof. See Appendix C.8.1. ■

Let us clarify and make some comments on the role of the decision matrix F and decision polynomials $\gamma_w(\Delta_t)$, $\gamma_u(\Delta_t)$, $\gamma_f(\Delta_t)$ and $\gamma_v(\Delta_t)$ in Theorem 8.1:

- Our approach uses updating gains $L(\alpha_{t+1}, \Delta_t)$ depending on the value of the control error statistic δ_t and δ_{t-1} . Then, gains $\gamma_{\_}(\Delta_t)$ (with $\gamma_{\_} = \{\gamma_w, \gamma_u, \gamma_v, \gamma_f\}$) are also related to Δ_t to better characterize the propagation of the state disturbances, control errors, measurements noises and fault changes to the fault estimation error characterized in (8.26) for all $\delta_t \in \mathcal{S}$.

- If we fix F to assure some minimum detectable faults, we can extract from (8.26) that minimizing $\gamma_f(\Delta_t)$ increases the sensitivity of the fault diagnoser to faults (i.e, decreases the response time to faults) for all the possible $\delta_t \in \mathcal{S}_1$ (as it minimizes the upper bound of $\mathbf{E}\{\|\tilde{f}\|^2_{\mathrm{RMS}}\}$). If δ_t is time-invariant ($\delta_t = \delta_{t-1}$ for all k, and thus vector Δ_t has equal row values), then (8.26) and (8.27) lead to

$$\mathbf{E}\{\|\tilde{f}\|^2_{\mathrm{RMS}}\} < \overline{\lambda}(F) \left(\gamma_w(\delta_t)\bar{w}^2_{\mathrm{rms}} + \gamma_v(\delta_t)\bar{v}^2_{\mathrm{rms}} + \gamma_u(\delta_t)\delta_t + \gamma_f(\delta_t)\, n_f\, \overline{\Delta f}^2\right). \tag{8.28}$$

The next theorem extends the previous one showing how to bound the sensitivity of the fault diagnoser to state disturbances, measurement noises and control errors to bound the FAR given by the fault detection law (8.21).

Theorem 8.2. *For a given threshold $r^{\mathrm{th}} \geq 0$ and $0 \leq \phi \leq 1$, and under the premisses of Theorem 8.1, if constraints* (8.25) *and*

$$\Phi(\Delta_t) = \gamma_w(\Delta_t)\, \bar{w}^2_{\mathrm{rms}} + \gamma_v(\Delta_t)\, \bar{v}^2_{\mathrm{rms}} + \gamma_u(\Delta_t)\, \delta_t < \phi\, r^{\mathrm{th}} \tag{8.29}$$

are fulfilled for all $\delta_t \in \mathcal{S}$, $\|w\|_{\mathrm{RMS}} \leq \bar{w}_{\mathrm{rms}}$ and $\|v\|_{\mathrm{RMS}} \leq \bar{v}_{\mathrm{rms}}$, then, the following additional statement holds:

iii) In the absence of faults and under null initial conditions, the fault detection logic (8.21) *assures an upper bound of the FAR* (8.22) *given by ϕ.*

Proof. See Appendix C.8.2.

■

Remark 8.5. In this work we propose a gain-scheduled fault diagnosis schema where the sensitivity to faults, through $\gamma_f(\Delta_t)$, is adapted to the control error (to improve the time response to faults) while the threshold r^{th} and the minimum detectable faults, defined by F, remain constant to guarantee the same minimum detectable faults over all the possible control errors. In the aim of [139], the presented method can be extended with not much effort to an adaptive threshold fault diagnosis procedure with a constant sensitivity to faults by imposing an invariant γ_f and a control error dependent matrix $F(\Delta_t)$. Then, the minimum detectable faults (which can also be seen as a part of the threshold, see (8.20) and (8.21)) would depend on the control error as proposed in [139] but with an observer that is also scheduled with the control error.

8.2.1 SOS decomposition

Conditions (8.25) and (8.29) lead to an infinite-dimensional problem. The main difficulty is how to verify the conditions over the entire parameter space. To deal with a finite-dimensional problem, we restrict the matrices and scalar functions in Theorem 8.2 to be polynomial functions of δ_t of fixed degree. Then, we can take advantage of SOS decompositions to turn the initial problem into a computationally tractable one.

Making use of the SOS decomposition results and notation in Appendix B, in the following theorem we present a sufficient condition to numerically find the parametric matrices and functions that guarantee the properties stated in Theorem 8.1. We will use δ_1, δ_2, δ_3, $\Delta_1 = \begin{bmatrix}\delta_1 & \delta_2\end{bmatrix}^T$ and $\Delta_2 = \begin{bmatrix}\delta_2 & \delta_3\end{bmatrix}^T$ to denote independent SOS variables representing de possible values of δ_t, δ_{t-1}, δ_{t-2}, Δ_t and Δ_{t-1} respectively where $\delta_t \in \mathcal{S}$ for all t.

Theorem 8.3. *For a given threshold $r^{\text{th}} > 0$ and $0 \leq \phi \leq 1$, if there exist a symmetric positive definite matrix $F \in \mathbb{R}^{n_f \times n_f}$, symmetric polynomial matrices*

$$P_i(\Delta_1) = \left(\Delta_1^{\{d_P\}} \otimes I_{\bar{n}}\right)^T P_i \left(\Delta_1^{\{d_P\}} \otimes I_{\bar{n}}\right) \tag{8.30}$$

$$P_i(\Delta_2) = \left(\Delta_2^{\{d_P\}} \otimes I_{\bar{n}}\right)^T P_i \left(\Delta_2^{\{d_P\}} \otimes I_{\bar{n}}\right) \tag{8.31}$$

with symmetric matrices $P_i \in \mathbb{R}^{\bar{n}\sigma(2,d_P)\times\bar{n}\sigma(2,d_P)}$ for $i = 0, \ldots, q$, polynomial matrices

$$G_i(\Delta_1) = G_i \left(\Delta_1^{\{d_G\}} \otimes I_{\bar{n}}\right), \quad X_i(\Delta_1) = X_i \left(\Delta_1^{\{d_P\}} \otimes I_{n_m}\right), \tag{8.32}$$

with $G_i \in \mathbb{R}^{\bar{n}\times\bar{n}\sigma(2,d_G)}$ and $X_i \in \mathbb{R}^{\bar{n}\times n_m\sigma(2,d_X)}$ for $i = 0, \ldots, q$, and polynomial functions

$$\gamma_w(\Delta_1) = \gamma_w^T \Delta_1^{\{d_\gamma\}}, \quad \gamma_u(\Delta_1) = \gamma_u^T \Delta_1^{\{d_\gamma - 1\}}, \quad \gamma_f(\Delta_1) = \gamma_f^T \Delta_1^{\{d_f\}}, \quad \gamma_v(\Delta_1) = \gamma_v^T \Delta_1^{\{d_\gamma\}} \tag{8.33}$$

with $\gamma_w \in \mathbb{R}^{\sigma(2,d_\gamma)}$, $\gamma_u \in \mathbb{R}^{\sigma(2,d_\gamma-1)}$, $\gamma_f \in \mathbb{R}^{\sigma(2,d_f)}$ and $\gamma_v \in \mathbb{R}^{\sigma(2,d_\gamma)}$, where $2d_P$, d_G, d_X, d_γ, $d_\gamma - 1$ and d_f are the degrees of the involved polynomials, that fulfill the following constraints

$$\mu^T P_i(\Delta_1)\,\mu - s_{P1,i}(\delta_1,\mu)\,h(\delta_1) - s_{P2,i}(\delta_2,\mu)\,h(\delta_2) \in \Sigma(\Delta_1,\mu), \tag{8.34a}$$

$$s_{P1,i}(\delta_1,\mu) \in \Sigma(\delta_1,\mu), \quad s_{P2,i}(\delta_2,\mu) \in \Sigma(\delta_2,\mu), \tag{8.34b}$$

$$\nu^T \Upsilon_i(\Delta_1,\Delta_2)\,\nu - s_{\Upsilon1,i}(\delta_1,\nu)\,h(\delta_1) - s_{\Upsilon2,i}(\delta_2,\nu)\,h(\delta_2) - s_{\Upsilon3,i}(\delta_3,\nu)\,h(\delta_3) \in \Sigma(\Delta_1,\Delta_2,\nu) \tag{8.34c}$$

$$s_{\Upsilon1,i}(\delta_1,\nu) \in \Sigma(\delta_1,\nu), \quad s_{\Upsilon2,i}(\delta_2,\nu) \in \Sigma(\delta_2,\nu), \quad s_{\Upsilon3,i}(\delta_3,\nu) \in \Sigma(\delta_3,\nu), \tag{8.34d}$$

$$\left(\phi\, r^{\text{th}} - \Phi(\Delta_t)\right) - s_{r1}(\delta_1)\,h(\delta_1) - s_{r2}(\delta_2)\,h(\delta_2) \in \Sigma(\Delta_1), \tag{8.34e}$$

$$s_{r1}(\delta_1) \in \Sigma(\delta_1), \quad s_{r2}(\delta_2) \in \Sigma(\delta_2), \tag{8.34f}$$

$$\gamma_j(\Delta_1) - s_{j1}(\delta_1)\,h(\delta_1) - s_{j2}(\delta_2)\,h(\delta_2) \in \Sigma(\Delta_1), \tag{8.34g}$$

$$s_{j1}(\delta_1) \in \Sigma(\delta_1), \quad s_{j2}(\delta_2) \in \Sigma(\delta_2), \quad j = \{w,\, u,\, f,\, v\}, \tag{8.34h}$$

for $i = 0, \ldots, q$ with $\Upsilon_i(\cdot)$ as in (8.25), $\Phi(\cdot)$ as in (8.29), $\mu \in \mathbb{R}^{\bar{n}}$, $\nu \in \mathbb{R}^{n_\nu}$ (with $n_\nu = \bar{n}\,(q+2) + 2\,n_f + n_w + n_u + n_m$) and

$$h(\delta) = \delta\,(\bar{\delta} - \delta),, \tag{8.35}$$

then constraints of Theorem 8.2 hold.

Proof. First, note that the set $\mathcal{S}$ is rewritten with its corresponding polynomial h as $\mathcal{S} = \{\delta : h(\delta) \geq 0\}$, see (8.35). Independent SOS variables δ_1, δ_2, δ_3 must fulfill $h(\cdot) \geq 0$ as $\delta_t \in \mathcal{S}$. Second, by Lemma B.3 and Lemma B.4 constraints (8.34c) and (8.34d) assure

the positive definiteness of $\Upsilon_i(\Delta_1, \Delta_2)$ for any $\delta_1, \delta_2, \delta_3 \in \mathcal{S}$, which guarantee (8.25) in Theorem 8.1. Third, by Lemma B.3 constraints in (8.34e) and (8.34f) asserts (8.29) in Theorem 8.2 for any $\delta_1, \delta_2 \in \mathcal{S}$. Finally, by Lemma B.3 and Lemma B.4 it follows that by constraints (8.34a), (8.34b), (8.34g) and (8.34h), we guarantee the positive definiteness of $P_i(\Delta_1)$, $\gamma_w(\Delta_1)$, $\gamma_u(\Delta_1)$, $\gamma_f(\Delta_1)$ and $\gamma_v(\Delta_1)$ for any $\delta_1, \delta_2 \in \mathcal{S}$ as required in Theorem 8.1.

■

In the above feasibility SOS problem μ and ν are scalarization vectors used to transform polynomial matrices in polynomials (see Lemma B.4). The decision variables are matrices P_i, G_i, X_i, F, γ_w, γ_u, γ_f and γ_v; and also the coefficients of SOS polynomials $s_{\_}$ in (8.34). We propose to choose the degree of these SOS polynomials in such a way that all the addends in each SOS expression have equal degree on all the variables. This can be performed by choosing d_P, d_G, d_X, d_γ and d_f, and then setting for all $j = 1, 2$ and $i = 0, \ldots, q$

$$\deg\, s_{Pj,i}(\delta_j, \mu) = \deg \left\{ \delta_j^{\max\{2d_P-2,\,0\}},\, \mu^2 \right\}, \tag{8.36a}$$

$$\deg\, s_{\Upsilon j,i}(\delta_j, \nu) = \deg \left\{ \delta^{\max\{2d_P-2,\,d_G-2,\,d_X-2,0\}},\, \nu^2 \right\}, \tag{8.36b}$$

$$\deg\, s_{\Upsilon 3,i}(\delta_3, \nu) = \deg \left\{ \delta^{\max\{2d_P-2,0\}},\, \nu^2 \right\}, \tag{8.36c}$$

$$\deg\, s_{rj}(\delta_j) = \deg\, \delta_j^{\max\{d_\gamma-2,\,0\}}, \tag{8.36d}$$

$$\deg\, s_{wj}(\delta_j) = \deg\, s_{vj}(\delta_j) = \deg\, \delta_j^{\max\{d_\gamma-2,\,0\}}, \tag{8.36e}$$

$$\deg\, s_{uj}(\delta_j) = \deg\, \delta_j^{\max\{d_\gamma-3,\,0\}}, \tag{8.36f}$$

$$\deg\, s_{fj}(\delta_j) = \deg\, \delta_j^{\max\{d_f-2,\,0\}}, \tag{8.36g}$$

where deg returns the maximum degree for each variable in the involved polynomial.

Remark 8.6. We have set the degree of polynomial $\gamma_u(\Delta_1)$ to be $d_\gamma - 1$ in order to assure the same degree on δ_t in the addends of expression (8.29).

Remark 8.7. The polynomial degrees defined by d_P, d_G, d_X, d_γ and d_f can be seen as trade-off parameters between conservativeness and computational effort. Moreover, if $d_G = 0$ and $d_X = 0$, the resulting updating gain L does not depend on Δ_t. If $d_G = 0$ and $d_X > 0$, matrix L has a polynomial form on Δ_t while if $d_G > 0$ and $d_X \geq 0$ it has a rational expression. Therefore, d_G and d_X define the dependency of L on Δ_t.

8.2.2 Fault diagnosis design strategy

Taking into consideration the fault diagnosis performances derived from Theorem 8.1 and Theorem 8.2, we propose the following strategy based on an optimization problem to design the fault diagnoser.

We force the fault diagnoser to only detect faults beyond some values (avoiding to rise alarms when faults are small), i.e., we impose each of the minimum detectable faults $f_{\min,l}$ (for $l = 1, \ldots, n_f$), while we intend to detect the presence of faults as fast as possible (higher fault sensitivity under faults) with a guaranteed FAR. We address the fulfillment of these constraints in the next optimization procedure.

Problem 8.1 (OP1)**.** For a unitary threshold $r^{\text{th}} = 1$ and a given desired FAR ψ, fix ϕ to be $\phi = \psi$. Let F be a diagonal matrix such as $F = \bigoplus_{l=1}^{n_f} f_{\min,l}^2$ where $f_{\min,l}$ stands for the minimum detectable fault. Then, the minimization problem

$$\begin{array}{ll} \text{minimize} & J \\ \text{subject to} & (8.34), \\ & J - \gamma_f(\Delta_1) - s_{J1}(\delta_1)\, h(\delta_1) - s_{J2}(\delta_2)\, h(\delta_2) \in \Sigma(\Delta_1), \\ & s_{J1}(\delta_1) \in \Sigma(\delta_1), \quad s_{J2}(\delta_2) \in \Sigma(\delta_2) \end{array} \tag{8.37}$$

with $\deg\, s_{J1}(\delta_1) = \deg\, \delta_1^{\max\{d_f-2,0\}}$ and $\deg\, s_{J2}(\delta_2) = \deg\, \delta_2^{\max\{d_f-2,0\}}$, assures fault detection over $f_{\min,l}$ (with $l = 1, \ldots, n_f$) with a FAR below ψ and maximizes in the worst case the sensitivity to faults of the resulting fault diagnoser for any possible δ_t .

Including constraints (8.34) in the above optimization problem guarantees the results of Theorem 8.2 as stated in Theorem 8.3. The new constraint imposes that

$$\gamma_f(\Delta_1) < J, \quad \forall \Delta_1 \in \{\delta_1, \delta_2 \,:\, h(\delta_1) \geq 0,\ h(\delta_2) \geq 0\},$$

which means that J is an upper bound of $\gamma_f(\Delta_t)$ for any k with $\delta_t \in \mathcal{S}$ (worst case). Then, $\bar{\gamma}_f < J$ (see (8.27)) and by minimizing J we minimize the upper bound of $\|\tilde{f}\|_{\text{RMS}}^2$ (see (8.26)) in the worst case.

Remark 8.8. Setting zero degree polynomials, (8.37) can be rewritten as a LMI optimization problem (worst case LMI design) such as

$$\begin{array}{ll} \text{minimize} & J \\ \text{subject to} & \Upsilon_i \succ 0, \\ & \gamma_w\, \bar{w}_{\text{rms}}^2 + \gamma_v\, \bar{v}_{\text{rms}}^2 + \gamma_u\, \bar{\delta} < 1, \\ & \gamma_f < J \end{array} \tag{8.38}$$

for all $i = 0, \ldots, q$ with Υ_i as in (8.25).

The previous optimization (8.37) may lead to quite conservative results because $\gamma_f(\Delta_1)$ is minimized for the worst case. In order to obtain less conservative results, we propose as an alternative to introduce some weighting function $g(\Delta_1)$ over $\gamma_f(\Delta_1)$ such that

$$\Gamma_f = \int_{\mathcal{S}\times\mathcal{S}} g(\Delta_1)\, \gamma_f(\Delta_1)\, \mathrm{d}\Delta_1. \tag{8.39}$$

The next optimization problem shows how to modify OP1 to include the weighting function $g(\Delta_1)$.

Problem 8.2 (OP2)**.** Consider some weighting function $g(\Delta_1)$, for a unitary threshold $r^{\text{th}} = 1$ and a given desired FAR Ψ, fix ϕ to be $\phi = \psi$. Let F be a diagonal matrix such as $F = \bigoplus_{l=1}^{n_f} f_{\min,l}^2$ where $f_{\min,l}$ stands for the minimum detectable fault. Then, the minimization problem

$$\begin{array}{ll} \text{minimize} & J \\ \text{subject to} & (8.34), \\ & \Gamma_f < J, \end{array} \tag{8.40}$$

where Γ_f is defined in (8.39), assures fault detection over $f_{\min,l}$ (with $l = 1, \ldots, n_f$) with a FAR below ψ and maximizes the sensitivity to faults of the resulting fault diagnoser under the weighting function $g(\Delta_1)$.

Remark 8.9. An interesting choice for function $g(\Delta_1)$ is the one that represents the case when δ_t is time invariant (constant or ramp-like transmitted control inputs, see (8.15)), that is $\delta_1 = \delta_2$, and all the possible values of $0 \leq \delta_t \leq \bar{\delta}$ are equally weighted (i.e., assuming no knowledge about which value is more likely). This weighting function can be defined as

$$g(\Delta_1) = \begin{cases} \dfrac{1}{\bar{\delta}} & \text{if } \delta_2 = \delta_1 \text{ and } 0 \leq \delta_1 \leq \bar{\delta}, \\ 0 & \text{otherwise.} \end{cases} \tag{8.41}$$

8.3 Examples

8.3.1 Example 1

For ease of analysis, let us first consider a simple linear time invariant discrete time system defined by (8.1)-(8.2) with

$$A = \begin{bmatrix} 0.48 & 0.11 \\ 0.11 & 0.97 \end{bmatrix}, \quad B_u = \begin{bmatrix} -0.5 \\ 0.7 \end{bmatrix}, \quad B_w = \begin{bmatrix} 0.2 \\ -0.6 \end{bmatrix}, \quad C = \begin{bmatrix} 0.18 & 0.8 \end{bmatrix},$$

where the measurable output is measured by just one sensor.

The state disturbances and measurement noises are Gaussian noises with zero mean and bounded RMS norms given by

$$\|w\|_{\text{RMS}} = 0.05, \quad \|v\|_{\text{RMS}} = 0.01.$$

The dropouts on the sensor to central unit link follow a Markov chain with

$$\mathbf{Pr}\{\alpha_{1,t} = 0 | \alpha_{1,t-1} = 0\} = 0.4, \quad \mathbf{Pr}\{\alpha_{1,t} = 1 | \alpha_{1,t-1} = 1\} = 0.7.$$

The transition probability matrix of the possible measurement transmission outcome is given by

$$\Lambda = \begin{bmatrix} 0.4 & 0.6 \\ 0.3 & 0.7 \end{bmatrix}.$$

The dropouts in the central unit to controller link follow a modified version of the above Markov chain with a maximum number of consecutive dropouts of $N_u = 6$ (see Remark 2.15). Then the probabilities of being using the control input sent $\tau - 1$ instants before are

$$\varphi = \begin{bmatrix} 0.668 & 0.2 & 0.08 & 0.032 & 0.0128 & 0.005 & 0.002 \end{bmatrix},$$

where $\varphi = [\varphi_0 \ \varphi_1 \ \varphi_2 \ \varphi_3 \ \varphi_4 \ \varphi_5 \ \varphi_6]$. Let us assume that in the worst case the control error statistic δ_t is bounded by $0 \leq \delta_t \leq 0.1$ for all k, i.e. $\bar{\delta} = 0.1$.

We address the problem of detecting possible faults from the actuator over 1.2 with a FAR under 0.1, which is the most interesting case due to the control input dropout (without delivery acknowledgement), i.e.

$$B_f = \begin{bmatrix} -0.5 \\ 0.7 \end{bmatrix}, \quad H = 0, \quad F = f_{\min}^2 = 1.2^2, \quad \phi = 0.1.$$

Table 8.1: Analyzed cases in Example 8.3.1.

Case	OP	d_P	d_G	d_X	d_γ	d_f	J
C1	1	0	0	0	0	0	154
C2	1	1	2	2	2	2	154
C3	2	1	2	2	2	2	63

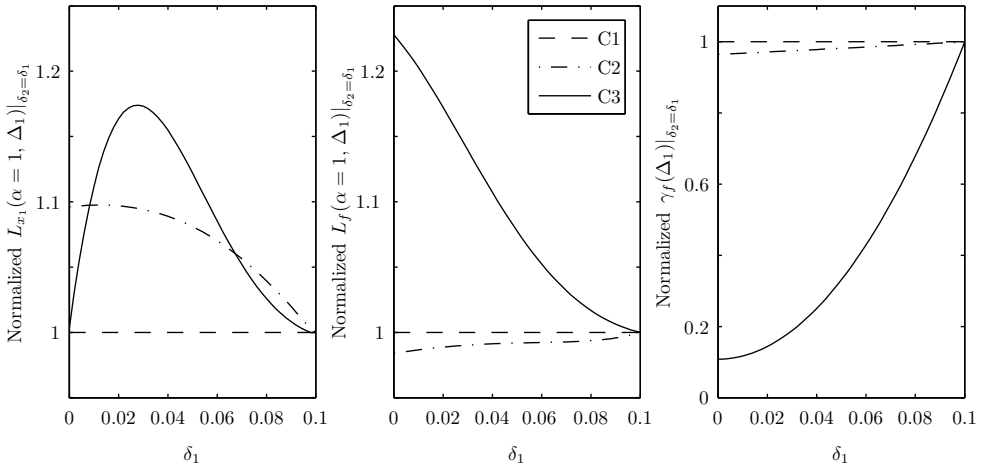

Figure 8.2: Comparison of the results given by optimization procedures C1, C2 and C3 normalized with respect to outcomes from C1 (see Table 8.1) when δ_t is time-invariant.

Let us first analyze the differences between using observer constant gains via the optimization problem in Remark 8.8 (worst case LMI design) and scheduling ones with second degree polynomials via design procedure OP1 (worst case SOS design) and OP2 with $g(\Delta_1)$ as defined in (8.41), see cases C1, C2 and C3 in Table 8.1 (all with $r^{\text{th}} = 1$). We represent the gain $L(\alpha, \Delta_1)$ as $L(\alpha, \Delta_1) = [L_{x_1}(\alpha, \Delta_1)\ L_{x_2}(\alpha, \Delta_1)\ L_f(\alpha, \Delta_1)]^T$ (we discard the analysis on $L_{x_2}(\alpha, \Delta_1)$ as its variation is not significant). Let us remember that $\Delta_1 = \begin{bmatrix}\delta_1 & \delta_2\end{bmatrix}^T$, where δ_1 models the current control error statistic and δ_2 de previous one. Fig. 8.2 illustrates, when $\delta_2 = \delta_1$ (i.e., δ_t time invariant), how the observer gains and the value of $\gamma_f(\Delta_1)|_{\delta_2=\delta_1}$ adapt their value to δ_1 when a measurement is received (i.e., $L(\alpha = 1,\ \Delta_1)|_{\delta_2=\delta_1}$). The values displayed in Fig. 8.2 have been normalized dividing them by the results from C1. Design C1 (constant gains) is the most conservative one as it keeps γ_f constant at the highest value for all δ_1. C2 improves the performance of C1 reducing γ_f up to a 5% (which increases the sensitivity under faults) when $\delta_1 = 0$ thanks to employing a scheduling observer gain. Design C3 requires selecting the weighting function $g(\Delta_1)$, but even with the simple choice proposed in Remark 8.9, it leads to the least conservative results, dividing by 10 the value of γ_f when $\delta_1 = 0$ with respect to its maximum value. Fig. 8.2 also shows that the proposed polynomial methods allow to obtain more sensitive fault diagnoser to faults (improving fault detection and estimation response) with respect to the constant gain observer, whenever δ_t is smaller than its

upper bound $\bar{\delta}$. From now on, we will only focus on C1 and C3.

Let us now examine for case C3 the full behavior of $L_f(\alpha = 1, \Delta_1)$ for any $\delta_1, \delta_2 \in \mathcal{S}$ normalized with respect to the correspondent gain of C1. Fig. 8.3 shows that the updating gain value becomes smaller as the control error increases. The maximum value of the gain occurs when there is no control error $\delta_1 = \delta_2 = 0$, while the minimum corresponds to the case when the control error is maximum ($\delta_1 = \delta_2 = \bar{\delta}$).

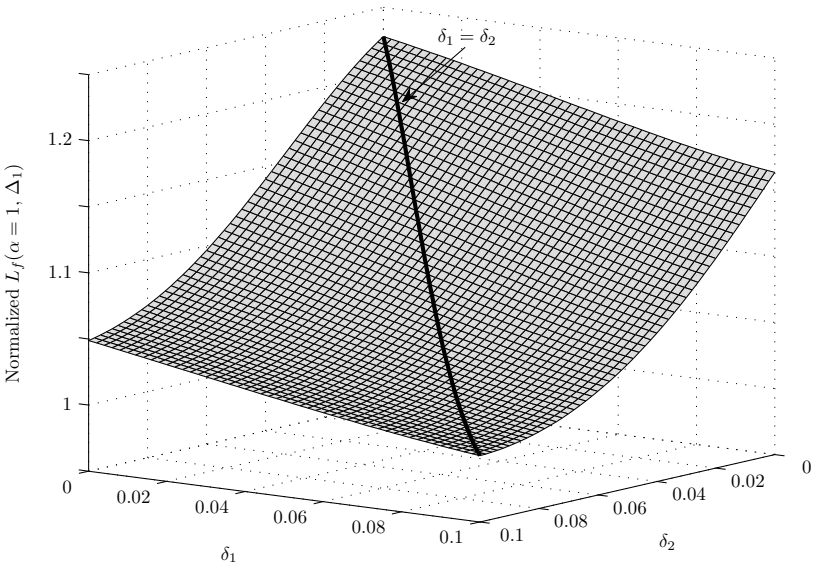

Figure 8.3: Normalized scheduled observer gain for C3 with respect to the one resulting from C1 in Table 8.1.

Finally, let us evaluate the behavior in simulation of the fault diagnosers for C1 and C3 under the appearance of step faults a 25% higher than $f_{\min}$ at $t = 10$ and $t = 60$ (vanishing at $t = 30$ and $t = 80$ respectively). Fig. 8.5 presents the involved control inputs in the networked fault diagnosis schema u_t, u_t^e and u_t^c, as well as the evolution in time of the squared control error $\tilde{u}_t^2$ and its statistic δ_t. We appreciate that while $\tilde{u}_t^2$ may have abrupt changes, δ_t changes slowly and smoothly. Fig. 8.4 shows the fault estimation and fault detection performances of the analyzed situation. The first fault appears when δ_t is near 0 and almost constant. Then, thanks to its scheduled updating gain the fault diagnoser for C3 reduces the fault detection time in a 40% and the fault estimation settling time (at the 95%) in a 50% with respect to C1. When the second fault occurs δ_t is more time-dependent and its value is near 0.07. In these conditions both fault diagnosers have the same performances. This proves that using a gain scheduling approach allows to improve the fault detection and estimation performances when δ_t is small, while for high δ_t values (near its maximum), our method retrieves the performances of the H_∞ constant gain design.

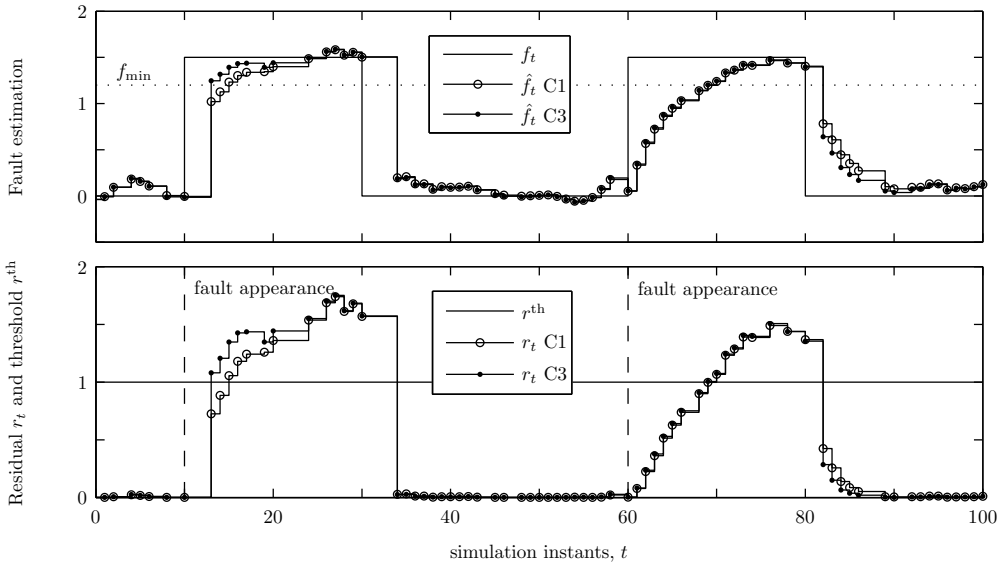

Figure 8.4: Fault estimation and fault detection performances in simulation for cases C1 and C3 in Table 8.1. Markers • and ∘ denote instants when a measurement sample is received.

8.3.2 Example 2

Let us now consider a more complex system by extending the previous one with

$$B_u = \begin{bmatrix} -0.5 & -0.3 \\ 0.7 & 0.2 \end{bmatrix}, \quad C = \begin{bmatrix} 0.18 & 0.8 \\ 0 & 1 \end{bmatrix}, \quad B_f = \begin{bmatrix} -0.5 & 0 \\ 0.7 & 0 \end{bmatrix}, \quad H = \begin{bmatrix} 0 & 1 \\ 0 & 0 \end{bmatrix}.$$

In this example, the system has two measured outputs, two control inputs and we desire to diagnose faults from the first actuator and first sensor. The successful transmissions from the new sensor to the central unit follow a Markov chain with

$$\mathbf{Pr}\{\alpha_{2,t} = 0 | \alpha_{2,t-1} = 0\} = 0.3, \quad \mathbf{Pr}\{\alpha_{2,t} = 1 | \alpha_{2,t-1} = 1\} = 0.5,$$

which is different and independent of the successful transmission from the existing sensor.

Similar than in Example 8.3.1 we aim to diagnose faults over $f_{\min} = 1.2$ (for both channels, $F = 1.2^2 \oplus 1.2^2$) with a FAR under 0.1 ($\phi = 0.1$). However, now we examine the obtained performances resulting from adapting the observer gain to the measurement reception scenarios α_t in addition to scheduling it with Δ_t, see cases C4 and C5 in Table 8.2.

Fig. 8.6 shows the estimation and detection performances of the fault diagnosers from C4 and C5 under the appearance of two faults given by

$$f_{1,k} = \begin{cases} 0, & \text{if } 0 \le t < 10 \\ 2\sin\left(\frac{t-10}{8}\right), & \text{if } 10 \le t < 85 \\ 0, & \text{if } t \ge 85 \end{cases}, \quad f_{2,k} = \begin{cases} 0, & \text{if } 0 \le t < 20 \\ 3\exp\left(-\frac{t-20}{10}\right), & \text{if } 20 \le t < 85 \\ 0, & \text{if } t \ge 85 \end{cases}$$

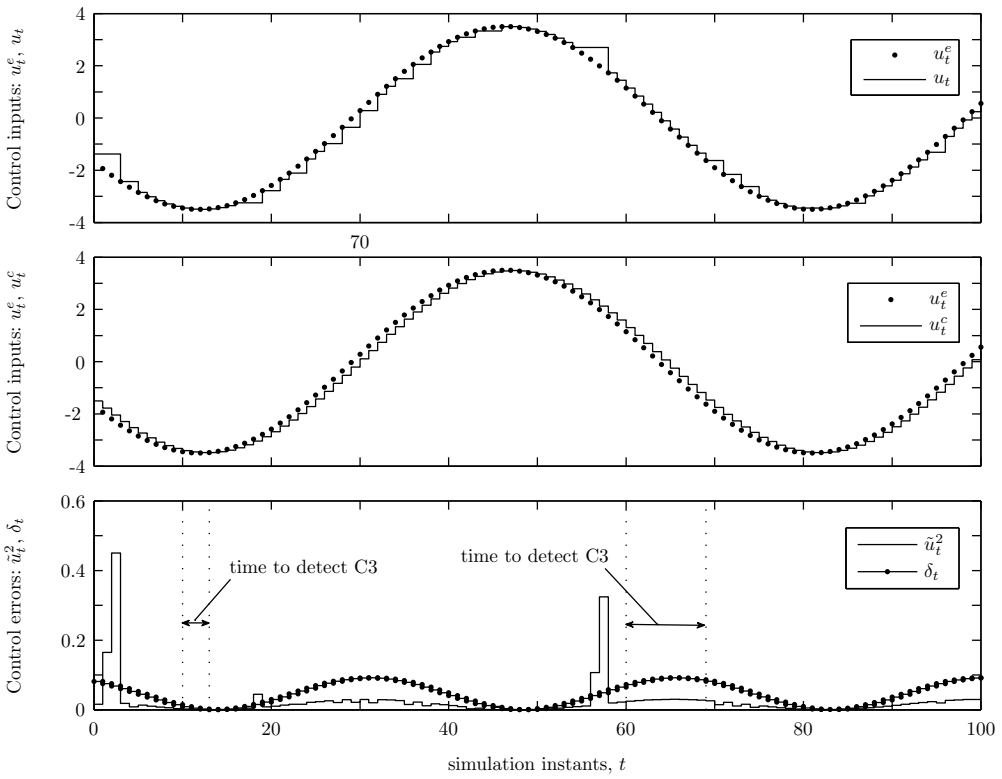

Figure 8.5: Control inputs involved in the NCS (control input applied in the plant u_t, transmitted control input u_t^e and control input used in the observer u_t^c), squared control error $\tilde{u}_t^2$ and its statistic δ_t in the simulation of Example 8.3.1.

Table 8.2: Analyzed cases in Example 8.3.2.

Case	Obsv. gain	OP	d_P	d_G	d_X	d_γ	d_f	J
C4	$L(\alpha_t, \Delta_{t-1})$	2	1	2	2	2	2	42
C5	$L(\Delta_{t-1})$	2	1	2	2	2	2	104

From Table 8.2 and Fig. 8.6 we appreciate that using an observer gain that jumps with the measurement reception scenarios (C4) improves the fault estimation and detection performances with respect to employing an observer gain that do not depend on α_t. For the analyzed case in Fig. 8.6, with C4 we reduce the RMS norm of the fault estimation error in simulation by a 23% with respect to C5.

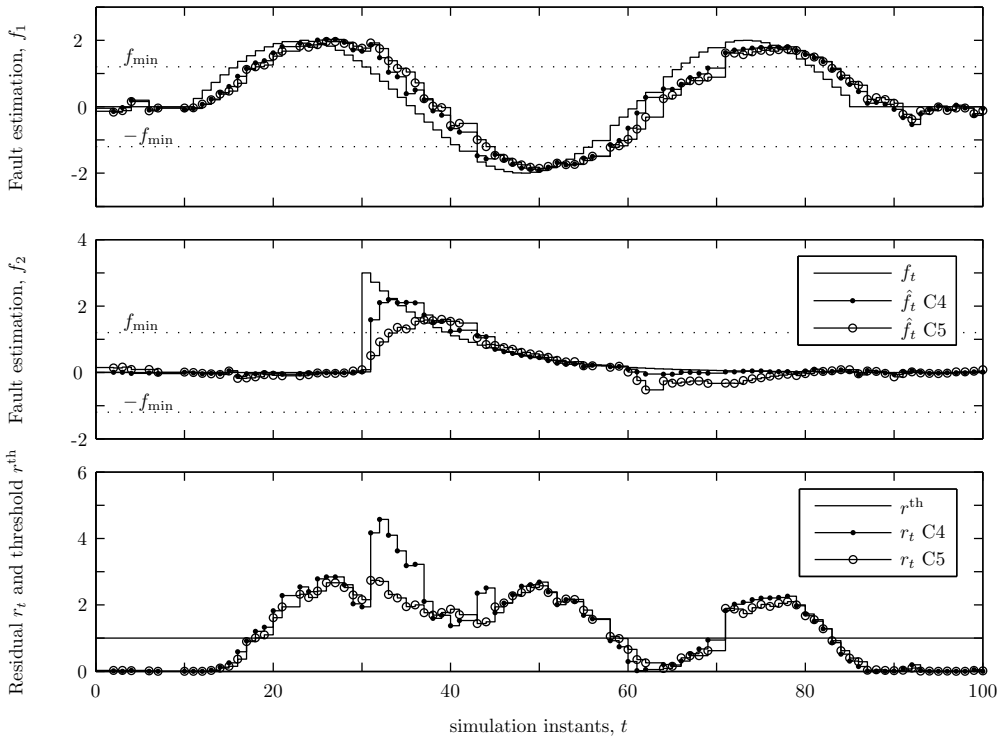

Figure 8.6: Fault estimation and fault detection performances in simulation for cases C4 and C5 in Table 8.2. Markers • and ○ denote instants when a measurement sample is received.

8.4 Conclusion

In the present chapter, we designed an observer-based fault diagnoser to operate under control input and measurement dropouts without successful delivery acknowledgement.

We characterized the sampling scenario with a Markov chain and described the control error between the control input being applied in the process and the one being used in the observer. With that, the observer gain is related to the sample transmission outcome and is scheduled in real time with a rational function of a control error statistic. We generated the residual signal using a quadratic form of the estimated faults provided by the observer, whose comparison to a threshold leads to fault detection.

The proposed design method allows minimizing the response time under faults while guaranteeing fault detection over some minimum detectable faults for a prescribed false alarm rate. We showed that our gain scheduling approach retrieves the performance of the worst case design with constant gains when the scheduling parameter is near to its upper bound, but improves it whenever the control error statistic is lower.

Part III

Conclusions of the thesis

Chapter 9

Conclusions and future work

In this final chapter, we present a short summary of the contributions of this thesis and conclude with some interesting future research lines.

9.1 Contributions

In this thesis we first studied the state estimation problem over networks. We focused on how to relate the gains of a Luenberg-like estimator to the network-induced data reception scenario. We proposed jump linear estimators whose gains are related to the data availability and gain-scheduled estimators whose gains are scheduled with the real time packet arrival rate estimation when it is time-varying. Second, we addressed the co-design estimation problem that consists of jointly designing the network operation conditions and the estimator, by minimizing the network resource consumption while assuring a predefined estimation performance. For the network operation, we analyzed two cases: event-based transmissions using the SOD protocol and power control of self-powered wireless nodes. Finally, we studied the fault diagnosis problem over networks. We developed fault diagnosis strategies that allow specifying the minimum detectable faults, the FAR and the dynamics of the fault diagnoser. Moreover we improved existing bounds on the FAR and extended the results when transmissions are performed through networks without delivery acknowledgement.

State estimation with jump observers

In Chapter 3 and Chapter 4 we designed jump state estimators for networked control systems where transmitted data is subject to time-varying delays and dropouts. In Chapter 3 the gains jump depending on the number of consecutive time instants without samples and on the available samples, while in Chapter 4 the gains are related with the measurement sample transmission outcomes on a finite interval. In both chapters, we analyzed some predefined cases to reduce the set of stored gains that allowed us exploring the trade-offs between estimator complexity, in terms of storage requirements, and estimation performance. We showed that the on-line computational effort of the jump estimators can be much lower than the optimal Kalman Filter, while achieving a similar estimation performance.

State estimation with gain-scheduled observers

In Chapter 5 we considered the case when the successful packet arrival probability varies slowly over time and is a priori unknown. We designed a gain-scheduled estimator whose gains are scheduled in real time with rational functions that depend on the PAR value. We formulated the problem as an optimization over polynomials that was then solved using tractable SOS-based techniques. In the example we illustrated the trade-offs between estimator complexity, in terms of polynomial degrees, and estimation performance.

Co-design

In Chapter 4 and Chapter 6 we studied the co-design problem by minimizing the number of successful data transmissions while guaranteeing a predefined estimation performance.

In Chapter 4 we considered that the sensor samples are transmitted over a multi-hop network with fading channels. Dropouts were induced by the fading links while delays were introduced when hopping through relay nodes. Higher power transmission levels alleviated the effect of the fading and reduced the end-to-end delay at the expense of a higher power budget. We jointly designed the power control policies and the jump linear estimator to minimize the power budget while guaranteeing a predefined state estimation error.

In Chapter 6 we used a simple SOD strategy to reduce the number of sensor transmissions and therefore alleviate the network resource consumption. Under this framework, we considered ideal transmissions without dropouts and delays. To reduce conservativeness, we derived a lower bound on the probability of receiving a measurement sample that is a priori unknown. We handled this uncertainty with SOS-based design. We jointly designed the transmission thresholds of the sensor nodes (which define the SOD strategy) and the jump estimator to minimize the network usage while guaranteeing a prescribed state estimation error.

Fault diagnosis with jump observers

In Chapter 7 and Chapter 8 we designed jump observer-based fault diagnosers to detect and estimate faults under transmission dropouts.

In Chapter 7 the design method allowed finding a favorable trade-off between the achievable minimum detectable faults and the response time to faults, while guaranteeing a prescribed FAR. In general, we bounded the FAR using Markov's inequality, which allows neglecting the probability distribution of the residual signal. Under the assumption of Gaussian disturbances and noises, we forced the residual to follow a Chi-squared distribution providing then an accurate FAR bound.

As a difference with Chapter 7, in Chapter 8 we considered networks without delivery acknowledgement which implied that the observer-based fault diagnoser ignored the control action being applied at the process. To improve fault diagnosis performance, we related the observer gains to the sampling scenario and scheduled them in real time with a rational function of a control error statistic (between the control input being applied at the process and the one at the observer). As in Chapter 7 the design procedure allowed trading between response time under faults and minimum detectable faults for a prescribed FAR. Again, we formulated the problem as an optimization over polynomials and solved it with a SOS-based tractable approach.

9.2 Future work

The following promising future work directions arise from the developed contributions of this thesis and other related works in which the author has participated during these years:

- Analytical characterization of the trade-offs between estimator complexity and estimation performance for jump linear estimators. This may be achieved by performing a sensitivity analysis of the optimized function through Lagrange multipliers. In that case, Lagrange multipliers can be seen as the cost of introducing an equality constraint over the estimator gain set on the estimation performance.

- Analysis of the a priori feasibility of the jump linear estimator design depending on the network transmission conditions and on the estimator complexity. This may be achieved by combining the Elimination Lemma with a similar analysis than the one proposed in the above item.

- Extension of the networked jump linear estimators design to uncertain systems. A preliminary work can be found in [31].

- Further research on reducing the gap between telecommunication theory and practice. Standard IEEE 802.15.4 transmitters send packets with at least 120 bits. The successful transmission probability expression (for a binary phase shift keying transmission) used in Chapter 4 has the number of used bits as the exponent, which narrows the power control values range to assure intermediate successful transmission probabilities between 0 and 1. Furthermore, IEEE 802.15.4 transmitters has at most 15 different discrete power control values to choose which may imply the impossibility of imposing intermediate probabilities. Then a good idea is to study the real degrees of freedom to impose a certain successful transmission probability between two node with discrete transmission power values.

- Extension of the co-design problem for the multi-hop network with fading channels where the channel fading gains are known with uncertainty.

- Design of the topology of a multi-hop wireless network with fading channels. This problem would consist on deciding the location of the relay nodes to minimize the power budget while assuring a certain end-to-end packet arrival rate. It can be seen as en extension of the presented co-design problem, where besides designing the estimator gains and the power control policies, we also decide the location of the relays, i.e., somehow the channel fading gains.

- Exploration of homogeneous polynomial methods to improve the SOS-based results. Homogeneous polynomials techniques alleviate conservativeness and provide necessary and sufficient conditions, while with SOS-based methods we can only derive sufficient ones.

- Design of estimators for networked multi-sensor systems where the data is transmitted through a network without delivery acknowledgement and time-varying packet arrival rate.

- Extension of the probability characterization of the SOD-based transmissions to a Markov framework instead of a Bernoulli one. This may be a reasonable extension, that would lead to less conservative results, as the probability of transmitting a new measurement sample at a given instant depends on whether we have just sent the previous one.
- Extension of the SOD-based jump linear estimation where transmission are subject to dropouts and time-varying delays. Dropouts can be seen as a reduction of the successful transmission probability, and therefore, as an increase of the virtual noise.
- Further characterization of the probability distribution of the considered residual signals to improve the FAR bound and enlarge the applicability domain of the fault diagnosis methods. One idea is to study whether we can apply the central limit theorem to characterize the probability distribution of the residual signal, which will imply that the proposed Chi-squared method is valid for a wider type of disturbances and measurement noises.
- Development of fault diagnosis procedures to deal with event-based measurements.
- Design of observer-based controllers that close the loop for the considered network scenarios. A preliminary work can be found in [110].
- Design of networked sparse controllers. A sparse controller controls a process with a reduced number of control inputs (less than the available ones) that may vary over time. A preliminary work can be found in [1].

Part IV

Appendixes and Bibliography

Appendix A

Linear matrix inequalities

In this appendix we present a brief review on convex optimization. First, we describe a general convex optimization problem and focus on linear matrix inequality (LMI) constraints. Second, we present some results that give necessary and sufficient conditions to fulfill a LMI constraint. Finally, we introduce some methods to deal with nonconvex constraints.

A.1 Convex optimization

A convex optimization problem is as follows

$$\begin{aligned} &\text{minimize} && f_0(x) \\ &\text{subjectto} && f_i(x) \leq b_i, \quad i = 1, \ldots, m, \end{aligned} \tag{A.1}$$

where the functions $f_0, \ldots, f_m : \mathbb{R}^n \to \mathbb{R}$ are convex, i.e., satisfy

$$f_i(\alpha x + \beta y) \leq \alpha f_i(x) + \beta f_i(y)$$

for all $x, y \in \mathbb{R}^n$ and all $\alpha, \beta \in \mathbb{R}$ with $\alpha + \beta = 1$, $\alpha > 0$, $\beta > 0$.

A specific convex constraint is the one given by

$$F(x) \triangleq F_0 + \sum_{i=1}^{m} x_i F_i \succ 0 \tag{A.2}$$

where $F_i = F_i^T \in \mathbb{R}^{n \times n}$. The convexity is assured because the set $\{x | F(x) \succ 0\}$ is convex. This constraint is a LMI one that constrains $F(x)$ to be positive definite . Expression (A.2) is equivalent to a set of n polynomial inequalities in x.

In mathematical programming terminology an optimization problem as in (A.1) with LMI constraints as in (A.2) is called a semi-definite programming problem.

A.2 Matrix inequalities

In this section we present some interesting reformulations of LMI providing necessary and sufficient conditions to fulfill it. Proofs can be found in the given literature.

The following lemma gives equivalent conditions to check the positive definiteness of a partitioned matrix.

Lemma A.1 (Schur's Complements [8])**.** *Let M be a partitioned matrix as*

$$M = \begin{bmatrix} A & B \\ C & D \end{bmatrix},$$

then, the following conditions are equivalent

(i) $M \succ 0$,

(ii) $D \succ 0,\ A - BD^{-1}C \succ 0$,

(iii) $A \succ 0,\ D - CA^{-1}B \succ 0$.

■

The next lemma allows reformulating LMI conditions. It can be used to transform bilinear matrix inequalities (BMIs) into LMIs.

Lemma A.2 (Dualiation Lemma [124]). *Let P be a non-singular symmetric matrix in $\mathbb{R}^{n\times n}$, and let $\mathcal{U}$, $\mathcal{V}$ be two complementary subspaces whose sum equals $\mathbb{R}^n$. Then*

$$x^T P x < 0\ \forall x \in \mathcal{U}\backslash\{0\} \quad \text{and} \quad x^T P x \geq 0\ \forall x \in \mathcal{V} \tag{A.3}$$

is equivalent to

$$x^T P^{-1} x > 0\ \forall x \in \mathcal{U}^\perp\backslash\{0\} \quad \text{and} \quad x^T P^{-1} x \leq 0\ \forall x \in \mathcal{V}^\perp \tag{A.4}$$

where $^\perp$ refers to the orthogonal subspace.

■

Corollary A.1. *Suppose $P = P^T = \begin{bmatrix} Q & S \\ S^T & R \end{bmatrix}$ is non-singular with $R \geq 0$, and let $\tilde{P} = P^{-1} = \begin{bmatrix} \tilde{Q} & \tilde{S} \\ \tilde{S}^T & \tilde{R} \end{bmatrix}$ with $\tilde{Q} \preceq 0$. Then*

$$\begin{bmatrix} I \\ W \end{bmatrix}^T P \begin{bmatrix} I \\ W \end{bmatrix} \prec 0 \quad \Leftrightarrow \quad \begin{bmatrix} W^T \\ -I \end{bmatrix}^T \tilde{P} \begin{bmatrix} W^T \\ -I \end{bmatrix} \succ 0. \tag{A.5}$$

■

The following three lemmas provide the possibility of rewriting LMI conditions by eliminating some of the variables.

Lemma A.3 (Finsler Lemma [21]). *Let $x \in \mathbb{R}^n$, $P = P^T \in \mathbb{R}^{n\times n}$, $V \in \mathbb{R}^{m\times n}$ such that $\operatorname{rank}(V) < n$, and $V^\perp$ be a basis matrix of $\ker(V)$, i.e. $\operatorname{im}(V^\perp) = \ker(V)$. Then the following statements are equivalent:*

(i) $x^T P x < 0 \ \ \forall V x = 0,\ x \neq 0$.

(ii) $(V^\perp)^T P V^\perp \prec 0$.

(iii) There exists $\mu \in \mathbb{R}$ such that $P - \mu V^T V \prec 0$.

(iv) There exist $Z \in \mathbb{R}^{n\times m}$ such that $P + ZV + V^T Z^T \prec 0$.

■

Remark A.1. $V^\perp$ is a basis for the null space of V. That is, all $x \neq 0$ such that $Vx = 0$ is generated by some $z \neq 0$ in the form $x = (V^\perp)z$.

Lemma A.4 (Projection Lemma [39]). *Suppose $P = P^T$, and let $U^\perp$, $V^\perp$ be matrices of $\ker(U)$, $\ker(V)$, i.e., $\operatorname{im}(U^\perp) = \ker(U)$, $\operatorname{im}(V^\perp) = \ker(V)$. Then the following statements are equivalent:*

(i) $Ux = 0$ *or* $Vx = 0$ *imply* $x^T P x < 0$ *or* $x = 0$.

(ii) $(U^\perp)^T P U^\perp \prec 0$ *and* $(V^\perp)^T P V^\perp \prec 0$.

(iii) There exist Z *such that* $P + U^T Z V + V^T Z^T U \prec 0$.

■

Lemma A.5 (Elimination Lemma [124])**.** *Suppose* $P = P^T = \begin{bmatrix} Q & S \\ S^T & R \end{bmatrix}$ *is non-singular with* $R \succeq 0$*, and let* $\tilde{P} = P^{-1} = \begin{bmatrix} \tilde{Q} & \tilde{S} \\ \tilde{S}^T & \tilde{R} \end{bmatrix}$ *with* $\tilde{Q} \preceq 0$*. Let* $U^\perp$*,* $V^\perp$ *be matrices of* $\ker(U)$*,* $\ker(V)$*, i.e.,* $\mathrm{im}(U^\perp) = \ker(U)$*,* $\mathrm{im}(V^\perp) = \ker(V)$*. Then there exists* Z *such that*

$$\begin{bmatrix} I \\ U^T Z V + W \end{bmatrix}^T P \begin{bmatrix} I \\ U^T Z V + W \end{bmatrix} \prec 0, \tag{A.6}$$

if and only if

$$(V^\perp)^T \begin{bmatrix} I \\ W \end{bmatrix}^T P \begin{bmatrix} I \\ W \end{bmatrix} V^\perp \prec 0 \quad \text{and} \quad (U^\perp)^T \begin{bmatrix} W^T \\ -I \end{bmatrix}^T \tilde{P} \begin{bmatrix} W^T \\ -I \end{bmatrix} U^\perp \succ 0. \tag{A.7}$$

■

A.3 Solving nonconvex inequalities

Sometimes, when dealing with complex problems, one encounters nonconvex inequality conditions. A first approach to solve these kind of problems is by using the results in precedent section.

For the cases where lemmas in Section A.2 cannot be applied, we present in the following some procedures that handle optimization problems with nonconvex constraints by iteratively solving convex ones.

A.3.1 Convexifying algorithm

Let us consider the following optimization problem.

Problem A.1. Let Ψ be a convex set, a scalar convex function $f(X)$, a matrix function $\mathcal{J}(X)$ (set of convex inequalities) and $\mathcal{H}(X)$ (set of nonconvex inequalities) be given, and consider the nonconvex optimization problem:

$$\min_{X \in \Psi} f(X), \ \Psi \triangleq \{X | \mathcal{J}(X) + \mathcal{H}(X) < 0\}. \tag{A.8}$$

Suppose $\mathcal{J}(X)$ is convex, $\mathcal{H}(X)$ is not convex, and $f(X)$ is a first order differentiable convex function bounded from below on the convex set Ψ.

A possible approach to solve this nonconvex problem is by a linearization of the nonconvex term. We next present the convexifying algorithm proposed in [46].

Theorem A.1 (Convexifying Linearization Algorithm [46])**.** *Problem A.1 can be solved (locally) by iterating a sequence of convex sub-problems if there exists a matrix function* $\mathcal{G}(X, X_k)$ *such that*

$$\begin{aligned} X_{k+1} = &\ \arg \min_{X \in \Psi_k} f(X) \\ \Psi_k \triangleq &\ \{X | \mathcal{J} + \mathrm{LIN}(\mathcal{X}, X_k) + \mathcal{G}(X, X_k) < 0 \\ &\ \mathcal{H}(X) \leq \mathcal{G}(X, X_k) + \mathrm{LIN}(\mathcal{H}(X), X_k)\} \end{aligned} \tag{A.9}$$

where $\mathrm{LIN}(\star, X_k)$ *is the linearization operator at given* X_k*.*

Proof. First note that every point $X_{k+1} \in \Psi_k$ is also in Ψ since

$$\mathcal{J}(X) + \mathcal{H}(X) \leq \mathcal{J} + \mathrm{LIN}(\mathcal{X}, X_k)\} + \mathcal{G}(X, X_k) < 0.$$

As long as $X_k \in \Psi_k$, $f(X_{k+1}) < f(X_k)$ holds strictly until $X_{k+1} = X_k$. The fact that $f(X)$ is bounded from below ensures that this strictly decreasing sequence converges to a stationary point.

■

The convexifying linearization algorithm is used to obtain a sufficient condition to guarantee the inequality conditions. This approach is conservative, but the conservatism will be minimized since we shall solve the problem iteratively. Due to the lack of convexity, only local optimality is guaranteed. This algorithm can be generalized using the results on [20] where the convexifying algorithm presented is based on finding a convexifying potential function.

The most frequent nonconvex term when dealing with matrix inequalities is the presence of inverse matrices. The following lemma provides the linearization of an inverse matrix.

Lemma A.6. *The linearization of* $X^{-1} \in \mathbb{R}^{n \times n}$ *about the value* $X_k \succ 0$ *(where* $X \succ 0$*) is*

$$\mathrm{LIN}(X^{-1}, X_k) = X_k^{-1} - X_k^{-1}(X - X_k)X_k^{-1} \tag{A.10}$$

If the convex part is zero, thus the matrix function is $\mathcal{G}(X, X_k) = 0$*.*

Proof. As X is positive definite, according to Theorem A.1, $\mathcal{H}(X) = -X^{-1} \prec 0$. $\mathrm{LIN}(-X^{-1}, X_k)$ can be easily developed using the Taylor series expansion for matrix variables. Then we have to find some $\mathcal{G}(X, X_k)$ such that

$$-X^{-1} - \mathrm{LIN}(X^{-1}, X_k) \prec \mathcal{G}(X, X_k).$$

Operating

$$\begin{aligned} -X^{-1} - \mathrm{LIN}(X^{-1}, X_k) &= -X^{-1} + X_k^{-1} - X_k^{-1}(X - X_k)X_k^{-1} = \\ &= X^{-1}(-I + 2XX_k^{-1} - XX_k^{-1}XX_k^{-1}) = -X^{-1}(XX_k^{-1} - I)^2 \end{aligned}$$

As $X^{-1} \succ 0$ and $(XX_k^{-1} - I)^2 \succeq 0$, then $-X^{-1}(XX_k^{-1} - I)^2 \preceq 0$. So $\mathcal{G}(X, X_k) = 0$.

■

For further information and examples the reader is referred to [20, 46].

Cone Complementarity Linearization algorithm

A particular case on inverse matrix convexification, more extended in the academic world, is the well known Cone Complementarity Algorithm (CCL).

Let us rewrite (A.8) as a feasibility problem such as

$$\text{find } X, S \in \Psi \text{ s.t } \Psi \triangleq \left\{ X | \mathcal{J}(X),\ \mathcal{K}(X,S) = \begin{bmatrix} X & I \\ I & S \end{bmatrix} \succeq 0 \right\} \tag{A.11}$$

where $S \in \mathbb{R}^{m \times m}$ and $\text{rank}(\mathcal{K}(X,S)) \leq n+m$. We seek to solve the above problem for $m = 0$ (i.e. $S = X^{-1}$).

To solve such a problem, a linearization method can be used. At a given point (X^0, S^0), a linear approximation of $\text{tr}(XS)$ takes the form

$$\text{LIN}(\text{tr}(XS), (X^0, S^0)) = \text{constant} + \text{tr}(S^0 X + X^0 S).$$

The linearization algorithm is conceptually described as follows.

Algorithm A.1. Cone Complementarity Algorithm.

Step 1 Find a feasible point X^0, S^0. If there are none, exit. Set $k = 0$.

Step 2 Set $V^k = S^k$, $W^k = X^k$, and find $X^{k+1},\ S^{k+1}$ that solve the LMI problem

$$\text{minimize } \text{tr}(V^k X + W^k S) \text{ subject to (A.11)}.$$

Step 3 If a stopping criterion is satisfied, exit. Otherwise, set $k = k+1$ and and go to Step 2.

For further information on the algorithm the reader is referred to [33].

Remark A.2. As the CCL only searches for feasibility, one may have to use an extern optimization procedure to search for an optimal solution, e.g., a bisection algorithm.

A.3.2 Rank-constrained problems

As we have seen, dealing with an inverse matrix is reduced to solve a rank-constrained problem. A rank-constrained LMI problem is an NP-hard optimization problem for which much work has been done and many iterative techniques have been developed to solve it. In the following we present an algorithm developed in [65, 66] to deal with rank constraints.

Let us rewrite a general rank-constrained LMI problem as

$$\begin{aligned} &\min_X f(X) \\ &\quad \text{s.t. } W(X) \succeq 0,\ \ \mathcal{J}(X) \succ 0,\ \ \text{rank}(W(X)) \leq r \end{aligned} \tag{A.12}$$

where X is the decision vector, $W(X) = W(X)^T \in \mathbb{R}^{n \times n}$ and $\mathcal{J}(X) = \mathcal{J}(X)^T \in \mathbb{R}^{n \times n}$ are symmetric matrices that are affine functions of X. The rank r is assumed to be less than the full rank of $W(X)$.

In [65, 66] a Penalty Fuction Method (PFM) [10] is proposed to solve this kind of problems. In their PFM, the rank-constrained problem (A.12) is first converted to an LMI

optimization problem without the rank condition by incorporating a penalty function into the objective function. Then, a sequence of convex LMI optimization problems are solved using an existing LMI solver. To select a penalty function reflecting the violation of the rank condition, they used the fact that the rank condition in (A.12) is satisfied if and only if the $n - r$ eigenvalues of $W(X)$ are zero. The following lemma provides the basis of their PFM.

Lemma A.7 ([65, 66])**.** *The rank of a symmetric positive semi-definite matrix $W \in \mathbb{R}^n$ is less than or equal to r if and only if there exists a matrix $V \in \mathbb{R}^{n\times(n-r)}$ with $V^TV = I_{n-r}$ such that* $\mathrm{tr}(V^TWV) = 0$.

Also, notice that if $\mathrm{rank}(W) > r$, then $\mathrm{tr}(V^TWV) > 0$. Therefore, they used $\mathrm{tr}(V^TWV)$ as a penalty function for the rank condition of the optimization problem. The following theorem present their PFM.

Theorem A.2 ([65, 66])**.** *Problem* (A.12) *can be solved (locally) by iterating a sequence of convex sub-problems such that*

$$X^k = \arg\min_X \{\phi(X; \rho^k, \mu^k, V^{k-1}) \ : \ X \in \Psi\}, \quad k = 1, 2, \ldots \tag{A.13}$$

where

$$\phi(X; \rho, \mu, V) = \rho\, f(X) + \mathrm{tr}(W) + \mu\, p(x; W), \tag{A.14}$$

$$p(x; W) = \mathrm{tr}(V^TWV), \tag{A.15}$$

$$\Psi = \{X : W(X) \succeq 0, \quad \mathcal{J}(X) \succ 0\}. \tag{A.16}$$

$p(x; W)$ is the penalty function with $V \in \mathbb{R}^{n\times(n-r)}$, $V^TV = I_{n-r}$. $\mu^k > 0$ is the penalty parameter and $\rho^k > 0$ is the optimization weight. Also, V_{k-1} is constructed from the eigenvectors corresponding to the $n - r$ smallest eigenvalues of $W(X^{k-1})$ since the eigenvectors of W can be taken to be orthonormal to each other.

For further information on the method the reader is referred to [65, 66].

Appendix B

SOS decomposition

This appendix aims to provide some useful definitions and results about SOS decomposition, which have been borrowed from [16, 50]. Le us first show how to build polynomials of a given degree.

Lemma B.1. *Let $x \in \mathbb{R}^n$ be a vector. $x^{\{d\}}$ is the vector of different monomials in x of degree not greater than d where its number is given by*

$$\sigma(n,d) = \frac{(n+d)!}{n!\,d!}.$$

With that, polynomial matrices $Q(x) \in \mathbb{R}^{N\times M}$ and polynomial symmetric matrices $P(x) \in \mathbb{R}^{N\times N}$ of degree $2d$ can be built with

$$Q(x) = Q\left(x^{\{2d\}} \otimes I_M\right),$$
$$P(x) = \left(x^{\{d\}} \otimes I_N\right)^T P\left(x^{\{d\}} \otimes I_N\right),$$

being matrix Q as $Q \in \mathbb{R}^{N\times M\sigma(n,2d)}$ and symmetric matrix P as $P \in \mathbb{R}^{N\sigma(n,d)\times N\sigma(n,d)}$.

Le us now characterize when a polynomial is said to be SOS.

Lemma B.2. *Let $p(x)$ be a polynomial in $x \in \mathbb{R}^n$ of degree $2d$. Let $Z(x) \in \mathbb{R}^n$ be a vector with all the monomials in x of degree $\leq d$ as entries. Then, $p(x)$ is said to be SOS if and only if there is a positive semidefinite matrix Q fulfilling*

$$p(x) = Z(x)^T QZ\,(x).$$

The set of SOS polynomials in x is denoted by $\Sigma(x)$.

The next results are derived from the Positivstellensatz (see [16, 50]) that states that polynomial feasibility conditions can be addressed by checking whether the condition is SOS.

Lemma B.3. *Let $p(x)$ be a polynomial in $x \in \mathbb{R}^n$, and let*

$$X = \{x \in \mathbb{R}^n : g_j(x) \geq 0,\, j = 1,\ldots,m\}.$$

Suppose there exist SOS polynomials

$$s_j(x) \in \Sigma(x), \quad j = 1,\ldots,m, \quad x \in \mathbb{R}^n$$

fulfilling

$$p(x) - \sum_{j=1}^{m} s_j(x)\, g_j(x) \in \Sigma(x),$$

then, the following condition holds:

$$p(x) \geq 0,\ \forall\, x \in X.$$

Lemma B.4. *Let $P(x) \in \mathbb{R}^{N\times N}$ be a symmetric polynomial matrix in $x \in \mathbb{R}^n$ and let*

$$X = \{x \in \mathbb{R}^n : g_j(x) \geq 0,\, j = 1, \ldots, m\}.$$

Suppose there exist SOS polynomials

$$s_j(x, v) \in \Sigma(x, v), \quad j = 1, \ldots, m$$

fulfilling

$$v^T P(x) v - \sum_{j=1}^{m} s_j(x, v)\, g_j(x) \in \Sigma(x, v)$$

with $v \in \mathbb{R}^N$ a scalarization vectors used to transform polynomial matrices in polynomials, then, the following condition holds:

$$P(x) \succeq 0,\ \forall\, x \in X.$$

The above lemmas show that verifying whether a polynomial function or a polynomial matrix is nonnegative over a domain defined by polynomial constraints can be formulated by means of sufficient LMI conditions. This kind of problems are handled by several LMI parsers as [80] and [113].

Auxiliary results and proofs

C.3 Proofs of Chapter 3

Let us first introduce the following lemma borrowed from [129].

Lemma C.1. *Define the linear operator*

$$\mathfrak{L}(Y) = \sum_{N=1}^{\bar{N}-1} p_0^{N-1} \sum_{i=1}^{r} p_i F_{N,i} \bar{A}^N Y (\bar{A}^N)^T F_{N,i}^T + \sum_{N=\bar{N}}^{\infty} p_0^{N-1} \sum_{i=1}^{r} p_i F_{\bar{N},i} \bar{A}^N Y (\bar{A}^N)^T F_{\bar{N},i}^T.$$

Suppose that there exists $\bar{Y} \succ 0$ such that $\mathfrak{L}(\bar{Y}) \prec \bar{Y}$. Then,

a) For all $W \succeq 0$, $\lim_{k\to\infty} \mathfrak{L}^k(W) = 0$[1]*.*

b) Let $U \succeq 0$ and consider the linear system $Y_{k+1} = \mathfrak{L}(Y_k) + U$, initialized at Y_0, then the sequence $\{Y_k\}$ is bounded.

C.3.1 Proof of Theorem 3.1

Let us assume that at $t = t_{k-1}$ a new sample is available and the state estimation is updated with equation (3.7) leading to a covariance matrix for the estimation error $\mathbf{E}\{\tilde{x}[t_{k-1}]\tilde{x}[t_{k-1}]^T\} = P_{k-1}$. The expected value of the covariance matrix for the estimation error at the next update time instant is

$$\begin{aligned}\mathbf{E}\{P_k\} = {} & \mathbf{E}\left\{(I - L_k\alpha_k\bar{C})\bar{A}^{N_k}P_{k-1}(\bar{A}^{N_k})^T(I - L_k\alpha_k\bar{C})^T\right\} \\ & + \mathbf{E}\left\{(I - L_k\alpha_k\bar{C})\sum_{i=0}^{N_k-1}\bar{A}^i\bar{B}_w W \bar{B}_w^T(\bar{A}^i)^T(I - L_k\alpha_k\bar{C})^T\right\} \\ & + \mathbf{E}\left\{L_k\alpha_k V \alpha_k L_k^T\right\},\end{aligned}$$

considering the independency between $x[t_{k-1}]$, v_k and $w[t_{k-1}+i]$ for $i = 0, \ldots, N_k-1$, and assuming $w[t]$ an uncorrelated noise. We express the different expectations considering the probability of the number of intersample instants N_k, the gain matrix dependency (3.17), and the rule of average conditional expectations. After algebraic computation and variable substitution it follows (3.19).

[1] $\mathfrak{L}^k\{\cdot\}$ represents the recursion of $\mathfrak{L}\{\cdot\}$.

C.3.2 Proof of Theorem 3.4

First, let us show the convergence of sequence $\{P_k\}$ with initial value $Q_0 = 0$. Let $Q_k = \mathfrak{E}\{Q_{k-1}\} = \mathfrak{E}^k\{Q_0\}$, then from (3.19), $Q_1 \succeq Q_0 = 0$ and $Q_1 = \mathfrak{E}\{Q_0\} \preceq \mathfrak{E}\{Q_1\} = Q_2$. By induction, $\{Q_k\}$ is non decreasing. Also, by Lemma C.1, $\{Q_k\}$ is bounded and by Theorem 3.3 there exists an M_{Q_0} such that $Q_k \preceq M_{Q_0}$ for any k. Hence, the sequence converges and $\lim_{k\to\infty} Q_k = \bar{P} \succeq 0$, where $\bar{P}$ is a fixed point, i.e, $\bar{P} = \mathfrak{E}\{\bar{P}\}$.

Second, we state the convergence of $G_k = \mathfrak{E}^k\{G_0\}$, initialized at $G_0 \succeq \bar{P}$. Since $G_1 = \mathfrak{E}\{G_0\} \succeq \mathfrak{E}\{\bar{P}\} = \bar{P}$, then $G_k \succeq \bar{P}$ for any k. Moreover

$$0 \preceq G_{k+1} - \bar{P} = \mathfrak{E}\{G_k\} - \mathfrak{E}\{\bar{P}\} = \mathfrak{L}(G_k - \bar{P}).$$

As $G_k - \bar{P} \succeq 0$, following the results on Lemma C.1, then $0 \preceq \lim_{k\to\infty}(G_k - \bar{P}) = 0$, i.e., the sequence $\{G_k\}$ converges to $\bar{P}$.

We demonstrate now that for any initial condition $P_0 \succeq 0$, the iteration $P_k = \mathfrak{E}\{P_{k-1}\}$ converges to $\bar{P}$. Since $0 \preceq Q_0 \preceq P_0 \preceq G_0$, we derive by induction that $0 \preceq Q_k \preceq P_k \preceq G_k$. Therefore, as $\{Q_k\}$ and $\{G_k\}$ converges to $\bar{P}$, then $\{P_k\}$ also converges to $\bar{P}$ and the convergence is demonstrated.

Finally, we demonstrate that

$$\bar{P} = \arg\min_{P} \operatorname{tr}(P) \text{ subject to } (3.26), (3.27).$$

Suppose this is not true, i.e. $\hat{P}$ solves the optimization problem but $\hat{P} \neq \mathfrak{E}\{\hat{P}\}$. Since $\hat{P}$ is a feasible solution, then $\hat{P} \succ \mathfrak{E}\{\hat{P}\} = \hat{\hat{P}}$. However, this implies $\operatorname{tr}(\hat{P}) > \operatorname{tr}(\hat{\hat{P}})$, which contradicts the hypothesis of optimality of matrix $\hat{P}$. Therefore $\hat{P} = \mathfrak{E}\{\hat{P}\}$. Furthermore $\bar{P}$ is unique since for a set of observer gains such that

$$[\bar{P},\ \mathcal{L}] = \arg\min_{P,\mathcal{L}} \operatorname{tr}(P) \text{ subject to } (3.26), (3.27),$$

we have shown that the sequence converges to $\bar{P}$, and this concludes the theorem.

C.3.3 Proof of Theorem 3.5

The expected value of the covariance matrix of the estimation error at instants t ($\mathbf{E}\{\tilde{x}[t]\,\tilde{x}[t]^T\}$) is computed as

$$\begin{aligned} P_t =& (1-p_0)P + \sum_{N=1}^{\infty} p_0^N \left(\bar{A}^N P (\bar{A}^N)^T + \sum_{i=1}^{N} \bar{A}^{i-1} \bar{B}_w W \bar{B}_w^T (\bar{A}^{i-1})^T \right) \\ =& (1-p_0)P + \sum_{N=1}^{\infty} p_0^N \bar{A}^N P (\bar{A}^N)^T + p_0 \left(\sum_{i=0}^{\infty} p_0^i \right) \sum_{j=0}^{\infty} p_0^j \bar{A}^j \bar{B}_w W \bar{B}_w^T (\bar{A}^j)^T, \end{aligned}$$

where the infinite addends can be written respectively as

$$\operatorname{vec}^{-1}\left((I - p_0 \bar{A} \otimes \bar{A}) \operatorname{vec}(p_0 \bar{A} P \bar{A}^T) \right), \tag{C.1}$$

$$\operatorname{vec}^{-1}\left((I - p_0 \bar{A} \otimes \bar{A}) \operatorname{vec}(\bar{B}_w W \bar{B}_w^T) \right). \tag{C.2}$$

Then, it finally leads to (3.29).

C.4 Proofs of Chapter 4

Let us first introduce the following lemma borrowed from [129] (which is similar to Lemma C.1).

Lemma C.2. *Define the linear operator*

$$\mathcal{T}_j(\mathcal{Y}) = \sum_{i=0}^{r} p_{i,j} \frac{\pi_i}{\pi_j} F_j \bar{A} Y_i \bar{A}^T F_j^T$$

where $\mathcal{T}(\cdot) \triangleq (\mathcal{T}_0(\cdot), \ldots, \mathcal{T}_r(\cdot))$ *and* $\mathcal{Y} \triangleq (Y_0, \ldots, Y_r)$. *Suppose that there exists* $\bar{\mathcal{Y}} \triangleq (\bar{Y}_0, \ldots, \bar{Y}_r) \succ 0$ *such that* $\mathcal{T}(\bar{\mathcal{Y}}) \prec \bar{\mathcal{Y}}$. *Then,*

a) For all $\mathcal{W} \triangleq (W_0, \ldots, W_r) \succeq 0$, $\lim_{t\to\infty} \mathcal{T}^t(\mathcal{W}) = 0$[2]

b) Let $U \succeq 0$ *and consider the linear system* $\mathcal{Y}_{t+1} = \mathcal{T}(\mathcal{Y}_t) + U$, *initialized at* $\mathcal{Y}_0$, *then the sequence* $\{\mathcal{Y}_t\}$ *is bounded.*

C.4.1 Proof of Theorem 4.1

Considering the independency between x_{t-1}, $\bar{v}_t$ and w_{t-1}, $P_{t,j} = \mathbf{E}\{\tilde{x}_t \tilde{x}_t^T | \theta_t = \vartheta_j\}$ can be computed as

$$\begin{aligned}
&\sum_{i=0}^{r} \mathbf{Pr}\{\theta_{t-1} = \vartheta_i | \theta_t = \vartheta_j\} \mathbf{E}\{\tilde{x}_t \tilde{x}_t^T | \theta_{t-1} = \vartheta_i, \theta_t = \vartheta_j\} = \\
&= \sum_{i=0}^{r} p_{i,j} \frac{\pi_i}{\pi_j} F_j (\bar{A} \mathbf{E}\{\tilde{x}_{t-1} \tilde{x}_{t-1}^T | \theta_{t-1} = \vartheta_i\} \bar{A}^T + \mathbf{E}\{w_{t-1} w_{t-1}^T\}) F_j^T \\
&+ \sum_{i=0}^{r} p_{i,j} \frac{\pi_i}{\pi_j} X_j \mathbf{E}\{\bar{v}_t \bar{v}_t^T\} X_j^T
\end{aligned}$$

which leads to (4.18) after having used

$$\mathbf{Pr}\{\theta_{t-1} = \vartheta_i | \theta_t = \vartheta_j\} = \mathbf{Pr}\{\theta_t = \vartheta_j | \theta_{t-1} = \vartheta_i\} \mathbf{Pr}\{\theta_{t-1} = \vartheta_i\} / \mathbf{Pr}\{\theta_t = \vartheta_j\}.$$

Finally, expression (4.20) can be derived with the law of total probabilities.

C.4.2 Proof of Theorem 4.3

Let us first show the convergence of sequence $\{\mathcal{P}_t\}$ with initial value $\mathcal{Q}_0 = 0$, where $\mathcal{Q}_t \triangleq (Q_{t,0}, \ldots, Q_{t,r})$. Let $\mathcal{Q}_t = \mathfrak{E}\{\mathcal{Q}_{t-1}\} = \mathfrak{E}^t\{\mathcal{Q}_0\}$, then from (4.18), $\mathcal{Q}_1 \succeq \mathcal{Q}_0 = 0$ and $\mathcal{Q}_1 = \mathfrak{E}\{\mathcal{Q}_0\} \preceq \mathfrak{E}\{\mathcal{Q}_1\} = \mathcal{Q}_2$. By induction, $\{\mathcal{Q}_t\}$ is non decreasing. Also, by Lemma C.2, $\{\mathcal{Q}_t\}$ is bounded and by Theorem 4.2 there exists an $M_{\mathcal{Q}} \triangleq (M_{Q_0}, \ldots, M_{Q_r})$ such that $\mathcal{Q}_t \preceq M_{\mathcal{Q}}$ for any t. Thus, the sequence converges and $\lim_{k\to\infty} \mathcal{Q}_t = \bar{\mathcal{P}} \succeq 0$, where $\bar{\mathcal{P}}$ is a fixed point, i.e, $\bar{\mathcal{P}} = \mathfrak{E}\{\bar{\mathcal{P}}\}$. Second, we demonstrate the convergence of $\mathcal{G}_t = \mathfrak{E}^k\{\mathcal{G}_0\}$, initialized at $\mathcal{G}_0 \succeq \bar{\mathcal{P}}$ where $\mathcal{G}_t \triangleq (G_{t,0}, \ldots, G_{t,r})$. Since $\mathcal{G}_1 = \mathfrak{E}\{\mathcal{G}_0\} \succeq \mathfrak{E}\{\bar{\mathcal{P}}\} = \bar{\mathcal{P}}$, then $\mathcal{G}_t \succeq \bar{\mathcal{P}}$ for any t. Moreover, we have that

$$0 \preceq \mathcal{G}_{t+1} - \bar{\mathcal{P}} = \mathfrak{E}\{\mathcal{G}_t\} - \mathfrak{E}\{\bar{\mathcal{P}}\} = \mathcal{T}(\mathcal{G}_t - \bar{\mathcal{P}}).$$

[2] $\mathcal{T}^t\{\cdot\}$ represents the recursion of $\mathcal{T}\{\cdot\}$.

As $\mathcal{G}_t - \bar{\mathcal{P}} \succeq 0$, following the results of Lemma C.2, then $0 \preceq \lim_{t\to\infty}(\mathcal{G}_t - \bar{\mathcal{P}}) = 0$, i.e., the sequence $\{\mathcal{G}_t\}$ converges to $\bar{\mathcal{P}}$.

We prove now that the convergence of iteration $\mathcal{P}_t = \mathfrak{E}\{\mathcal{P}_{t-1}\}$ to $\bar{\mathcal{P}}$ for any initial condition $\mathcal{P}_0 \succeq 0$. Since $0 \preceq \mathcal{Q}_0 \preceq \mathcal{P}_0 \preceq \mathcal{G}_0$, we derive by induction that $0 \preceq \mathcal{Q}_t \preceq \mathcal{P}_t \preceq \mathcal{G}_t$. Therefore, as $\{\mathcal{Q}_t\}$ and $\{\mathcal{G}_t\}$ converge to $\bar{\mathcal{P}}$, then $\{\mathcal{P}_t\}$ also does, and the convergence is shown. Finally, we need to show that

$$\bar{\mathcal{P}} = \arg\min_{\mathcal{P}} \ \mathrm{tr}\left(\sum_{j=0}^{r} P_j \pi_j\right) \ \text{subject to (4.22)}.$$

Suppose this is false, i.e. $\hat{\mathcal{P}}$ solves the optimization problem, but $\hat{\mathcal{P}} \neq \mathfrak{E}\{\hat{\mathcal{P}}\}$. Since $\hat{\mathcal{P}}$ is a feasible solution, then $\hat{\mathcal{P}} \succ \mathfrak{E}\{\hat{\mathcal{P}}\} = \hat{\hat{\mathcal{P}}}$. But, this implies $\mathrm{tr}\left(\sum_{j=0}^{r} \hat{P}_j \pi_j\right) > \mathrm{tr}\left(\sum_{j=0}^{r} \hat{\hat{P}}_j \pi_j\right)$, which contradicts the hypothesis of optimality of matrix $\hat{\mathcal{P}}$. Then, $\hat{\mathcal{P}} = \mathfrak{E}\{\hat{\mathcal{P}}\}$. Furthermore $\bar{\mathcal{P}}$ is unique since for a set of filter gains such that

$$[\bar{\mathcal{P}},\ \mathcal{L}] = \arg\min_{\mathcal{P},\mathcal{L}} \ \mathrm{tr}\left(\sum_{j=0}^{r} P_j \pi_j\right) \ \text{subject to (4.22)},$$

we have shown that the sequence converges to $\bar{\mathcal{P}}$, and this concludes the proof.

C.4.3 Proof of Theorem 4.4

Constraint (4.22) can be rewritten as

$$p_{j,j} F_j \bar{A} P_j \bar{A}^T F_j^T - P_j \preceq \sum_{i=0}^{r} p_{i,j} \frac{\pi_i}{\pi_j} \left(F_j(\bar{A} P_i \bar{A}^T + \bar{B}_w W \bar{B}_w^T) F_j^T + X_j V X_j^T\right) - P_j \preceq 0 \ \forall j,$$

with $j = 0, \ldots, r$. Therefore, a necessary condition for (4.22) to hold is

$$p_{j,j}(I - L_j\, \psi(\vartheta_j)\bar{C})\bar{A} P_j \bar{A}^T (I - L_j\, \psi(\vartheta_j)\bar{C})^T - P_j \preceq \ \forall j. \tag{C.3}$$

Let us first prove inequality (4.23a). When $\psi(\vartheta_j) = 0$, we have that

$$p_{j,j} \bar{A} P_j \bar{A}^T - P_j \preceq 0, \ \ \forall j : \psi(\vartheta_j) = 0.$$

Then a necessary condition for the existence of the filter is that

$$p_{j,j} \rho(\bar{A})^2 - 1 \leq 0, \quad \forall j : \psi(\vartheta_j) = 0,$$

which proves (4.23a). Let us now prove constraint (4.23b). Following the elimination lemma result (see Appendix A), the existence of matrices L_j and P_j such that the strict inequality (C.3) holds is equivalent to the existence of a matrix P_j with $\psi(\vartheta_j) = \eta_l$ such that

$$(\eta_l \bar{C} \bar{A})^{\perp^T} \left(p_{jj} (\bar{A})^T P_j \bar{A} - P_j\right) (\eta_l \bar{C} \bar{A})^{\perp} \succ 0,$$

where $(\eta_l \bar{C} \bar{A})^{\perp}$ is a basis for the null space of $(\eta_l \bar{C} \bar{A})$ containing a basis of the unobservable subspace from reception scenario η_l. Then a necessary condition for the existence of the filter is that

$$p_{j,j} \rho(\bar{A}_l)^2 - 1 \leq 0, \quad \forall j : \psi(\vartheta_j) = \eta_l,$$

which proves (4.23b).

C.5 Proofs of Chapter 5

C.5.1 Proof of Theorem 5.1

If (5.16) holds, then, it is obvious that $G(\hat{\beta}_t)^T + G(\hat{\beta}_t) - P(\beta_t) \succ 0$ and, therefore, $G(\hat{\beta}_t)$ is a nonsingular matrix. In addition, as $P(\beta_t)$ is a positive definite matrix, it is always true that

$$(P(\beta_t) - G(\hat{\beta}_t))^T P(\beta_t)^{-1} (P(\beta_t) - G(\hat{\beta}_t)) \succeq 0,$$

implying that $G(\hat{\beta}_t)^T + G(\hat{\beta}_t) - P(\beta_t) \succeq G(\hat{\beta}_t)^T P(\beta_t)^{-1} G(\hat{\beta}_t)$. Using this fact, replacing $X(\hat{\beta}_t)$ by $G(\hat{\beta}_t)L(\hat{\beta}_t)$ in (5.16), performing congruence transformation by matrix $G(\beta_t)^{-1} \oplus I \oplus I \oplus 1$ and applying Schur complements it leads to

$$\begin{bmatrix} P(\beta_t - \delta_t) - I & 0 & 0 \\ 0 & \gamma_w(\beta_t) I & 0 \\ 0 & 0 & \gamma_v(\beta_t) \end{bmatrix} - \beta_t \underbrace{\begin{bmatrix} ((I - L(\hat{\beta}_t)C)A)^T \\ ((I - L(\hat{\beta}_t)C)B_w)^T \\ -L(\hat{\beta}_t)^T \end{bmatrix}}_{\star\star} P(\beta_t)[\star\star]^T$$
$$-(1 - \beta_t) \underbrace{\begin{bmatrix} A^T \\ B_w^T \\ 0 \end{bmatrix}}_{\star\star\star} P(\beta_t)[\star\star\star]^T \succ 0. \qquad \text{(C.4)}$$

Now, let us define a Lyapunov function depending on the actual PAR as $V_t = V(\tilde{x}_t, \beta_t) = \tilde{x}_t^T P(\beta_t) \tilde{x}_t$. Multiplying expression (C.4) by $[\tilde{x}_{t-1}^T, w_{t-1}^T, v_t^T]$ by its left, and by its transpose on the right it leads to

$$(1 - \beta_t) V_{t|0} + \beta_t V_{t|1} - V_{t-1} + \tilde{x}_{t-1}^T \tilde{x}_{t-1} < \gamma_w(\beta_t) w_{t-1}^T w_{t-1} + \gamma_v(\beta_t) v_t^T v_t, \qquad \text{(C.5)}$$

being $V_{t|i}$ the value of the Lyapunov function when $\alpha_t = i$, $i = \{0, 1\}$. The first two addends of the previous expression can be interpreted as the expected value of the Lyapunov function over α_t for a given β_t

$$\mathbf{E}\{V_t|\beta_t\} = \mathbf{Pr}\{\alpha_t = 0|\beta_t\} V_{t|0} + \mathbf{Pr}\{\alpha_t = 1|\beta_t\} V_{t|1}.$$

If we assume null disturbances, (C.5) leads to $\mathbf{E}\{V_t|\beta_t\} < V_{t-1}$, i.e., the asymptotical mean square stability of the observer is assured for any β_t. Now, if expression (C.5) is multiplied by the PDF $g(\beta_t)$ and integrated from $\beta_t = 0$ to 1, the expectation over β_t is obtained leading to

$$\mathbf{E}\{V_t\} - V_{t-1} + \tilde{x}_{t-1}^T \tilde{x}_{t-1} < \bar{\gamma}_w w_{t-1}^T w_{t-1} + \bar{\gamma}_v v_t^T v_t, \qquad \text{(C.6)}$$

where $\mathbf{E}\{V_t\} = \int_0^1 g(\beta_t) \mathbf{E}\{V_t|\beta_t\} \mathrm{d}\beta_t$, $\int_0^1 g(\beta_t) \tilde{x}_{t-1} \mathrm{d}\beta_t = \tilde{x}_{t-1}$, and $\bar{\gamma}_w$ and $\bar{\gamma}_v$ as defined in (5.18). Assuming a null initial state estimation error ($\tilde{x}_{-1} = 0$, $V_{-1} = 0$), and adding the previous expression from $t = 0$ to $t = T$ one obtains

$$\mathbf{E}\{V_T\} + \sum_{j=0}^{T-1} (\mathbf{E}\{V_j\} - V_j) + \sum_{t=0}^{T} \tilde{x}_{t-1}^T \tilde{x}_{t-1} < \sum_{t=0}^{T} \left(\bar{\gamma}_w w_{t-1}^T w_{t-1} + \bar{\gamma}_v v_t^T v_t \right). \qquad \text{(C.7)}$$

Dividing by T and taking the limit when T tends to infinity, and taking into account that $\mathbf{E}\{V_T\} > 0$ and that

$$\lim_{T\to\infty} \frac{1}{T} \sum_{j=0}^{T-1} (\mathbf{E}\{V_j\} - V_j) \to 0,$$

condition $\mathbf{E}\{V_T\} > 0$ leads to (5.17).

C.6 Proofs of Chapter 6

C.6.1 Proof of Theorem 6.1

If (6.10) holds, then $Q_j + Q_j^T - P_j \succ 0$ and Q_j is a nonsingular matrix. If P_j is a positive definite matrix, then $(P_j - Q_j)^T P_j^{-1}(P_j - Q_j) \succeq 0$, implying that $Q_j + Q_j^T - P_j \succeq Q_j^T P_j^{-1} Q_j$. If we replace X_j by $Q_j L_j$, in (6.10), perform congruence transformation by matrix $Q_j \oplus I \oplus I \oplus I \oplus I$ and apply Schur complements, we obtain that

$$\begin{bmatrix} P_i - I & \star & \star & \star \\ 0 & \gamma_w I & \star & \star \\ 0 & 0 & \Gamma_v & \star \\ 0 & 0 & 0 & \Gamma_\delta \end{bmatrix} - \underbrace{\begin{bmatrix} ((I - L_j C)A)^T \\ ((I - L_j C)B_w)^T \\ -(L_j)^T \\ -(I - \eta_j) \cdot (L_j)^T \end{bmatrix}}_{\star} P_j (\star)^T \succ 0. \tag{C.8}$$

Consider a Lyapunov function depending on the sampling scenario as

$$V[t] = V(\tilde{x}[t], \alpha[t]) = \tilde{x}[t]^T P(\alpha[t]) \tilde{x}[t],$$

with $P(\alpha[t])$ taking values on the set $\{P_0, \ldots, P_q\}$ depending on the value $\alpha[t]$ as

$$P(\alpha[t]) = P_j, \quad \text{if } \alpha[t] = \eta_j, \ \forall\, j \in [0, \ldots, q].$$

Multiplying expression (C.8) by $[\tilde{x}[t]^T, w[t]^T, v[t]^T, \delta[t]^T]$ on the left, and by its transpose on the right, and assuming $\alpha[t+1] = j$ and $\alpha[t] = i$, it leads

$$\tilde{x}[t+1]^T P_j \tilde{x}[t+1] - \tilde{x}[t]^T P_k \tilde{x}[t] + \tilde{x}[t]^T \tilde{x}[t] < \gamma_w w[t]^T w[t] + v[t]^T \Gamma_v v[t] + \delta[t]^T \Gamma_\delta \delta[t] \tag{C.9}$$

for any pair i, j in $\{0, \ldots, q\} \times \{0, \ldots, q\}$. If we consider null disturbances, then $V[t+1] < V[t]$, demonstrating the asymptotic stability of the observer. If we assume null initial state estimation error ($\tilde{x}[0] = 0$, $V[0] = 0$) and we add expression (C.9) from $t = 0$ to T, we obtain

$$V[T+1] + \sum_{t=0}^{T} \tilde{x}[t]^T \tilde{x}[t] < \sum_{t=0}^{T} \left(\gamma_w w[t]^T w[t] + v[t]^T \Gamma_v v[t] + \delta[t]^T \Gamma_\delta \delta[t] \right)$$

As $V[T+1] > 0$, if we divide by T and take the limit when T tends to infinity, we obtain (6.11).

C.6.2 Probabilities and variances computation

On the following results we derive the expressions used in Chapter 6 to compute the probability of sending new samples and the associated variance of the virtual noise during the less excited instants.

Theorem C.1. *Let us assume that each sample from sensor s is independent and uniformly distributed within the range $\bar{m}_{s,\min} \leq m_s \leq \bar{m}_{s,\max}$, being $r_s = \bar{m}_{s,\max} - \bar{m}_{s,\min}$ as given in* (6.12)*, for the instants t_{k_s} and $t_{k_s}+1$, thus fulfilling $m_s[t] - m^e_{s,k_s}] \in [-r_s, r_s]$. Then, the probability of having a new sample from sensor s at instant $t = t_{k_s} + 1$ with law* (6.2) *is given by*

$$\beta_s = \mathbf{Pr}\{|m_s[t] - m^e_{s,k_s}| \geq \Delta_s\} = \frac{1}{r_s^2}(r_s - \Delta_s)^2. \tag{C.10}$$

The variance of the virtual noise related to this Δ_s is given by

$$\sigma^2_{\delta_s} = Var\{\delta_s[t]\} = E\{\delta_s[t]^2\} = \frac{2\Delta_s^3}{r_s^2}\left(\frac{r_s}{3} - \frac{\Delta_s}{4}\right). \tag{C.11}$$

Proof. Let us call the random variable m^e_{s,k_s} as u, denoting the sample at t_{k_s}, the last time it was sent from sensor to the central unit. Then, the PDF of u is

$$f_U(u) = \begin{cases} \frac{1}{r_s}, & u \in [\bar{m}_{s,\min}, \bar{m}_{s,\max}] \\ 0, & \text{otherwise} \end{cases}$$

Let us also call the random variable $m_s[t]$ as v, denoting the posterior sample at $t = t_{k_s}+1$, with a PDF

$$f_V(v) = \begin{cases} \frac{1}{r_s}, & v \in [\bar{m}_{s,\min}, \bar{m}_{s,\max}] \\ 0, & \text{otherwise} \end{cases}$$

The PDF of the random variable $w = m_s[t] - m^e_{s,k_s} = u - v$ is given by the convolution

$$f_W(w) = \int_{-\infty}^{\infty} f_U(v+w) f_V(v) dv.$$

Since $f_V(v) = 1/r_s$ if $\bar{m}_{s,\min} \leq v \leq \bar{m}_{s,\max}$ and 0 otherwise, this becomes

$$f_W(w) = \frac{1}{r_s} \int_{\bar{m}_{s,\min}}^{\bar{m}_{s,\max}} f_U(v+w) dv.$$

The integrand is 0 unless $\bar{m}_{s,\min} \leq v + w \leq \bar{m}_{s,\max}$ (i.e., unless $\bar{m}_{s,\min} - w \leq v \leq \bar{m}_{s,\max} - w$) and in that case, it is $\frac{1}{r_s}$. So it leads

$$f_W(w) = \begin{cases} \frac{1}{r_s} \int_{\bar{m}_{s,\min}-w}^{\bar{m}_{s,\max}} \frac{1}{r_s} dv = \frac{r_s + w}{r_s^2}, & -r_s \leq w \leq 0, \\ \frac{1}{r_s} \int_{\bar{m}_{s,\min}}^{\bar{m}_{s,\max}-w} \frac{1}{r_s} dv = \frac{r_s - w}{r_s^2}, & 0 \leq w \leq r_s, \\ 0, & w^2 > r_s. \end{cases}$$

The probability of having two consecutive samples with an absolute difference greater than Δ_s is

$$\beta_s = \mathbf{Pr}\{|m_s[t] - m^e_{s,k_s}| \geq \Delta_s\} = 1 - \mathbf{Pr}\{-\Delta_s < w < \Delta_s\}.$$

Using the above probability density function this can be computed by

$$\beta_s = 1 - \int_{-\Delta_s}^{\Delta_s} f_W(w) = \frac{(r_s - \Delta_s)^2}{r_s^2}$$

The virtual noise signal can be obtained as a function of the previous random variable w as

$$\delta[t] = g(w) = \begin{cases} w, & -\Delta_s < w < \Delta_s \\ 0, & \text{otherwise} \end{cases}$$

Its expected value is given by

$$E\{\delta[t]\} = \int_{-\infty}^{\infty} g(w) f_W(w) dw = 0,$$

and the variance is given by

$$Var\{\delta[t]\} = E\{\delta[t]^2\} = \int_{-\infty}^{\infty} g(w)^2 f_W(w) dw = \frac{2\Delta_s^3}{r_s^2}\left(\frac{r_s}{3} - \frac{\Delta_s}{4}\right),$$

■

Theorem C.2. *Let us assume that the difference $m_s[t] - m^e_{s,k_s}$ is normally distributed with zero mean and variance σ_s^2 given by (6.14) for $t = t_{k_s} + 1$. Then, the probability of having a new sample from sensor s at each instant $t = t_{k_s} + 1$ with law (6.2) is given by*

$$\beta_s = \mathbf{Pr}\{|m_s[t] - m^e_{s,k_s}| \geq \Delta_s\} = 1 - \text{erf}\left(\frac{\Delta_s}{\sqrt{2}\sigma_s}\right), \tag{C.12}$$

being $\text{erf}(x) = \frac{2}{\sqrt{\pi}} \int_0^x e^{-t^2} dt$ *the error function. The variance of the virtual noise related to this Δ_s is given by*

$$\sigma^2_{\delta_s} = Var\{\delta[t]\} = E\{\delta[t]^2\} = \sigma_s^2 \text{erf}\left(\frac{\Delta_s}{\sqrt{2}\sigma_s}\right) - \frac{\sqrt{2}\Delta_s\sigma_s}{\sqrt{\pi}} e^{\frac{-\Delta_s^2}{2\sigma_s^2}}. \tag{C.13}$$

Proof. The variable $w = m_s[t] - m^e_{s,k_s}$ has the PDF

$$f_W(w) = \frac{1}{\sigma_s\sqrt{2\pi}} e^{\frac{-w^2}{2\sigma_s^2}}.$$

The probability of having a new sample available is

$$\beta_s = 1 - \int_{-\Delta_s}^{\Delta_s} f_W(w) dw = 1 - \frac{2}{\sqrt{\pi}} \int_0^{\Delta_s} h'(w) e^{-(h(w))^2} dt$$

with $h(w) = \frac{w}{\sqrt{2}\sigma_s}$ and $h'(w) = \frac{1}{\sqrt{2}\sigma_s}$, and where we accounted that $f_W(w)$ is symmetric with respect to $w = 0$. Applying the definition of the error function, it leads (6.16).

We express the virtual noise signal as a function of the previous random variable w as

$$\delta[t] = g(w) = \begin{cases} w, & -\Delta_s < w < \Delta_s \\ 0, & \text{otherwise} \end{cases}$$

Its expected value is given by

$$E\{\delta[t]\} = \int_{-\infty}^{\infty} g(w) f_W(w) dw = 0$$

and the variance is given by (with $E\{\delta[t]^2\} = 0$)

$$Var\{\delta[t]\} = \int_{-\infty}^{\infty} g(w)^2 f_W(w) dw = \int_{-\Delta_s}^{\Delta_s} w^2 \frac{1}{\sigma_s\sqrt{2\pi}} e^{\frac{-w^2}{2\sigma_s^2}} dw.$$

Integrating this expression, it follows straightforwardly (6.27).

■

C.6.3 Proof of Theorem 6.2

Following similar steps than those in the proof of Theorem 6.1, inequalities (6.19) imply

$$\mathbf{E}\{V[t+1]\} - V[t] + \tilde{x}[t]^T\tilde{x}[t] < \gamma_w w[t]^T w[t] + v[t]^T\Gamma_v v[t] + \delta[t]^T\Gamma_\delta\delta[t], \qquad \text{(C.14)}$$

where $\mathbf{E}\{V[t+1]\}$ is the expected value of the Lyapunov function $V[t] = \tilde{x}[t]^T P\tilde{x}[t]$ at the next time instant over the possible modes of the system ($\alpha[t] = \{\eta_0, \ldots, \eta_q\}$ in (6.9)). Assuming null disturbances we obtain $\mathbf{E}\{V[t+1]\} < V[t]$, assuring the asymptotical mean square stability of the observer. Assuming initial state estimation error ($\tilde{x}[0] = 0$, $V[0] = 0$) and adding expression (C.14) from $t = 0$ to T, we obtain

$$\mathbf{E}\{V[T+1]\} + \sum_{t=0}^{T} \tilde{x}[t]^T\tilde{x}[t] < \sum_{t=0}^{T} \left(\gamma_w w[t]^T w[t] + v[t]^T\Gamma_v v[t] + \delta[t]^T\Gamma_\delta\delta[t]\right). \qquad \text{(C.15)}$$

As $\mathbf{E}\{V[T+1]\} > 0$, dividing by T and taking the limit when T tends to infinity, one finally obtains (6.21).

C.7 Proofs of Chapter 7

Let us first introduce the following lemmas to be used in the proof of Theorem 7.5.

Lemma C.3 ([131]). *Let ω be a stochastic vector with mean μ and a covariance matrix W, and P a symmetric matrix. Then*

$$\mathbf{E}\{\omega^T P\omega\} = \mu^T P\mu + \mathrm{tr}(PW). \qquad \text{(C.16)}$$

Lemma C.4 ([79]). *Let P be a positive semidefinite matrix, x_i a vector with appropriate dimensions and $\mu_i \geq 0$ scalar constants (with $i = 1, 2, \ldots$). If the series concerned is convergent, then we have*

$$\left(\sum_{i=1}^{\infty} \mu_i x_i\right)^T P \left(\sum_{i=1}^{\infty} \mu_i x_i\right) \leq \left(\sum_{i=1}^{\infty} \mu_i\right) \sum_{i=1}^{\infty} \mu_i x_i^T P x_i. \qquad \text{(C.17)}$$

C.7.1 Proof of Theorem 7.1

Let us define the Lyapunov function at instant $t = t_k$ as $V_k = \tilde{z}_k^T P \tilde{z}_k$.

i) In the absence of disturbances, faults and measurement noises, after taking Schur's complements on (7.16a) and premultiplying the result by $\tilde{z}_k^T$ and postmultipliying by its transpose, we obtain that $V_{k+1} - V_k \leq 0$ that assures that the extended state estimation error (7.12) converges to zero under standard sampling.

ii) Performing similar steps on (7.16b) (Schur's complements and operations with w_k^T, v_k^T and Δf_k), taking expected value on the results and adding the obtained constraints with the one from (7.16a) we get

$$\begin{aligned} &\mathbf{E}\{V_{k+1}\} - \mathbf{E}\{V_k\} + \mathbf{E}\{\tilde{f}_k^T F^{-1} \tilde{f}_k\} - \mathbf{E}\{w_k^T \Gamma_w w_k\} \\ &- \mathbf{E}\{v_{k+1}^T \Gamma_v v_{k+1}\} - \Delta {f_k}^T \Gamma_f \Delta f_k \leq 0 \end{aligned} \tag{C.18}$$

where we have considered the uncorrelation between $\tilde{z}_k$, w_k, v_{k+1} and Δf_k. Applying Lemma C.3 over w_k^T and v_k^T, considering null initial conditions ($V(0) = 0$) and adding the result from $k = 0$ to $K - 1$ we get

$$\sum_{k=0}^{K-1} \mathbf{E}\{\tilde{f}_k^T F^{-1} \tilde{f}_k\} \leq K \operatorname{tr}(\bar{\Gamma}) + \sum_{k=0}^{K-1} \Delta f_k^T \Gamma_f \Delta f_k^T \tag{C.19}$$

where we have taken into account that $P \succeq 0$ and that $\bar{\Gamma} = \Gamma_w W + \Gamma_v V$. Dividing the above expressions by K, taking the limit when $K \to \infty$ and considering that

$$\begin{aligned} &\mathbf{E}\{\tilde{f}_k^T F^{-1} \tilde{f}_k\} \geq \underline{\lambda}(F^{-1}) \mathbf{E}\{\tilde{f}_k^T \tilde{f}_k\}, \\ &\Delta {f_k}^T \Gamma_f \Delta f_k \leq n_f \overline{\lambda}(\Gamma_f) \|\Delta f\|_\infty^2 \leq n_f \overline{\lambda}(\Gamma_f) \Delta f_{\max}^2, \end{aligned}$$

and that $\underline{\lambda}(F^{-1}) = 1/\overline{\lambda}(F)$ (as F is a positive definite matrix), it leads to (7.17), which concludes this proof.

C.7.2 Proof of Theorem 7.2

If there is no fault on the system (i.e. $\tilde{f}_k = -\hat{f}_k$ and $\Delta f_k = 0$ for all k), we have that $\mathbf{E}\{\tilde{f}_k^T F^{-1} \tilde{f}_k\} = \mathbf{E}\{\hat{f}_k^T F^{-1} \hat{f}_k\} = \mathbf{E}\{r_k\}$. Then, following the proof of Theorem 7.1, dividing expression (C.19) by K, taking the limit when K tends to infinity and considering constraint (7.18), we obtain

$$\lim_{K \to \infty} \frac{1}{K} \sum_{k=0}^{K-1} \mathbf{E}\{r_k\} \leq \phi \, r^{\text{th}}. \tag{C.20}$$

Considering the above result and the FAR definition given in (7.14), we can employ Markov's inequality[3] to obtain

$$\Psi \leq \lim_{K \to \infty} \frac{1}{K} \sum_{k=0}^{K-1} \frac{\mathbf{E}\{r_k\}}{r^{\text{th}}} \leq \phi,$$

proving that ϕ bounds the FAR.

[3] If x is a positive random variable and $a > 0$, then $\mathbf{Pr}\{x > a\} \leq \frac{\mathbf{E}\{x\}}{a}$.

C.7.3 Proof of Theorem 7.3

Let us define vector $\tilde{f}'_k$ by $\tilde{f}'_k = F^{-\frac{1}{2}}\tilde{f}_k$. With that, (C.18) can be rewritten as

$$\mathbf{E}\{V_{k+1}\} - \mathbf{E}\{V_k\} \leq -\mathbf{E}\{\|\tilde{f}'_k\|_2^2\} + r^{\text{th}} + n_f\overline{\lambda}(\Gamma_f)\Delta f_{\max}^2. \tag{C.21}$$

Inequality (7.19) implies that Γ_f minus the diagonal block of P corresponding to the fault estimation error is positive semidefinite. Then, there exists a finite real constant $d_1 \geq 0$ that fulfills

$$\begin{aligned}\mathbf{E}\{V_k\} &\leq \mathbf{E}\{\tilde{f}_k^T\Gamma_f\tilde{f}_k\} + d_1 = \mathbf{E}\{\tilde{f}_k'^T {F^{\frac{1}{2}}}^T\Gamma_f F^{\frac{1}{2}}\tilde{f}'_k\} + d_1 \\ &\leq \overline{\lambda}(\Gamma_f F)\mathbf{E}\{\|\tilde{f}'_k\|_2^2\} + d_1\end{aligned} \tag{C.22}$$

for all k, considering the fact that $\Gamma_f F$ and ${F^{\frac{1}{2}}}^T\Gamma_f F^{\frac{1}{2}}$ are similar matrices[4]. From this expression we can upper bound $-\mathbf{E}\{\|\tilde{f}'_k\|_2^2\}$ allowing us to rewrite expression (C.21) as

$$\mathbf{E}\{V_{k+1}\} \leq \rho\mathbf{E}\{V_k\} + \varepsilon + (1-\rho)d_1, \tag{C.23}$$

for all k with ρ as defined in (7.20) and

$$\varepsilon = r^{\text{th}} + n_f\overline{\lambda}(\Gamma_f)\Delta f_{\max}^2.$$

Expressions (7.16a) imposes that $\bar{B}_f^T P\bar{B}_f \succeq F^{-1}$ which combined with (7.19) leads to $\Gamma_f F \succeq I$ guaranteing that $0 \leq \rho \leq 1$. Going backwards from k to $k=0$, expression (C.23) becomes

$$\mathbf{E}\{V_{k+1}\} \leq \rho^{k+1}\mathbf{E}\{V_0\} + \sum_{l=0}^{k}\rho^l\left(\varepsilon + (1-\rho)d_1\right).$$

Taking into account that $\sum_{l=0}^{k}\rho^l = \frac{1-\rho^{k+1}}{1-\rho} \leq \frac{1}{1-\rho}$, then

$$\mathbf{E}\{V_{k+1}\} \leq \rho^{k+1}\mathbf{E}\{V_0\} + \frac{1}{1-\rho}\varepsilon + d_1. \tag{C.24}$$

Constraint (7.16a) implies also that $\mathbf{E}\{V_k\} \geq \mathbf{E}\{\|\tilde{f}'_k\|_2^2\}$. Considering this, inequality (C.22) and the fact that

$$\underline{\lambda}(F^{-1})\|\tilde{f}_k\|_2^2 \leq \|\tilde{f}'_k\|_2^2 \leq \overline{\lambda}(F^{-1})\|\tilde{f}_k\|_2^2,$$

expression (C.24) leads to

$$\mathbf{E}\{\|\tilde{f}_{k+1}\|_2^2\} \leq \rho^{k+1}\frac{\kappa(F)}{(1-\rho)}\mathbf{E}\{\|\tilde{f}_0\|_2^2\} + \frac{\overline{\lambda}(F)}{(1-\rho)}\varepsilon + \overline{\lambda}(F)d_1, \tag{C.25}$$

where $\kappa(F) = \overline{\lambda}(F)/\underline{\lambda}(F)$ is the condition number of matrix F and where we have considered that $\underline{\lambda}(F^{-1}) = 1/\overline{\lambda}(F)$ because F is positive definite. Expression (C.25) proves that $\mathbf{E}\{\|\tilde{f}_k\|_2^2\}$ decays with ρ.

[4]Matrices A and B are similar if $B = C^{-1}AC$. Similar matrices share the same eigenvalues.

C.7.4 Proof of Theorem 7.4

First, in the absence of faults and under null initial conditions, $\tilde{f}_k$ is normally distributed and has zero mean because the disturbances and measurement noises are normally distributed with zero mean. Second, let $Z_{k-1} = \mathbf{E}\{\tilde{z}_{k-1}\tilde{z}_{k-1}^T\}$ be the covariance matrix for the state estimation error updated at instants t_{k-1} (which is also the covariance at instants t, since we are dealing with standard sampling). Then, its expected value at instant t_k is given by

$$\mathbf{E}\{Z_k\} = G(\bar{A}Z_{k-1}\bar{A}^T + \bar{B}_w W \bar{B}_w^T)G^T + L\,V\,L^T. \tag{C.26}$$

As the observer gain L assures the stability of (7.12) (by Theorem 7.1), the series in (C.26) converges to a symmetric positive definite matrix $\Sigma_f = \mathbf{E}\{Z_k\} = Z_{k-1}$ when $k \to \infty$ (see Chapter 3) given in (7.23). Then we have that $\tilde{f}_k^T \Sigma_f^{-1} \tilde{f}_k$ is distributed as $\mathcal{X}^2_{n_f}$ (see [63]). Considering (7.22), the signal $r_k/\phi = \tilde{f}_k^T F^{-1} \tilde{f}_k$ is then distributed as $\mathcal{X}^2_{n_f}$. From Theorem 7.2 we know that $\mathbf{E}\{r_k\}/\phi \leq r^{\text{th}}$, see (C.20). As the expected value of random variable that follows a $\mathcal{X}^2_{n_f}$ is n_f, if we fix the threshold to be $r^{\text{th}} = n_f$, then we have that the FAR is

$$\Psi = \mathbf{Pr}\left\{ \frac{r_k}{\phi} > \frac{r^{\text{th}}}{\phi} \middle| f_k = 0 \right\}, \tag{C.27}$$

and using the definition of the CDF, we obtain (7.24).

C.7.5 Proof of Theorem 7.5

Let us define the Lyapunov function at instant $t = t_k$ as $V_k = \tilde{z}_k^T P \tilde{z}_k$. Let us first study the evolution of the Lyapunov function. The expected value of the Lyapunov function at the next update instant $t = t_{k+1}$ given that a measurement was obtained at t_k, denoted by $\mathbf{E}\{V_{k+1}\}$, is

$$\begin{aligned}
&\sum_{N=1}^{\infty} p_0^{N-1} \sum_{i=1}^{q} p_i\, \mathbf{E}\{\tilde{z}_{k+1}^T P \tilde{z}_{k+1} | N_{k+1} = N, \alpha_{k+1} = \eta_i\} \\
&\quad = \mathbf{E}\left\{ \tilde{z}_k^T \left(\sum_{N=1}^{\infty} p_0^{N-1} (\bar{A}^N)^T \mathcal{Q} \bar{A}^N \right) \tilde{z}_k \right\} \\
&\quad + \mathbf{E}\left\{ w_k^T \left(\sum_{N=1}^{\infty} p_0^{N-1} \left(\sum_{l=0}^{N-1} \bar{B}_w^T \left(\bar{A}^l\right)^T \mathcal{Q} \bar{A}^l \bar{B}_w \right) \right) w_k \right\} \\
&\quad + \mathbf{E}\left\{ v_k^T \left(\sum_{N=1}^{\infty} p_0^{N-1} \sum_{i=1}^{r} \eta_i^T L_i^T P L_i \eta_i \right) v_k \right\} \\
&\quad + \sum_{N=1}^{\infty} p_0^{N-1} (\star)^T \mathcal{Q} \underbrace{\left(\sum_{l=0}^{N-1} \bar{A}^l \bar{B}_f \Delta f[t_k + l] \right)}_{\star}
\end{aligned} \tag{C.28}$$

considering the uncorrelation between $\tilde{z}[t_k]$, $w[t_k + l - 1]$, $v[t_{k+1}]$ and $\Delta f[t_k + l - 1]$ for $l = 1, \ldots, N_k - 1$ and the uncorrelation in time of $w[t]$. Matrix $\mathcal{Q}$ is defined by $\mathcal{Q} = \sum_{i=1}^{q} p_i G_i^T P G_i$, where $G_i = I - L_i \eta_i \bar{C}$ and $L_i = P^{-1} X_i$.

Le us denote by $\mathcal{V}_{k+1}$ the result of replacing in (C.28) $\mathcal{Q}$ by Q where $\mathcal{Q} \preceq Q$. We rewrite $\mathcal{V}_{k+1}$ as

$$\mathcal{V}_{k+1} = \mathcal{V}^z_{k+1} + \mathcal{V}^w_{k+1} + \mathcal{V}^v_{k+1} + \mathcal{V}^f_{k+1}.$$

Since $\mathcal{Q} \preceq Q$, we have that $\mathbf{E}\{V_{k+1}\} \leq \mathcal{V}_{k+1}$. If $p_0\overline{\lambda}(\bar{A})^2 < 1$, the series involve in (C.28), and therefore in $\mathcal{V}_{k+1}$, are convergent. Then, the summatory in $\mathcal{V}^f_{k+1}$, which implies dealing with cross products between the different $\Delta f[t_k + l]$, can be bounded with Lemma C.4 as $\mathcal{V}^f_{k+1} \leq \overline{\mathcal{V}}^f_{k+1}$ with $\overline{\mathcal{V}}^f_{k+1}$ given by (7.27). Therefore, defining $\overline{\mathcal{V}}_{k+1}$ as

$$\overline{\mathcal{V}}_{k+1} = \mathcal{V}^z_{k+1} + \mathcal{V}^w_{k+1} + \mathcal{V}^v_{k+1} + \overline{\mathcal{V}}^f_{k+1}, \tag{C.29}$$

we have that $\mathbf{E}\{V_{k+1}\} \leq \mathcal{V}_{k+1} \leq \overline{\mathcal{V}}_{k+1}$. Let us now analyze constraints (7.25a)-(7.25e). If (7.25e) holds, then matrix Q is such as $Q \succeq \mathcal{Q}$. Matrices M_1, M_2, M_5, M_6 can be rewritten as

$$\begin{aligned}
M_1 &= \sum_{N=1}^{\infty} p_0^{N-1} (\bar{A}^N)^T Q \bar{A}^N, \\
M_2 &= \sum_{N=1}^{\infty} p_0^{N-1} \left(\sum_{l=0}^{N-1} \bar{B}_w^T \left(\bar{A}^l\right)^T Q \bar{A}^l \bar{B}_w \right), \\
M_5 + M_6 &= \sum_{N=1}^{\infty} N p_0^{N-1} \sum_{j=0}^{N-1} (\bar{A}^j)^T Q \bar{A}^j.
\end{aligned}$$

Then taking Schur's complement from (7.25a) to (7.25d); premultiplying the result by $\tilde{z}_k^T$, w_k^T, v_k^T and $\overline{\Delta f}_k{}^T$ and postmultipliying by its transpose respectively; and taking expected values in both sides, we obtain

$$\begin{aligned}
&\mathbf{E}\left\{\tilde{z}_k^T M_1 \tilde{z}_k\right\} \leq \mathbf{E}\left\{V_k\right\} - \mathbf{E}\left\{\tilde{f}_k^T F^{-1} \tilde{f}_k\right\}, \\
&\mathbf{E}\left\{w_k^T M_2 w_k\right\} \leq \mathbf{E}\left\{w_k^T \Gamma_w w_k\right\}, \\
&\mathbf{E}\left\{ v_k^T \left(\sum_{N=1}^{\infty} p_0^{N-1} \sum_{i=1}^{r} \eta_i^T L_i^T P L_i \eta_i \right) v_k \right\} \leq \mathbf{E}\left\{v_k^T \Gamma_v v_k\right\}, \\
&\overline{\Delta f}_k{}^T \left(\bar{B}_f^T (M_5 + M_6) \bar{B}_f\right) \overline{\Delta f}_k \leq \overline{\Delta f}_k{}^T \Gamma_f \overline{\Delta f}_k,
\end{aligned}$$

Adding all the above expressions leads to

$$\begin{aligned}
\Upsilon = \overline{\mathcal{V}}_{k+1} &- \mathbf{E}\{V_k\} + \mathbf{E}\{\tilde{f}_k^T F^{-1} \tilde{f}_k\} \\
&- \mathbf{E}\{w_k^T \Gamma_w w_k\} - \mathbf{E}\{v_k^T \Gamma_v v_k\} - \overline{\Delta f}_k{}^T \Gamma_f \overline{\Delta f}_k \leq 0
\end{aligned} \tag{C.30}$$

where $\overline{\mathcal{V}}_{k+1}$ is as defined in (C.29). Let us define Θ as

$$\Theta = \Upsilon - \overline{\mathcal{V}}_{k+1} + \mathbf{E}\{V_{k+1}\} \leq 0.$$

Therefore, as $\mathbf{E}\{V_{k+1}\} \leq \overline{\mathcal{V}}_{k+1}$, if (C.30) holds, then we have that $\Theta \leq 0$ (analogous to (C.18)), since $\Theta \leq \Upsilon \leq 0$.

Using the fact that $\Theta \leq 0$ and following similar steps than in the proofs of Theorems 7.1, 7.2 and 7.3 we can prove with not much effort that the statements of Theorem 7.5 hold.

C.7.6 Proof of Theorem 7.6

Let $Z_{k-1} = \mathbf{E}\{\tilde{z}_{k-1}\tilde{z}_{k-1}^T\}$ be the covariance matrix for the state estimation error updated at the measurement instant t_{k-1}. Then, its expected value at instant t_k is given by

$$\begin{aligned}\mathbf{E}\{Z_k\} = &\sum_{i=1}^{q} p_i G_i(\bar{A}R_{k-1}\bar{A}^T + S_W)G_i^T \\ &+ \frac{1}{1-p_0}\sum_{i=1}^{q} p_i L_i\,\eta_i V \eta_i^T L_i^T \end{aligned} \tag{C.31}$$

where $\sum_{N=1}^{\infty} p_0^{N-1} = 1/(1-p_0)$ and $R_{k-1} = \sum_{i=0}^{\infty} p_0^i \bar{A}^i Z_{k-1}(\bar{A}^i)^T$ expressed as

$$\mathrm{vec}(R_{k-1}) = (I - p_0\bar{A}\otimes\bar{A})^{-1}\mathrm{vec}(Z_{k-1}).$$

Following similar arguments than in the proof of Theorem 7.4, the series in (C.31) converges to a symmetric positive definite matrix Σ_f and $r_k/\phi = \tilde{f}_k^T\Sigma_f^{-1}\tilde{f}_k$ is distributed as $\mathcal{X}^2_{n_f}$, leading to a FAR given by (7.24).

C.8 Proofs of Chapter 8

C.8.1 Proof of Theorem 8.1

If (8.25) holds, then we have $G_j(\Delta_t) + G_j(\Delta_t)^T - P_j(\Delta_t) \succ 0$ and thus, $G_j(\Delta_t)$ is a nonsingular matrix. As $P_j(\Delta_t)$ is a symmetric positive definite matrix, we can always state that

$$(\,P_j(\Delta_t) - G_j(\Delta_t)\,)\;P_j(\Delta_t)^{-1}\,(\,P_j(\Delta_t) - G_j(\Delta_t))^T \succeq 0,$$

which implies that $G_j(\Delta_t)+G_j(\Delta_t)^T - P_j(\Delta_t) \preceq G_j(\Delta_t)\,P_j(\Delta_t)^{-1}\,G_j(\Delta_t)^T$. Substituting $X_j(\Delta_t)$ by $G_j(\Delta_t)\,L_j(\Delta_t)$, applying a congruence transformation on (8.25) by matrix

$$\left(\bigoplus_{j=0}^{q} G_j(\Delta_t)^{-1}\right) \oplus I \oplus I \oplus I,$$

taking Schur's complements and premultiplying the result by $\begin{bmatrix}\tilde{z}_t^T & w_t^T & \tilde{u}_t^T & \Delta f_t^T & v_{t+1}^T\end{bmatrix}$ and postmultiplying by its transpose leads to

$$\begin{aligned}&\sum_{j=0}^{q} p_{i,j}\,(\mathcal{A}_j(\Delta_t)\,\tilde{z}_t + \mathcal{B}_j(\Delta_t)\,\mathcal{W}_t)^T\,P_j(\Delta_t)\,(\mathcal{A}_j(\Delta_t)\,\tilde{z}_t + \mathcal{B}_j(\Delta_t)\,\mathcal{W}_t) - \tilde{z}_t^T\,P_i(\Delta_{-1})\,\tilde{z}_t \\ &+ \tilde{f}_t^T\,F^{-1}\,\tilde{f}_t - \gamma_w(\Delta_t)\,w_t^T\,w_t - \gamma_u(\Delta_t)\,\tilde{u}_t^T\,\tilde{u}_t - \gamma_f(\Delta_t)\,\Delta f_t^T\,\Delta f_t - \gamma_v(\Delta_t)\;v_{t+1}^T\,v_{t+1} < 0,\end{aligned} \tag{C.32}$$

for all $i = 0,\ldots,q$ and $\delta_t \in \mathcal{S}$, where

$$\begin{aligned}\mathcal{A}_j(\Delta_t) &= (I - L_j(\Delta_t)\,\eta_j\,\bar{C})\bar{A}, \\ \mathcal{B}_j(\Delta_t) &= \begin{bmatrix}(I - L_j(\Delta_t)\,\eta_j\,\bar{C})\begin{bmatrix}\bar{B}_w & \bar{B}_u & \bar{B}_f\end{bmatrix} & -L_j(\Delta_t)\,\eta_j\end{bmatrix}, \\ \mathcal{W}_t &= \begin{bmatrix}w_t^T & \tilde{u}_t^T & \Delta f_t^T & v_{t+1}^T\end{bmatrix}^T.\end{aligned}$$

Now, let us define the Lyapunov function as $V_t = V(\tilde{z}_t, \alpha_t, \Delta_{t-1}) = \tilde{z}_t^T\, P_i(\Delta_{t-1})\, \tilde{z}_t$ for $\alpha_t = \eta_i$ and $i = 0, \ldots, q$.

i) In the absence of disturbances ($w_t = 0$), faults ($\Delta f_t = 0$), control errors ($\tilde{u}_t = 0$) and measurement noises ($v_t = 0$), expression (C.32) leads to

$$\tilde{z}_t^T \left(\sum_{j=0}^{q} p_{i,j} \mathcal{A}_j(\Delta_t)^T\, P_j(\Delta_t)\, \mathcal{A}_j(\Delta_t) \right) \tilde{z}_t - \tilde{z}_t^T\, P_i(\Delta_{t-1})\, \tilde{z}_t < 0 \tag{C.33}$$

for all $i = 0, \ldots, q$ and $\delta_t \in \mathcal{S}$, which assures $\mathbf{E}\{V_{t+1}|\alpha_t = \eta_i\} - V_t < 0$ guaranteeing that the extended state estimation error (8.19) converges asymptotically to zero in average for all the possible parameter values. This proves the first statement.

ii) For ease of notation let us write $\mathbf{E}\{V_{t+1}|\alpha_t = \eta_i\}$ as $\mathbf{E}\{V_{t+1}|\alpha_t\}$. Then, taking conditional expectation given α_{t-1} over expression (C.32), remembering that α_t is known at instant k, leads to

$$\begin{aligned} &\mathbf{E}\{V_{t+1}|\alpha_t\} - \mathbf{E}\{V_t\} + \mathbf{E}\{\tilde{f}_t^T\, F^{-1}\, \tilde{f}_t\} - \gamma_w(\Delta_t)\, \|w\|^2_{\mathrm{RMS}} \\ &\quad - \gamma_u(\Delta_t)\, \delta_t - \gamma_f(\Delta_t)\, \Delta f_t^T\, \Delta f_t - \gamma_v(\Delta_t)\, \|v\|^2_{\mathrm{RMS}} < 0, \end{aligned} \tag{C.34}$$

for all $\alpha_t \in \Xi$ and $\delta_t \in \mathcal{S}$, where we have considered the assumptions on w_t and v_t, and that $\delta_t = \mathbf{E}\{\tilde{u}_t^T\, \tilde{u}_t\}$. For brevity, let us not include in the next the fact that the inequalities are fulfilled for all $\alpha_t \in \Xi$ and $\delta_t \in \mathcal{S}$. If (C.34) is fulfilled, then

$$\begin{aligned} &\mathbf{E}\{V_{t+1}|\alpha_t\} - \mathbf{E}\{V_t\} + \mathbf{E}\{\tilde{f}_t^T\, F^{-1}\, \tilde{f}_t\} - \gamma_w(\Delta_t)\ \bar{w}^2_{\mathrm{rms}} \\ &\quad - \gamma_u(\Delta_t)\, \delta_t - \gamma_f(\Delta_t)\, \Delta f_t^T\, \Delta f_t - \gamma_v(\Delta_t)\, \bar{v}^2_{\mathrm{rms}} < 0 \end{aligned} \tag{C.35}$$

holds because $\|w\|^2_{\mathrm{RMS}} \leq \bar{w}^2_{\mathrm{rms}}$, $\|v\|^2_{\mathrm{RMS}} \leq \bar{v}^2_{\mathrm{rms}}$. Under null initial conditions ($V_0 = 0$), adding the above expression from $t = 0$ to $T - 1$ we obtain that

$$\begin{aligned} &\mathbf{E}\{V_T|\alpha_{T-1}\} + \sum_{t=0}^{T-1} \left(\mathbf{E}\{V_t|\alpha_{t-1}\} - \mathbf{E}\{V_t\}\right) + \sum_{t=0}^{T-1} \mathbf{E}\{\tilde{f}_t^T\, F^{-1}\, \tilde{f}_t\} - \sum_{t=0}^{T-1} \gamma_w(\Delta_t) \bar{w}^2_{\mathrm{rms}} \\ &- \sum_{t=0}^{T-1} \gamma_u(\Delta_t) \delta_t - \sum_{t=0}^{T-1} \gamma_f(\Delta_t)\, \Delta f_t^T\, \Delta f_t - \sum_{t=0}^{T-1} \gamma_v(\Delta_t) \bar{v}^2_{\mathrm{rms}} < 0. \end{aligned} \tag{C.36}$$

Considering that $\mathbf{E}\{V_{T+1}|\alpha_T\} > 0$, dividing (C.36) by T and taking the limit when T tends to infinity we get

$$\lim_{T\to\infty} \frac{1}{T} \sum_{t=0}^{T-1} \mathbf{E}\{\tilde{f}_t^T\, F^{-1}\, \tilde{f}_t\} < \bar{\gamma}_w \bar{w}^2_{\mathrm{rms}} + \bar{\gamma}_u + \bar{\gamma}_v \bar{v}^2_{\mathrm{rms}} + \frac{1}{T} \sum_{t=0}^{T-1} \gamma_f(\Delta_t)\, \Delta f_t^T\, \Delta f_t \tag{C.37}$$

where we have taken into account the definition of $\bar{\gamma}_{\_}$ given in (8.27) and that

$$\lim_{T\to\infty} \frac{1}{T} \sum_{t=0}^{T-1} \left(\mathbf{E}\{V_t|\alpha_{t-1}\} - \mathbf{E}\{V_t\}\right) = 0.$$

Finally, due to the facts that

$$\begin{aligned} &\mathbf{E}\{\tilde{f}_t^T\, F^{-1}\, \tilde{f}_t\} \geq \underline{\lambda}(F^{-1})\, \mathbf{E}\{\tilde{f}_t^T\, \tilde{f}_t\}, \\ &\gamma_f(\Delta_t)\, \Delta f_t^T\, \Delta f_t \leq \gamma_f(\Delta_t)\, n_f\, \|\Delta f\|^2_\infty \leq \gamma_f(\Delta_t)\, n_f\, \overline{\Delta f}^2, \end{aligned}$$

and that $\underline{\lambda}(F^{-1}) = 1/\overline{\lambda}(F)$ (as F is a positive definite matrix), expression (C.37) leads to (8.26).

C.8.2 Proof of Theorem 8.2

Following the proof of Theorem 8.1, taking into account constraint (8.29), expression (C.37) leads to

$$\lim_{T\to\infty} \frac{1}{T} \sum_{t=0}^{T-1} \mathbf{E}\{\tilde{f}_t^T \, F^{-1} \, \tilde{f}_t\} < \phi \, r^{\text{th}} + \frac{1}{T} \sum_{t=0}^{T-1} \gamma_f(\Delta_t) \, \Delta f_t^T \, \Delta f_t. \tag{C.38}$$

In the absence of faults (i.e. $\tilde{f}_t = -\hat{f}_t$ and $\Delta f_t = 0$ for all k), we have that $\mathbf{E}\{\tilde{f}_t^T \, F^{-1} \, \tilde{f}_t\} = \mathbf{E}\{\hat{f}_t^T \, F^{-1} \, \hat{f}_t\} = \mathbf{E}\{r_t\}$. Then, in the fault free case, (C.38) becomes

$$\lim_{T\to\infty} \frac{1}{T} \sum_{t=0}^{T-1} \mathbf{E}\{r_t | f_t = 0\} < \phi \, r^{\text{th}}. \tag{C.39}$$

Considering the above result and the FAR definition given in (8.22), we can employ Markov's inequality[5] to obtain

$$\Psi = \lim_{T\to\infty} \frac{1}{T} \sum_{t=0}^{T-1} \Pr\left\{r_t > r^{\text{th}} \,\middle|\, f_t = 0\right\} \leq \lim_{T\to\infty} \frac{1}{T} \sum_{t=0}^{T-1} \frac{\mathbf{E}\{r_t | f_t = 0\}}{r^{\text{th}}} < \phi, \tag{C.40}$$

which ends this proof.

[5] If x is a positive random variable and $a > 0$, then $\mathbf{Pr}\{x > a\} \leq \frac{\mathbf{E}\{x\}}{a}$.

Bibliography

[1] R. P. Aguilera, R. Delgado, D. Dolz, and J. C. Agüero. Quadratic MPC with ℓ_0-input constraint. In *19th World Congress of The International Federation of Automatic Control*, pages 10888–10893, 2014.

[2] P. Albertos and A. Sala. *Multivariable control systems: an engineering approach*. Springer, 2004.

[3] J. Anderson and A. Papachristodoulou. Robust nonlinear stability and performance analysis of an F/A-18 aircraft model using sum of squares programming. *International Journal of Robust and Nonlinear Control*, 23(10):1099–1114, 2013.

[4] K. J. Åström and B. Bernhardsson. Comparison of Riemann and Lebesque sampling for first order stochastic systems. In *41st IEEE Conference on Decision and Control*, volume 2, pages 2011–2016. IEEE, 2002.

[5] K. J. Åström and T. Hägglund. Automatic tuning of simple regulators with specifications on phase and amplitude margins. *Automatica*, 20(5):645–651, 1984.

[6] G. Battistelli, A. Benavoli, and L. Chisci. Data-driven communication for state estimation with sensor networks. *Automatica*, 48(5):926–935, 2012.

[7] J. A. Bondy and U. S. R. Murty. *Graph theory with applications*, volume 6. Macmillan London, 1976.

[8] S. Boyd, L. Gaoui, E. Feron, and V. Balakrishnan. *Linear Matrix Inequalities in Systems and Control Theory*. SIAM. Philadelphia, 1994.

[9] P. Brémaud. *Markov Chains*. Springer, New York, 1999.

[10] J. V. Burke, A. S. Lewis, and M. L. Overton. Two numerical methods for optimizing matrix stability. *Linear Algebra and its Applications*, 351:117–145, 2002.

[11] G. Caire, G. Taricco, and E. Biglieri. Optimum power control over fading channels. *IEEE Transactions on Information Theory*, 45(5):1468–1489, 1999.

[12] G. Cembrano, G. Wells, J. Quevedo, R. Pérez, and R. Argelaguet. Optimal control of a water distribution network in a supervisory control system. *Control engineering practice*, 8(10):1177–1188, 2000.

[13] J.-L. Chang. Applying discrete-time proportional integral bbservers for state and disturbance estimations. *IEEE Transactions on Automatic Control*, 51(5):814–818, 2006.

[14] J. Chen, K. H. Johansson, S. Olariu, I. C. Paschalidis, and I. Stojmenovic. Guest editorial special issue on wireless sensor and actuator networks. *IEEE Transactions on Automatic Control*, 56(10):2244–2246, 2011.

[15] J. Chen and R. J. Patton. *Robust model-based fault diagnosis for dynamic systems*, volume 3. Springer Publishing Company, Incorporated, 1999.

[16] G. Chesi. LMI techniques for optimization over polynomials in control: a survey. *IEEE Transactions on Automatic Control*, 55(11):2500–2510, 2010.

[17] A. Chiuso, N. Laurenti, L. Schenato, and A. Zanella. Analysis of delay-throughput-reliability tradeoff in a multihop wireless channel for the control of unstable systems. In *IEEE International Conference on Communications*, 2014.

[18] F. N. Chowdhury. Ordinary and neural Chi-squared tests for fault detection in multi-output stochastic systems. *IEEE Transactions on Control Systems Technology*, 8(2):372–379, 2000.

[19] S.-L. Dai, H. Lin, and S. S. Ge. Scheduling-and-control codesign for a collection of networked control systems with uncertain delays. *IEEE Transactions on Control Systems Technology*, 18(1):66 –78, 2010.

[20] M. C. de Oliveira, J. F. Camino, and R. E. Skelton. A convexifying algorithm for the design of structured linear controllers. In *39th IEEE Conference on Decision and Control*, volume 3, pages 2781–2786. IEEE, 2000.

[21] M. C. de Oliveira and R. E. Skelton. Stability tests for constrained linear systems. In *Perspectives in robust control*, pages 241–257. Springer, 2001.

[22] J.-D. Decotignie. Ethernet-based real-time and industrial communications. *Proceedings of the IEEE*, 93(6):1102–1117, 2005.

[23] D. Dolz, I. Peñarrocha, N. Aparicio, and R. Sanchis. Control de aerogeneradores mediante controladores dependientes de la velocidad y turbulencia del viento. In *XXXIII Jornadas de Automática*, pages 443–450, 2012.

[24] D. Dolz, I. Peñarrocha, N. Aparicio, and R. Sanchis. Virtual torque control in wind generation with doubly fed induction generator. In *38th Annual Conference on IEEE Industrial Electronics Society*, pages 2536–2541, 2012.

[25] D. Dolz, I. Peñarrocha, and R. Sanchis. Estrategias de control y estimacion robustas para sistemas de control en red. In *XI Simposio CEA de ingeniería de control*, pages 67–73, 2013.

[26] D. Dolz, I. Peñarrocha, and R. Sanchis. Jump state estimation with multiple sensors with packet dropping and delaying channels. *International Journal of Systems Science*, pages 1–12, 2014.

[27] D. Dolz, I. Peñarrocha, and R. Sanchis. Networked gain-scheduled fault diagnosis under control input dropouts without data delivery acknowledgement. *Submitted for journal publication*, july and november 2014.

[28] D. Dolz, I. Peñarrocha, and R. Sanchis. Performance trade-offs for networked jump observer-based fault diagnosis. *Submitted for journal publication*, may and november 2014.

[29] D. Dolz, I. Peñarrocha, and R. Sanchis. Accurate fault diagnosis in sensor networks with markovian transmission dropouts. *Submitted for journal publication*, september 2014.

[30] D. Dolz, D. E. Quevedo, I. Peñarrocha, A. S. Leong, and R. Sanchis. Co-design of Markovian jump estimators for wireless multi-hop networks with fading channels. *To be submitted for journal publication*, 2014.

[31] D. Dolz, D. E. Quevedo, I. Peñarrocha, and R. Sanchis. A jump filter for uncertain dynamic systems with dropouts. In *To appear in 53rd IEEE Conference on Decision and Control*, 2014.

[32] D. Dolz, D. E. Quevedo, I. Peñarrocha, and R. Sanchis. Performance vs complexity trade-offs for markovian networked jump estimators. In *19th World Congress of The International Federation of Automatic Control*, pages 7412–7417, 2014.

[33] L. El Ghaoui, F. Oustry, and M. AitRami. A cone complementarity linearization algorithm for static output-feedback and related problems. *IEEE Transactions on Automatic Control*, 42(8):1171–1176, 1997.

[34] D. Estrin. Wireless sensor networks tutorial part IV: sensor network protocols. In *The Eighth Annual International Conference on Mobile Computing and Networking (Mobicom)*, pages 23–28, 2002.

[35] H. Fang, H. Ye, and M. Zhong. Fault diagnosis of networked control systems. *Annual Reviews in Control*, 31(1):55–68, 2007.

[36] M. Felser. Real-time ethernet-industry prospective. *Proceedings of the IEEE*, 93(6):1118–1129, 2005.

[37] A. Fletcher, S. Rangan, V. Goyal, and K. Ramchandran. Causal and strictly causal estimation for jump linear systems: An LMI analysis. In *40th Annual Conference on Information Sciences and Systems*, pages 1302–1307, Princeton, NJ, march 2006.

[38] H. C. Foundation. Control with wirelesshart. 2009.

[39] P. Gahinet and P. Apkarian. A linear matrix inequality approach to h_∞ control. *International Journal of Robust and Nonlinear Control*, 4(4):421–448, 1994.

[40] M. Gaid, A. Cela, and Y. Hamam. Optimal integrated control and scheduling of networked control systems with communication constraints: application to a car suspension system. *IEEE Transactions on Control Systems Technology*, 14(4):776 – 787, 2006.

[41] H. Gao, T. Chen, and L. Wang. Robust fault detection with missing measurements. *International Journal of Control*, 81(5):804–819, 2008.

[42] G. C. Goodwin, S. F. G., and M. E. Salgado. *Control system design*, volume 240. Prentice Hall New Jersey, 2001.

[43] V. C. Gungor and G. P. Hancke. Industrial wireless sensor networks: challenges, design principles, and technical approaches. *IEEE Transactions on Industrial Electronics*, 56(10):4258–4265, 2009.

[44] R. A. Gupta and M. Y. Chow. Networked control system: Overview and research trends. *IEEE Transactions on Industrial Electronics*, 57(7):2527–2535, 2010.

[45] C. Han, H. Zhang, and M. Fu. Optimal filtering for networked systems with markovian communication delays. *Automatica*, 49(10):3097 – 3104, 2013.

[46] J. Han and R. E. Skelton. An LMI optimization approach for structured linear controllers. In *42nd IEEE Conference on Decision and Control*, volume 5, pages 5143–5148. IEEE, 2003.

[47] X. He, Z. Wang, Y. D. Ji, and D. H. Zhou. Robust Fault Detection for Networked Systems with Distributed Sensors. *IEEE Transactions on Aerospace and Electronic Systems*, 47(1):166 – 177, 2011.

[48] X. He, Z. Wang, and D. H. Zhou. Robust fault detection for networked systems with communication delay and data missing. *Automatica*, 45(11):2634–2639, 2009.

[49] W. Heemels and M. Donkers. Model-based periodic event-triggered control for linear systems. *Automatica*, 49(3):698–711, 2013.

[50] D. Henrion and A. Garulli. *Positive polynomials in control*, volume 312. Springer, 2005.

[51] J. P. Hespanha, P. Naghshtabrizi, and Y. Xu. A survey of recent results in networked control systems. *Proceedings of the IEEE*, 95(1):138–162, 2007.

[52] L. Hetel, J. Daafouz, and C. Iung. Equivalence between the Lyapunov–Krasovskii functionals approach for discrete delay systems and that of the stability conditions for switched systems. *Nonlinear Analysis: Hybrid Systems*, 2(3):697–705, 2008.

[53] D. Hongli, W. Zidong, and G. Huijun. Robust $\mathcal{H}_\infty$ filtering for a class of nonlinear networked systems with multiple stochastic communication delays and packet dropouts. *IEEE Transactions on Signal Processing*, 58(4):1957–1966, 2010.

[54] D. Huang and S. K. Nguang. Robust fault estimator design for uncertain networked control systems with random time delays: An ILMI approach. *Information Sciences*, 180(3):465–480, 2010.

[55] I. Hwang, S. Kim, Y. Kim, and C. E. Seah. A survey of fault detection, isolation, and reconfiguration methods. *IEEE Transactions on Control Systems Technology*, 18(3):636–653, 2010.

[56] G. Irwin, J. Chen, A. McKernan, and W. Scanlon. Co-design of predictive controllers for wireless network control. *Control Theory Applications, IET*, 4(2):186 –196, 2010.

[57] R. Isermann. Process fault detection based on modeling and estimation methodsŮa survey. *Automatica*, 20(4):387–404, 1984.

[58] R. Isermann. *Fault-diagnosis systems: an introduction from fault detection to fault tolerance*. Springer, 2006.

[59] Z. Jarvis-Wloszek, R. Feeley, W. Tan, K. Sun, and A. Packard. *Control applications of sum of squares programming*, volume 312 of *Lecture Notes in Control and Information Sciences*. 2005.

[60] T. Jia, Y. Niu, and Y. Zou. Sliding mode control for stochastic systems subject to packet losses. *Information Sciences*, 217(June):117–126, Dec. 2012.

[61] K. H. Johansson, M. Törngren, and L. Nielsen. Vehicle applications of controller area network. In *Handbook of networked and embedded control systems*, pages 741–765. Springer, 2005.

[62] K. E. Johnson and N. Thomas. Wind farm control: addressing the aerodynamic interaction among wind turbines. In *American Control Conference*, pages 2104–2109. IEEE, 2009.

[63] R. A. Johnson and D. W. Wichern. *Applied Multivariate Statistical Analysis (6th Edition)*. Pearson, 2007.

[64] R. E. Kalman. A new approach to linear filtering and prediction problems. *Journal of Fluids Engineering*, 82(1):35–45, 1960.

[65] S.-J. Kim and Y.-H. Moon. Structurally constrained and control: a rank-constrained LMI approach. *Automatica*, 42(9):1583–1588, 2006.

[66] S.-J. Kim, Y.-H. Moon, and S. Kwon. Solving rank-constrained LMI problems with application to reduced-order output feedback stabilization. *IEEE Transactions on Automatic Control*, 52(9):1737–1741, 2007.

[67] D. Lehmann. *Event-based state-feedback control*. Logos Verlag Berlin GmbH, 2011.

[68] A. S. Leong and S. Dey. Power allocation for error covariance minimization in Kalman filtering over packet dropping links. *51st IEEE Conference on Decision and Control*, pages 3335–3340, 2012.

[69] A. S. Leong and D. E. Quevedo. Kalman filtering with relays over wireless fading channels. 2014.

[70] J. Li and G.-Y. Tang. Fault diagnosis for networked control systems with delayed measurements and inputs. *IET Control Theory & Applications*, 4(6):1047, 2010.

[71] W. Li and S. X. Ding. Remote fault detection system design with online channel reliability information. *International Journal of Systems Science*, 41(8):957–970, 2010.

[72] W. Li, Z. Zhu, and S. Ding. Fault detection design of networked control systems. *IET Control Theory & Applications*, 5(12):1439, 2011.

[73] Y. Li, D. Quevedo, V. Lau, and L. Shi. Optimal periodic transmission power schedules for remote estimation of ARMA processes. *IEEE Transactions on Signal Processing*, 61(24):6164–6174, 2013.

[74] Z. Li, E. Mazars, Z. Zhang, and I. M. Jaimoukha. State-space solution to the $\mathcal{H}_-/\mathcal{H}_\infty$ fault-detection problem. *International Journal of Robust and Nonlinear Control*, 22(3):282–299, 2012.

[75] Y. Liang, T. Chen, and Q. Pan. Multi-rate stochastic $\mathcal{H}_\infty$ filtering for networked multi-sensor fusion. *Automatica*, 46(2):437–444, Feb. 2010.

[76] Q. Ling. Optimal dropout policies for networked control systems. *Optimal control applications and methods*, 2012.

[77] Q. Liu, Z. Wang, X. He, and D. H. Zhou. A survey of event-based strategies on control and estimation. *Systems Science & Control Engineering: An Open Access Journal*, 2(1):90–97, 2014.

[78] X. Liu and A. Goldsmith. Kalman filtering with partial observation losses. In *43rd IEEE Conference on Decision and Control*, volume 4, pages 4180–4186. IEEE, 2004.

[79] Y. Liu, Z. Wang, J. Liang, and X. Liu. Synchronization and state estimation for discrete-time complex networks with distributed delays. *IEEE Transactions on Systems, Man, and Cybernetics, Part B: Cybernetics*, 38(5):1314–1325, 2008.

[80] J. Löfberg. Pre-and post-processing sum-of-squares programs in practice. *IEEE Transactions on Automatic Control*, 54(5):1007–1011, 2009.

[81] Y. Long and G.-H. Yang. Fault detection filter design for stochastic networked control systems. *International Journal of Robust and Nonlinear Control*, 2013.

[82] Y. Long and G.-H. Yang. Fault detection for networked control systems subject to quantisation and packet dropout. *International Journal of Systems Science*, 44(6):1150–1159, 2013.

[83] Y. Long and G.-H. Yang. Fault detection and isolation for networked control systems with finite frequency specifications. *International Journal of Robust and Nonlinear Control*, 24(3):495–514, 2014.

[84] X. Lu, H. Zhang, W. Wang, and K.-L. Teo. Kalman filtering for multiple time-delay systems. *Automatica*, 41(8):1455–1461, 2005.

[85] J. Lunze and D. Lehmann. A state-feedback approach to event-based control. *Automatica*, 46(1):211–215, 2010.

[86] M. Mahmoud, S. Selim, P. Shi, and M. Baig. New results on networked control systems with non-stationary packet dropouts. *IET Control Theory & Applications*, 6(15):2442–2452, Oct. 2012.

[87] Z. Mao, B. Jiang, and P. Shi. H_∞ fault detection filter design for networked control systems modelled by discrete Markovian jump systems. *IET Control Theory & Applications*, 1(5):1336, 2007.

[88] C. Meng, T. Wang, W. Chou, S. Luan, Y. Zhang, and Z. Tian. Remote surgery case: robot-assisted teleneurosurgery. In *IEEE International Conference on Robotics and Automation*, volume 1, pages 819–823. IEEE, 2004.

[89] P. Millán, L. Orihuela, I. Jurado, C. Vivas, and F. R. Rubio. Distributed estimation in networked systems under periodic and event-based communication policies. *International Journal of Systems Science*, i-First(ahead-of-print):1–13, 2013.

[90] M. Miskowicz. Send-on-delta concept: an event-based data reporting strategy. *sensors*, 6(1):49–63, 2006.

[91] M. Moayedi, Y. K. Foo, and Y. C. Soh. Filtering for networked control systems with single/multiple measurement packets subject to multiple-step measurement delays and multiple packet dropouts. *International Journal of Systems Science*, 42(3):335–348, 2011.

[92] A. F. Molisch. *Wireless Communications*. Wiley, 2010.

[93] M. Nagahara, D. E. Quevedo, and J. Ø stergaard. Sparse packetized predictive control for networked control over erasure channels. *IEEE Transactions on Automatic Control*, 2013.

[94] P. Neumann. Communication in industrial automation–What is going on? *Control Engineering Practice*, 15(11):1332–1347, 2007.

[95] V. H. Nguyen and Y. S. Suh. Improving estimation performance in networked control systems applying the send-on-delta transmission method. *Sensors*, 7(10):2128–2138, 2007.

[96] V. H. Nguyen and Y. S. Suh. Networked estimation with an area-triggered transmission method. *Sensors*, 8(2):897–909, 2008.

[97] V. H. Nguyen and Y. S. Suh. Networked estimation for event-based sampling systems with packet dropouts. *Sensors*, 9(4):3078–3089, 2009.

[98] B. A. Ogunnaike. *Random phenomena: fundamentals of probability and statistics for engineers*. Taylor & Francis US, 2011.

[99] A. Papachristodoulou and S. Prajna. *Analysis of non-polynomial systems using the sum of squares decomposition*, volume 312 of *Lecture Notes in Control and Information Sciences*. 2005.

[100] I. Peñarrocha, A. Dinu, and R. Sanchis. Experimental test of power saving strategies in a networked based control over a wireless platform. In *39th Annual Conference of the IEEE Industrial Electronics Society*, pages 5650–5655. IEEE, 2013.

[101] I. Peñarrocha, R. Sanchis, and P. Albertos. Estimation in multisensor networked systems with scarce measurements and time varying delays. *Systems & Control Letters*, 61(4):555–562, Apr. 2012.

[102] I. Peñarrocha, D. Dolz, N. Aparicio, and R. Sanchis. Synthesis of nonlinear controller for wind turbines stability when providing grid support. *International Journal of Robust Nonlinear Control*, 2013.

[103] I. Peñarrocha, D. Dolz, N. Aparicio, R. Sanchis, R. Vidal, and E. Belenguer. Power analysis in wind generation with doubly fed induction generator with polynomial optimization tools. In *20th Mediterranean Conference on Control & Automation*, pages 1316–1321, 2012.

[104] I. Peñarrocha, D. Dolz, J. Romero, and R. Sanchis. State estimation and Send on Delta strategy codesign for networked control systems. In *9th International Conference on Informatics in Control, Automation and Robotics*, pages 499–504, 2012.

[105] I. Peñarrocha, D. Dolz, J. A. Romero, and R. Sanchis. Codesign strategy of inferential controllers for wireless sensor networks. In *4th International Congress on Ultra Modern Telecommunications and Control Systems and Workshops*, pages 28–33, 2012.

[106] I. Peñarrocha, D. Dolz, J. A. Romero, and R. Sanchis. Estrategia de codiseño de controladores inferenciales para su implementación mediante sensores inalámbricos. In *XXXIII Jornadas de Automática*, pages 361–367, 2012.

[107] I. Peñarrocha, D. Dolz, J. A. Romero, and R. Sanchis. Co-design of H-infinity jump observers for event-based measurements over networks. *Submitted for journal publication*, may 2014.

[108] I. Peñarrocha, D. Dolz, and R. Sanchis. Estimación óptima en redes de sensores con pérdida de datos aleatoria y retardos variantes. In *XXXII Jornadas de Automática*, 2011.

[109] I. Peñarrocha, D. Dolz, and R. Sanchis. A polynomial approach for observer design in networked control systems with unknown packet dropout rate. In *52nd IEEE Conference on Decision and Control*, pages 5933–5938, 2013.

[110] I. Peñarrocha, D. Dolz, and R. Sanchis. Inferential networked control with accessibility constraints in both the sensor and actuator channels. *International Journal of Systems Science*, 45(5):1180–1195, 2014.

[111] I. Peñarrocha and R. Sanchis. Fault detection and estimation in systems with scarce measurements. In *7th IFAC Symposium on Fault Detection, Supervision and Safety of Technical Processes*, pages 113–118, 2009.

[112] C. Peng, D. Yue, E. Tian, and Z. Gu. Observer-based fault detection for networked control systems with network Quality of Services. *Applied Mathematical Modelling*, 34(6):1653–1661, 2010.

[113] S. Prajna, A. Papachristodoulou, and P. A. Parrilo. Introducing SOSTOOLS: A general purpose sum of squares programming solver. In *41st IEEE Conference on Decision and Control*, pages 741–746, 2002.

[114] J. Proakis. *Digital Communications*. 1995.

[115] D. E. Quevedo, A. Ahlén, A. S. Leong, and S. Dey. On Kalman filtering over fading wireless channels with controlled transmission powers. *Automatica*, 48(7):1306–1316, 2012.

[116] D. E. Quevedo, A. Ahlén, and J. Østergaard. Energy efficient state estimation with wireless sensors through the use of predictive power control and coding. *IEEE Transactions on Signal Processing*, 58(9):4811–4823, Sept. 2010.

[117] D. E. Quevedo, J. Østergaard, and A. Ahlén. Power control and coding formulation for state estimation with wireless sensors. *IEEE Transactions on Control Systems Technology*, (2):413–427.

[118] Z. Ren, P. Cheng, J. Chen, L. Shi, and H. Zhang. Dynamic sensor transmission power scheduling for remote state estimation. *Automatica*, 50(4):1235–1242, 2014.

[119] M. Sahebsara, T. Chen, and S. L. Shah. Optimal $\mathcal{H}_2$ filtering in networked control systems with multiple packet dropout. *IEEE Transactions on Automatic Control*, 52(8):1508–1513, Aug. 2007.

[120] R. Sanchis, I. Peñarrocha, and P. Albertos. Design of robust output predictors under scarce measurements with time-varying delays. *Automatica*, 43(2):281–289, Feb. 2007.

[121] D. Sauter, S. Li, and C. Aubrun. Robust fault diagnosis of networked control systems. *International Journal of Adaptive Control and Signal Processing*, 23(8):722–736, 2009.

[122] L. Schenato. Optimal sensor fusion for distributed sensors subject to random delay and packet loss. *46th IEEE Conference on Decision and Control*, pages 1547–1552, 2007.

[123] L. Schenato. Optimal estimation in networked control systems subject to random delay and packet drop. *IEEE Transactions on Automatic Control*, 53(5):1311–1317, 2008.

[124] C. Scherer and S. Weiland. Linear matrix inequalities in control. *Lecture Notes, Dutch Institute for Systems and Control, Delft, The Netherlands*, 2000.

[125] B. Shen, S. X. Ding, and Z. Wang. Finite-horizon H_∞ fault estimation for linear discrete time-varying systems with delayed measurements. *Automatica*, 49(1):293–296, 2013.

[126] L. Shi, Q.-S. Jia, Y. Mo, and B. Sinopoli. Sensor scheduling over a packet-delaying network. *Automatica*, 47(5):1089–1092, 2011.

[127] L. Shi and L. Xie. Optimal sensor power scheduling for state estimation of gaussian markov systems over a packet-dropping network. *IEEE Transactions on Signal Processing*, 60(5):2701–2705, May 2012.

[128] J. Sijs and M. Lazar. Event based state estimation with time synchronous updates. *IEEE Transactions on Automatic Control*, 57(10):2650–2655, 2012.

[129] B. Sinopoli, L. Schenato, M. Franceschetti, K. Poolla, M. I. Jordan, and S. S. Sastry. Kalman filtering with intermittent observations. *IEEE Transactions on Automatic Control*, 49(9):1453–1464, 2004.

[130] S. C. Smith and P. Seiler. Estimation with lossy measurements : jump estimators for jump systems. *IEEE Transactions on Automatic Control*, 48(12):2163–2171, 2003.

[131] T. Söderström. Discrete-time stochastic systems. estimation and control. 1994.

[132] H. Song, L. Yu, and W. Zhang. Networked $\mathcal{H}_\infty$ filtering for linear discrete-time systems. *Information Sciences*, 181(3):686–696, Mar. 2011.

[133] J. Song, S. Han, A. K. Mok, D. Chen, M. Lucas, and M. Nixon. Wirelesshart: applying wireless technology in real-time industrial process control. In *IEEE Real-Time and Embedded Technology and Applications Symposium*, pages 377–386. IEEE, 2008.

[134] Y. S. Suh, V. H. Nguyen, and Y. S. Ro. Modified Kalman filter for networked monitoring systems employing a send-on-delta method. *Automatica*, 43(2):332 – 338, 2007.

[135] X. Wan, H. Fang, and S. Fu. Observer-based fault detection for networked discrete-time infinite-distributed delay systems with packet dropouts. *Applied Mathematical Modelling*, 36(1):270–278, 2012.

[136] X. Wang and M. Lemmon. Self-triggered feedback control systems with finite-gain stability. *IEEE Transactions on Automatic Control*, 54(3):452 –467, 2009.

[137] Y. Wang, S. X. Ding, H. Ye, and G. Wang. A new fault detection scheme for networked control systems subject to uncertain time-varying delay. *IEEE Transactions on Signal Processing*, 56(10):5258–5268, 2008.

[138] Y. Wang, H. Ye, S. X. Ding, Y. Cheng, P. Zhang, and G. Wang. Fault detection of networked control systems with limited communication. *International Journal of Control*, 82(7):1344–1356, 2009.

[139] Y. Wang, H. Ye, S. X. Ding, G. Wang, and D. Zhou. Residual generation and evaluation of networked control systems subject to random packet dropout. *Automatica*, 45(10):2427–2434, 2009.

[140] Z. Wang, B. Shen, and X. Liu. $\mathcal{H}_\infty$ Filtering With Randomly Occurring Sensor Saturations and Missing Measurements. *Automatica*, 48(3):556–562, Mar. 2012.

[141] Z. Wang, F. Yang, D. W. C. Ho, and X. Liu. Robust H_∞ filtering for stochastic time-delay systems with missing measurements. *IEEE Transactions on Signal Processing*, 54(7):2579–2587, 2006.

[142] A. Willig. Recent and emerging topics in wireless industrial communications: a selection. *IEEE Transactions Industrial Informatics*, 4(2):102–124, 2008.

[143] F. Wu and S. Prajna. SOS-based solution approach to polynomial LPV system analysis and synthesis problems. *International Journal of Control*, 78(8):600–611, 2005.

[144] J. Wu, Y. Mo, and L. Shi. Stochastic online sensor scheduler for remote state estimation. In *1st International Conference on Cyber-Physical Systems, Networks, and Applications*, pages 84–89. IEEE, 2013.

[145] Y. L. Wu, Z. P. Shen, and Y. Y. Liu. Mean square detectability of multi-output systems over stochastic multiplicative channels. *IET Control Theory & Applications*, 6(6):796, June 2012.

[146] X. Yao, L. Wu, and W. X. Zheng. Fault detection filter design for markovian jump singular systems with intermittent measurements. *IEEE Transactions on Signal Processing*, 59(7):3099–3109, 2011.

[147] J. Yick, B. Mukherjee, and D. Ghosal. Wireless sensor network survey. *Computer networks*, 52(12):2292–2330, 2008.

[148] J. Yu, M. Liu, W. Yang, P. Shi, and S. Tong. Robust fault detection for Markovian jump systems with unreliable communication links. *International Journal of Systems Science*, 44(11):2015–2026, 2013.

[149] K. Zhang, B. Jiang, and P. Shi. Fault estimation observer design for discrete-time Takagi-Sugeno fuzzy systems based on piecewise lyapunov functions. *IEEE Transactions on Fuzzy Systems*, 20(1):192–200, 2012.

[150] L. Zhang, H. Gao, and O. Kaynak. Network-induced constraints in networked control systems-A survey. *IEEE Transactions on Industrial Informatics*, 9(1):403–416, 2013.

[151] P. Zhang and S. X. Ding. An integrated trade-off design of observer based fault detection systems. *Automatica*, 44(7):1886–1894, 2008.

[152] C. Zhu, Y. Xia, L. Yan, and M. Fu. Centralised fusion over unreliable networks. *International Journal of Control*, 85(4):409–418, Apr. 2012.